SAPIENZA
UNIVERSITÀ DI ROMA

Motor patterns evaluation of people with neuromuscular disorders for biomechanical risk management and job integration/reintegration

Facoltà di Medicina e Odontoiatria
Dipartimento di Neuroscienze Umane
Dottorato in Neuroscienze Clinico-Sperimentali e Psichiatria
Curriculum Neuroriabilitazione

Antonella Tatarelli
Matricola 1244988

Relatore
Dott. Mariano Serrao

Correlatori
Dott. Francesco Draicchio
Ing. Alberto Ranavolo

A.A. 2021-2022

Motor patterns evaluation of people with neuromuscular disorders for biomechanical risk management and job integration/reintegration

Table of Contents

- *The effectiveness of a soft passive trunk exoskeleton on the motor coordination in patients with cerebellar ataxia.*
- *Exploring Risk of Falls and Dynamic Unbalance in Cerebellar Ataxia by Inertial Sensor Assessment.*
- *Identification of Gait Unbalance and Fallers Among Subjects with Cerebellar Ataxia by a Set of Trunk Acceleration-Derived Indices of Gait.*

4.1.2 Parkinson's disease

- *Ability of a Set of Trunk Inertial Indexes of Gait to Identify Gait Instability and Recurrent Fallers in Parkinson's Disease.*
- *Harmonic ratio is the most responsive trunk acceleration derived gait index to rehabilitation in people with Parkinson's disease at moderate disease stages.*
- *An artificial neural network approach to detect presence and severity of Parkinson's disease via gait parameters.*

4.1.3 Hemiparesis

- *Ability of a set of trunk-acceleration derived gait indexes to characterize gait instability and asymmetry in stroke survivors.*

5. Gait analysis of people with lower limb amputation

- *Characterizing the gait of people with different types of amputation and prosthetic components through multimodal measurements: a methodological perspective.*

5.1 Kinematic, kinetic and energy consumption

- *Common and specific gait patterns in people with varying anatomical levels of lower limb amputation and different prosthetic components.*

5.1.1 Kinematic data

5.1.1.Spatio-temporal parameters

5.1.1.2 Joint angles

5.1.2 Kinetic data

5.1.3 Energy consumption

- *Pelvic obliquity as a compensatory mechanism leading to lower energy recovery: Characterization among the types of prostheses in subjects with transfemoral amputation.*

5.2 Electrophysiological features of prosthetic gait

- *Global Muscle Coactivation of the Sound Limb in Gait of People with Transfemoral and Transtibial Amputation.*

6. Job integration/reintegration of people with neuromuscular disorders

- *Indexes for motor performance assessment in Job Integration/Reintegration of People with Neuromuscular Disorders-A Systematic Review.*

7. Discussion and Conclusion

7.1 Kinematic indices

7.2 Kinetic indices

7.3 Surface electromyography indices

Keywords

Neuromuscular disorders

Job integration/reintegration

Gait analysis

Kinematics

Kinetics

Surface electromyography

Wearable sensors

Publications

International Journal Papers

1. Chini G, Fiori L, **Tatarelli A**, Varrecchia T, Draicchio F, Ranavolo A. 2022. *Indexes for motor performance assessment in job integration/reintegration of people with neuromuscular disorders: A systematic review*. Front. Neurol., 8;13:968818. doi: 10.3389/fneur.2022.968818
2. Castiglia S.F, Trabassi D, De Icco R, **Tatarelli A**, Avenali M, Corrado M, Grillo V, Coppola G, Denaro A, Tassorelli C, Serrao M. 2022. *Harmonic ratio is the most responsive trunk acceleration derived gait index to rehabilitation in people with Parkinson's disease at moderate disease stages.* Gait & Posture, 97:152-158. doi: 10.1016/j.gaitpost.2022.07.235.
3. Chini G, Varrecchia T, **Tatarelli A**, Silvetti A, Fiori L, Draicchio F, Ranavolo A. 2022. *Trunk muscle co-activation and activity in one-and two-person lifting*. International Journal of Industrial Ergonomics, 89, 103297. https://doi.org/10.1016/j.ergon.2022.103297
4. De Marchis C, Ranaldi S, Varrecchia T, Serrao M, Castiglia S.F, **Tatarelli A**, Ranavolo A, Draicchio F, Lacquaniti F, Conforto S. 2022. *Characterizing the gait of people with different types of amputation and prosthetic components through multimodal measurements: a methodological perspective.* Front. Rehabilit. Sci., 3:804746. doi: 10.3389/fresc.2022.804746
5. Castiglia S.F, Trabassi D, **Tatarelli A**, Ranavolo A, Varrecchia T, Fiori L, Di Lenola D, Cioffi E, Raju M, Coppola G, Caliandro P, Casali C, Serrao M. 2022. *Identification of Gait Unbalance and Fallers Among Subjects with Cerebellar Ataxia by a Set of Trunk Acceleration-Derived Indices of Gait*. Cerebellum, doi: 10.1007/s12311-021-01361-5.
6. Castiglia S.F, **Tatarelli A,** Trabassi D, De Icco R, Grillo V, Ranavolo A, Varrecchia T, Magnifica F, Di Lenola D, Coppola G, et al. 2021. *Ability of a Set of Trunk Inertial Indexes of Gait to Identify Gait Instability and Recurrent Fallers in Parkinson's Disease*. Sensors, 15;21(10):3449. doi: 10.3390/s21103449.
7. Varrecchia T, Castiglia SF, Ranavolo A, Conte C, **Tatarelli A**, Coppola G, et al. 2021. *An artificial neural network approach to detect presence and severity of Parkinson's disease via gait parameters*. PLoS ONE, 16(2): e0244396.https://doi.org/10.1371/journal.pone.024439.
8. Fiori L, Ranavolo A, Varrecchia T, **Tatarelli A**, Conte C, Draicchio F, Castiglia S.F, Coppola G, Casali C, Pierelli F, Serrao M. 2020. *Impairment of Global Lower Limb Muscle Coactivation During Walking in Cerebellar Ataxias*. The Cerebellum, 19:583–596, https://doi.org/10.1007/s12311-020-01142-6.

9. Castiglia S.F, Ranavolo A, Varrecchia T, De Marchis C, **Tatarelli A**, Magnifica F, Fiori L, Conte C, Draicchio F, Conforto S, Serrao M. 2020. *Pelvic obliquity as a compensatory mechanism leading to lower energy recovery: Characterization among the types of prostheses in subjects with transfemoral amputation*. Gait & Posture, 80, 280–284.
10. **Tatarelli A**, Serrao M, Varrecchia T, Fiori L, Draicchio F, Silvetti A, Conforto S, De Marchis C, Ranavolo A. 2020. *Global Muscle Coactivation of the Sound Limb in Gait of People with Transfemoral and Transtibial Amputation*. Sensors 20, 2543; doi:10.3390/s20092543.
11. P Caliandro, Conte C, Iacovelli C, **Tatarelli A**, Castiglia S.F, Reale G, Serrao M. 2019. *Exploring Risk of Falls and Dynamic Unbalance in Cerebellar Ataxia by Inertial Sensor Assessment*. Sensors, 19, 5571; doi:10.3390/s19245571.

International Conference Papers

1. Alessio Silvetti, Alberto Ranavolo, Giorgia Chini, Tiwana Varrecchia, **Antonella Tatarelli**, Lorenzo Fiori, Adriano Papale, Ari Fiorelli, and Francesco Draicchio. Integrating sEMG into NIOSH Protocol: A Manual Material Handling Risk Assessment in the Fruit and Vegetable Department of a Supermarket. Physical Ergonomics and Human Factors, Vol. 63, 2022, 71–78 https://doi.org/10.54941/ahfe1002598.
2. Alessio Silvetti, Lorenzo Fiori, Alberto Ranavolo, Giorgia Chini, Tiwana Varrecchia, **Antonella Tatarelli**, Adriano Papale, Ari Fiorelli, and Francesco Draicchio. Biomechanical Risk Assessment of Kerbside Waste Collection Round Through Heart Rate and GPS Data. Social and Occupational Ergonomics, Vol. 65, 2022, 213–220 https://doi.org/10.54941/ahfe1002678.
3. Stefano Filippo Castiglia, **Antonella Tatarelli** , Alberto Ranavolo, Fabrizio Magnifica, Dante Trabassi, Roberto De Icco, Valentina Grillo, Alessandro Denaro, Cristina Tassorelli, Mariano Serrao. Ability of a set of trunk acceleration-derived gait stability indexes to identify gait unbalance and recurrent fallers in subjects with parkinson's disease. 25th World Congress of Neurology (SIN). Fully virtual, 3-7 ottobre 2021
4. Alessio Silvetti, Lorenzo Fiori, **Antonella Tatarelli**, Alberto Ranavolo, Francesco Draicchio. Kerbside Waste Collection Round Risk Assessment by Means of Physiological Parameters: sEMG and Heart Rate. International Ergonomics Association, IEA 2021. Virtual, Online,13 June 2021 through 18 June 2021.

5. Alberto Ranavolo, Giorgia Chini, Francesco Draicchio, Alessio Silvetti, Tiwana Varrecchia, Lorenzo Fiori, **Antonella Tatarelli**, Patricia Helen Rosen, Sascha Wischniewski, Philipp Albrecht, Lydia Vogt, Matteo Bianchi, Giuseppe Averta, Andrea Cherubini, Lars Fritzsche, Massimo Sartori, Bram Vanderborght, Renee Govaerts, and Arash Ajoudani. Human-Robot Collaboration (HRC)Technologies for Reducing Work-Related Musculoskeletal Diseases in Industry 4.0. International Ergonomics Association, IEA 2021. Virtual, Online 13 June 2021 through 18 June 2021.
6. Alessio Silvetti, Elio Munafò, Ari Fiorelli, Lorenzo Fiori, **Antonella Tatarelli**, Alberto Ranavolo, and Francesco Draicchio. Ergonomic Risk Assessment of Sea Fisherman Part IV: Tunisian Chapter. AHFE Conferences on Physical Ergonomics and Human Factors, Social and Occupational Ergonomics, and Cross-Cultural Decision Making, 2021. Virtual, Online 25 July 2021 through 29 July 2021
7. Lorenzo Fiori, Alessio Silvetti, **Antonella Tatarelli**, Alberto Ranavolo, Francesco Draicchio. sEMG and Postural Analysis for Biomechanical Risk Assessment in a Banknotes Printing Process. AHFE Conferences on Physical Ergonomics and Human Factors, Social and Occupational Ergonomics, and Cross-Cultural Decision Making, 2021. Virtual, Online, 25 July 2021 through 29 July 2021.
8. Alessio Silvetti, Lorenzo Fiori, **Antonella Tatarelli**, Alberto Ranavolo, Eleonora Spagnoli, Francesco Draicchio. Ergonomic Risk Assessment in Kerbside Waste Collection Through Dynamic REBA Protocol. 21st Congress of the International Ergonomics Association, IEA 2021. Virtual, Online, 13 June 2021 through 18 June 2021.
9. **Tatarelli A.**, Serrao M., Varrecchia T., Fiori L., Silvetti A., De Marchis C., Ranaldi S., Draicchio F., Conforto S., Ranavolo A. Global lower limb muscle coactivation during walking in trans-femoral and trans-tibial amputees. 15th IEEE International Symposium on Medical Measurements and Applications, MeMeA 2020. Bari, June 2020 through 3 June 2020.
10. Alessio Silvetti, Lorenzo Fiori, **Antonella Tatarelli**, Alberto Ranavolo, Francesco Draicchio. Back and Shoulder Biomechanical Load in Curbside Waste Workers. AHFE Virtual Conference on Physical Ergonomics and Human Factors, the Virtual Conference on Social and Occupational Ergonomics, and the Virtual Conference on Cross-Cultural Decision Making, 2020. San Diego16 July 2020 through 20 July 2020.

National Conference Papers

1. **A. Tatarelli**, M. Serrao, C. Casali, E. Cioffi, L. Fiori, T. Varrecchia, G. Chini, F. Draicchio, B. Montante, R. Ciancia, M. Michieli, M. Rupolo, A. Ranavolo. The effectiveness of a soft passive trunk exoskeleton on the motor coordination in patients with cerebellar ataxia. SIAMOC 2022 (5-8/10/2022) Bari.
2. L. Fiori, I.B. Marc, S. Ramawat, **A. Tatarelli**, T. Varrecchia, G. Chini, A. Ranavolo, F. Draicchio, P. Pani, S. Ferraina, E. Brunamonti, Motor inhibition parameters are reflected in the kinetic and kinematic of gait initiation in a step version of the Stop Signal Task, Gait & Posture, Volume 97, Supplement 2, 2022, Page 9, ISSN 0966-6362, https://doi.org/10.1016/j.gaitpost.2022.09.021.(https://www.sciencedirect.com/science/article/pii/S0966636222005227)
3. G. Chini, T. Varrecchia, A. Silvetti, **A. Tatarelli**, L. Fiori, F. Draicchio, M. Serrao, B. Montante, R. Ciancia, M. Michieli, M. Rupolo, A. Ranavolo, The effect of a passive exoskeleton on trunk co-activation during liftings at different risk levels, Gait & Posture, Volume 97, Supplement 2, 2022, Pages 34-35, ISSN 0966-6362, https://doi.org/10.1016/j.gaitpost.2022.09.058.(https://www.sciencedirect.com/science/article/pii/S0966636222005598)
4. Adriano Papale, Alessio Silvetti, Lorenzo Fiori, **Antonella Tatarelli**, Alberto Ranavolo, Tiwana Varrecchia, Giorgia Chini, Ari Fiorelli, Francesco Draicchio. Valutazione della postazione videoterminale (VDT) del check-in di un Aeroporto. AIDII (22-24/06/2022) Cagliari.
5. Alessio Silvetti, Lorenzo Fiori, **Antonella Tatarelli**, Alberto Ranavolo, Tiwana Varrecchia, Giorgia Chini, Adriano Papale, Ari Fiorelli, Francesco Draicchio. Valutazione del rischio biomeccanico del giro di raccolta rifiuti porta a porta tramite analisi della frequenza cardiaca degli operatori e dei dati GPS. AIDII (22-24/06/2022) Cagliari.
6. Caratteristiche comportamentali e correlati cinematici dell'inibizione motoria durante l'inizio del passo L. Fiori, S. Colangeli, G. Chini, **A. Tatarelli**, T. Varrecchia, A. Ranavolo, F. Draicchio, P. Pani, S. Ferraina, E. Brunamonti. Congresso SIE 2022 (2-4/05/2022) Lucca.
7. Analisi di stabilità dinamica locale L5/S1 in soggetti con lombalgia durante attività di sollevamento faticose dipendenti dalla frequenza G. Chini, T. Varrecchia, S. Conforto, A. Silvetti, L. Fiori, **A. Tatarelli**, A. De Nunzio, D. Falla, A. Ranavolo, F. Draicchio. Congresso SIE 2022 (2-4/05/2022) Lucca.

8. Elettromiografia di superficie ad alta densità in persone con e senza lombalgia durante faticose attività di sollevamento dipendenti dalla frequenza. T. Varrecchia, G. Chini, S. Conforto, A. Silvetti, **A. Tatarelli**, L. Fiori, A. De Nunzio, D. Falla, F. Draicchio, A. Ranavolo. SIE 2022 (2-4/05/2022) Lucca.
9. L'effetto di un esoscheletro del tronco assistivo indossabile sulla coordinazione motoria delle persone con atassia cerebellare. **A. Tatarelli**, M. Serrao, C. Casali, E. Cioffi, L. Fiori, T. Varrecchia, G .Chini, F. Draicchio, B. Montante, R. Ciancia, M. Michieli, A. Ranavolo. SIE 2022 (2-4/05/2022) Lucca.
10. Valutazione posturale e biomeccanica nel lavoro di acconciatura prima e dopo un intervento Ergonomico. A. Silvetti, A. Fiorelli, V. Rocchi, **A. Tatarelli**, L. Fiori, A. Ranavolo, A. Papale, T. Varrecchia, G. Chini, F. Draicchio. SIE 2022 (2-4/05/2022) Lucca.
11. Stefano Filippo Castiglia, Dante Trabassi, **Antonella Tatarelli**, Giorgia Chini, Lorenzo Fiori, Tiwana Varrecchia, Alberto Ranavolo, Carlo Casali and Mariano Serrao. Ability of a set of trunk inertial indexes of gait to identify gait unbalance and fallers in subjects with cerebellar ataxia. SIAMOC 2021, Virtual edition, 30 Settembre-1 Ottobre .
12. Stefano Filippo Castiglia, Dante Trabassi, **Antonella Tatarelli**, Tiwana Varrecchia, Lorenzo Fiori, Alberto Ranavolo and Mariano Serrao. Responsiveness to rehabilitation of a set of gait stability indexes in persons with Parkinson's disease. SIAMOC 2021, Virtual edition, 30 Settembre-1 Ottobre .
13. Giorgia Chini, Alberto Ranavolo, Tiwana Varrecchia, **Antonella Tatarelli**, Lorenzo Fiori, Mariano Serrao and Francesco Draicchio. Trunk muscles co-activation in single vs team lifting at different risk levels. SIAMOC 2021, Virtual edition, 30 Settembre-1 Ottobre
14. Tiwana Varrecchia, Silvia Conforto, Mariano Serrao, Alessandro Marco De Nunzio, Deborah Falla, Francesco Draicchio, Giorgia Chini, **Antonella Tatarelli**, Lorenzo Fiori and Alberto Ranavolo. High-Density surface electromyography during fatiguing frequency-dependent lifting activities at different risk levels in people with and without low back pain. SIAMOC 2021, Virtual edition, 30 Settembre-1 Ottobre .
15. Lorenzo Fiori, **Antonella Tatarelli**, Tiwana Varrecchia, Giorgia Chini, Francesco Draicchio, Mariano Serrao and Alberto Ranavolo. Global lower limb muscle coactivation from slow walking to running. SIAMOC 2021, Virtual edition, 30 Settembre-1 Ottobre .

Abstract

Neurological diseases are now the most common pathological condition and the leading cause of disability, progressively worsening the quality of life of those affected. Because of their high prevalence, they are also a social issue, burdening both the national health service and the working environment. It is therefore crucial to be able to characterize altered motor patterns in order to develop appropriate rehabilitation treatments with the primary goal of restoring patients' daily lives and optimizing their working abilities.

In this thesis, I present a collection of published scientific articles I co-authored as well as two in progress in which we looked for appropriate indices for characterizing motor patterns of people with neuromuscular disorders that could be used to plan rehabilitation and job accommodation programs. We used instrumentation for motion analysis and wearable inertial sensors to compute kinematic, kinetic and electromyographic indices.

These indices proved to be a useful tool for not only developing and validating a clinical and ergonomic rehabilitation pathway, but also for designing more ergonomic prosthetic and orthotic devices and controlling collaborative robots.

CHAPTER 1

1. INTRODUCTION

The research activity carried out during the PhD programme was based on the study and characterization of motor disorders, mainly resulting from neurological diseases, for the purposes of functional evaluation in the clinical and occupational fields. Neurological diseases are now the most common pathological condition and the leading cause of disability, progressively worsening the affected people's quality of life. They are also a social issue because of their high prevalence, which burdens both the national health service and the working environment. In order to fully characterize motor disorders caused by neurological diseases, I decided to evaluate three different pathologies involving the central nervous system (CNS), such as cerebellar ataxia, Parkinson's disease, and hemiparesis. Cerebellar ataxia is a neurological condition characterized by a lesions at different regions of cerebellum that plays a primary role in static and dynamic balance control and in modulating the rhythmic flexor and extensor muscle activity [1]. It has been showed that patients suffering from cerebellar ataxia exhibit several deficit in locomotion [2], such as peculiar spatiotemporal and kinematic features that contribute to an unstable gait [3-7], as well as a widened muscle activation patterns [1]. Parkinson's disease is an extrapyramidal syndrome caused by a malfunction of neuronal circuits in the basal ganglia that are in charge of regulating automatic and involuntary movements as well as motor learning [8]. Among the various symptoms, gait abnormality is the most invalidating for patients with Parkinson’s disease [9] and closely parallels disease progression, leading to a high risk of falls [10], impaired patient autonomy, and reduced quality of life [11]. Hemiparesis, on the other hand, is defined as a partial loss of voluntary motility on one side of the body caused by damage to the pyramidal system, which is responsible for muscle contraction [12]. Muscle tone is more pronounced as a result of this change, and movements are altered. For instance, stroke survivors with hemiparesis have abnormal gait patterns as a result of sensorimotor impairments, such as the inability to generate normal levels of force, spasticity, impaired motor control, and proprioceptive deficits [13-17]. Although lower limb amputation is an orthopedic pathology, it also involves significant neural reorganization within CNS [18,19], and thus the prosthetic gait reflects a mixture of deviations from normal gait. In light of this, it is critical to define a global characterization of these motor patterns in order to design an appropriate rehabilitation pathway as well as to assess the efficacy of the treatment

itself. In addition to the more purely clinical aspect, it is also important to consider that many patients with neuromuscular disorders are still working due to the increase in working age, which means they frequently struggle with employability, work challenges, and job loss [3,20, 21]. For example, Parkinson's disease, which was previously thought to be a disease of the elderly, now increasingly affects younger individuals as well, both for early forms and for other cases of the disease itself. For these reasons, a quantitative assessment of residual motor skills is necessary, and it could be a key factor in the design and evaluation of innovative ergonomic interventions for effective occupational integration/reintegration. As a result, it is important to characterize altered motor patterns in order to develop appropriate pharmacological, surgical, and rehabilitation treatments with the primary goal of restoring patients' motor performance, autonomy, and daily life, and if they are of working age allowing them also to return to work and optimize their working abilities.

To achieve this, we used the instrumentation for motion analysis (i.e. an optoelectronic system that permits a three-dimensional quantitative motion analysis, dynamometric platforms that measure the reaction forces in space during ground contact, as well as the moments and powers acting on joint structures, and the surface electromyography, an instrumental approach that provides a comprehensive view of human movement by measuring and analyzing electrical activity generated by muscles). Furthermore, thanks to wearable sensors, we were able to leave the laboratory's enclosed setting and assess the patient/worker directly in his/her daily environment. Moreover, the fourth industrial revolution has recently opened up new employment scenarios in which, using wearable technologies and artificial intelligence, it is possible to characterize the motor capabilities of individuals who have motor impairments, and use these information to control human-robot collaboration (HRC) technologies, such as collaborative robots and exoskeletons. HRC technologies support workers in the workplace by adapting to their specific demands and individual needs.

In this scenario, the first aim of my thesis work was to identify, using movement analysis technologies, appropriate indices for characterizing pathologic conditions in patients with cerebellar ataxia, Parkinson’s disease, hemiparesis and lower limb amputation. These indices could support the process for identifying the correct rehabilitation pathway and be useful for verifying the effectiveness of the treatment itself. The second aim was the identification of quantitative biomechanical and physiological indices for motor monitoring in job accommodation programs of people with neuromuscular disorders.

My overall role in the scientific articles reported in this thesis remained consistent in the following activities: scientific literature search and analysis; experimental procedure design; data recordings; data processing and analysis; statistical analysis; articles writing. Writing, coordination, and finalization of results have been emphasized in scientific works for which I am the first author.

Bibliography

[1]. Martino G, Ivanenko YP, Serrao M, Ranavolo A, d'Avella A, Draicchio F, et al. 2014. Locomotor patterns cerebellar ataxia. J Neurophysiol., 112:2810–21.

[2]. Thach WT, Bastian AJ. 2004. Role of the cerebellum in the control and adaptation of gait in health and disease. Prog Brain Res., 143:353-66.

[3]. Klockgether T. 2010 Sporadic ataxia with adult onset: classification and diagnostic criteria. Lancet Neurol., 9(1): 94-104.

[4]. Ranavolo A, Serrao M, Draicchio F. 2020. Critical Issues and Imminent Challenges in the Use of sEMG in Return-To-Work Rehabilitation of Patients Affected by Neurological Disorders in the Epoch of Human–Robot Collaborative Technologies. Front. Neurol., 11:572069.

[5]. Serrao M, Pierelli F, Ranavolo A, Draicchio F, Conte C, Don R, Di Fabio R, Le Rose M, Padua L, Sandrini G, et al. 2012. Gait pattern in inherited cerebellar ataxias. Cerebellum Lond. Engl., 11, 194–211.

[6]. Serrao M, Ranavolo A, Casali C. 2018. Neurophysiology of gait. Handb. Clin. Neurol., 154, 299–303.

[7]. Chini G, Ranavolo A, Draicchio F, Casali C, Conte C, Martino G, Leonardi L, Padua L, Coppola G, Pierelli, F, et al. 2017. Local Stability of the Trunk in Patients with Degenerative Cerebellar Ataxia DuringWalking. Cerebellum Lond. Engl., 16, 26–33.

[8]. Yanagisawa N. 2018. Functions and dysfunctions of the basal ganglia in humans. Proc Jpn Acad Ser B Phys Biol Sci., 94(7):275-304.

[9]. Morris M.E, Iansek R, Matyas T.A., Summers J.J. 1994. The pathogenesis of gait hypokinesia in parkinson's disease. Brain, 117, 1169–1181.

[10]. Amboni M, Iuppariello L, Iavarone A, Fasano A, Palladino R, Rucco R, Picillo M, Lista I, Varriale P, Vitale C, et al. 2018. Step length predicts executive dysfunction in Parkinson's disease: A 3-year prospective study. J. Neurol., 265, 2211–2220.

[11]. De Boer A.G.E.M., Wijker W, Speelman J.D, De Haes J.C.J.M. 1996. Quality of life in patients with Parkinson's disease: Development of a questionnaire. J. Neurol. Neurosurg. Psychiatry, 61, 70–74.

[12]. Otsuka N, Miyashita K, Krieger DW, Naritomi H. 2013. Compensatory contribution of the contralateral pyramidal tract after stroke. Front Neurol Neurosci., 32:45-53.

[13]. Tok F. Balaban B. Yas¸ar E. Alaca R. Tan AK. 2012. The effects of on a botulinum toxin A injection into rectus femoris muscle in hemiplegic stroke patients with stiff-knee gait: A placebo-controlled. nonrandomized trial. Am J Phys Med Rehabil., 91:321-326.

[14]. Balaban B. Tok F. Yavuz F. Yas¸ar E. Alaca R. 2011. Early rehabilitation outcome in patients with middle cerebral artery stroke. Neurosci Lett., 498:204-207.

[15]. Tok F. Ozçakar L. Safaz I. Alaca R. 2011. Effects of botulinum toxin-A on the muscle architecture of stroke patients: The first ultrasonographic study. J Rehabil Med., 43:1016-1019.

[16]. Perry J. Garrett M. Gronley JK. Mulroy SJ. 1995. Classification of walking handicap in the stroke population. Stroke, 26:982-989.

[17]. Krasovsky T. Levin MF. 2010. Review: Toward a better understanding of coordination in healthy and poststroke gait. Neurorehabil Neural Repair., 24:213-224.

[18]. Geurts A.C, Mulder T.W, Nienhuis B, Rijken R.A. 1991. Dual-task assessment of reorganization of postural control in persons with lower limb amputation. Arch. Phys. Med. Rehabil., 72, 1059–1064.

[19]. Chen R, Corwell B, Yaseen Z, Hallett M, Cohen L.G. 1998. Mechanisms of cortical reorganization in lower-limb amputees. J. Neurosci., 18, 3443–3450.

[20]. Miller A, Dishon, S. 2006. Health-related quality of life in multiple sclerosis: the impact of disability, gender and employment status. Quality of life research, 15(2):259–271.

[21]. Ranavolo A, Serrao M and Draicchio F. 2020. Critical Issues and Imminent Challenges in the Use of sEMG in Return-To-Work Rehabilitation of Patients Affected by Neurological Disorders in the Epoch of Human–Robot Collaborative Technologies. Front. Neurol., 11:572069.

CHAPTER 2

2. GAIT ANALYSIS

Gait is defined as a repetitive sequence of limb motions used to propel the body forward, with one limb acting as a support while the other advances to a new support site [1]. The limbs then reverse their roles, with both feet in contact with the ground for the transfer of body weight from one limb to the other. This sequence of events is repeated by each limb alternately until the desired destination is reached. Gait is the most common movement performed by humans, and autonomy and safety during gait represent an important aspect of daily life for the individual in a variety of contexts. As a result, a detailed characterization of gait is essential for defining motor ability.

Gait analysis is a relevant discipline for the characterization of human movement, and it is a viable assessment tool not only used in sports science or basic biomechanical research, but has also expanded to be a very valuable instrument in clinical diagnostics, monitoring functional recovery and musculoskeletal rehabilitation [2]. In fact, it allows for the quantification of gait deviations, the informing of clinical decision making, the providing of useful elements to define an appropriate rehabilitation strategy [3,4] and the monitoring of the efficacy of therapy in movement disorders[5,6]. In this context, this method has long been used to treat neurological disorders such as cerebellar ataxia, Parkinson's disease, and post-stroke hemiplegia [7]; however, in the meantime, the benefits have become apparent in other medical fields such as foot surgery, orthopedic technology, and patients who have had lower limb amputations [2].
Therefore, robust investigation of impaired gait mechanisms, as well as precise measurement, may be critical in targeted physical and/or pharmaceutical intervention.

The use of motion analysis begins in the nineteenth century, but technological and electronic advancements continue to provide new solutions for increasing and improving measurement techniques [8]. Specifically, movement analysis can currently be performed using marker-based systems or wearable systems, both of which will be described in this thesis.

Bibliography

[1]. Whittle M.W. 1993. Gait analysis. The soft tissues. Butterworth-Heinemann, 187-199.

[2]. Klöpfer-Krämer I, Brand A, Wackerle H, Müßig J, Kröger I, Augat P. 2020. Gait analysis - Available platforms for outcome assessment. Injury, 51 Suppl 2:S90-S96. doi: 10.1016/j.injury.2019.11.011. Epub 2019 Nov 11.

[3]. Saunders J.B, Inman V.T, Eberhart H.D. 1953. The major determinants in normal and pathological gait." The Journal of Bone and Joint Surgery, American vol. 35-A, pp. 543– 558.

[4]. Whittle M.W. 1996. Clinical gait analysis: A review. Human Movement Science, vol. 15, no. 3, pp. 369-387.

[5]. Cimolin V, Galli M. 2014. Summary measures for clinical gait analysis: a literature review. Gait Posture 39, 1005–1010.

[6]. Armand S, Decoulon G, Bonnefoy-Mazure A. 2016. Gait analysis in children with cerebral palsy. EFORT Open Rev. 1, 448–460.

[7]. Celik Y, Stuart S, Woo WL, Godfrey A. 2021 Gait analysis in neurological populations: Progression in the use of wearables. Med Eng Phys., 87:9-29.

[8]. Akhtaruzzaman M, Shafie A.A, Khan M.R. 2016. Gait Analysis: Systems, Technologies, and Importance. Journal of Mechanics in Medicine and Biology, vol. 16, no. 7, 1630003.

CHAPTER 3

3. Materials and Methods

3.1 Biomechanical characterization

Motion analysis based on the study of kinematic, kinetic and electromyographic parameters.

Kinematics describes the spatial variations of anatomical references and body segments involved independent of the forces that cause the movement through variables such as linear and angular displacements, velocities, and accelerations [1-3].

The definition of space and anatomical plane with respect to which the measurement is made is required for the calculation of these variables. The plan chosen refers to standardized definitions based on the human body: three fundamental planes are defined, namely the frontal or coronal plane, the sagittal plane, and the transverse plane. The origin axes are defined as anteroposterior, mediolateral, and longitudinal (or craniocaudal) (Figure 3.1).

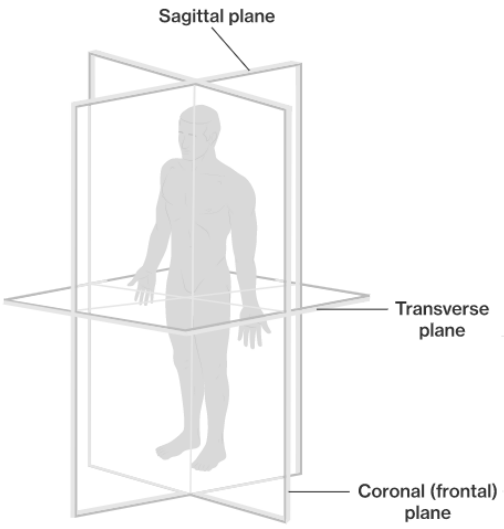

Figure 3.1 *Anatomical planes*

Just for simplicity, the body is represented as a rigid body composed of a series of segments; the length of these anatomical segments is reported in the literature as a percentage of body weight, as defined by Drillis and colleagues [4,5] (Figure 3.2):

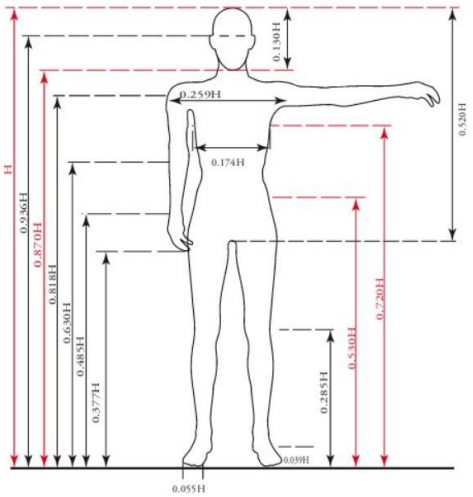

Figure 3.2 *The length of body segments as a function of height H*

Kinetics studies the forces and angular moments at the base of motor acts to describe the role of forces in generating movement [6]. Internal and external forces are studied, and both types play a role in motor performance.

Surface electromyography (sEMG) has recently been used in clinical and research settings for assessing muscular activity, performing isometric tests, studying muscle fatigue, pain, movement control, and performance analysis in sports medicine [3]. sEMG is also used in the research of muscle tremors, muscle contraction biofeedback, and muscle spasticity. sEMG investigates the electrical signals produced by muscle contraction; these signals travels through the tissues and can be recorded on the surface.

3.2 Instrumentation

3.2.1 Stereo-photogrammetric system

3.2.1.1 Kinematics

The kinematics is investigated using stereo-photogrammetric systems.

A stereo-photogrammetric system collects kinematic data using video cameras to record movements in the two- or three-dimensional acquisition space. The cameras may be based on various types of technology, necessitating a variety of experimental setups. Markers are typically used to reconstruct kinematics [1-3,7], which can be both active and passive. The most common are passive markers, that combine ease of use and low cost with high operational reliability. The position of the markers in space allows for the reconstruction of the body, resulting in the so-called stick diagram, and they are recognized as clear spots on a homogeneous background.
The position and number of markers must adhere to specific protocols in order to ensure a standardized description of the movement, and they are heavily dependent on the type of movement to be analyzed.

The studies reported in this thesis were carried out mainly using the system SMART DX Motion Capture system, BTS, Milan, whose components are shown in Figure 3.3.
This system allowed for the acquisition of synchronized and integrated kinematic, kinetic, sEMG, and video signals.

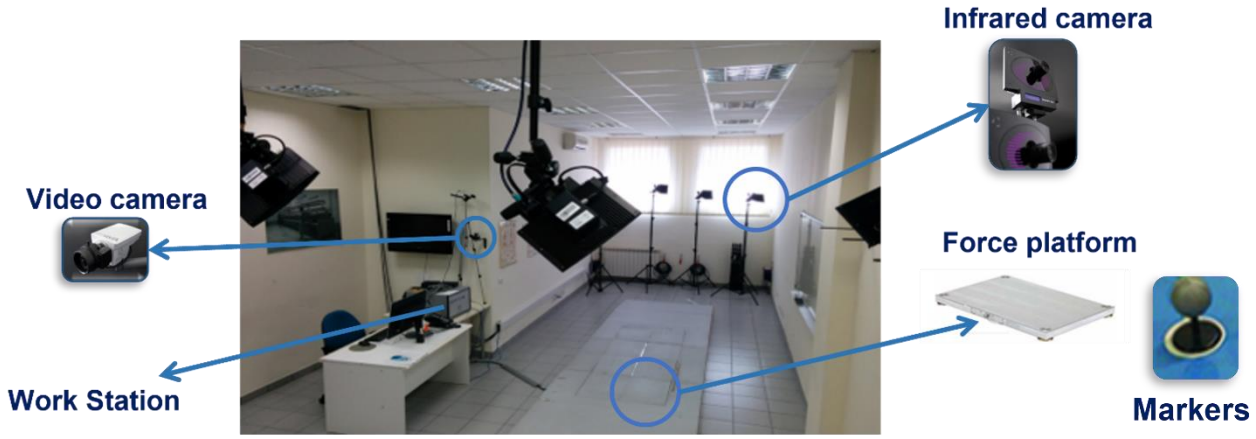

Figure 3.3 *Components of SMART system.*

The Davis protocol [8] is the most commonly used marker positioning protocol in gait analysis; developed in 1991 at the NCH (Newington Children 's Hospital, USA) [6], this protocol uses 22 passive markers (Figure 3.4), which represent the minimum set-up required for the 3D description of the gait. The kinematics of the trunk and lower limbs are defined by the Davis protocol; in fact, the 22 passive markers are arranged at the landmarks of these body segments, as shown in the table / figure.

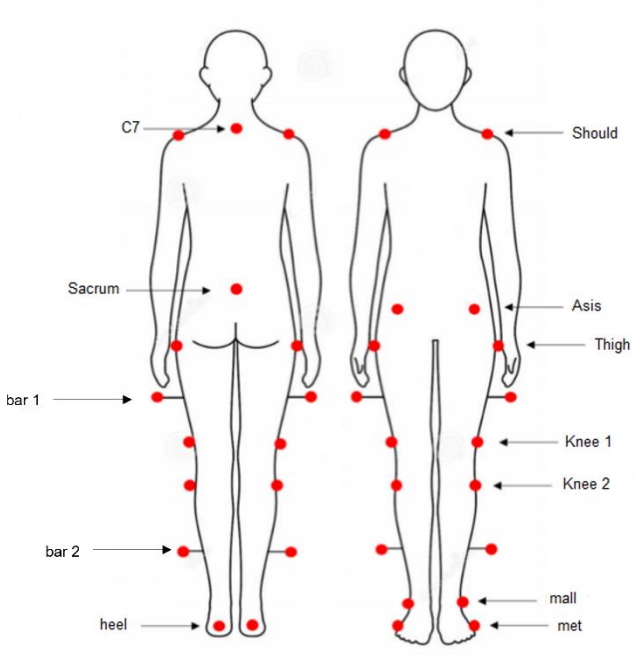

Figure 3.4 *Kinematic Davis model*

Sticks or wands varying in length from 7 to 10 cm and placed at 1/3 of the length of the body segment were used in addition to markers directly applied to the skin. A wand on the femur and a leg were used in particular, so that the plane containing the three points was parallel to the frontal plane. In some studies reported in this thesis , we used a modified version of the Davis protocol by adding the elbow and wrists as well. Anthropometric measurements were collected for each subject in order to determine the joint offset angles; these included the subject's mass and height, as well as the length of the main segments of the body as described by Winter [1]: height, weight, length of the subject's shank, diameter of the knee, diameter of the ankle, distance between the anterior iliac crests, and pelvic thickness.

Multiple cameras are required for the acquisition of movement in a three-dimensional space, and in a motion analysis laboratory 6-12 cameras are typically used for the complete capture of the movements.

The cameras are equipped with an infrared illuminator, which is typically made up of a series of LEDs, as well as a camera sensor, which is typically a CCD sensor; the capture volume is illuminated with infrared light, which is reflected by the markers and captured by the cameras [1]. The active infrared lights form a ring around the chamber's lens and are pulsed at 120 Hz for less than a millisecond. Because the light is pulsed, the images of the markers are captured at very precise times.

The sequence of images will allow us to reconstruct the trajectory of each marker and therefore of the body segments.
It is necessary to define the reference system and the protocol on which the markers are positioned in order to provide an accurate and complete description of the kinematics.
Before each acquisition, the space is calibrated using a two-step procedure. To begin, a triad of axes equipped with markers at a defined and known distance is positioned in a point of the capture space for the definition of the global reference system. The capture volume is then calibrated using a wand moved by an operator.

Static acquisitions must be performed, as well as dynamic acquisitions, to record the individual recordings of the twenty-two reference points required for the protocol's construction, while dynamics acquisitions are required to record some samples of the subject's gait.

3.2.1.2 Kinetics

The kinetics was investigated by analyzing the ground reaction forces recorded at 1200 Hz by means of two force platforms (0.6 x 0.4 m; Kistler 9286B, Winterthur, Switzerland), placed at the center of the walkway, attached to each other in the longitudinal direction but displaced by 0.2 m in the lateral direction (Figure 3.5).

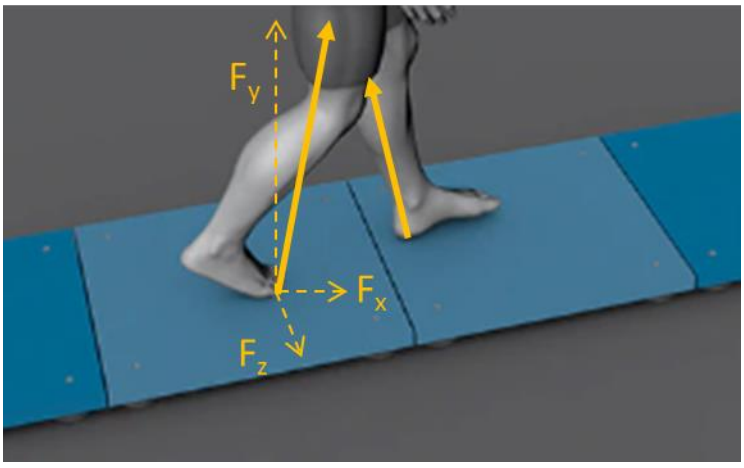

Figure 3.5 *Force platforms and ground reaction force with the three components in space*

The force platforms are made up of four load cells, each of which is placed in one of the platform's four angles. They are made up of three force transducers, each idealized and designed to detect only one of the three components of force or moment. Force transducers use sensors to convert applied force into deformation, which results in an electrical signal output. The ground reaction resultant is measured by the force platforms at the time of the subject's impact.

The forces were examined in the three components F_x, F_y, F_z along the anterior-posterior, medio-lateral, and vertical directions.
The measured forces, combined with the kinematic analysis, allowed the researchers to investigate the moments at the hip, knee, and ankle articulations.

3.2.1.3 Surface electromyography (sEMG)

The surface electromyography analyzed in some studies reported in this thesis was recorded at 1000 Hz using a 16-channel wireless system (FreeEMG1000 System; BTS, Milan, Italy); to record EMG activity from body muscles, bipolar Ag-AgCl surface electrodes (H124SG, Kendall ARBO, Donau, Germany) (Figure 3.6) were prepared with electro-conductive gel (diameter 1 cm, distance between electrodes 2 cm) and placed over the muscle belly in the direction of the muscle fibers.

Figure 3.6 *Bipolar Ag-AgCl surface electrodes.*

A critical aspect of the surface electromyography technique is the proper placement of the electrodes. The sEMG signal allows information about skeletal muscle activity to be extracted, but this information may be incorrect if electrodes are placed near the innervation zone (IZ) or tendon regions, which have a strong influence on sEMG amplitude and frequency. We were able to locate the innervation zone using SENIAM guidelines (European Recommendations for Surface Electromyography) [9,10], improving the correct placement of sEMG electrodes and the quality of the electromyographic signal acquired.

Data acquisition from the integrated surface EMG system, optoelectronic system and force platforms were integrated and synchronized.

3.2.2 Inertial wearable sensors

Wearable sensors are increasingly being used in clinical settings to obtain more objective measures of walking performance [11-16].

Based on the inverted pendulum gait model [17], mobile inertial measurement units (IMU) with accelerometers, gyroscopes and magnetometers can objectively capture the ability to control the body center of mass while moving the base of support, resulting in an effective tool to monitor dynamic balance during gait [13,18]. Ideally, using several combined IMUs to analyze a subject's gait would improve overall accuracy, but this benefit would be offset by the wearability burden. A single lumbar-mounted IMU, on the other hand, provides sensitive information on gait and allows clinicians to monitor it even in free-living conditions [19]. IMUs directly provide trunk acceleration measurements and make it easier to record patient gaits for many steps during follow-up clinical assessments in outpatient facilities, making them ideal tools for studying gait stability.

The G-Walk (BTS, Milan, Italy) was used in the studies reported in this thesis. It consists of an inertial sensor G-SENSOR, the G-Studio software and a set of protocols for the analysis of the specific movements. It represents indeed one of the best solutions for fast and objective assessment of the walking, running and jumping parameters. Thanks to a Bluetooth connection, the sensor acquires and transmits the data to the PC to process and automatically create the report. The other components of the G-WALK are:

- Belt with pocket for the sensor positioning;
- Up to 2 webcam for video recording;
- Bluetooth dongle;
- Bluetooth extension cable;
- USB Charge cable;

The G-SENSOR (Figure 3.7) is a wearable device housed in a specialized belt that allows the patient to walk, run, and jump completely free. It is made up of a triaxial accelerometer, a magnetic sensor, and a triaxial gyroscope that is mounted on the L5 vertebrae and allows for functional gait analysis.

Figure 3.7 *Wearable device G-Sensor*

G-Studio (Figure 3.8) is an easy-to-use software that allows for the easy management of patient databases, the organization of system acquisitions, and the creation of extensive analytical reports.

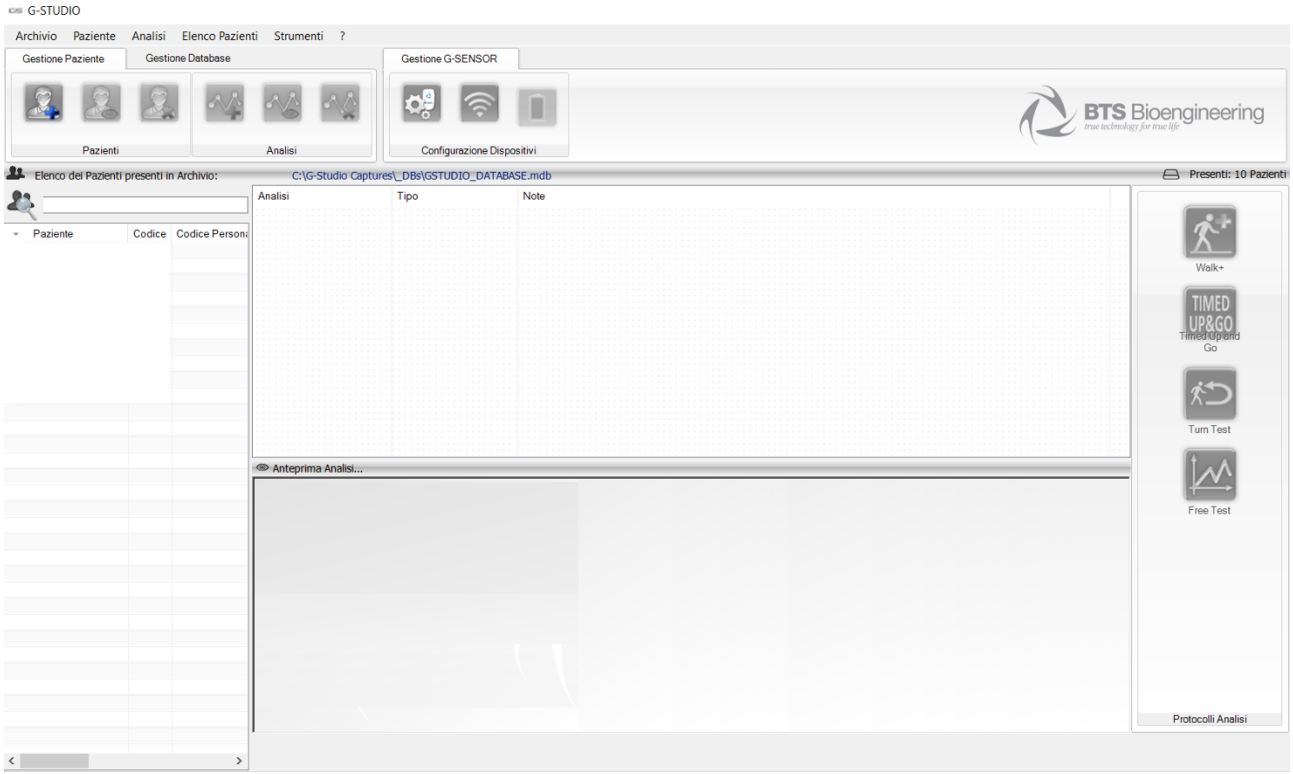

Figure 3.8 *G-Studio software screen*

After processing the data, the software generates a report (Figure 3.9) that includes the parameters calculated during the test. It is also possible to extract raw accelerometer and gyroscope data in all three spatial directions.

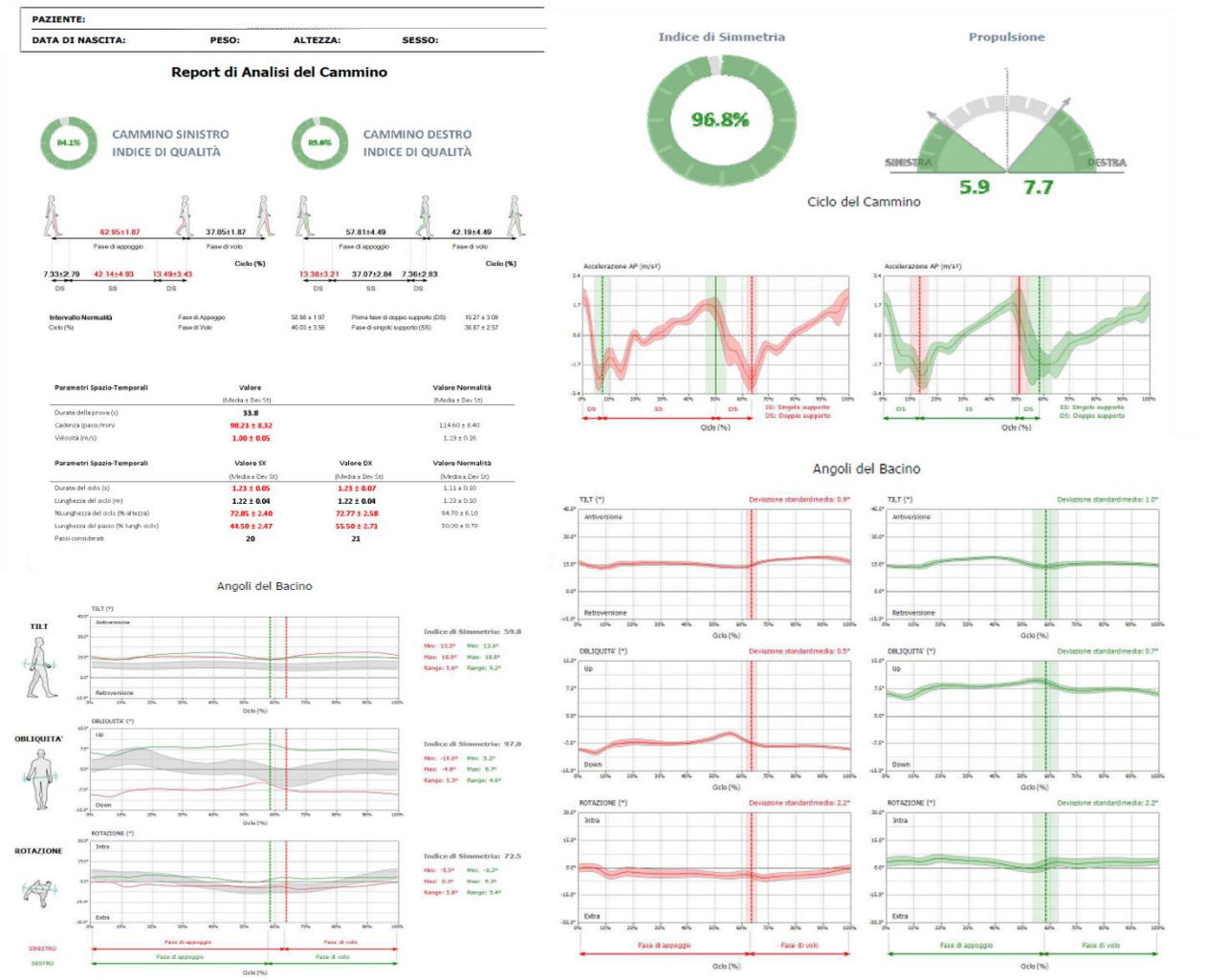

Figure 3.9 *An example of a report generated with gait analysis results*

3.2.3 MATLAB

Matlab is a high-level programming language for scientific and engineering computing, as well as a tool for matrix manipulation, signal processing, data classification, and graphical visualization, among other things. It was used for algorithm implementation, graphical visualization, and data classification in many processing sections of the studies described in this thesis.

3.3 Data analysis

To process data recorded by stereo-photogrammetric system, a reconstruction of the tridimensional position of each marker from the images of each camera was required (Figure 3.10). This procedure was carried out using the SMART Software Tracker (BTS, Milan, Italy), and it consists of matching the individual points of the Davis model to the marker represented in the file acquisition by labeling each marker (labeling). The first stage of data processing was the tracking operation, which

represented the logical connection of two successive frames in order to identify the time curve of each single marker. Thus, the kinematic speed and acceleration were deduced from the trajectories of the markers. In this step, force signals from the platform can be labeled. These signals are displayed as a vector with the origin in the center of pressure and magnitude and direction equal to the vector sum of the three components of force.

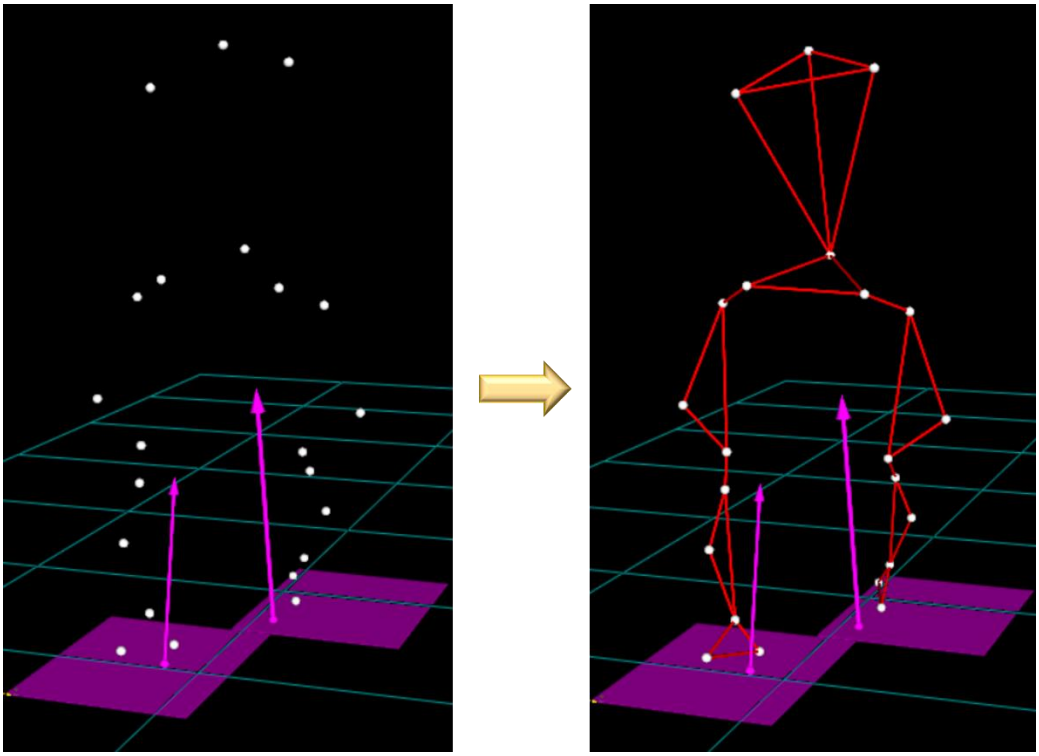

Figure 3.10 *Reconstruction of the 3D position of each marker according to Davis model (left) and tracking procedure (right).*

Following the tracking procedure, the data was processed using 3D reconstruction software (SMART Analyzer, BTS, Milan, Italy) and protocols that calculated all biomechanical parameters of interest, such as the relative angles between two body segments, speeds, distances, forces, and moments acting on the joints. During this phase, a temporal analysis of the signals was performed in order to manually define events in the gait cycle. The trajectories of the foot markers were used to correctly identify the instants of support and toe-off.

3.3.1 Gait events estimation

Gait is defined by a cyclic pattern of motor activity in the lower limbs and trunk that allows weight to be transferred to the limb support and forward movement against the limb-side. The gait cycle, which is defined as the time between two consecutive foot contacts of the same leg, is the functional unit of reference for gait analysis.

In the studies described in this thesis, heel strike (HS) was determined as the minimum point of the heel trajectory while the toe-off (TO) was determined by the metatarsal trajectory (Figure 3.11). When subjects step onto the force platforms, these kinematic criteria can be verified using information from the force platforms' signals.

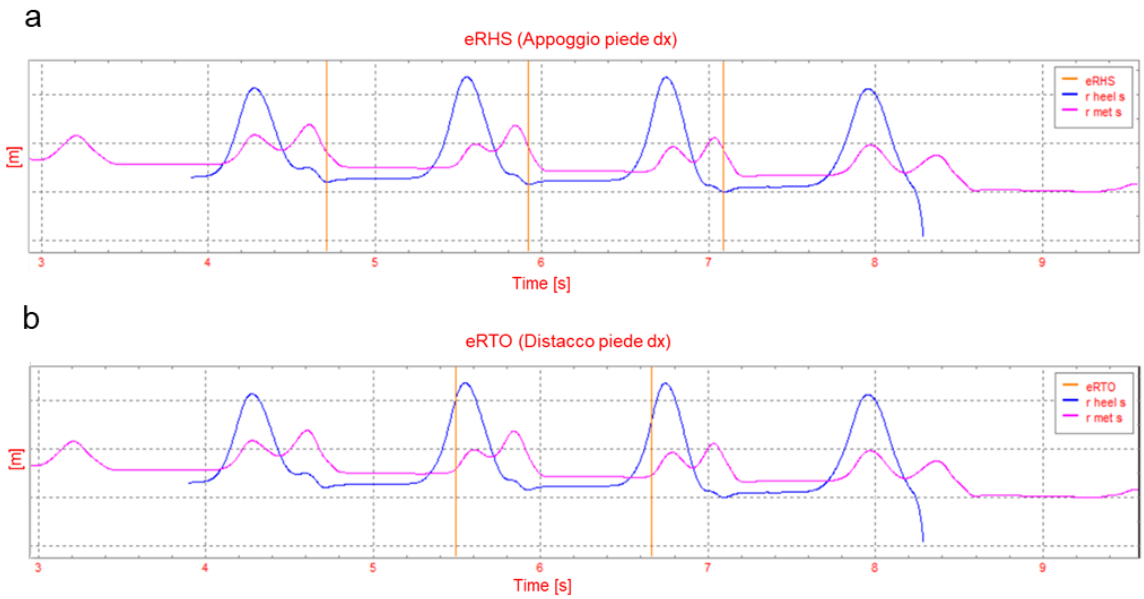

Figure 3.11 *Definition of the instants of heel strike (a) and toe-off (b).*

Normally, two major phases of a gait cycle are distinguished (Figure 3.12): the *stance phase* (from first contact to foot-off) and the *swing phase* (from foot-off to the successive initial contact). Finally, three subphases were considered within the stance phase:

- *initial double support* (first double support): both feet are in contact with the ground;
- *single support*: the reference foot is in contact with the ground while the counter-side swings;
- *terminal double support* (second double support): both feet are in contact with the ground again.

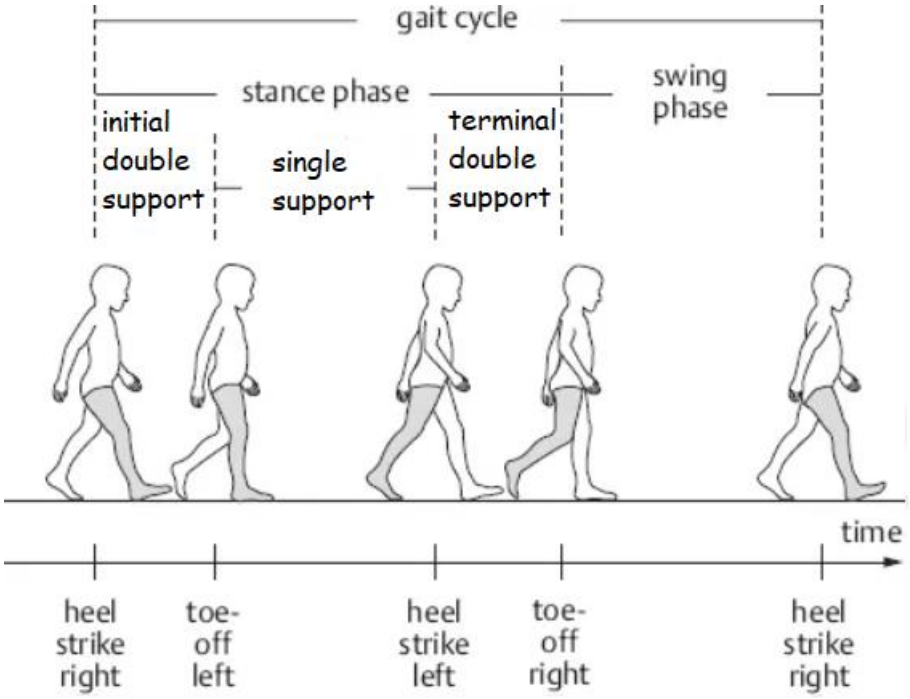

Figure 3.12 *Normal gait cycle*

3.3.2 Time-distance parameters

The most important time-distance gait parameters are listed in Table 3.1.

Table 3.1 *General time-distance parameters*

Gait parameters	
Walking speed (m/s)	
Cycle duration (s)	Time interval between two successive initial contact of the same foot
Cycle length (m)	Distance between two successive supports of the same foot
Step length (m)	Distance between the heel of one foot and the heel of the contralateral foot
Step width (m)	Mediolateral distance between the feet
Stance duration (s)	The entire period during which the foot is in contact with the ground
Swing duration (s)	The entire period during which the foot is not in contact with the ground
1st double support duration (s)	Time in which both feet are in contact with the ground after the initial contact
2st double support duration (s)	Time in which both feet are in contact with the ground after single standby
Cadence (steps/min)	Number of steps in the time unit

3.3.2.1 Speed matching procedure

To compare data between healthy subjects and patients, we used a matching procedure based on speed in our studies. In fact, because many spatio-temporal parameters are dependent on gait speed, to collect the largest possible sample size for speed-matched comparisons, the healthy subjects were also asked to walk at a slower speed [20-25]. The speed matching procedure was performed as follows: for each healthy subject, we considered only those trials in which gait speed fell within the range identified by patients mean gait speed ± standard deviation. In one of the studies 1:1 optimal matching procedure using propensity scores method was used. Propensity scores were calculated through logistic regression analysis using age and speed as covariates [26,27].

3.3.3 Kinematic data

The frontal, sagittal, and transverse plane anatomical and joint angles for the hip, knee, ankle, trunk, and pelvis were computed. The joint range of motion (RoM) was calculated based on these variables as the difference between the maximum and minimum values during the gait cycle.

3.3.3.1 Energy consumption measurement

The mechanical behavior was measured in terms of energy recovery and consumption in relation to the whole-body center of mass (CoM) and provides information on mechanical energy expenditure involving the entire skeletal muscle system while walking. the kinetic energy (Ek) associated with CoM displacements was calculated as the sum of kinetic energy on the x (Ek_x), y (Ek_y), and z (Ek_z) axes:

$$E_k = E_{kx} + E_{ky} + E_{kz} = \frac{1}{2}m(v_x^2 + v_y^2 + v_z^2)$$

where m and v_x, v_y, and v_z are the mass and velocity components of the CoM, respectively. Furthermore, the potential energy (Ep) associated with the CoM was calculated as

$$E_p = mgh$$

where h is the vertical component of the CoM, and g is the acceleration of gravity (m/s^2). The sum of E_k and E_p was used to calculate the total mechanical energy (E_{tot}) associated with the CoM. The fraction of mechanical energy (R-step) recovered during each walking step was calculated as follows [28]:

$$R_{step} = \frac{W_p^+ + W_{kf}^+ - W_{tot}^+}{W_p^+ + W_{kf}^+} x100 = \left(1 - \frac{W_{tot}^+}{W_p^+ + W_{kf}^+}\right) x100$$

where W_p^+, W_{kf}^+, and W_{tot}^+ represent the positive work produced by gravitational potential energy, forward motion kinetic energy, and total mechanical energy, respectively. The total energy consumption (TEC) was then calculated as the sum of the negative (W_{tot}) and positive work (W_{tot}^+), each divided by their respective efficiencies [29], as follows:

$$TEC = \frac{W_{tot}^+}{1.20} + \frac{W_{tot}^-}{0.25}$$

Because walking is cyclical, the positive work done at each step equals the negative work, changing the previous formula to

$$TEC = \frac{W_{tot}^+}{0.21}$$

For each subject, the R-step and TEC values were normalized to the body weight and step length, respectively, and were averaged.

3.3.4 Kinetic data

We considered the vertical component along the y-axis of the ground reaction force recorded by the force platforms normalized with respect to the subject's weight [30] in the studies reported in this thesis. With this parameter, we analyzed the subject's behavior in terms of the force it exchanges with the ground. Furthermore, we considered the force data when only one foot is exactly inside the platform (Figure 3.13).

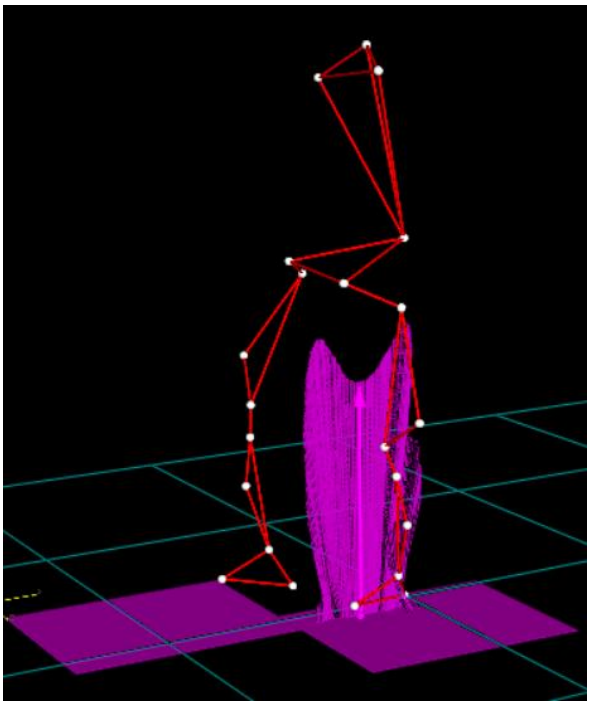

Figure 3.13 *Three-dimensional representation of the data recorded by the force platform*

Kinetic data, in conjunction with kinematic analysis, allow for the investigation of the internal moments of the hip, knee, and ankle, as well as the support moment.

3.3.5 Electromyographic parameter: muscle co-activation

The recorded raw sEMG signals were band-pass filtered (3rd order Butterworth filter at 30–450 Hz), rectified, and low-pass filtered (zero-lag 4th order Butterworth filter at 10 Hz).

Muscle co-activation is the mechanism that regulates simultaneous activity of agonist and antagonist muscles crossing the same joint [31]and it has been shown to be important for ensuring adequate spine and joint stability, movement accuracy (as in precision tasks), and energy efficiency [32,33], as well as adapting to environmental demands [34].

When significant antagonist activations counteract the agonist actions, resulting in moments that do not contribute to the required net joint moments, co-activation may become functionally unfavorable, if not harmful. It may, in fact, be a factor that contributes to the inefficiency of human movement by increasing the physiological and metabolic cost, lowering net moment and power development. Excessive muscle co-activation also increases compressive loading across the joint, which can lead to cartilage loss. [34-37].

For an accurate determination of muscle co-activation during functional movements, robust measurement techniques are required [38].

To quantify muscle co-activation, several computational approaches have been used: ratio, overlapping, or cross-sectional areas of simultaneous activation of opposite muscles [39]. These mathematical tools are based on an agonist–antagonist approach to EMG signals recorded from two antagonist muscles or from two antagonist muscles in the same joint. The results of these tools are expressed in terms of the time of overlapping between the linear envelopes of two opposing muscles as well as the magnitude of muscle co-activation [40,41].

Furthermore, Ranavolo et al. 2015 [42] proposed a method based on the time-varying multi-muscle co-activation function (TMCf), which may enable understanding of the global strategy achieved by the CNS in modulating the activation/deactivation of many lower limb muscles during gait, irrespective of both the agonist antagonist interaction at a single-joint level [23] and the modular architecture [43]. The TMCf is calculated as follow:

$$TMCf(d(i),i) = \left(1 - \frac{1}{1 + e^{-12(d(i)-0.5)}}\right) \cdot \frac{\left(\sum_1^M m\, EMG_m(i)/M\right)^2}{max_{m=1\ldots M}[EMG_m(i)]}$$

where M is the number of muscles considered, $EMG_m(i)$ is the sEMG sample value of the m_{th} muscle at instant i, d(i) is the mean of the differences between each pair among the twelve $EMG_m(i)$ samples at instant i:

$$d(i) = \left(\frac{\sum_1^{M-1} m \sum_{m+1}^{M} n \ \left| EMG_m(i) - EMG_n(i) \right|}{\left(\frac{M!}{2!\,(M-2)!}\right)} \right)$$

where M!/(2!(M-2)!) is the total number of possible differences between each pair of $EMG_m(i)$. Next, starting from TMCf, we calculated synthetic indices for each condition, among which the coactivation index (CI) as the mean value of the TMCf [42]:

$$CI = \sum_{i=1}^{201} \frac{TMCf(d(i),i)}{201}$$

Other parameters are:

- the Full Width at Half Maximum (FWHM) which characterize the TMCf curves in terms of time amplitude. The FWHM is calculated as the sum of the durations of the intervals Δt_j in which the TMCf curve exceeded half of its maximum [44]:

$$FWHM = \sum_j \Delta t_j$$

- the Center of Activity (CoA) which determine where the majority of coactivation occurs during the gait cycle [45]. It is calculated by combining Labini's [46] formula with the circular transformation, yielding the following expression:

$$coa = tan^{-1}\left(\frac{\sum_0^{201} i\ EMG_i * sin\vartheta_i}{\sum_0^{201} i\ EMG_i * \cos\vartheta_i}\right)$$

- the Coefficient of Multiple Correlation (CMC) which expresses the waveforms similarity, and it is calculated as [47,48] :

$$CMC = \sqrt{1 - \frac{(1/\ (\mathrm{T}\ (\mathrm{N} - 1)))\sum_1^N i \sum_1^T t\ (y_{it} - \bar{y}_t)^2}{(1/\ (\mathrm{T}\ \mathrm{N} - 1))\sum_1^N i \sum_1^T t\ (y_{it} - \bar{y})^2}}$$

- Deviation Phase (DP) is calculated by averaging the standard deviations of the ensemble TMCf curves for each group using the following equation [47]:

$$DP = \frac{\sum_{i=1}^p SD_i}{p}$$

where p is the number of time points.

All measurement techniques are susceptible to error, which can reduce validity and reliability while also complicating interpretation of the results. Several factors in the sEMG measurement process, such as signal acquisition and signal analysis procedures, may influence the establishment of representative envelope profiles and, as a result, the outcome of co-activation evaluated from the signal envelope. An important consideration is the variation of the signal-to-noise ratio (SNR) level: the sensitivity of the algorithm's performance may change as the SNR level varies [49].
Muscle joint coactivation varies throughout the gait cycle, depending on the functional role of the lower limb joints along gait phases, reaching higher values during weight acceptance and transition from stance to swing subphases [34] and lower values during mid-stance [50]. Other factors that influence the muscle coactivation during locomotion are age [51], speed, and motor context, i.e., stable vs. unstable conditions [52].

3.3.6 Wearable sensors parameters

The “Walk+” protocol of the G-STUDIO software (G-STUDIO, BTS, Milan, Italy) was used to detect trunk acceleration patterns, right and left heel strikes, toe-off, spatiotemporal parameters, and pelvis kinematics (Table 3.2).

Table 3.2 *Spatio-temporal and kinematic parameters recorded by the sensor*

Spatio-temporal parameters	***Pelvic kinematics***
Analysis duration (s)	TILT: pelvic movement along the sagittal plane
Cadence (steps/min)	
Gait cycle duration (s)	
Stride length (m)	
% Stride length (%height)	OBLIQUITY: pelvic movement along the frontal plane
Step length (%str. length)	
Stance phase (%cycle)	
Swing phase (%cycle)	ROTATION: pelvic movement along the transversal plane
Double support phase (%cycle)	
Single support phase (%cycle)	
Elaborated steps	

3.3.7 Trunk acceleration-derived indices

We calculated the following indices from raw trunk acceleration data:

1. Harmonic Ratio (HR) and Improved Harmonic Ratio (iHR):

The Harmonic Ratio is an index that expresses the smoothness and rhythmicity of trunk acceleration patterns. The calculation of HR for continuous walking trials is based on a stride (two steps) [53]. Acceleration signals in AP and VT axes are characterized by the even harmonics, as trunk movements in these directions are biphasic for any given stride. In contrast, ML accelerations are characterized by the odd harmonics, as the ML movement is limb-dependent and only repeated once for any give stride. Therefore, using the first twenty harmonic amplitudes derived from the discrete Fourier transform of trunk accelerations, the HR for AP and VT accelerations is calculated by dividing the sum of the even harmonics by the sum of the odd harmonics while for ML accelerations, the HR is calculated by dividing the sum of the odd harmonics by the sum of the even harmonics. A forth order low-pass Butterworth filter with a 20 Hz cutoff was used to eliminate noise signals and the HR values were calculated as follows [54]:

$$HR_{AP,VT} = \frac{\sum_i A_{i*2}}{\sum_i A_{i*2-1}}$$

$$HR_{ML} = \frac{\sum_i A_{i*2-1}}{\sum_i A_{i*2}}$$

where Ai represents the amplitudes of the first 20 even harmonics and A2i−1 represents the amplitudes of the first 20 odd harmonics. A greater HR represents a more stable walking pattern [55,56]. The index definition was then modified to overcome its large variability in highly symmetrical gait due to the small contribution of the extrinsic harmonics (at the denominator), its unintuitive interpretation and its lack of mathematical rigor. An improved Harmonic Ratio was therefore defined as the ratio between the power (P) of the considered k intrinsic harmonics over the total power of the signal, thus obtaining a normalized index, ranging from 0 (total asymmetry) to 100 (total symmetry) [57] :

$$iHR_k = \frac{\sum_{j=1}^{k} P_I^j}{\sum_{j=1}^{k}(P_I^j + P_E^j)} * 100 = \frac{\sum_{j=1}^{k}(A_I^j)^2}{\sum_{j=1}^{k}(A_I^j)^2 + \sum_{j=1}^{k}(A_E^j)^2} * 100$$

2. Coefficient of Variation (CV)

To compute the Coefficient of Variation, the step length was estimated by using the inverted pendulum model, in which the body's center of mass (CoM) movements in the sagittal plane follow a circular trajectory during each single-support phase and its height changes depend on the step length [58]. Therefore, the step length is calculated as follows:

$$step\ length = 2\sqrt{2lh - h^2}$$

where h is the height of the CoM and l represents the pendulum length. A double integration of the vertical acceleration was implemented to calculate changes in the vertical position. A fourth-order zero-lag Butterworth high-pass filter, with cutoff frequency of 20 Hz, was used to avoid integration drift. The amplitude of the changes in the vertical position [59] was calculated as the difference between the highest and lowest positions during a step cycle. The leg length was considered to be the pendulum length (l). The step length CV was computed as follows:

$$CV = \frac{SD}{mean} * 100$$

where mean is the mean step length and SD is the standard deviation over all step lengths for each subject [60]. The higher the CV, the higher the variability in step length.

3. Normalized Jerk Score (NJS)

The Normalized Jerk Score measures the time-normalized rate of change in the acceleration signals during stepping [61,62]. The acceleration data were first low pass filtered using a fourth-order zero-lag Butterworth filter with a cutoff frequency of 20 Hz. We then calculated the NJS from the time duration between each foot contact as follows [62]:

$$NJS = \frac{1}{N}\sum_{i=1}^{N}\sqrt{\frac{(hs_{i+1} - hs_i)^5}{2}}\int_{hs_i}^{hs_{i+1}}(a)^2 dt$$

where hsi is the time of the ith heel strike and a is the acceleration. The next step consists of low pass filtering of the NJS using a fourth-order zero-lag Butterworth filter with a cutoff frequency of 5 Hz [61]. A high index value indicates a smoother gait.

4. Log Dimensionless Jerk (LDJ)

The log dimensionless jerk is an acceleration-based parameter examining the rate of change of movement acceleration and it results from the logarithm naturalis of the sum of the squared acceleration multiplied with the trial duration to the power of three and divided by the squared peak velocity [63]:

$$LDJ \triangleq -\ln\left(\frac{t^2 - t^1}{v_{peak}^2}\int_{t_1}^{t_2}\left|\frac{d^2v}{dt^2}\right| dt\right)$$

An index value closer to zero represent smoother movements.

5. Recurrence Quantification Analysis (RQA)

The Recurrence Quantification Analysis can provide useful information regarding the pattern and structure of system dynamics even for short duration and non-stationary data [64] . As already shown by Poincaré in 1890, recurrence is one of the fundamental features of dynamical systems and can be used to characterize the specifc behaviour of a system in phase space, including the quantification of deterministic structures and non-stationarity, based on the construction of recurrence plots [65]. A detailed description of RQA calculation was provided by Webber et al. (1994) [66]. Acceleration and angular velocity data are embedded in “m” dimensions using “m” copies of the original time series, where each copy is shifted in time by integer multiples of “τ” samples. The embedding dimension “m” is the first recurrence parameter estimated using the nearest-neighbor method [67], which compares the distances between neighboring trajectories at successively higher dimensions. “False neighbors” occur when trajectories that overlap in dimension m_i are distinguished in dimension m_{i+1}

. As i increases, the total percentage of false neighbors decrease, and m is chosen where this percentage approaches 0. False neighbors analysis was performed using values of R_{tol} = 17 and A_{tol} = 2 [68,69]. We considered a maximum embedding dimension of 10, and m = 5 was considered as the optimal embedding dimension. "τ" represents the second recurrence parameter selected to minimize the interaction between the points in the measured time series. Two methods can be used to determine the appropriate delay, namely find the first minimum in either the (linear) autocorrelation function or (nonlinear) mutual information function of the continuous time series. τ was calculated from the first minimum of the average mutual information (AMI) function [70], which evaluates the shared amount of information in bits between two data sets over a range of time delays. By choosing the first minimum of the AMI function, adjacent delay coordinates with a minimum of redundancy are provided. The time delay computed by the first minimum of the AMI considered as optimal was 10 samples [66,69]. A distance matrix is then computed by calculating the Euclidean distances between all embedded vectors. A recurrence matrix is computed by selecting a threshold (radius) of 10% of the maximum distance, where all cells with values below this threshold are identified as recurrent points. RQA variables are used to quantify the structure of the recurrence matrix. Percent recurrence (RQA_{rec}) can be calculated to understand how often a trajectory visits similar locations in the state space and it is computed as the percentage of recurrent points in the recurrence matrix. Percent determinism (RQA_{det}) can be calculated to understand how often a trajectory repeatedly revisits similar state space locations and it is quantified as the percentage of recurrent points in the diagonal line structures (at least four consecutive points in length) parallel to the main diagonal. Therefore, RQA_{rec} quantifies the number of potentially recurrent points, where only a portion of these points recur periodically and are related to the predictability of the target dynamical system. The higher the RQA_{rec} and RQA_{det} values, the higher the predictability of the system [64].

6. Largest Lyapunov Exponent (LLE)

The Largest Lyapunov exponent measures gait stability by calculating the average logarithmic rate of divergence after infinitesimal perturbations. An LLE less than zero represents the system's rate of convergence to its nearest neighboring trajectory, whereas an LLE greater than zero represents the rate of divergence. When trajectories converge, the observed system is said to be local dynamically stable, whereas divergence indicates local dynamically unstable. In our study, the LLE was estimated using the method described by Van Schooten et al [71]. To avoid the loss of spatiotemporal fluctuations and nonlinearities, no filtering was applied to the triaxial accelerations, and the accelerations were time-normalized to obtain 100 data points per stride, excluding the effects of data

series time duration on dynamic stability measures. For each triaxial trunk acceleration over the strides considered in each trial, local dynamic stability was calculated. Based on the AP, ML, and VT trunk accelerations, we calculated the short-term maximum finite-time LE (lmax) for each stride. Using the Lyaprosen MATLAB toolbox for nonlinear time series analysis, the value of lmax was determined using Rosenstein's algorithm for short time series. To evaluate dynamic perturbations, a multidimensional state space whose dimensions were determined using the classical global false-nearest-neighbor method was reconstructed from the recorded one-dimensional time series data by juxtaposing the original data and delayed copies (the time delay was determined using the first minimum of the average mutual information function) [72]. This index's low values indicate more stable trunk dynamics, while high values indicate less stable trunk dynamics.

7. Root Mean Square (RMS)

The root mean square of acceleration represents a statistical measure of the magnitude of the trunk acceleration in each direction. It was calculated as follows:

$$RMS = \sqrt{\frac{\sum_{i=1}^{n} a_i^2}{n}}$$

Where a_i is the acceleration measured at the i-th sampled value and n is the length of the acceleration vector.

The RMSR represents the ratio between the RMS in each direction and the RMS vector magnitude (RMS_T) and was calculated using the following equations [73]:

$$RMS_T = \sqrt{RMS_{AP}^2 + RMS_{ML}^2 + RMS_V^2}$$

$$RMSR_k = \frac{RMS_k}{RMS_T}$$

Bibliography

[1]. Winter D. A.. 2009. Biomechanics and motor control of human movement, Fourth Edition, John Wiley & Sons.

[2]. Ceseracciu E, Sawacha Z, Cobelli C. 2014. Comparison of Markerless and Marker-Based Motion Capture Technologies through Simultaneous Data Collection during Gait: Proof of Concept. PLoS One., 4;9(3):e87640.

[3]. Leardini A, Chiari L, Della Croce U, Cappozzo A. 2005. Human movement analsysis using stereophotogrammetry Part 3. Soft tissue artifact assessment and compensation, Gait Posture, 21(2):212-25.

[4]. Contini R, Drillis R.J, Bluestein M. 1963. Determination of Body Segment Parameters. Human Factors The Journal of the Human Factors and Ergonomics Society, 5(5):493-504

[5]. Bannier P, Jin H, Goodrum P. Modeling of work envelope requirements in the piping and steel trades and the influence of global anthropomorphic characteristics. 2016. Electronic Journal of Information Technology in Construction, 21:292-314

[6]. Whittle M. W. 2007. Gait Analisys An Introduction, Fourth Edition, Elsevier.

[7]. Della Croce U, Leardini A, Chiari L, Cappozzo A. 2005. Human movement analysis using stereophotogrammetry part 4: assessment of anatomical landmark misplacement and its effects on joint kinematics. Gait Posture, 21(2):226-37.

[8]. Davis R. B, Ounpuu S, Tyburski D, Gage J. R. 1991. A gait analysis data collection and reduction technique, Human movement Science, 10: 575-587.

[9]. Barbero M, Merletti R, Rainoldi A. Atlas of Muscle Innervation Zones; Springer: Milan, Italy, 2012.

[10]. Hermens HJ, Freriks B, Disselhorst-Klug C, Rau G. 2000. Development of recommendations for SEMG sensors and sensor placement procedures, 10(5):361-74.

[11]. Zampogna A, Mileti I, Palermo E, Celletti C, Paoloni M, Manoni A, Mazzetta I, Costa G.D, Pérez-López C, Camerota F, et al. 2020. Fifteen years of wireless sensors for balance assessment in neurological disorders. Sensors, 20, 3247.

[12]. Brognara L, Palumbo P, Grimm B, Palmerini L. 2019. Assessing Gait in Parkinson's Disease UsingWearable Motion Sensors: A Systematic Review. Diseases, 7, 18.

[13]. Schlachetzki J.C.M, Barth J, Marxreiter F, Gossler J, Kohl Z, Reinfelder S, Gassner H, Aminian K, Eskofier B.M, Winkler J, et al. 2017. Wearable sensors objectively measure gait parameters in Parkinson's disease. PLoS ONE, 12, e0183989.

[14]. Rovini E, Maremmani C, Cavallo F. 2017. How wearable sensors can support parkinson's disease diagnosis and treatment: A systematic review. Front. Neurosci., 11, 555.

[15]. Maetzler W, Domingos J, Srulijes K, Ferreira J.J, Bloem B.R. 2013. Quantitative wearable sensors for objective assessment of Parkinson's disease. Mov. Disord., 28, 1628–1637.

[16]. Ramdhani R.A, Khojandi A, Shylo O, Kopell B.H. 2018. Optimizing clinical assessments in Parkinson's disease through the use of wearable sensors and data driven modeling. Front. Comput. Neurosci., 12, 72.

[17]. Kuo A.D, Donelan J.M. 2010. Dynamic principles of gait and their clinical implications. Phys. Ther., 90, 157–174.

[18]. Horak F.B, Mancini M. 2013. Objective biomarkers of balance and gait for Parkinson's disease using body-worn sensors. Mov. Disord., 28, 1544–1551.

[19]. Czech M, Demanuele C, Erb M.K, Ramos V, Zhang H, Ho B, Patel S. 2020. The impact of reducing the number of wearable devices on measuring gait in parkinson disease: Noninterventional exploratory study. JMIR Rehabil. Assist. Technol., 7.

[20]. Morris M.E, Iansek R, Matyas T.A, Summers J.J. 1994. The pathogenesis of gait hypokinesia in parkinson's disease. Brain, 117:1169–1181.

[21]. Serrao M, Chini G, Caramanico G, Bartolo M, Castiglia S.F, Ranavolo A, Conte C, Venditto T, Coppola G, Di Lorenzo C, et al. 2019. Prediction of responsiveness of gait variables to rehabilitation training in Parkinson's disease. Front. Neurol., 10, 826.

[22]. Rinaldi M, Ranavolo A, Conforto S, Martino G, Draicchio F, Conte C, Varrecchia T, Bini F, Casali C, Pierelli F, et al. 2017. Increased lower limb muscle coactivation reduces gait performance and increases metabolic cost in patients with hereditary spastic paraparesis. Clin. Biomech., 48:63–72.

[23]. Mari S, Serrao M, Casali C, Conte C, Martino G, Ranavolo A, Coppola G, Draicchio F, Padua L, Sandrini G, et al. 2014. Lower limb antagonist muscle co-activation and its relationship with gait parameters in cerebellar ataxia. Cerebellum, 13: 226–236.

[24]. Cofré L.E, Lythgo N, Morgan D, Galea M.P. 2011. Aging modifies joint power and work when gait speeds are matched. Gait Posture, 33:484–489.

[25]. Peterson D.S, Mancini M, Fino P.C, Horak F, Smulders K. 2020. Speeding Up Gait in Parkinson's Disease. J. Parkinsons Dis., 10:245–253.

[26]. Fukuchi CA, Fukuchi RK, Duarte M. 2019. Effects of walking speed on gait biomechanics in healthy participants: a systematic review and meta-analysis. Syst. Rev. BioMed Central Ltd.

[27]. Craig JJ, Bruetsch AP, Huisinga JM. 2018. Coordination of trunk and foot acceleration during gait is affected by walking velocity and fall history in elderly adults. Aging Clin Exp Res., 31:943–50.

[28]. Cavagna G, Willems P.A, Legramandi M.A, Heglund N.C. 2002. Pendular energy transduction within the step in human walking. J. Exp. Biol., 205: 3413–3422.

[29]. Cavagna G.A, Thys H, Zamboni A. 1976. The sources of external work in level walking and running. J. Physiol., 262: 639–657.

[30]. Serrao M, Rinaldi M, Ranavolo A, Lacquaniti F, Martino G, Leonardi L, Pierelli F. 2016. Gait patterns in patients with hereditary spastic paraparesis. PLoS ONE, 11(10).

[31]. Busse ME, Wiles CM, et al. 2005. Muscle co-activation in neurological conditions. Phys Ther Rev., 7(4):247–53.

[32]. Darainy M, Ostry DJ. 2008. Muscle cocontraction following dynamics learning. Exp Brain Res., 190:153–63.

[33]. Boudarham J, Hameau S, Zory R, Hardy A, Bensmail D, Roche N. 2016. Coactivation of Lower Limb Muscles during Gait in Patients with Multiple Sclerosis. PLoS One 11 (6).

[34]. Higginson JS, Zajac FE, et al. 2006. Muscle contributions to support during gait in an individual with post-stroke hemiparesis. J Biomech., 39(10):1769–77.

[35]. Falconer K, Winter,D.A. 1985. Quantitative assessment of co-contraction at the ankle joint in walking. Electromyography and clinical neurophysiology 25, 135–149.

[36]. Lewek M.D, Rudolph K.S, Snyder-Mackler L. 2004. Control of Frontal Plane Knee Laxity During Gait in Patients with Medial Compartment Knee Osteoarthritis. Osteoarthritis Cartilage 12 (9), 745–751.

[37]. Childs J.D, Sparto P.J, Fitzgerald G.K, Bizzini M, Irrgang J.J. 2004. Alterations in Lower Extremity Movement and Muscle Activation Patterns in Individuals with Knee Osteoarthritis. Clinical Biomechanics (Bristol, Avon) 19 (1), 44–49.

[38]. Den Otter A, Geurts A, et al. 2004. Speed related changes in muscle activity from normal to very slow walking speeds. Gait Posture, 19(3):270– 8.

[39]. Fonseca ST, Silva PLP ST, Ocarino JM, Ursine PGS. 2001. Analysis of an EMG method for quantification of muscular co-contraction. Rev Bras Ciên e Mov., 9(3):23-30.

[40]. Den Otter A, Geurts A, Mulder T, Duysens J. 2006. Gait recovery is not associated with changes in the temporal patterning of muscle activity during treadmill walking in patients with post-stroke hemiparesis. Clin Neurophysiol: Off J Int Fed Clin Neurophysiol., 117(1):4–15.

[41]. Unnithan VB, Dowling JJ, Frost G, Volpe Ayub B, et al. 1996. Cocontraction and phasic activity during GAIT in children with cerebral palsy. Electromyogr Clin Neurophysiol., 36(8):487–94.

[42]. Ranavolo A, Mari S, Conte C, Serrao M, Silvetti A, Iavicoli S, Draicchio F. 2015. A new muscle co-activation index for biomechanical load evaluation in work activities. Ergonomics, 58(6):966-79.

[43]. Ivanenko YP, Cappellini G, Solopova IA, Grishin AA, MacLellan MJ, Poppele RE, et al. 2013. Plasticity and modular control of locomotor patterns in neurological disorders with motor deficits. Front Comput Neurosci., Frontiers,7: 123.

[44]. Varrecchia T, Rinaldi M, Serrao M, Draicchio F, Conte C, Conforto S, et al. 2018. Global lower limb muscle coactivation during walking at different speeds: Relationship between spatio-temporal, kinematic, kinetic, and energetic parameters. J Electromyogr Kinesiol., 43:148–57.

[45]. Martino G, Ivanenko Y, Serrao M, Ranavolo A, D'Avella A, Draicchio F, Conte C, Casali C, Lacquaniti F. 2014. Locomotor patterns in cerebellar ataxia. J. Neurophysiol., 112:2810–2821.

[46]. Labini F.S, Ivanenko Y, Cappellini G, Gravano S, Lacquaniti F. 2011. Smooth changes in the EMG patterns during gait transitions under body weight unloading. J. Neurophysiol., 106: 1525–1536.

[47]. Ranavolo A, Donini L.M, Mari S, Serrao M, Silvetti A, Iavicoli S, Cava E, Asprino R, Pinto A, Draicchio F.2013. Lower-limb joint coordination pattern in obese subjects. BioMed Res. Int., 2013, 1–9.

[48]. Steinwender G, Saraph V, Scheiber S, Zwick E, Uitz C, Hackl K. 2000. Intrasubject repeatability of gait analysis data in normal and spastic children. Clin. Biomech., 15:134–139.

[49]. Bonato P, D'Alessio T, Knaflitz M. A 1998. statistical method for the measurement of muscle activation intervals from surface myoelectric signal during gait. IEEE Trans Biomed Eng., 45(3):287-299.

[50]. Olney SJ. 1985. Quantitative evaluation of cocontraction of knee and ankle muscles in normal walking. Champaign: Human Kinetics Publishers.

[51]. Franz JR, Kram R. 2013. How does age affect leg muscle activity/coactivity during uphill and downhill walking? Gait Posture, 37:378–84.

[52]. Martino G, Ivanenko YP, d'Avella A, Serrao M, Ranavolo A, Draicchio F, Cappellini G, Casali C, Lacquaniti F. 2015. Neuromuscular adjustments of gait associated with unstable conditions. J Neurophysiol., 114(5):2867-82.

[53]. Menz HB, Lord SR, Fitzpatrick RC. 2003. Acceleration patterns of the head and pelvis when walking on level and irregular surfaces. Gait Posture, 18:35–46.

[54]. Iosa M, Picerno P, Paolucci S, Morone G. 2016. Wearable inertial sensors for human movement analysis. Expert Rev. Med. Devices, 13. 641–659.

[55]. Doi T, Hirata S, Ono R, Tsutsumimoto K, Misu S, Ando H. 2013. The harmonic ratio of trunk acceleration predicts falling among older people: results of a 1-year prospective study. J Neuroeng Rehabil., 10:7.

[56]. Latt MD, Menz HB, Fung VS, Lord SR. 2009. Acceleration patterns of the head and pelvis during gait in older people with Parkinson's disease: a comparison of fallers and nonfallers. J Gerontol A Biol Sci Med Sci., 64:700–6.

[57]. Tok F, Balaban B, Yas¸ar E, Alaca R, Tan AK. 2012. The effects of on a botulinum toxin A injection into rectus femoris muscle in hemiplegic stroke patients with stiff-knee gait: A placebo-controlled. nonrandomized trial. Am J Phys Med Rehabil., 91:321-326.

[58]. Zijlstra, W. 2004. Assessment of spatio-temporal parameters during unconstrained walking. Eur. J. Appl. Physiol., 92: 39–44.

[59]. Lisa A, Zukowski. Jody A, Feld. Carol A, Giuliani & Prudence Plummer. 2019. Relationships between gait variability and ambulatory activity post stroke. Topics in Stroke Rehabilitation.

[60]. Serrao M, Pierelli F, Ranavolo A, Draicchio F, Conte C, Don R, Di Fabio R, Lerose M, Padua L, Sandrini G, et al. 2012. Gait pattern in inherited cerebellar ataxias. Cerebellum, 11:194–211.

[61]. Miller Koop M, Ozinga S.J, Rosenfeldt A.B, Alberts J.L. 2018. Quantifying turning behavior and gait in Parkinson's disease using mobile technology. IBRO Rep., 5:10–16.

[62]. Palmerini L, Mellone S, Avanzolini G, Valzania. F, Chiari L. 2013. Quantification of motor impairment in Parkinson's disease using an instrumented timed up and go test. IEEE Trans. Neural Syst. Rehabil. Eng., 21:664–673.

[63]. Gulde P, Hermsdörfer J. 2018. Smoothness Metrics in Complex Movement Tasks. Front. Neurol.

[64]. Labini FS, Meli A, Ivanenko YP, Tufarelli D. 2012. Recurrence quantification analysis of gait in normal and hypovestibular subjects. Gait Posture, 35(1):48-55.

[65]. Afsar O, Tirnakli U, Marwan N. 2018. Recurrence Quantification Analysis at work: Quasi-periodicity based interpretation of gait force profiles for patients with Parkinson disease. Sci Rep., 14;8(1):9102.

[66]. Webber C.L, Zbilut, J.P. 1994. Dynamical assessment of physiological systems and states using recurrence plot strategies. J. Appl. Physiol., 76: 965–973.

[67]. Kennel M.B, Abarbanel H.D.I. 2002. False neighbors and false strands: A reliable minimum embedding dimension algorithm. Phys. Rev. E Stat. Phys. Plasmas Fluids Relat. Interdiscip. Top.

[68]. Dingwell J.B, Cusumano J.P. 2000. Nonlinear time series analysis of normal and pathological human walking. Chaos, 10: 848–863.

[69]. Riva F, Bisi M.C, Stagni R. 2014. Gait variability and stability measures: Minimum number of strides and within-session reliability. Comput. Biol. Med., 50: 9–13.

[70]. Fraser A.M, Swinney H.L. 1986. Independent coordinates for strange attractors from mutual information. Phys. Rev. A, 33: 1134–1140.

[71]. Van Schooten K.S, Rispens S.M, Elders P.J.M, van Dieën J.H, Pijnappels M. 2014. Toward ambulatory balance assessment: Estimating variability and stability from short bouts of gait. Gait Posture, 39: 695–699.

[72]. Chini G, Ranavolo A, Draicchio F, Casali C, Conte C, Martino G, Leonardi L, Padua L, Coppola G, Pierelli F, et al. 2017. Local Stability of the Trunk in Patients with Degenerative Cerebellar Ataxia During Walking. Cerebellum, 16:26–33.

[73]. Sekine M, Tamura T, Yoshida M, Suda Y, Kimura Y, Miyoshi H, et al. 2013. A gait abnormality measure based on root mean square of trunk acceleration. J NeuroEngineering Rehabil., 10:1–7.

CHAPTER 4

4. GAIT ANALYSIS OF PEOPLE WITH NEUROLOGICAL DISEASES

4.1. Characterization of pathologies under investigation

Gait analysis in subjects with motor disabilities provides critical information because it allows for the determination of the degree of limitation caused by the pathology and, as a result, the definition of an appropriate rehabilitation path.

Walking disorders are among the most visible symptoms of the pathologies studied in this thesis. For example, the first symptoms of Parkinson's disease are a shorter and more crawled locomotion, as well as a decrease in the angular movements of the joints [1]. A progressive loss of muscle coordination has been observed in diseases caused by a cerebellum deficit, such as cerebellar ataxia, making voluntary movements difficult [2]. Furthermore, upper motor neuron syndrome caused by stroke involves a various of sensorimotor impairments including spasticity, impaired motor control and proprioceptive deficits that interfere with normal gait [3-7].

It has also been demonstrated in subjects who have had lower limb amputations that prosthetic gait reflects a mixture of deviations from normal gait and adaptive and compensatory motions dictated by residual limb function after amputation [8].

Consequently, a complete characterization of these patients' locomotion could be a useful tool for identifying the motor strategies put in place to ensure stability and progression.

4.1.1 Cerebellar Ataxia

Gait ataxia is a common feature of cerebellar disorders, and patients exhibit unusual spatiotemporal and kinematic characteristics that contribute to an unstable gait [9-13].

Gait impairment has a significant impact on a person's autonomy and daily life activities, as well as significantly increasing the risk of falling [14,15]. Because walking is such an important function in everyday life, longitudinal gait assessment is critical for measuring the actual progression of gait impairment, determining if there are differences in the progression of gait impairment for different ataxic disorders, and identifying which gait parameters are more sensitive to gait decline. Modern motion analysis systems have recently been used to quantify the nature and degree of walking dysfunction in patients with cerebellar ataxia. Several abnormalities in spatiotemporal parameters,

muscle activation patterns, and upper body control have been observed, as well as increased variability in global and segmental gait parameters [9,16].

Furthermore, the evaluation of gait instability and fall risk is critical in the study of ataxic gait to prevent further disabilities, and it should be performed in a real-life environment outside the motion analysis laboratory for a long period of time in order to maximize and optimize the information we gather from such evaluation. Investigating the patterns of trunk acceleration during gait of people with cerebellar ataxia, in particular, may allow clinicians to quantify the level of trunk instability during gait as a generator of dynamic imbalance and provide clinicians with useful information for designing specific devices and rehabilitative interventions [17-20]. For these reasons, we examined the kinematics, kinetics, surface electromyography and stability in gait of subjects with cerebellar ataxia using both motion capture systems and wearable inertial sensors in our studies.

Ataxic gait reflects both the primary deficit, which is related to the cerebellum's lost ability to process multisensory features and provide a "error-correction mechanism" [17,21,22], and the compensatory mechanisms, which patients use to maintain dynamic stability while walking [9,10,23-25].

One of the most important motor compensatory strategy used by patients with cerebellar ataxia (CA) is to increase antagonist muscle coactivation at a single-joint level. The aims of the study "*Impairment of Global Lower Limb Muscle Coactivation During Walking in Cerebellar Ataxias*" (2020) were: (i) to investigate the TMCf in the lower limbs during gait in patients with CA; (ii) to compare the data of patients with CA with those of healthy subjects (HS); and (iii) to correlate the global coactivation parameters with the biomechanical (i.e., Center of Mass (CoM) displacement) and clinical features.

Subjects

Twenty-three patients with degenerative CA were enrolled. Fourteen patients had a diagnosis of autosomal dominant ataxia (spinocerebellar ataxia [SCA]; eight with SCA1 and six with SCA2), whereas the other seven had sporadic adult-onset ataxia of unknown etiology (SAOA). The severity of the disease was rated using the Scale for the Assessment and Rating of Ataxia (SARA)[26]. No patient was found to have visual impairment, whereas almost all patients had oculomotor abnormalities such as gaze nystagmus or square wave jerks during pursuit movements. All patients exhibited cerebellar atrophy on magnetic resonance imaging. Moreover, all patients were able to walk alone without any kind of aid on a level surface and to perform the required task. Because patients with SCA may show signs other than cerebellar features, we only included those who exhibited gait disturbances that were exclusively cerebellar in nature at the initial evaluation. A total of 23 age-,

sex-, and speed-matched HS were also enrolled as a control group. All subjects provided informed consent before taking part in the study, which complied with the Helsinki Declaration and had local ethics committee approval.

Instrumentation and procedure

All participants involved in the study were preliminary instructed about the correct experimental procedures and underwent practice tests to familiarize themselves with the experimental set up. Each participant was asked to walk barefoot for approximately 8 m along the laboratory pathway while looking straight ahead. Patients with CA were asked to walk 10 trials at a self-selected, comfortable speed. On the other hand, the HS were asked to walk 10 times at a self-selected speed and 10 times at a slow speed (slower than self-selected). Because we were interested in natural locomotion, only general, qualitative, and verbal instructions were provided. A 1- min break was provided between each walking trial to avoid the onset of muscle fatigue.

For the acquisition of gait kinematics, a stereophotogrammetric motion analysis system with optoelectronic technology was used (SMART-D System; BTS, Italy, Milan). Eight infrared cameras (sampling rate 300 Hz) and 22 reflective markers positioned above the anatomical reference points were used according to Davis' protocol.

A wireless (Wi-Fi) 16-channel acquisition system (FreeEMG1000; BTS SpA, Milan, Italy) was used to measure the superficial myoelectric activity. The probes were placed over the muscles of interest using Ag/AgCl pregelled electrodes (H124SG; Kendall ARBO, Donau). As the motor disturbances were symmetrical in our patients, we focused our analyses on the right-leg locomotor output. Therefore, the electrodes were placed over the following right-sided muscles: gluteus medius, rectus femoris, vastus lateralis, vastus medialis, tensor fascia latae, semitendinosus, biceps femoris, tibialis anterior, gastrocnemius medialis, gastrocnemius lateralis, soleus, and peroneus longus.

Data analysis

The following parameters within the gait cycle were calculated: (i) the synthetic coactivation index (CI; (ii) the full width at half maximum of the TMCf ($FWHM_{TMCf}$); (iii) the CoA of the TMCf (CoA_{TMCf}). The vertical component of GRFs was measured and normalized both to the stance phase duration and to each subject's body weight. To characterize the spatial and temporal profile of the VF curves, the indexes of the full width at half maximum ($FWHM_{VF}$) and that of the CoA (CoA_{VF}) were measured.

Cross-correlation analysis was used to evaluate the similarity in shape and timing between the VF and TMCf curves. The normalized cross-correlation function (Rxy(k)) was calculated between the VF and TMCf mean curves of all subjects only for the stance phase. To obtain information on the mechanical energy expenditure involving the whole skeletal muscle system during walking, we measured energy recovery and energy consumption parameters.

Statistical Analysis

The Shapiro-Wilk test was used for the preliminary study of normal data distribution. The unpaired two-sample t test (ttest) or Mann-Whitney (MW) test was used to evaluate differences in kinematic, kinetic, spatiotemporal, energetic, and EMG data between patients with CA and HS. We used the Watson-Williams test for circular data which allows to compare mean angles with two or more samples and is equivalent, for angles, of an ANOVA/Kruskal-Wallis test. Specifically, we used this test to evaluate differences in CoA values, reported with polar representation, of both the TMCf and VF curves between patients with CA and HS. A p value of < 0.05 was considered statistically significant. Cohen's d values were evaluated to estimate the effect size, considering small (< 0.5), medium (from 0.5 to 0.8), and large (> 0.8) effects. The Pearson or Spearman test was used to investigate any correlations between global coactivation parameters and clinical and gait variables. Partial correlations were used to control for gait speed. Statistical analysis was performed using MATLAB R2018b.

Results

The global coactivation, in terms of both CI and FWHM of the TMCf, was significantly increased in patients with CA compared with HS (Figure 4.1a, b). Furthermore, patients with CA shifted the global activation (i.e., CoA_{TMCf}) toward the initial contact (Figure 4.1c). Specifically, patients with CA showed CI values of 17.18 ± 3.35% vs values of 11.01 ± 1.81% of the HS ($p_{ttest} < 0.001$, $d = 2.28$; see Figure 4.1a) and $FWHM_{TMCf}$ values of 43.95 ± 9.19% vs values of 37.57 ± 8.70% of the HS ($p_{ttest} = 0.02$, $d = 0.75$; see Figure 4.1b), indicating a higher coactivation level. In addition, patients with CA showed lower values of CoA than HS ($p = 0.001$; Figure 4.1c), indicating a shift of the global activation toward the initial contact (Figure 4.1c). Moreover, the CA patients showed higher TMCf waveform similarity both within and between subjects: the CMC_{WS} values were significantly higher than HS and the CMC_{BS} values higher than HS. Lastly, a lower value of TMCf waveform similarity between groups was found.

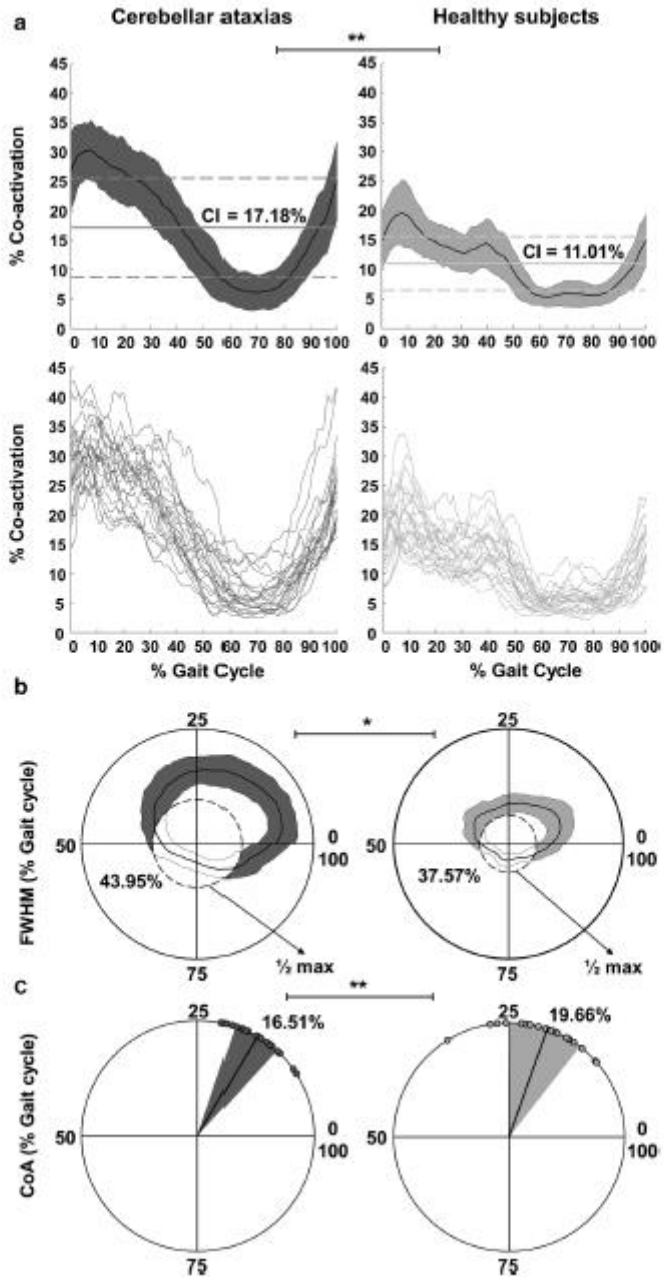

Figure 4.1 *Simultaneous coactivation of 12 lower limb muscles in patients with cerebellar ataxia (CA) and healthy subjects (HS).* ***a*** *Time-varying multi-muscle coactivation function (TMCf) curves: the upper graphs represent all TMCf curves of the 23 patient swith CA and the 23 HS, whereas the lower graphs show the mean values of TMCf (average value in solid line and standard deviation [SD] in light color) with the coactivation index (CI) (average value in solid line and SD in dotted line).* ***b*** *Full width at half maximum (FWHM) of the TMCf: the TMCf (average and SD) is presented as a polar graph and the FWHM is the colored area subtending the curve. All quantities shown are expressed as a percentage of the gait cycle.* ***c*** *Center of activity (CoA) of the TMCf: each dot in the circumference represents an individual subject's mean CoA value, whereas the mean value and SD of the CoA of all subjects are represented by the solid line and the width of the circular sector (in light color), respectively.*

The VFs of both patients with CA and the HS are shown in Figure 4.2a as averaged curves and standard deviations, while Figure 4.2b and c show the mean values of FWHM (identified by the

colored area between the curves) and of CoA (average values are the solid line and SD the circular sector in light color), respectively. No significant difference was observed for $FWHM_{VF}$ whereas a significantly lower value of CoA_{VF} was found in patients with CA than in HS (Figure 4.2c).

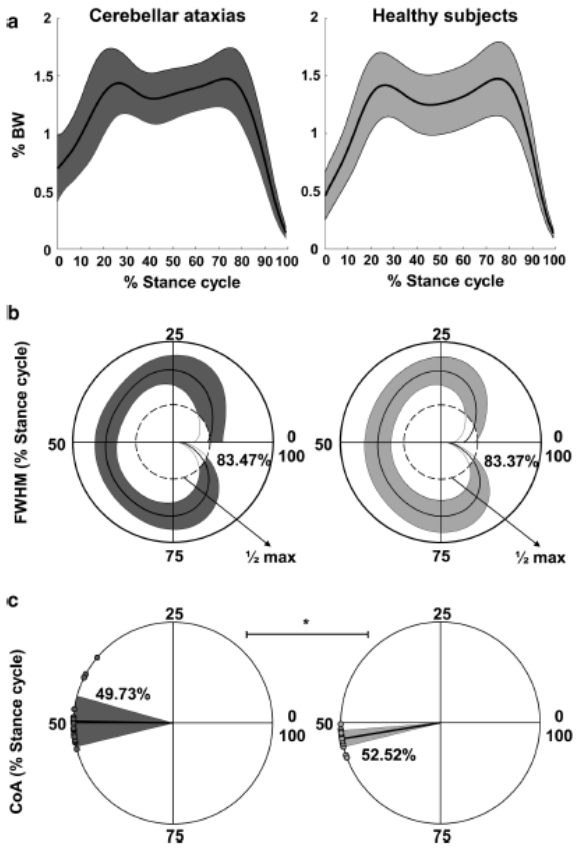

Figure 4.2 *Vertical component (VF) of the ground force reaction (GFR) in patients with cerebellar ataxia (CA) and healthy subjects (HS).* ***a*** *VF curves (average in solid line and standard deviation [SD] in light color).* ***b*** *Full width at half maximum (FWHM) of the VF: the VF (average and SD) is presented as a polar graph and the FWHM is the colored area subtending the curve. All quantities shown are expressed as a percentage of the stance phase of the gait cycle.* ***c*** *Center of activity (CoA) of the VF: each dot in the circumference represents a single subject's mean CoA value, whereas the mean value and SD of the CoA of all subjects are represented by the solid line and the width of the circular sector, respectively*

Figure 4.3 shows the results of the cross-correlation between the TMCf and VF averaged curve values within the HS (Figure 4.3a) and CA groups (Figure 4.3b), with the maximum point (R_{max}) and the time of its occurrence (τ^*) obtained through a comparison of the curves. The figure demonstrates that both the groups showed a high degree of similarity: RHS_max was 0.96 and RCA_max was 0.94. Furthermore, the same values of τ^* were observed for the two groups: τ^*HS and τ^*CA were 9% (Figure 4.3b).

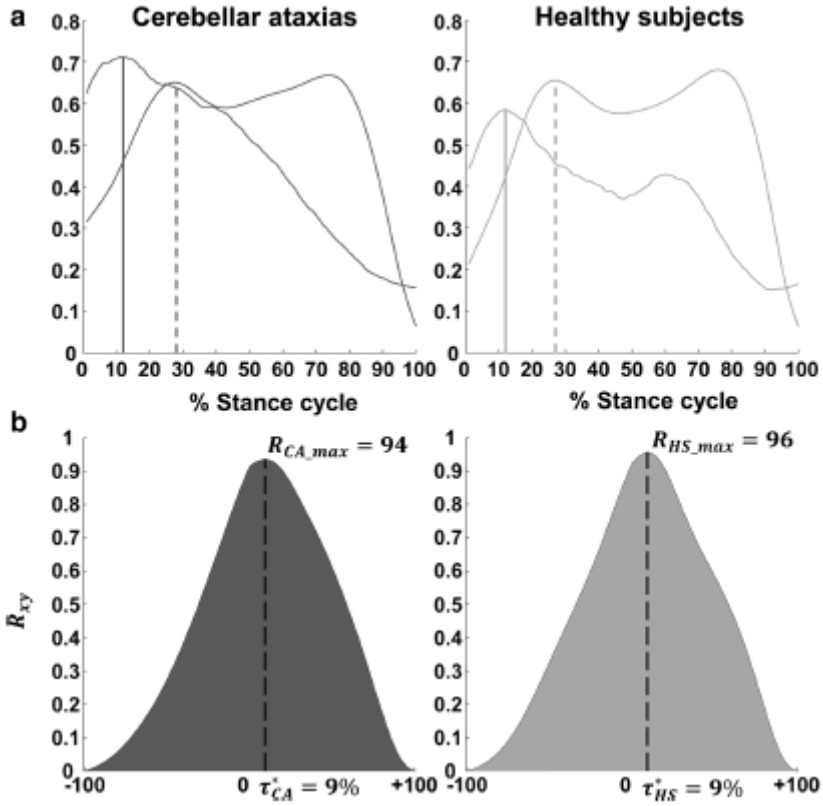

Figure 4.3 *Cross-correlation. a Mean curves of time-varying multi-muscle coactivation function (TMCf) (continuous line) and vertical force (VF) (dashed line), normalized to the maximum value among all subjects, presented in the range of 0–1. b Cross-correlation curves between the TMCf and the VF curves and their relative maximum value (Rmax,). The dashed lines represent the temporal shift (τ*) of the cross-correlation. All quantities shown are expressed as a percentage of the stance phase of the gait cycle.*

Figure 4.4 shows the negative moderate correlation between gait speed and CI, CoA_{TMCf} and $FWHM_{TMCf}$. Furthermore, Figure 4.4 shows a significant positive partial correlation between CI and both CoM mediolateral displacement values and SARA scores and between CoA_{TMCf} and both CoM mediolateral displacement values and SARA scores.

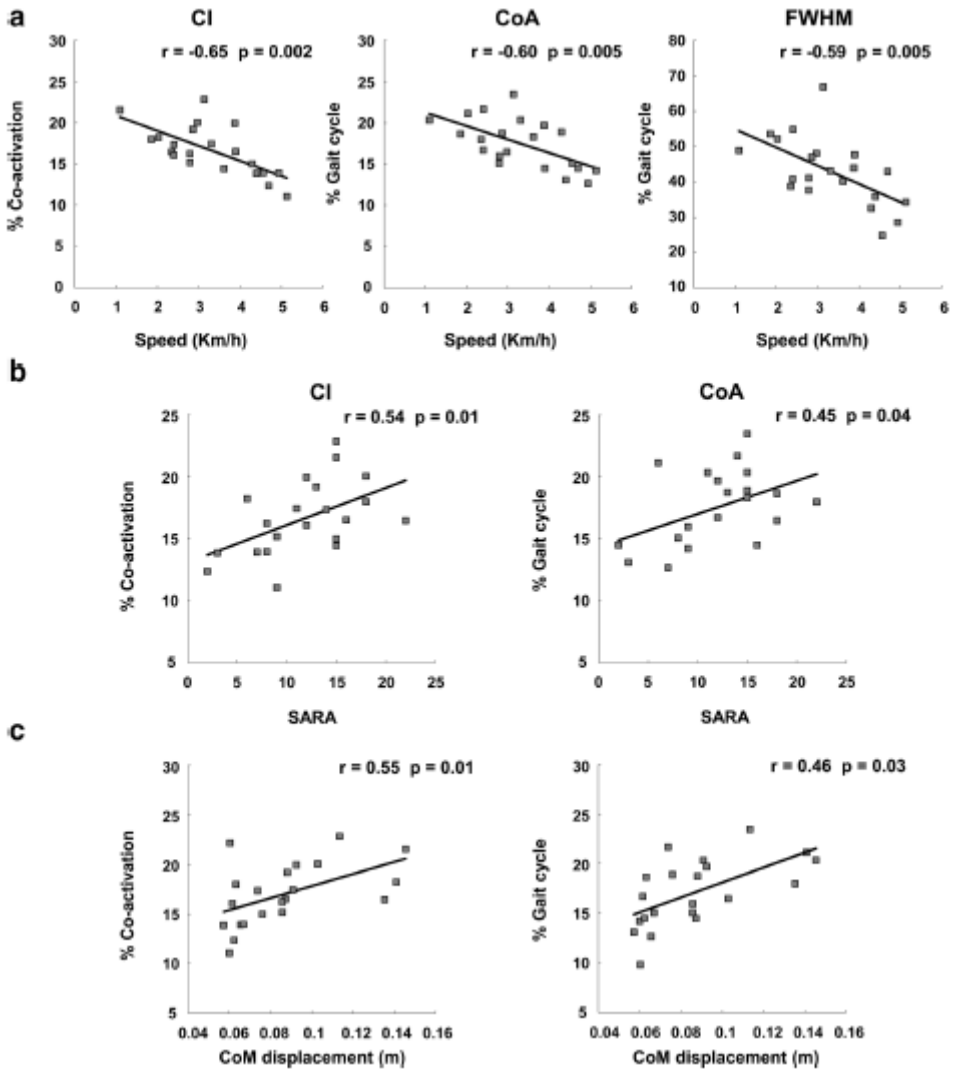

Figure 4.4 *Correlations among the time-varying multi-muscle coactivation function (TMCf) parameters, gait parameters, and clinical scores. Only parameters that significantly differed between patients with cerebellar ataxia and healthy subjects are plotted in this figure. Each point on the graphs represents the value for the individual patient, and linear regression lines (solid line) with corresponding r and p values are reported. A Relationships of the coactivation index (CI), center of activity (CoA), and full width at half maximum (FWHM) to the mean gait speed. b CI and CoA with the Scale for the Assessment and Rating of Ataxia (SARA) score. c CI and CoA with the center-of-mass mediolateral displacement.*

In addition to altered muscle behavior, recent studies in the literature have demonstrated that upper body oscillations are another clinical feature of ataxic patients [2,13,27]. These oscillations shift the center of mass to the edges of the base of support, which can worsen gait instability, increase body sway while walking, and increase the risk of falling [20]. For these reasons, ataxic patients must use special devices designed to stabilize the upper body, reduce body sway while walking, and reduce walking variability. In particular, ataxic patients may benefit from using elastic or semi-rigid orthoses that can reduce trunk oscillations and stabilize joint trajectories without restricting lower limb movements during walking.

In the study "*The effectiveness of a soft passive trunk exoskeleton on the motor coordination in patients with cerebellar ataxia*" (in progress) we analyzed the gait of patients with cerebellar ataxia using a suit made of lycra fabric woven with carbon thread, with a pocket on the back that houses a passive exoskeleton. We then compared the gait of these patients without and with the use of the device; in particular, the aim of the study was to compare the following parameters between the two conditions:

(i) spatio-temporal parameters;

(ii) kinematic of the trunk and lower limb joints;

(iii) the device's effectiveness in terms of mechanical energy expenditure and recovery;

(iv) vertical ground reaction force;

(v) stability in terms of center of mass and center of pressure behavior.

Subjects

Eight patients (3 females, 5 males; mean age: 55,5 ± 9,47 years) affected by degenerative cerebellar ataxia were enrolled in this study. Four were diagnosed with autosomal dominant ataxia (spinocerebellar ataxia [SCA]; 4 patients with SCA1 ,SCA2, SCA8, SCA40) while the other 4 had sporadic adult-onset ataxia (SAOA). We excluded patients with major involvement of neurological systems other than cerebellar impairment (e.g., extrapyramidal, pyramidal, peripheral nerve, or muscle), as well as those with orthopedic disorders that could cause further gait impairment. The Scale for the Assessment and Rating of Ataxia (SARA)[26] was used to assess the disease's characteristics; the characteristics of patients are described in Table 4.1. All the participants gave a written informed consent according to the Declaration of Helsinki. The local research ethics committee approved the study (CE Lazio 2, protocol number 0139696/2021).

Table 4.1 *Patients' characteristics*

Patients	Age	Gender	Diagnosis	SARA Tot	SARA Gait
P1	67	F	SAOA	18	4
P2	57	F	SAOA	5	2
P3	37	M	SCA1	14	3
P4	54	M	SCA2	14	3
P5	59	M	SAOA	12	3
P6	51	M	SAOA	7	2
P7	66	M	SCA40	6	2
P8	53	F	SCA1	2	1

A soft passive exoskeleton made of lycra fabric woven with carbon thread is used. The textile module of this exoskeleton has a specific tension and force direction that is useful in ensuring the patient's body alignment in three-dimensional space. These typically extend from the shoulders to the hips, creating a force that opposes trunk movements. The passive exoskeletons designed to be accommodated in the patient's spine using computerized tomography and optoelectronic methods are attached to the textile module. Because these devices are typically made of shape memory material, they operate on the principle of energy restitution.

Instrumentation and procedure

A six infrared cameras optoelectronic motion analysis system at sample frequency of 340 Hz (SMART-DX 6000 System, BTS, Milan, Italy) was used to detect the movement of twenty-seven passive markers placed according to a modified Davis' protocol [28]. The gait analysis began with a standing position on a platform. The procedure continued by asking the patient to walk at their preferred speed and in their own shoes without wearing the device; at least ten trials were recorded in this condition. Following that, the patients were made to wear the suit with the exoskeleton inserted, and was asked again to walk at least ten times at their preferred speed and in their shoes.

Data analysis

We calculated the spatio-temporal parameters, the trunk range of motions and the flexion-extension range of motion of hip, knee and ankle joints. We examined the vertical component of the ground reaction force and the corresponding FWHM for kinetics. To evaluate the effectiveness of the device in terms of mechanical energy recovery and expenditure, we calculated the R-step and TEC parameters. Finally, to evaluate the device's effect on stability, we examined the displacement of the center of mass (COM) as well as the b_{min} parameter. The COM was calculated according to the reconstructed pelvis method [29] , considering the markers on the sacrum and the two anterior iliac spines. The b_{min} parameter was calculated as the difference between CoP and XCoM in the medio-lateral direction during the double support phase. The XCoM was determined using the extrapolated centre of mass:

$$\zeta(t) = x(t) + \frac{\dot{x(t)}}{\omega_0}$$

$$\xi(t) = z(t) + \frac{\dot{z(t)}}{\omega_0}$$

where ζ(t), ξ(t) and x(t), z(t) are the instantaneous anterior– posterior and lateral XCoM and CoM positions respectively, $\dot{x(t)}$ and $\dot{z(t)}$ are the instantaneous anterior– posterior and lateral CoM velocities, and ω_0 is the Eigen frequency calculated by the following equation:

$$\omega_0 = \sqrt{\frac{g}{h}}$$

where g is the acceleration due to gravity and h is the effective height of the body's CoM above the floor. For the anterior–posterior and lateral directions, h was calculated as 1.24 and 1.34 times the trochanteric height, respectively [30]. The center of pressure (CoP) position was calculated from the distribution of the forces on the platforms as the point location of the ground reaction force vector. Positive and negative values of b_{min} indicate, respectively, a condition of stability and instability.

Statistical Analysis

Statistical analysis was performed using MATLAB R2021b. All data were expressed as mean± standard deviation; $p < 0.05$ was considered statistically significant. We assessed the normality of distributions using the Shapiro-Wilk test. Mean and standard deviation within subjects were computed for all parameters. We used the independent-samples t test to compare the parameters calculated in the two conditions, without and with the soft passive exoskeleton.

Results

There was no statistically significant difference in the spatio-temporal gait parameters between the two conditions, with the exception of step length variability, which is significantly lower in the presence of the device (Table 4.2).

Table 4.2 *Comparison of space-time parameters between the two conditions*

Spatio-temporal parameters	Withouth exoskeleton	With exoskeleton	p-value
Step Length (m)	0.41±0.02	0.44±0.07	>0.05
CV Step length	6.5±0.8	5.3±1.4	**0.02**
Step Width (m)	0.17±0.06	0.14±0.04	>0.05
CV step Width	5.7±1.8	5.4±2.3	>0.05
Stance phase (% gait cycle)	66±2.6	65±2.2	>0.05
Swing phase (% gait cycle)	34±2.1	35±3.06	>0.05
Double support phase (% gait cycle)	16±2.5	18±3.8	>0.05
Speed (m/s)	0.7±0.05	0.8±0.1	>0.05

Mean ± standard deviation values and the result of the independent samples t-test are reported. p values lower than 0,05 were considered statistically different

When comparing the two conditions, statistically significant differences in trunk ranges of motion in the sagittal and transverse planes were found (Figure 4.5). There were no differences in the flexion-extension ranges of motion of the hip, knee, and ankle joints (Figure 4.5).

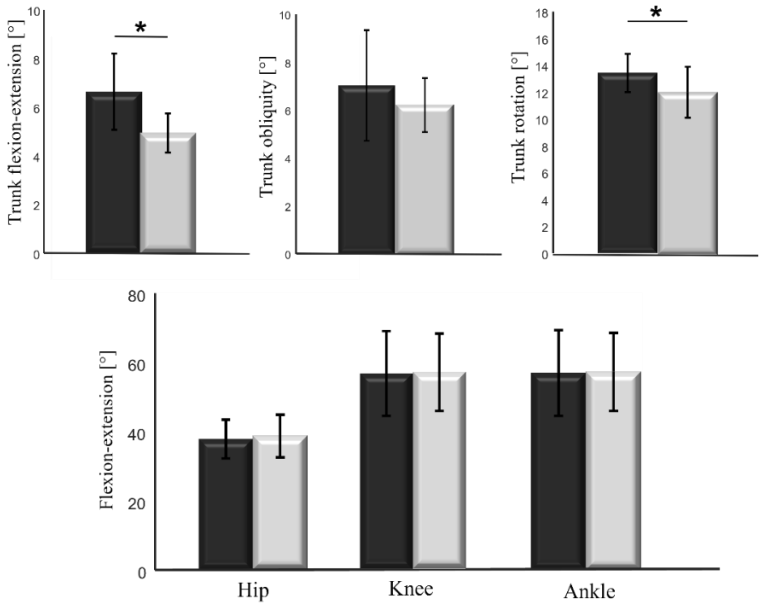

Figure 4.5 *Range of motion of the trunk in three planes of space (above) and flexion-extension of the hip, knee, and ankle joints (below) without exoskeleton (black) and with exoskeleton (grey)*

A comparison of the profiles of the vertical component of the ground reaction force in the two conditions revealed that in the presence of the device, a peak in the 10% of the stance phase disappeared. Furthermore, a statistically significant difference was found when comparing the FWHM values (Figure 4.6).

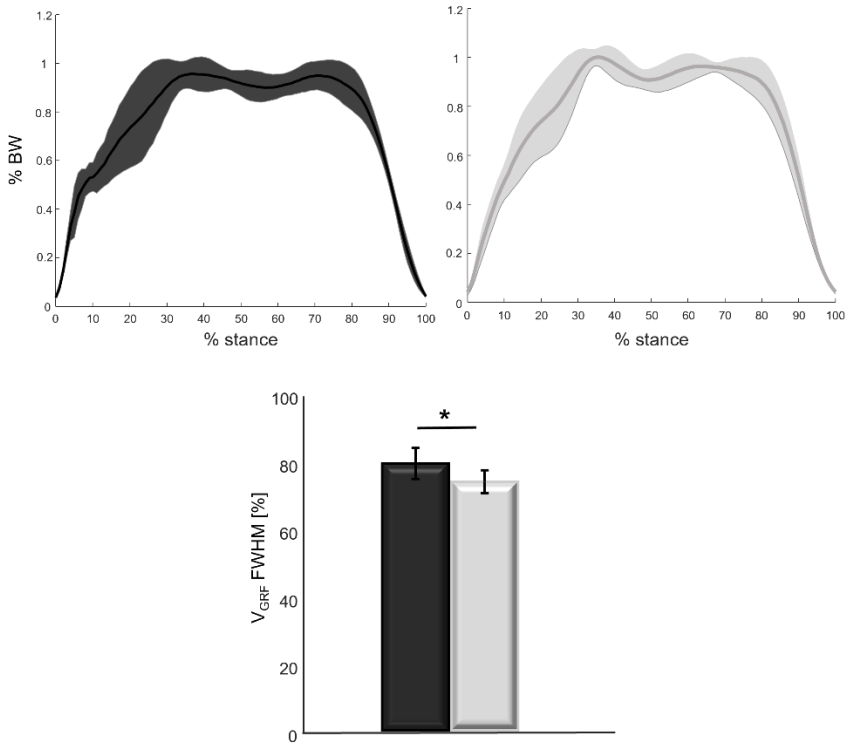

Figure 4.6 *Vertical ground reaction force components, means, standard deviations and statistical results of FWHM values without exoskeleton (black) and with exoskeleton (grey)*

In terms of energy behavior, statistically significant differences were found for both energy consumption and energy recovery, with the parameters improving in the presence of the device (Figure 4.7).

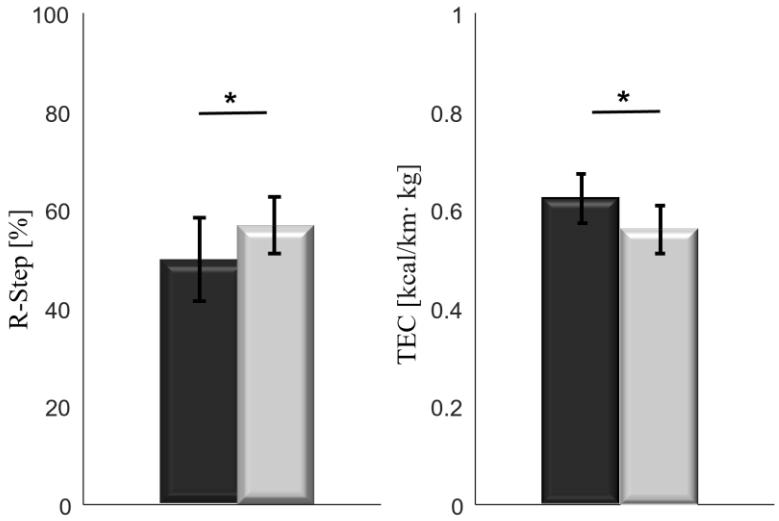

Figure 4.7 *Means, standard deviations, and statistical results of fraction of mechanical energy recovered (R-step) and total energy consumption (TEC) values without exoskeleton (black) and with exoskeleton (grey)*

No significant differences were found for the stability index b_{min}. However, there were significant differences in the displacement of the COM in the medio-lateral direction (COM_{ML} displacement without exoskeleton= 0.123±0.02, COM_{ML} displacement with exoskeleton= 0.094±0.02, p=0.018) , which is statistically smaller in the presence of the device (Figure 4.8).

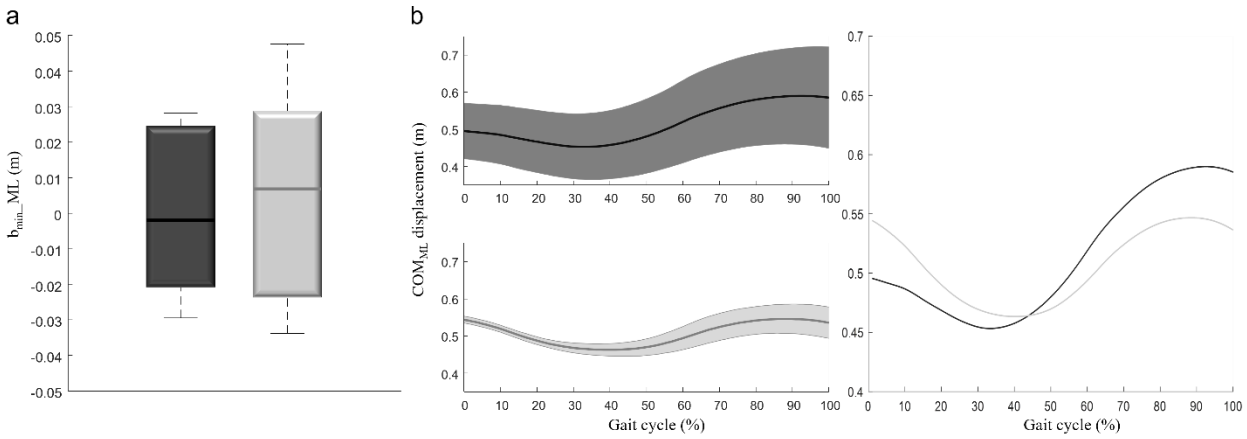

Figure 4.8 *a)Boxplot of dynamic stability index in both conditions (black: without exoskeleton, grey: with exoskeleton) during the double support phase in the medio-lateral direction. b)center of mass displacement in medio-lateral direction for both conditions for a representative patient.*

As a result, patients with cerebellar ataxia exhibit peculiar spatiotemporal and kinematic characteristics, as well as muscle activation patterns that contribute to an unstable gait [9-11,31]. Furthermore, ataxic gait is extremely variable across gait cycles [9] and exhibits inefficient coordination between upper and lower body segments, even in the absence of external disturbances

[32]. Given these circumstances, it is reasonable to hypothesize that when perturbation occurs in ataxic patients, the risk of falling increases, and the gait pattern can be classified as unstable.
The evaluation of gait instability and fall risk is thus critical in the study of ataxic gait to prevent further disabilities, and it should be performed in a real-life environment outside the motion analysis laboratory to maximize and optimize the information we gather from such evaluation. In this context, wearable magnetic and inertial measurement units (MIMUs), consisting of a three-axial accelerometer, a gyroscope, and a magnetometer, represent a self-contained alternative to conventional laboratory-based motion capture systems [33-35].

The study "*Exploring Risk of Falls and Dynamic Unbalance in Cerebellar Ataxia by Inertial Sensor Assessment*" (2019) evaluated whether and how wearable inertial sensors can describe the gait kinematic features among ataxic patients.

Subjects

Seventeen patients affected by primary degenerative cerebellar ataxia were enrolled in the study. The complete neurological assessment included (1) cognitive evaluation according to mini-mental state examination (MMSE) scale, (2) cranial nerve evaluation, (3) muscle tone evaluation, (4) muscle strength evaluation, (5) joint coordination evaluation, (6) sensory examination, (7) tendon reflex elicitation, and (8) disease severity measured by International Cooperative Ataxia Rating Scale (ICARS) and Scale for the Assessment and Rating of Ataxia (SARA) [26]. All patients were able to walk alone without any kind of assistance or aid, and were receiving physical therapy, including active and passive exercises for upper and lower limbs as well as balance and gait re-education. The number of falls in the last year was used for correlation analysis. Sixteen age-matched healthy adults were enrolled as the control group. We obtained informed consent from each patient and healthy subject, which complied with the Helsinki Declaration and was approved by the local ethics committee.

Instrumentation and procedure

We acquired data with an inertial sensor (BTSGWALK, BTS, Milan, Italy), attached to an ergonomic belt placed around the pelvis at the level of the L5 vertebra, connected to a portable computer via Bluetooth. The sampling rate was 100 Hz, and the sensor, endowed with a tri-axial accelerometer (16 bit/axes), a tri-axial magnetometer (13 bit), and a tri-axial gyroscope (16 bit/axes), measured the linear

trunk accelerations and the trunk angular velocities in three space directions.

Before starting the experimental session, participants were asked to walk along a predetermined route in order to familiarize themselves with the procedure. Recordings of all the patients were obtained during overground walking. We asked participants to walk along a corridor (3 m wide and 20 m long) at their preferred speed. Control subjects were asked to walk at a low speed in order to match the two groups for speed.

Data analysis

The 'walking protocol' of the inertial sensor (G-STUDIO, BTS, Milan, Italy) was used to detect: (1) trunk acceleration patterns, (2) right and left heel strikes, and (3) toe-off. The HR and the CV were calculated using MATLAB software (MATLAB 7.4.0, MAthWorks, Natick, MA, USA).

Statistical Analysis

We used the SPSS 17.0 software (SPSS Inc. Chicago, IL, USA) for statistical analysis. All data were expressed as mean ± standard deviation; $p < 0.05$ was considered statistically significant. We assessed the normality of distributions using the Shapiro-Wilk test. Mean and standard deviation within subjects were computed for speed and stability indexes. We used the independent-samples t test to look for differences between the stability indexes of ataxic patients vs. controls. Cohen's d index was used to assess the effect size of the stability indexes int he three spatial directions. We used the Pearson's test to investigate any correlation. We used the Pearson test to investigate any correlation of acceleration HR and step length CV with age, height, weight, disease duration, total ICARS and SARA scores and number of falls in the last year.

Results

HR in all three directions and step length CV were all significantly different when compared to the controls (Table 4.3). Briefly, the HR of patients was lower than the HR of healthy subjects, meaning a less harmonic and rhythmic acceleration pattern of the trunk, while the CV of step length was greater in patients than in the controls, indicating a more variable step length in ataxic patients. Both HR and CV of step length showed a high effect size in distinguishing patients and controls, but HR in all three directions showed a higher effect size score when compared to the CV (Table 4.3).

Table 4.3. *Comparisons of the stability indexes between 17 ataxic patients and 16 controls at matched gait speed.*

Parameter	Patients	Controls	t	p	Cohen's d
HR-AP	1.665 ± 0.300	2.414 ± 0.540	4.964	<0.001	1.714
HR-ML	1.639 ± 0.282	2.347 ± 0.559	4.631	<0.001	1.599
HR-VT	1.694 ± 0.304	2.549 ± 0.715	4.519	<0.001	1.556
Step length CV (%)	21.249 ± 10.293	13.205 ± 6.004	−2.720	0.011	0.955
Step length (m)	0.499 ± 0.087	0.569 ± 0.067	−2.382	0.024	0.112
Speed (m/s)	0.939 ± 0.195	0.924 ± 0.239	−0.207	0.838	0.069

Mean ± standard deviation values, the results of the independent samples t-test and Cohen's d are reported. Values of p lower than 0.05 were considered statistically significant. HR-AP: harmonic ratio in the anterior–posterior direction; HR-ML: harmonic ratio in the mediolateral direction; and HR-VT: harmonic ratio in the vertical direction.

Surprisingly, no correlation was found between HR in all directions, falls/year, and clinical severity (ICARS and SARA scores) (Table 4.4), while a significant positive correlation was found between the CV of step length and the falls/years and ICARS and SARA scores (Figure 4.9).

Table 4.4. *Correlation analysis between HR in all directions and ICARS, SARA, and falls/year.*

Parameter	ICARS (R, p)	SARA (R, p)	falls/year (R, p)
HR-AP	−0.35, 0.24	−0.35, 0.13	−0.10, 0.66
HR-ML	−0.47, 0.10	−0.36, 0.11	0.02, 0.92
HR-VT	−0.41, 0.88	−0.43, 0.06	−0.01, 0.99

The reported values represent Pearson correlation value (R) and statistical significance value (p). HR-AP: harmonic ratio in the anterior–posterior direction; HR-ML: harmonic ratio in the mediolateral direction; and HR-VT: harmonic ratio in the vertical direction.

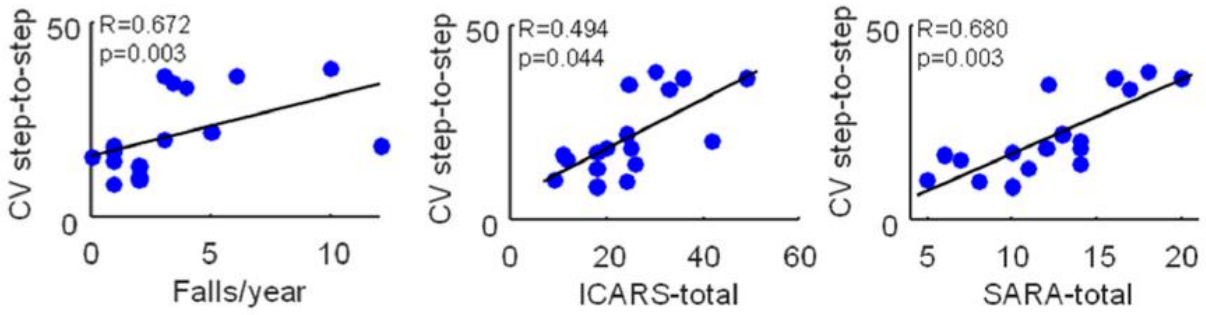

Figure 4.9 *Correlations between the maximum step-to-step coefficient of variation and the falls/year, ICARS-total, and SARA-total scores in 17 ataxic patients. Pearson's R coefficient (R) and significance (p) are reported.*

The sample and number of stability indices analyzed were expanded in the subsequent study "*Identification of Gait Unbalance and Fallers Among Subjects with Cerebellar Ataxia by a Set of*

Trunk Acceleration-Derived Indices of Gait" (2022), and their correlation with clinical and kinematic variables was investigated.

Subjects

Thirty-two subjects with primary degenerative CA (pwCA), 13 females and 19 males, aged 5 1.87 ± 12.54 years, were included in this study. All subjects were assessed at the Academic Neurorehabilitation Unit of the Traumatic Orthopedic Surgical Institute (ICOT), Latina, Italy. The Scale for the Assessment and Rating of Ataxia (SARA) [26] was administered to assess disease severity, and data on the patient-reported number of falls during the last year were collected [36]. We only included subjects who were able to walk without assistance and who had gait problems that were exclusively cerebellar in nature at the time of their initial evaluation within a broader group of CA patients from a rare disease center. Because many spatio-temporal parameters are dependent on gait speed and we expected a slower gait speed in pwCA , to avoid any bias due to this feature, a 1:1 optimal data matching procedure using the propensity score difference method. After the matching procedure, 32 age- and speed-matched healthy subjects ($HS_{matched}$) were included as the control group. In accordance with the Declaration of Helsinki, informed consent was obtained from both pwCA and HS before the experimental procedure. The study was approved by the local ethics committee (CE Lazio 2, protocol number 0139696/2021).

Instrumentation and procedure

An inertial sensor (BTS GWALK, BTS, Milan, Italy) positioned at the L5 level through an ergonomic belt was used to acquire the data. The "Walk+ " protocol of the G-STUDIO software (G-STUDIO, BTS, Milan, Italy) was used to detect the linear trunk acceleration patterns during gait at a sampling rate of 100 Hz in the antero-posterior, medio-lateral and vertical directions, spatio-temporal parameters, and pelvis kinematics. The sensor was equipped with a triaxial accelerometer and gyroscope (16 bit/axes) and a triaxial magnetometer (13 bits). Subjects were asked to walk barefoot along a 30-m-long corridor at a self-selected speed. Since natural locomotion was the focus of this study, subjects were free to choose their preferred speed without interfering with their pacing or rhythm through external sensory cues. To facilitate the largest sample for speed-matched comparison, HS were also asked to walk at a slower speed .

Data analysis

MATLAB software (MATLAB 7.4.0, MAthWorks, Natick, MA, USA) was used to calculate the gait stability indices: HR, CV, RQA, NJS, LDLJ-A, RMS and RMSR in all three directions (AP: anterior-posterior, ML: medio-lateral, V:vertical).

Statistical Analysis

An unpaired sample t-test or Mann–Whitney U test was performed to identify significant differences in the gait stability indexes between pwCA and $HS_{matched}$. Cohen's d was calculated to assess the magnitude of the differences. To assess the ability of the gait stability indices to characterize the gait of pwCA compared to that of $HS_{matched}$ and characterize the gait of pwCA who reported a history of frequent falls, receiver operating characteristic (ROC) curves were plotted, and the area under the curve (AUC) was calculated. AUC values greater than 0.60, with a confidence interval lower bound greater than 0.50, were considered for sufficient overall discriminative ability. The optimal cutoff point was calculated as the point of the ROC curve, maximizing the sum of sensitivity and specificity. Positive and negative likelihood ratios (LR+ and LR− , respectively) were calculated and transformed into positive and negative post-test probabilities using Fagan's nomogram [37]. We used the 35.6% prevalence of frequent fallers among people with CA walking without support as the prior probability in the post-test probabilities calculations, to improve the generalizability of the findings. To assess the speed-independent correlation between the identified discriminant indexes, SARA scores, history of falls, and gait variables, a partial correlation analysis excluding the effects of gait speed was performed. Because eventual correlations between the gait indexes and the history of falls could be reflective of general motor disability rather than a specific relationship between the trunk behavior and the risk of falls, we also performed a partial correlation analysis excluding the effects of the SARA PG scores. The significance level was set at 95% confidence level. Statistical analysis was performed using IBM SPSS Statistics for Windows, version 27.0. (IBM Corp, Armonk, NY, USA) and NCSS 2020 statistical software (2020) (NCSS, LLC. Kaysville, Utah, USA).

Results

After the matching procedure, no significant differences in age and gait speed between the pwCA and $HS_{matched}$ groups were found. Significant differences between pwCA and $HS_{matched}$ were found for HR, RMS, and sLLE in the three directions, $RMSR_{AP}$ and $RMSR_{ML}$, CV and LDLJ-A in the V direction. The HRs and CV showed a good ability to discriminate between pwCA and HS (AUCs > 0.80, Table 4.5). The sLLE and RMS in three directions, $RMSR_{AP}$, $RMSR_{ML}$, and $LDLJA_{V}$, showed

sufficient ability to discriminate between pwCA and HS (AUCs > 0.60; Table 4.5). HRs, CV, RMS_{AP}, RMS_V, and $RMSR_{AP}$ showed the highest probabilities of characterizing the gait of pwCA at the optimal cutoff point, regardless of gait speed. HRs and sLLEs were also able to characterize the gait of fallers (AUCs ≥ 0.70; Table 4.5 and Figure 4.10). HR_{AP} values ≤ 1.53, HR_{ML} values ≤ 1.80, and HR_V values ≤ 1.87 characterize the gait of fallers with 71%, 61%, and 61% probability, respectively.

Table 4.5. *Discriminative ability and cutoff analysis*

	Criterion	AUC (95% CI)	OCP	Se (95% CI)	Sp (95% CI)	LR+	LR−	PTP+	PTP−
HR_{AP}	*pwCA vs HS*	0.87 (0.75–0.94)	≤ 1.99	0.72(0.54–0.87)	0.97(0.85–0.99)	24.72	0.28	96%	21%
	Fallers	0.73 (0.48–0.87)	≤ 1.53	0.53(0.28–0.77)	0.82(0.56–0.96)	4.53	0.41	71%	18%
HR_{ML}	*pwCA vs HS*	0.84 (0.72–0.91)	≤ 1.89	0.67(0.48–0.82)	0.91(0.76–0.98)	7.55	0.36	88%	26%
	Fallers	0.75 (0.52–0.88)	≤ 1.80	0.82(0.56–0.96)	0.70(0.44–0.89)	2.88	0.24	61%	12%
HR_V	*pwCA vs HS*	0.84 (0.71–0.92)	≤ 2.06	0.79(0.61–0.91)	0.85(0.69–0.95)	5.36	0.26	84%	20%
	Fallers	0.76 (0.51–0.89)	≤ 1.87	0.76(0.50–0.53)	0.70(0.44–0.89)	2.88	0.24	615%	12%
CV	*pwCA vs HS*	0.82 (0.68–0.90)	≥ 35.14	0.66(0.49–0.82)	0.88(0.72–0.96)	5.50	0.36	85%	26%
	Fallers	0.56 (0.29–0.74)	-	-	-	-	-	-	-
$sLLE_{AP}$	*pwCA vs HS*	0.75 (0.60–0.84)	≥ 0.44	0.66(0.47–0.84)	0.76(0.57–0.87)	2.75	0.44	73%	31%
	Fallers	0.63 (0.35–0.80)	-	-	-	-	-	-	-
$sLLE_{ML}$	*pwCA vs HS*	0.69 (0.52–0.81)	≥ 0.43	0.68(0.47–0.84)	0.73(0.55–0.87)	2.75	0.44	73%	31%
	Fallers	0.62 (0.35–0.79)	-	-	-	-	-	-	-
$sLLE_V$	*pwCA vs HS*	0.79 (0.63–0.87)	≥ 0.56	0.86(0.67–0.96)	0.65(0.47–0.80)	2.55	0.22	72%	18%
	Fallers	0.65 (0.38–0.82)	-	-	-	-	-	-	-
RMS_{AP}	*pwCA vs HS*	0.62 (0.46–0.75)	≥ 1.88	0.33(0.22–0.56)	0.94(0.80–0.99)	5.50	0.71	85%	42%
	Fallers	0.60 (0.27–0.80)	-	-	-	-	-		
RMS_{ML}	*pwCA vs HS*	0.67 (0.51–0.79)	≥ 1.22	0.66(0.46–0.83)	0.63(0.45–0.79)	1.93	0.46	66%	32%
	Fallers	0.63 (0.29–0.82)	-	-	-	-	-		
RMS_V	*pwCA vs HS*	0.60 (0.43–0.73)	≥ 1.49	0.33(0.16–0.53)	0.88(0.72–0.96)	3.66	0.73	79%	42%
	Fallers	0.63 (0.29–0.82)	-	-	-	-	-		
$RMSR_{AP}$	*pwCA vs HS*	0.62 (0.45–0.75)	≥ 0.89	0.33(0.16–0.54)	0.97(0.84–0.99)	11.00	0.68	92%	40%
	Fallers	0.59 (0.29–0.78)	-	-	-	-	-		
$RMSR_{ML}$	*pwCA vs HS*	0.71 (0.55–0.83)	≥ 0.58	0.74(0.58–0.89)	0.58(0.43–0.77)	1.88	0.43	65%	30%
	Fallers	0.60 (0.29–0.79)	-	-	-	-	-		
$LDLJA_V$	*pwCA vs HS*	0.64 (0.49–0.75)	< − 11.80	0.77(0.57–0.91)	0.48(0.31–0.66)	1.51	0.45	60%	31%
	Fallers	0.55 (0.27–0.74)	-	-	-	-	-		

AUC , area under the receiver operating characteristics curve; OCP, optimal cutoff point; Se, sensitivity; Sp, specificity; CI, confidence interval; LR + , positive likelihood ratio; LR − , negative likelihood ratio; PTP + , positive post-test probability; PTP − , negative post-test probability; pwCA, persons with cerebellar ataxia; HS, speed-matched healthy subjects; HR, harmonic ratio; CV, coefficient of variation; sLLE, short-term largest Lyapunov exponent; RMS, root mean square of the acceleration signals; RMSR, root mean square ratio; LDLJ-A, acceleration-based log dimensionless jerk

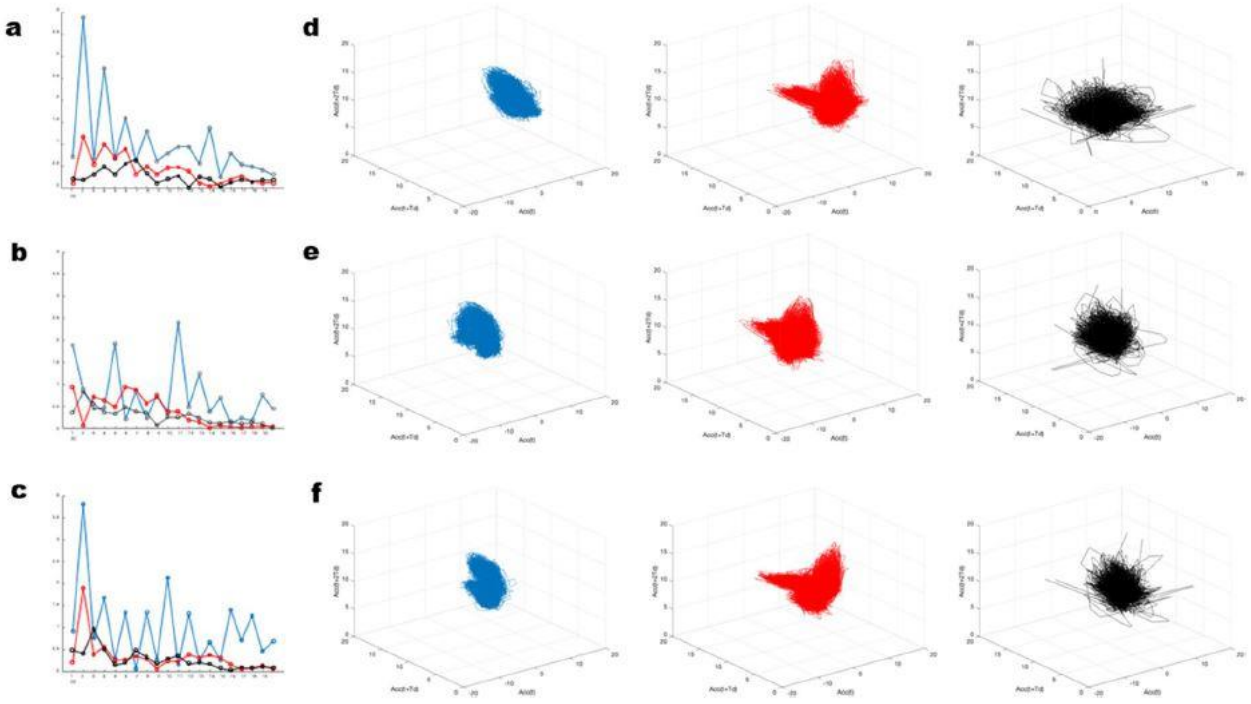

Figure 4.10 *Harmonic Ratios values for each of the considered strides in the antero-posterior (a), medio-lateral (b), and vertical (c) and 3D-reconstructed state space of the acceleration and its time-delayed copies (time delay of 10 data samples) in the antero-posterior (d), medio-lateral (e), and vertical (f) directions of a representative ageand-speed-matched healthy subject (blue), a non-faller subject with CA (red), and a faller subject with CA (black)*

The results of the partial correlation analysis are presented in Table 4.6. HRs were significantly correlated with the history of falls, SARAPG, stance, swing, and double support duration by excluding gait speed. CV was significantly correlated with $SARA_{PG}$, stance, and swing duration. $sLLE_{AP}$ correlated with step length, and pelvic rotation. $sLLE_{ML}$ was pelvic tilt and pelvic rotation. $sLLE_{V}$ was correlated with pelvic tilt and rotation. The RMS values in the AP direction were correlated with step length (Table 4.6). LDLJ-Av did not show any correlation with clinical and kinematic parameters. The HR_{AP}, HR_{ML}, and HR_{V} still correlated with the history of falls when excluding the effects of SARAPG scores.

Table 4.6. *Partial correlation analysis*

	SARA	SARAPG	Disease duration	Falls	Step length	Stance duration	Swing duration	Double support	Cadence	Pelvic tilt	Pelvic obliquity	Pelvic rotation
HRAP	−0.26	**−0.39**	−0.22	**−0.37**	0.18	**−0.51**	**0.51**	**−0.51**	−0.03	0.04	0.06	−0.06
HRML	−0.26	**−0.33**	−0.25	**−0.37**	0.05	**−0.45**	**0.45**	**−0.46**	0.09	0.03	−0.02	−0.11
HRV	**−0.32**	**−0.33**	−0.25	**−0.37**	0.07	**−0.53**	**0.53**	**−0.55**	−0.12	0.06	−0.03	−0.11
CV	0.23	**0.30**	0.21	0.24	−0.20	**0.28**	**−0.28**	0.27	0.14	0.16	0.05	0.09
sLLEAP	−0.06	−0.19	−0.14	−0.20	**−0.46**	−0.20	0.20	−0.19	0.03	0.24	0.18	**0.37**
sLLEML	0.02	−0.13	**−0.30**	−0.19	−0.22	−0.39	0.39	−0.28	−0.17	**0.41**	0.17	**0.29**
sLLEV	0.04	−0.06	0.11	−0.74	−0.25	−0.21	0.21	−0.10	0.25	**0.37**	0.25	**0.50**
RMSAP	0.10	0.18	−0.11	0.05	**0.40**	−0.01	0.01	0.04	−0.14	−0.20	0.18	0.06
RMSML	−0.07	−0.07	−0.13	0.09	0.24	−0.01	0.01	0.01	−0.03	0.01	0.14	0.13
RMSV	−0.07	−0.07	−0.13	0.10	0.24	−0.01	0.01	0.01	−0.03	−0.01	0.14	0.13
RMSRAP	0.14	0.22	−0.08	0.04	**0.39**	0.01	−0.01	0.07	−0.12	−0.24	0.19	0.06
RMSRML	−0.11	−0.04	−0.13	0.14	0.15	0.05	−0.01	0.04	0.03	0.07	0.12	0.16
LDLJ-AV	0.12	−0.05	0.19	−0.15	0.20	0.05	−0.05	0.06	−0.23	0.08	−0.09	−0.15

SARA , scale for the assessment and rating of ataxia; SARA PG, posture and gait subscore of the SARA scale; HR, harmonic ratio; CV, coefficient of variation; LLE, short-term largest Lyapunov exponent; RMS, root mean square of the acceleration signals; RMSR, root mean square ratio; LDLJ-A, acceleration-based log dimensionless jerk. Significant speed-independent correlation coefficients at $p < 0.05$ are highlighted in bold

4.1.2 Parkinson's Disease

Patients with Parkinson's disease (PwPD) have gait deficits, which are one of the most debilitating aspects of the disease because they inevitably deteriorate over time, increasing the risk of falls and significantly reducing patient autonomy and quality of life. The mechanism underlying gait impairment is multi-factorial, involving both the dopaminergic and non-dopaminergic mechanisms related to bradykinesia, rigidity, impaired balance and postural control, visual motor deficiency, and cognition [38,39].

Because of these characteristics, as well as the impact of social and economic costs, treating gait abnormalities should be one of the primary foci of intervention in patients with Parkinson's disease.

Gait analysis has become an essential tool for objective evaluation of gait performance in recent years; in particular, a single lumbar-mounted IMU provides sensitive information on the gait of PwPD and allows clinicians to monitor their gait even when they are free-living [40]. IMUs directly provide trunk acceleration measurements and make it easier to record patient gaits for many steps during follow-up clinical assessments in outpatient facilities, making them ideal tools for studying gait stability in people with Parkinson's disease.

Therefore, the purpose of the study "*Ability of a Set of Trunk Inertial Indexes of Gait to Identify Gait Instability and Recurrent Fallers in Parkinson's Disease*" (2021) was to determine the accuracy of a set of trunk stability indexes in detecting gait instability in PwPD compared to healthy subjects, to

assess the ability of each index to characterize the gait of PwPD who fall recurrently, and to investigate the correlations of each index with clinical and biomechanical variables.

Subjects

We collected data samples from 62 subjects diagnosed with idiopathic PD who enrolled for our study at "ICOT" in Latina Italy, and the "IRCCS Mondino Foundation" in Pavia, Italy. The inclusion criteria were defined as follows: (i) diagnosis of idiopathic PD according to the UK bank criteria, (ii) Hoehn and Yahr (HY) stages 1 to 3 , (iii) ability to walk independently for at least 8 m along a laboratory pathway without exhibiting gait freezing and the ability to perform repeated walking trials with at least 10 consecutive strides, and (iv) on a stable drug program and acclimated to their current medication use for at least two weeks. For group comparisons, a group of 55 HS were recruited. Each HS repeated the tests twice: once walking at a self-selected speed and once walking at a slower directed speed.

Informed consent was obtained from all participants in compliance with the Helsinki Declaration and local ethics committee approval was obtained (CE Lazio2, protocol number: 0053667/2021).

Instrumentation and procedure

An inertial sensor (BTS GWALK, BTS, Milan, Italy) attached to an ergonomic belt placed around the pelvis at the level of the L5 vertebra and connected to a laptop via Bluetooth was used to acquire data. This sensor is equipped with a tri-axial accelerometer (16 bit/axes), tri-axial magnetometer (13 bits), and tri-axial gyroscope (16 bit/axes). Linear trunk accelerations and trunk angular velocities in the three directions were measured at a sampling rate of 100 Hz. To familiarize themselves with the experimental procedure, the participants were asked to walk on the ground along a predetermined pathway before the experimental session. Both the PwPD and HS were asked to walk barefoot at a self-selected speed along a corridor (approximately 3 m wide and 10 m long). To avoid the influence of gait speed on other gait parameters and collect the largest possible sample size for speed-matched comparisons, the HS were also asked to walk at a slower speed .

Data analysis

The "Walk+" protocol of the G-STUDIO software (G-STUDIO, BTS, Milan, Italy) was used to detect trunk acceleration patterns, right and left heel strikes, toe-off, spatiotemporal parameters, and pelvis kinematics. The HR, RQA, CV, NJS, and LLE were calculated using MATLAB (MATLAB 7.4.0, MAthWorks, Natick, MA, USA).

Statistical Analysis

After checking the normality of the distributions and homoscedasticity of the variances using the Shapiro-Wilk test for all variables and Levene's test, respectively, univariate ANOVA with Bonferroni's post-hoc analysis and the Kruskal-Wallis H test with Dunn's post-hoc analysis was performed to identify differences in the gait stability indexes between PwPD and $HS_{matched}$, as well as across the HY stages within the PwPD. To assess the ability of the identified indexes to discriminate between PwPD and $HS_{matched}$, characterize the gait of PwPD according to the HY stages, and characterize the gait of recurrent fallers, ROC curves were plotted and AUCs were calculated with the presence of PD, HY stages, and a reported number of falls ≥5 as anchors, respectively. AUC values greater than 0.60 with a confidence interval lower bound greater than 0.50 were considered for sufficient overall discriminative ability. The optimal cutoff points (OCPs) for each discriminative index were calculated as the points on the ROC curves that maximized the sum of sensitivity (Se) and specificity (Sp) values. Positive and negative likelihood ratios (LR+ and LR-) were also computed and transformed into post-test probabilities by using Fagan's nomogram to analyze the probability of being correctly classified by a given index at the OCP. Because the prevalence of recurrent fallers in our sample was low, to improve the generalizability of our results, the previously reported 39% prevalence of recurrent fallers in the general PD population was used to calculate post-test probabilities for the identification of recurrent fallers. Partial correlation coefficients (r) after removing the effects of age and gait speed were calculated to identify correlations between the identified indexes and UPDRS-III scores, history of falls, and spatiotemporal and kinematic parameters. Statistical analyses were performed using the IBM SPSS ver. 27 and NCSS 2019 software.

Results

After the matching procedure, 55 walking trials from PwPD and 55 age-and-speed matched walking trials from 30 HS ($HS_{matched}$) were included in our analysis. The final PwPD group consisted of 16 females and 39 males diagnosed with PD. Twelve subjects were assessed at the HY = 1 disability stage, 19 subjects at the HY = 2 stage, and 24 at the HY = 3 stage. The mean UPDRS-III score was 39.48 ± 16.91. Nineteen subjects had experienced at least one fall in the previous year with 1.63 ± 4.54 falls an average. Seven subjects reported more than five falls during the past six months and were classified as recurrent fallers [41]. The final $HS_{matched}$ group consisted of 55 walking trials from a sample of 30 subjects. Eighteen of the 55 $HS_{matched}$ trials were recorded at self-selected speeds and 37 were recorded at a reduced speed. No significant overall differences between group means were

identified for age or gait speed after the matching procedure. Post-hoc analysis revealed no significant differences for and gait speed between the HY stage subgroups and HS, neither between the HY subgroups.

Significant main effects of the group on HR_{AP} (H = 9.48, p = 0.024), HR_{ML} (H = 10.24, p = 0.017), HR_{V} (H = 14.30, p = 0.003), RQA_{det} in the AP direction (RQA_{detAP}) (H = 8.27, p = 0.041), and CV (H = 10.41, p = 0.015) were identified (Figure 4.11, Table 4.7).

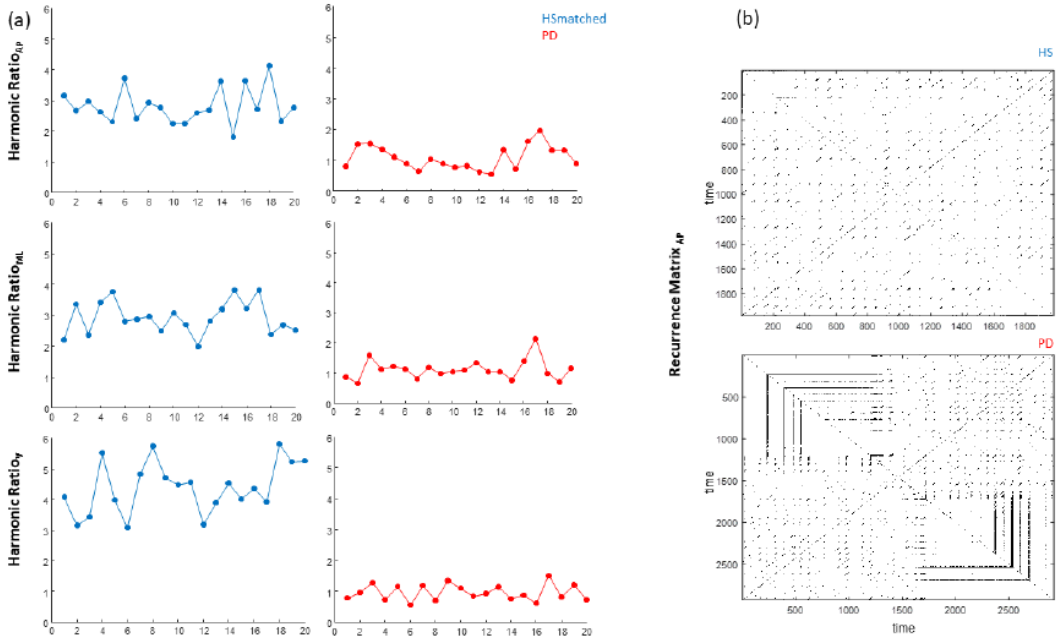

Figure 4.11 *(a) Graphical representation of the Harmonic Ratios in the antero-posterior, medio-lateral, and vertical directionsof a representative age-and-speed-matched healthy subject (blue) and a subject with PD at Hoehn and Yahr stage = 3 (red);(b) recurrence matrices in the antero-posterior direction of the same representative subject.*

Post-hoc analysis revealed significant differences in HR_{AP} between PwPD at HY stage = 3 and $HS_{matched}$, between PwPD at HY = 3 and HY = 1, and between PwPD at HY = 3 and HY = 2. A significant difference was identified in HR_{ML} between PwPD at HY = 3 and $HS_{matched}$. Significant differences were identified in HRV between PwPD at HY = 3 and $HS_{matched}$, and between PwPD at HY = 3 and HY = 2. Significant differences were identified in RQA_{detAP} between PwPD at all HY stages and $HS_{matched}$. A significant difference in CV was identified between PwPD at HY = 3 and $HS_{matched}$ (Table 4.7).

Table 4.7: *Comparison of the gait stability indexes between subjects with PD and HSmatched.*

	HY 1	HY 2	HY 3	HSmatched
	Mean (SD)	Mean (SD)	Mean (SD)	Mean (SD)
HR_{AP}	2.00 (0.55)	1.94 (0.51)	1.65 (0.34) * #	2.08 (0.67)
HR_{ML}	1.82 (0.49)	1.84 (0.48)	1.63 (0.37) *	1.97 (0.51)
HR_{V}	1.93 (0.53)	1.86 (0.41)	1.64 (0.37) *	2.05 (0.50)
RQA_{recAP}	3.13 (2.04)	4.21 (2.91)	4.35 (4.10)	5.24 (3.54)
RQA_{recML}	4.43 (4.83)	3.80 (4.08)	2.53 (3.77)	3.86 (3.31)
RQA_{recV}	4.73 (5.50)	3.44 (4.65)	5.38 (7.62)	2.76 (2.25)
RQA_{detAP}	23.20 (15.94) *	30.23 (17.89) *	28.37 (22.74) *	41.75 (27.07)
RQA_{detML}	31.09 (26.35)	33.93 (26.27)	22.63 (25.10)	34.93 (25.38)
RQA_{detV}	27.17 (28.83)	20.61 (20.05)	25.40 (23.67)	23.78 (16.04)
CV	39.36 (17.85)	35.56 (16.94)	40.92 (18.30) *	28.72 (14.08)
NJS_{AP}	2261.67 (1387.79)	4157.58 (3465.20)	4061.89 (2839.03)	3512.49 (3047.39)
NJS_{ML}	1169.38 (959.77)	1518.38 (1115.65)	1622.29 (1217.89)	1558.43 (1221.20)
NJS_{V}	1127.09 (808.44)	1526.17 (1166.67)	1591.34 (1925.34)	1656.37 (1169.45)
LLE_{AP}	0.53 (0.26)	0.49 (0.20)	0.60 (0.23)	0.53 (0.26)
LLE_{ML}	0.64 (0.23)	0.58 (0.18)	0.63 (0.20)	0.54 (0.28)
LLE_{V}	0.82 (0.28)	0.88 (0.21)	0.88 (0.21)	0.86 (0.29)

** significant differences between subjects with PD and HSmatched; #, significant differences between subjects with PD at HY 1,2 and HY 3; HY, Hoehn and Yahr disease staging classification system; HR, harmonic ratio; RQArec, recurrence quantification analysis, percent recurrence; RQAdet, recurrence quantification analysis, percent determinism; CV, coefficient of variation of the step length; NJS, normalized Jerk score; LLE, largest Lyapunov exponent.*

A good ability (AUC > 0.70) to discriminate between PwPD at HY = 3 and $HS_{matched}$ was identified for HR_{AP}, HR_{ML}, HR_{V}, CV (Table 4.8, Figures 4.12 and 4.13). A moderate ability (AUC = 0.65) to discriminate between PwPD at HY = (1, 2, 3) and $HS_{matched}$ was identified for RQA_{detAP} (Table 4.8, Figure 4.9). HR_{AP} values ≤ 1.50 identified PwPD at HY = 3 with 67% probability, HR_{ML} values ≤ 1.58 identified PwPD at HY = 3 with 54% probability, HR_{V} values ≤ 1.74 identified PwPD at HY = 3 with 57% probability, and CV values ≥ 38.06 identified PwPD at HY = 3 with 58% probability. RQA_{detAP} values ≤ 38.85 identified PwPD with 67% probability, regardless of the HY stage.

Table 4.8: *ROC curve and cutoff analysis results.*

Gait Index	Subjects	AUC (95% CI)	OCP	Se (95% CI)	Sp (95% CI)	LR+	LR−	PTP+	PTP−
HR_{AP}	HY = 3 vs. $HS_{matched}$	0.71 (0.56–0.81)	≤1.50	0.42 (0.22–0.63)	0.91 (0.80–0.97)	4.58	0.64	67%	22%
	HY = 3 vs. HY = 1.2	0.70 (0.53–0.80)	≤1.50	0.46 (0.25–0.67)	0.87 (0.70–0.96)	3.55	0.62	73%	32%
	recurrent fallers (≥5)	0.80 (0.52–0.92)	≤1.50	0.85 (0.42–0.98)	0.83 (0.70–0.92)	5.14	0.17	77%	10%
HR_{ML}	HY = 3 vs. $HS_{matched}$	0.72 (0.56–0.82)	≤1.58	0.58 (0.36–0.78)	0.78 (0.65–0.88)	2.67	0.53	54%	19%
HR_{V}	HY = 3 vs. $HS_{matched}$	0.76 (0.61–0.86)	≤1.74	0.71 (0.49–0.87)	0.76 (0.63–0.87)	3.00	0.38	57%	14%
RQA_{detAP}	All subjects with PD vs. $HS_{matched}$	0.65 (0.53–0.75)	≤38.85	0.74 (0.61–0.85)	0.63 (0.49–0.76)	2.05	0.40	67%	29%
CV	HY = 3 vs. $HS_{matched}$	0.72 (0.57–0.82)	≥38.06	0.58 (0.36–0.78)	0.81 (0.69–0.91)	3.21	0.51	58%	18%

AUC, area under the ROC curve; OCP, optimal cutoff point; Se, sensitivity; Sp, specificity; LR+, positive likelihood ratio; LR-, negative likelihood ratio; PTP+, positive post-test probability; PTP-, negative post-test probability; HR, harmonic ratio; $RQAdet_{AP}$. Recurrence quantification analysis, percent determinism in the antero-posterior direction; CV, coefficient of variation. of the step length.

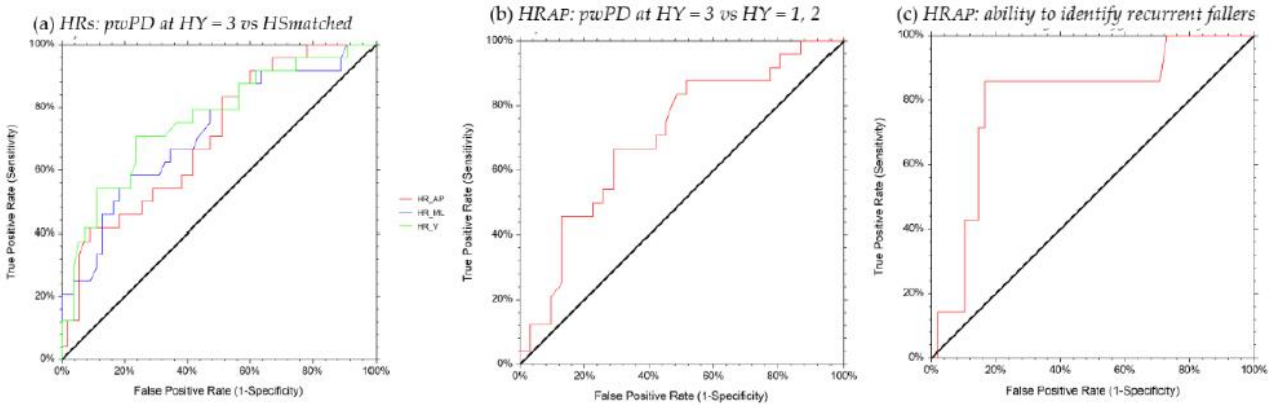

Figure 4.12 *ROC curves for the HRs in identifying PwPD vs. $HS_{matched}$, PwPD at HY = 3 from milder HY and recurrent fallers. The red line represents the HR_{AP}, the blue line the HR_{ML}, and the green line the HR_{V} fallers. The red line represents the HR_{AP}, the blue line the HR_{ML}, and the green line the HR_{V}.*

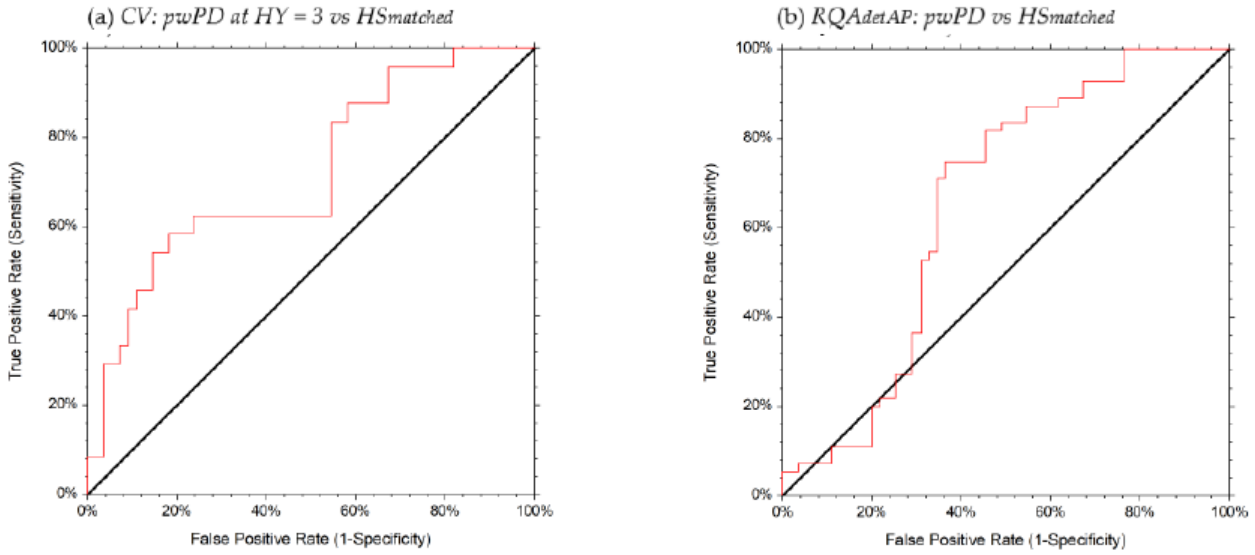

Figure 4.13 *ROC curves of the CV (a) and RQA_{detAP} (b) in discriminating PwPD from $HS_{matched}$.*

HR_{AP} exhibited a good ability to discriminate between PwPD at HY = 3 and HY = (1, 2) (Table 4.8, Figure 4.8). HR_{AP} values ≤ 1.50 discriminated PwPD at HY = 3 from subjects at lower HY stages with 73% probability. Furthermore, HR_{AP} exhibited a strong ability to identify recurrent fallers (Table 4.8, Figure 4.8). HR_{AP} values ≤ 1.50 identified frequent fallers with 77% probability.

After removing the effects of gait speed and age, HR_{AP} was negatively correlated with the history of falls (r = -0.45, p = 0.004) and positively correlated with pelvic obliquity (r = 0.37, p = 0.024) and pelvic rotation (r = 0.31, p = 0.040). RQA_{detAP} was negatively correlated with gait cadence (r = -0.35, p = 0.031) and positively correlated with stride time (r = 0.36, p = 0.030) and UPDRS III score (r = 0.385, p = 0.004). HR_{ML}, HR_{V}, and CV exhibited no correlations with clinical features or gait kinematics.

This study showed that the Harmonic Ratio, which measures the smoothness of the trunk acceleration patterns, the percent determinism in the antero-posterior direction of the accelerative pattern, which expresses the predictability of acceleration trajectories during the gait, and the coefficient of variation of the stride length, which reflects the continuous step-by-step adjustments of the gait strategy accurately characterize the gait of PwPD with a mild-to-moderate disability. Furthermore, HR_{AP} was discovered to be a potential marker of fall risk and to correlate with trunk rigidity and a decrease in pelvic motion [42]. These gait instability indexes could be useful outcome measures for evaluating the efficacy of rehabilitative interventions. However, before suggesting these indices as outcome measures in a clinical setting, their ability to change meaningfully over time and to parallel clinical changes following a rehabilitation intervention [43] should be studied.

As a result, the primary goal of the study *"Harmonic ratio is the most responsive trunk-acceleration derived gait index to rehabilitation in people with Parkinson's disease at moderate disease stages*" (2022) is to evaluate the internal responsiveness to rehabilitation of HR, RQA_{detAP}, and CV. Furthermore, we intend to determine: the external responsiveness of the gait stability indexes, as well as the minimal clinically significant differences that characterize PwPD who approach normative values after rehabilitation; the baseline gait parameters that predict the improvements of the gait stability indexes and the spatiotemporal and kinematic gait parameters that correlate with the improvements in the gait stability indexes following rehabilitation.

Subjects

We collected data samples from 21 subjects diagnosed with idiopathic PD (9 females and 12 males) with the following inclusion criteria: i) a diagnosis of idiopathic Parkinson's disease (PD) based on UK bank criteria; ii) HY stage 3; iii) the ability to walk repeatedly without assistance for at least 10 walking strides without exhibiting gait freezing; and iv) a stable and accustomed drug program for at least two weeks before baseline. Subjects with cognitive deficits (Mini Mental State Examination < 26), moderate-to-severe depression (Back Depression Inventory > 17), orthopedic and/or other gait-affecting diseases, including other neurological diseases, clinically defined osteoarthritis referring pain in hip or knee joints, reduced hip internal rotation, visible anatomic abnormalities of the joints, or total hip joint replacement, were all ruled out. The severity of PD was assessed using the HY disease staging system and the motor examination section of the Unified Parkinson's Disease Rating Scale (UPDRS-III) at baseline (T_0) and after (T_1) the rehabilitation period. For group comparison, a 1:1 optimal data matching procedure using propensity score difference method was performed to match pwPD with a dataset of 89 walking trials recorded in healthy subjects (HS). The propensity scores were computed using logistic regression analysis with age and speed as covariates. Following the matching procedure,21 age-and-speed-matched healthy subjects were included as a control group. Informed consent was obtained from all participants in compliance with the Helsinki Declaration and local ethics committee approval was obtained (CE Lazio2, protocol number: 0053667/2021).

Instrumentation and procedure

The data acquisition instrumentation is the same as in the previous study. Before the experimental session, the participants were asked to walk on the ground along a predetermined pathway to become acquainted with the procedure. PwPD were asked to walk at their self-selected speed along a corridor

(approximately 3 m wide and 30 m long) with no external sensory cues to interfere with their pacing and rhythm. PwPD were assessed before (T_0) and at the end (T_1) of their scheduled rehabilitation period during their "ON phase".

Data analysis

HRs in the three spatial directions, RQA_{detAP}, and CV were calculated using MATLAB (MATLAB 7.4.0, MathWorks, Natick, MA, USA) at T_0 and T_1. Walking trials with at least 10 consecutive correctly recorded strides were input into the analyses.

Statistical Analysis

After checking for the normality of the distributions through the Shapiro-Wilk test, a paired T-test or Wilcoxon test was performed to identify significant modifications in clinical and gait parameters at T_1. Cohen's d with Hedge's correction was calculated to assess internal responsiveness. Unpaired t-test or Mann-Whitney test was used to identify significant differences between PwPD and $HS_{matched}$ at T_0 and normalization at T_1. Changes in gait variables and UPDRS-III scores at T_1 were expressed as delta (Δ) values according to the following formula:

$$\Delta = 100 * \frac{value_{T1} - value_{T0}}{value_{T0}}$$

Multiple linear regression analysis with "backward" procedure was performed to identify the clinical and gait parameters that predicted the improvements of the gait stability indexes. Spearman's correlation coefficients were calculated to identify the correlations between the Δs of the modified gait stability indexes and the Δ_s of the clinical, spatio-temporal, and kinematic gait parameters. To exclude a carry-over effect of Δ_{gait} speed on the Δ_{gait} stability indexes, partial correlation analysis adjusting for the Δ_{gait} speed was also performed. An anchor-based method was used to assess the external responsiveness of the normalized parameters. AUCs were calculated to assess the ability of the correlated Δs to identify the subjects who improved and normalized the modified stability indexes, using the normalization of the gait stability indexes as the anchor. Each improved subject with PD was individually categorized as having the gait stability indexes "normalized" at T_1 if the thresholds characterizing PwPD at HY3 had been exceeded. The minimally clinically important differences (MCID) were calculated as the Δvalues that maximize the sum of sensitivity and specificity. Positive and negative likelihood ratios (LRs) were calculated at the MCID value and transformed into post-test probabilities through Fagan's nomograms. The probability to be identified as PwPD by the

threshold values was used as pre-test probabilities. All the statistical tests were set at 95 % significance level and 80 % power. Statistical analyses were performed using the IBM SPSS ver. 27 and NCSS 2019 software.

Results

No differences in age and gait speed between PwPD and $HS_{matched}$ were found, as shown in Table 4.9.

Table 4.9 *Results of the assessments at baseline and at T1 in PwPD and comparison with $HS_{matched}$.*

HSmatched		pwPD		p-value T0 vs. T1	d
		T0	T1		
UPDRSIII	–	43.85 (16.28)	30.80 (10.30)	0.00	0.97
Speed (m/s)	0.80 (0.21)	0.71 (0.21)	0.85 (0.26)	0.01	0.65
HRAP	2.00 (0.48)	1.55 (0.35) *	1.81 (0.35)	0.00	0.82
HRML	1.90 (0.38)	1.54 (0.30) *	1.67 (0.24)	0.03	0.52
HRV	2.02 (0.44)	1.61 (0.37) *	1.70 (0.32) *	0.22	0.28
RQAdetAP	40.56 (28.51)	34.12 (23.44)	30.45 (27.27)	0.71	0.03
CV	25.11 (10.47)	39.26 (20.63)*	36.87 (18.02)*	0.58	0.12
Stance duration (%)	62.32 (4.63)	61.45 (2.48)	61.01 (1.91)	0.46	0.17
Swing duration (%)	37.67 (4.63)	38.57 (2.32)	38.85 (2.09)	0.61	0.12
DS (%)	12.22 84.54)	11.30 (2.51)	10.80 (2.07)	0.35	0.21
SS (%)	38.06 (4.42)	38.53 (2.49)	38.99 (1.92)	0.42	0.18
Stride duration (s)	1.31 (0.23)	1.25 (0.27)	1.24 (0.41)	0.90	0.03
Stride length (m)	1.10 (0.19)	0.85 (0.22) *	0.98 (0.25)	0.01	0.62
Cadence (steps/min)	95.48 (13.77)	98.60 (23.35)	105.08 (22.63)	0.02	0.49
Pelvic Tilt (°)	2.76 (0.77)	3.01 (1.15)	3.46 (1.08) *	0.13	0.36
Pelvic Obliquity (°)	4.02 (1.39)	3.28 (2.38)	3.80 (2.10)	0.02	0.43
Pelvic Rotation (°)	7.00 (4.41)	4.44 (2.28) *	6.29 (3.55)	0.01	0.70

**Significant difference between pwPD and $HS_{matched}$ ($p < 0.05$); pwPD, persons with Parkinson Disease; $HS_{matched}$, age-and-speed matched healthy subjects; T0, baseline assessment; T1, assessment at the end of the rehabilitation period; AP, antero-posterior direction; ML, medio-lateral direction; V, vertical direction; HR, harmonic ratio; RQA_{det}, %determinism in the recurrence quantification analysis; CV, step length coefficient of variation; DS, double support phase; SS, single support phase; p-value, 95 % significance level of the paired samples tests; d, Cohen's effect size.*

At T_0, there were significant differences in HRs, CV, stride length, and pelvic rotation between PwPD and $HS_{matched}$. After rehabilitation, PwPD improved in HR_{AP}, HR_{ML}, gait speed, stride length, cadence, pelvic obliquity, pelvic rotation, and UPDRS-III, with medium-to-large effect sizes. At T_1, HR_{AP}, HR_{ML}, stride length, and pelvic rotation were no different from $HS_{matched}$, suggesting a normalization of these parameters. According to the multiple linear regression analysis models, lower HRs values, and higher pelvic rotation values at baseline predicted ΔHR_{AP} and ΔHR_{ML} (Table 4.10).

Table 4.10 *Multiple regression analysis findings.*

	Baseline variables	B	SE	*b*	t	p
ΔHR_{AP}	Constant	69.75	25.63		2.72	0.01
R^2_{adj}: 0.43,	HR_{AP}	-25.55	13.60	-0.57	-3.32	0.00
F = 8.34,	pelvic rotation	5.71	2.39	0.41	2.38	0.03
p = 0.00						
ΔHR_{ML}	Constant	57.85	17.23		3.36	0.00
R^2_{adj}: 0.45,	HR_{ML}	-40.57	10.52	-0.66	-3.85	0.00
F = 8.92,	pelvic rotation	3.19	1.51	0.36	2.11	0.05
p = 0.00						

With regard to correlations, Figure 4.14 show that ΔHR_{AP} correlated with ΔHR_{ML}, and both were positively correlated with Δ_{stride} length and Δ_{pelvic} rotation, regardless of Δ_{gait} speed.

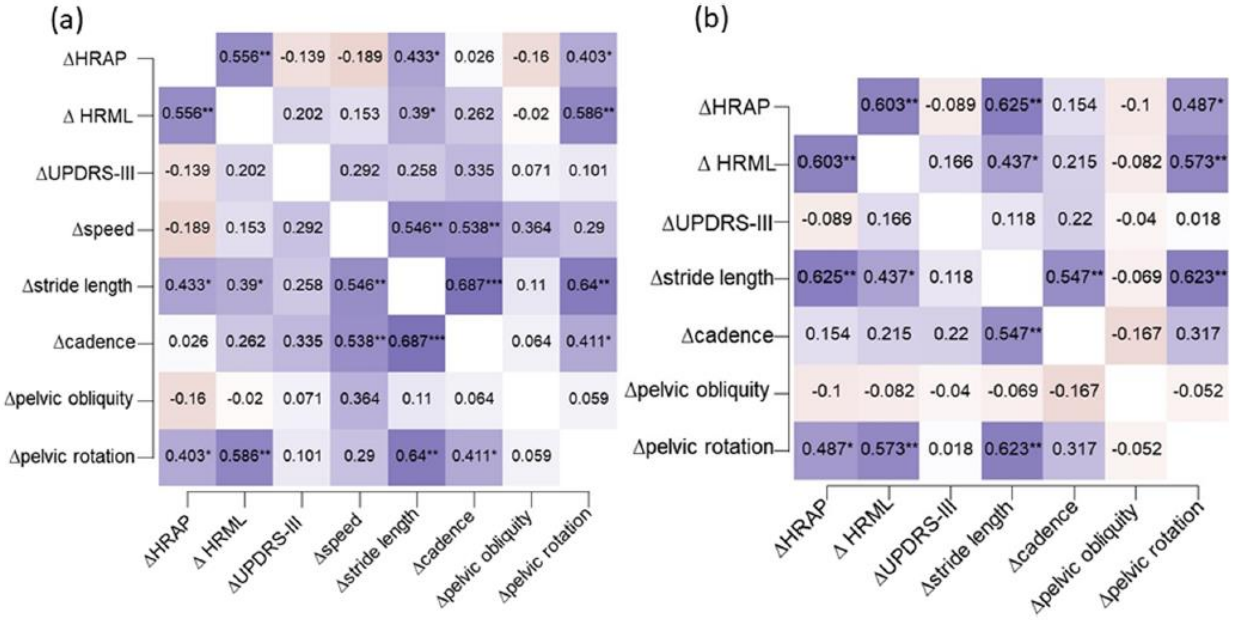

Figure 4.14 *a) Spearman's correlation coefficients between the improvements in gait parameters; b) Partial Spearman's correlation coefficients excluding the effects of the improvements in gait speed.*

Assuming the normalization of the gait stability indexes as anchor, HR_{AP}, HR_{ML}, stride length, and pelvic rotation revealed good-to-optimal responsiveness to rehabilitation (Table 4.11). Eight (38 %) and 6 (28 %) pwPD normalized their HR_{AP} and HR_{ML} values at T1, respectively. At the analysis of MCID, $\Delta HR_{AP} \geq 21.47$ %, $\Delta HR_{ML} \geq 11.31$ %, Δstride length ≥ 10.09 %, and Δpelvic rotation ≥ 8.59 % were needed to normalize HR_{AP} with 95 %, 88 %, 74 %, and 81 % probability, respectively (Table 4.11). $\Delta HR_{ML} \geq 36.94$ %, $\Delta HR_{AP} \geq 16.79$ %, Δstride length ≥ 22.67 %, and Δpelvic rotation ≥ 37.67

%, were needed to normalize HR_{ML} with 92 %, 71 %, 73 %, and 90 % probability, respectively (Table 4.11).

Table 4.11 *External responsiveness and minimal clinically important differences (MCID) analysis of normalized parameters.*

Criterion		AUC (95 % CI)	MCID	Se (95 % CI)	Sp (95 % CI)	LR+	LR-	PTP+	PTP-
HR_{AP} normalization	ΔHR_{AP}	0.87 (0.52–0.97)	≥ 21.47 %	0.66 (0.22–0.98)	0.92 (0.64–0.98)	8.67	0.36	95 %	42 %
	ΔHR_{ML}	0.84 (0.53–0.95)	≥ 11.31 %	0.83 (0.36–0.99)	0.77 (0.46–0.94)	3.61	0.21	88 %	30 %
	Δstride length	0.63 (0.42–0.78)	≥ 10.09 %	0.87 (0.47–0.93)	0.59 (0.21–0.80)	1.37	0.21	74 %	34 %
	Δpelvic rotation	0.70 (0.50–0.83)	≥ 8.59 %	0.87 (0.47–0.99)	0.58 (0.28–0.85)	2.10	0.21	81 %	30 %
HR_{ML} normalization	ΔHR_{ML}	0.90 (0.64–0.97)	≥ 36.94 %	0.60 (0.14–0.95)	0.94 (0.70–0.99)	9.60	0.42	92 %	33 %
	ΔHR_{AP}	0.74 (0.42–0.89)	≥ 16.79 %	0.80 (0.28–0.99)	0.62 (0.35–0.85)	2.13	0.32	71 %	27 %
	Δstride length	0.76 (0.44–0.90)	≥ 22.67 %	0.66 (0.27–0.96)	0.71 (0.42–0.92)	2.33	0.46	73 %	35 %
	Δpelvic rotation	0.81 (0.43)	≥ 37.67 %	0.60 (0.14–0.95)	0.94 (0.70–0.99)	7.50	0.38	90 %	38 %

Δ, difference between T_1 and T_0 values; HR_{AP}, harmonic ratio in the antero-posterior direction; HR_{ML}, harmonic ratio in the medio-lateral direction; AUC, area under the receiver operating characteristics curve; CI, confidence interval; MCID, minimal clinically important difference; Se, sensitivity; Sp, specificity; LR+ , positive likelihood ratio; LR-, negative likelihood ratio; PTP+ , positive post-test probability; PTP-, negative post-test probability.

In recent years, an innovative approach to assessing quantitative gait measures to qualitative clinical features for clinical practice purposes has been the use of quantitative machine-learning techniques such as artificial neural networks (ANNs), which, like real neural networks, are mathematical models that represent a distributed adaptive system built using multiple interconnecting processing elements [44,45]. However, few studies have attempted to identify and classify gait deficits using machine-learning approaches in neurological disorders such as Huntington's disease [46] and Parkinson's disease [47-49].

The goals of the study "*An artificial neural network approach to detect the presence and severity of Parkinson's disease via gait parameters*" (2021) were to develop a diagnostic algorithm based on machine-learning techniques (i.e., ANNs) capable of classifying the gait deficit of PwPD according to disease progression as assessed by the H–Y staging system and to identify the minimum set of gait time distance and kinematic parameters capable of distinguishing the H–Y stage gait pattern from each other.

Subjects

This study enrolled 76 PwPD. Clinical evaluation of the severity of Parkinsonism included neurological and functional assessments using the UPDRS III (18±12) and the H-Y staging system[26] (20 with H-Y = 1, 17 with H-Y = 2, 27 with H-Y = 3), and 12 with H-Y = 4. The inclusion criteria were: a diagnosis of idiopathic PD according to the UK Brain Bank Diagnostic Criteria [50], H-Y stages 1–4, stable drug program and the ability to walk independently on at least the laboratory pathway without showing freezing of gait. The exclusion criteria were: cognitive deficit (defined as

scores <24 on the Mini-Mental State Examination, moderate or severe depression (defined as scores ≥ 20 on the Beck Depression Inventory), and presence of orthopedic and/or other gait-influencing conditions such as arthrosis or total hip joint replacement. Medication was kept constant throughout the trial period and all interventions were performed at the same time of day for each patient during the "ON phase." The participants were asked to maintain their usual activity levels and current medication dosage when not in the laboratory. The assessments for both clinical and instrumental evaluations were not involved in the treatment of the patients and were blinded to the time of the evaluation. The patients were on oral levodopa (16 patients), dopamine agonists (27 patients), or both (33 patients) and were recorded to be in the "ON phase." Sixty-seven healthy subjects (HS) were enrolled as the healthy control group. All participants provided written informed consent before taking part in the study, which was approved by a local ethics committee (Sapienza University of Rome, Policlinico Umberto I, UP 00988_2020) and complied with the principles of the Declaration of Helsinki.

Instrumentation and procedure

An optoelectronic motion analysis system (SMART-DX 6000 System, BTS, Milan, Italy) consisting of six infrared cameras (sample frequency, 340 Hz) was used to collect data from the movement of twenty-two passive spherical markers covered with reflective aluminum powder placed over prominent bony landmarks, according to the International Society of Biomechanics recommendations and Davis's protocol.

The patients and controls were asked to walk barefoot at a comfortable, self-selected speed along a walkway approximately 10 m in length while looking forward; the HSs were also instructed to walk at low speeds in order to compare the parameters between groups without potential velocity bias. For PwPD, at least ten trials were recorded. For HSs, at least ten trials were recorded at a self-selected speed and ten trials at a slow speed. To avoid potential velocity bias, gait speed was matched between groups.

Data analysis

After each acquisition performed by Smart Capture (BTS, Milan, Italy), three-dimensional marker trajectories were reconstructed using a frame-by-frame tracking system (SMART Tracker, BTS, Milan, Italy). Then, the data were processed using SMART Analyzer (BTS, Milan, Italy) and MATLAB (version 7.10.0, MathWorks, Natick, MA, USA) software. In this study, heel strike and toe-off events were determined by maximum and minimum limb angle excursions. The limb angle

was calculated as the angle between the vertical axis from the greater trochanter and a vector drawn from the greater trochanter to the lateral malleolus projected on the sagittal plane: a 0˚ limb angle meant that the leg was positioned vertically under the body; positive angles denoted and negative angles denoted extension. After this preprocessing procedure, the time-distance and kinematic parameters were evaluated and the kinematic data were normalized to the duration of the gait cycle (defined as the interval between two successive foot contacts of the same leg) and interpolated to 101 samples using a polynomial procedure.

The following time-distance gait parameters were calculated: for each subject and for each stride: walking speed (m/s), cadence (step/s), step width (m), step length (m) (defined as the distance from the heel strike of a limb and the subsequent heel strike of the other limb), stance, swing, and double support phase durations (expressed as percentages of the gait cycle duration). Step length and step width were normalized to the limb length of each subject. For each subject, the average value of each gait feature was calculated.

The anatomical joint angles of the hip, knee, ankle, trunk, and pelvis (frontal, sagittal, and transverse planes) and the corresponding ranges of motion (RoMs) of the joints (defined as the differences between the maximum and minimum values during the gait cycle) were computed. For each subject, the average value of each RoM was calculated.

ANN approach for the diagnosis and staging of the gait deficit in PwPD. HS vs PwPD classification. A principal component analysis (PCA), using a threshold of 98% on the cumulative variance was used to define a subset of features starting from all time-distance and kinematic HS and PwPD features. An ANNs approach based on Levenberg-Marquardt back-propagation algorithm [51], was used for diagnosis of Parkinson disease using the features selected by PCA. We trained different topologies of feedforward networks with different numbers of hidden layers (HL) and different numbers of neurons (N) in each HL. Thus, the combination of L layers and N nodes in the first HL hidden layer led to the six different network architectures. To verify the repeatability of our results, each of the six network topologies was trained ten times by using a random 10% of samples as the validation set and a random 10% as the testing set. For each trained network, a confusion matrix was calculated based on the real value (HS or PwPD) and the one estimated on the randomly extracted testing set. The mean 2×2 confusion matrix was then obtained by averaging the confusion matrixes of the trained ANNs. A performance parameter (P) was calculated as the mean (%) of the elements on the diagonal of the mean confusion matrix, where 100% indicates the absence of misclassifications. Furthermore, the sensitivity and specificity of each group were calculated.

The entire system is schematically described in Figure 4.15. Then, to reduce the features, we also used subsets of features from the selected features with PCA and, for each subset, we trained the six ANNs ten times to evaluate the confusion matrix and performance. An ANN approach was also used to stages the gait deficits in PD in terms of the H-Y scale using the features selected by PCA and walking speed. We trained the six different topologies of feedforward networks. For each trained network, a confusion matrix was calculated based on the real H-Y value and the one estimated on the randomly extracted testing set. The mean 4×4 confusion matrix was then obtained by averaging the confusion matrices of the trained ANNs and the P was calculated. To reduce the features, we also used subsets of features from among the features selected by PCA and, for each subset, we trained the six ANNs ten times, evaluating the confusion matrix and performance. We started with all combination of two features subsets and continued until we found a subset whose performance was no different from that of the set with all features selected by PCA (Figure 4.15).

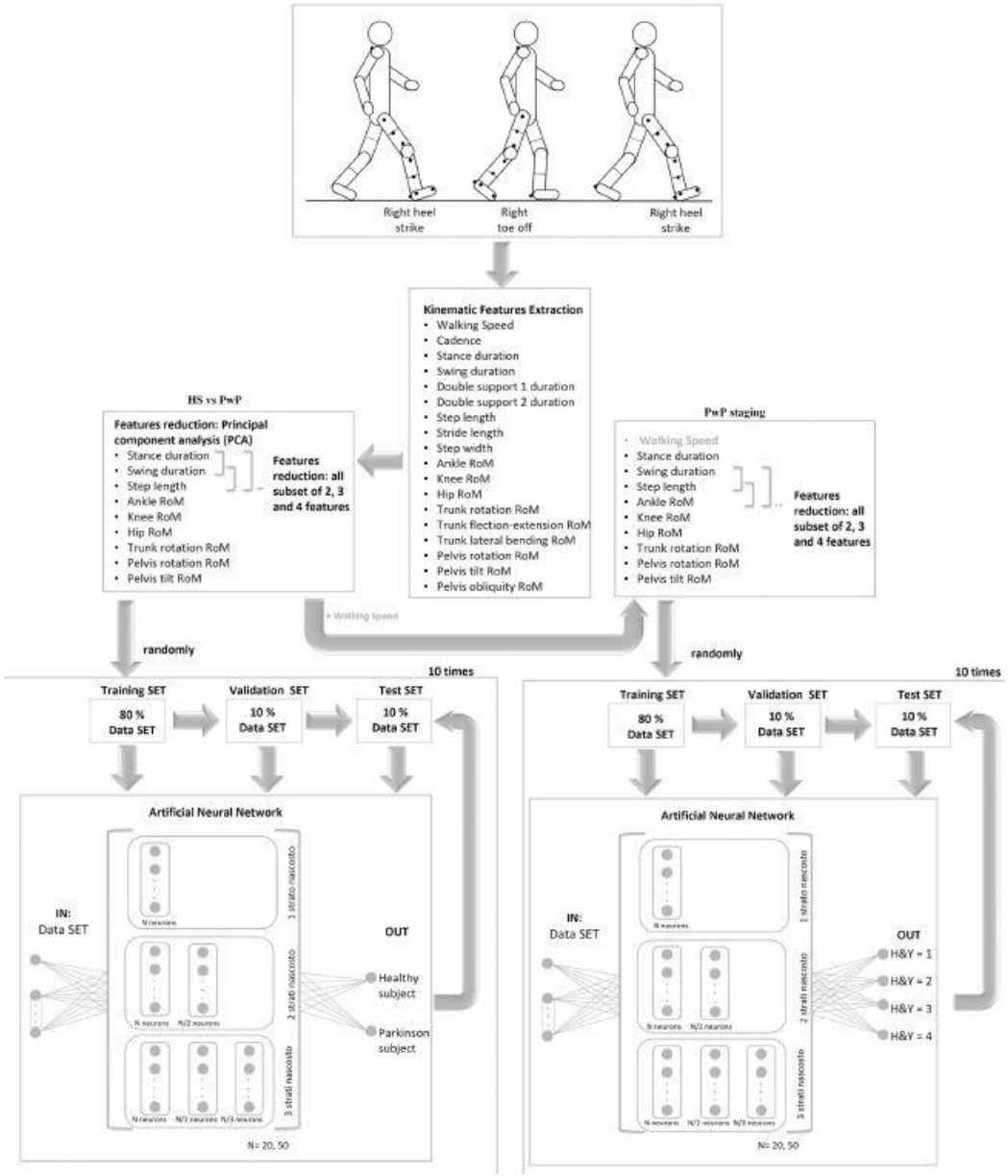

Figure 4.15 *Description of experimental set-up and methodological approach. A schematic description of the walking and artificial neural network method used to map time-distance and kinematic features on the H&Y (1, 2, 3 and 4) levels*

Statistical Analysis

The Shapiro–Wilk test for normal distribution was preliminarily executed on all gait parameters. Unpaired two-sample t-tests or Mann–Whitney tests (two-tailed) were used for assessment of between-group differences in the time-distance parameters and joint kinematics values. Then, we performed a two-way analysis of variance (ANOVA) test with L and N as factors to determine the possible significant effects on ANN performance, sensitivity and specificity caused by the listed factor. Separate ANOVAs test were performed for performance, sensitivity and specificity. Post-hoc

analysis with Bonferroni's corrections was performed when significant differences were observed in the ANOVA results. P values < 0.05 were considered statistically significant. Statistical analysis was performed to check if the results of the performance obtained using all features of PCA differed significantly from those obtained considering the subsets of two, three, or four features. As a confirmative analysis, independent samples t-tests and univariate ANOVA with Bonferroni post-hoc analysis were performed to test the ability of the identified minimum sets of gait parameters to differentiate between PwPD and HS, and PwPD across the H-Y stages, respectively. Receiver operating characteristic (ROC) curves were plotted to assess the discriminative ability of the identified minimum sets of gait parameters in differentiating PwPD from HS and PwPD across the H-Y stages. Area under the curve (AUC), sensitivity and specificity, and positive (LR+) and negative (LR-) likelihood ratios were calculated. The optimal cutoff points (OCP) for the cumulative indices of the combinations of gait parameters included in the identified sets were calculated as the point of the ROC curve where the sum of sensitivity and specificity was highest. Post-test probabilities were inferred by transforming LRs into odds ratios using the Fagan nomogram [52,53].

Results

Compared with HCs, PwPD showed significantly lower step length; stride length; hip, knee, and ankle RoMs; trunk flexion-extension; trunk rotation and pelvis rotation values; and higher cadence (Table 4.12)

Table 4.12: *kinematic parameters*

	Parameters	PwPD	HS
Spatio-temporal parameters	Gait speed (km/h)	2.87±1.07	3.18±0.91
	Stance duration (*% gait cycle*)	65.66±3.49	65.54±3.13
	Swing duration (*% gait cycle*)	34.34±3.49	34.46±3.13
	1st double support (*% gait cycle*)	15.74±3.68	15.40±3.16
	2nd double support (*% gait cycle*)	15.48±3.42	15.50±3.20
	Step length (*% limb length*)	0.68±0.14*	0.77±0.10
	Step width (*% limb length*)	0.30±0.05	0.28±0.05
	Stride length (*% limb length*)	1.19±0.32*	1.43±0.23
	Cadence	0.89±0.22*	0.77±0.15
Range of motion	RoM Hip	32.97±11.89*	37.38±5.23
	RoM Knee	52.28±9.39*	60.09±10.62
	RoM Ankle	24.19±7.26*	32.00±12.05
	Trunk lateral bending [°]	3.31±2.05	4.05±1.66
	Trunk flexion-extension [°]	2.84±1.10*	5.99±2.45
	Trunk rotation [°]	8.64±5.05 *	14.36±11.12
	Pelvis obliquity [°]	4.82±3.37	5.77±2.06
	Pelvis rotation [°]	11.20±8.55*	16.48±13.26
	Pelvis tilt [°]	67.78±21.98*	84.25±24.43

*Mean ± SD of time-distance and kinetic parameters in patients with Parkinson disease (PwPD) patients and healthy subjects (HS). * p-value<0.05.*

The PCA showed that a set of nine features (stance duration, swing duration, step length, ankle, knee, hip, trunk rotation, pelvis rotation, and pelvis tilt RoM) expressed 98% of the cumulative variance of the data (Figure 4.16A).

The ANNs analysis revealed a mean performance range of 82–98% (Figure 4.16A), a mean sensitivity range of 81–89% (Table 4.13), and a mean specificity range of 81–89% (Table 4.13) for all features detected by PCA for each number of neurons and HL. The number of neurons did not affect the performance ($F1 = 0.15$, $p = 0.699$), sensitivity ($F1 = 0.5$, $p = 0.482$), or specificity ($F1 = 0.5$, $p = 0.482$) in two-way ANOVA. Furthermore, the HL did not affect the performance ($F2 = 0.48$, $p = 0.621$), sensitivity ($F2 = 0.32$, $p = 0.724$), or specificity ($F2 = 0.48$, $p = 0.621$) in two way ANOVA. By analyzing all the possible combinations, we found that one combination of two features was the minimum set of gait parameters able to distinguish PwPD from controls (knee RoM, trunk rotation RoM) and whose performance (Figure 4.16A) did not significantly differ ($p>0.05$) from that of all PCA features.

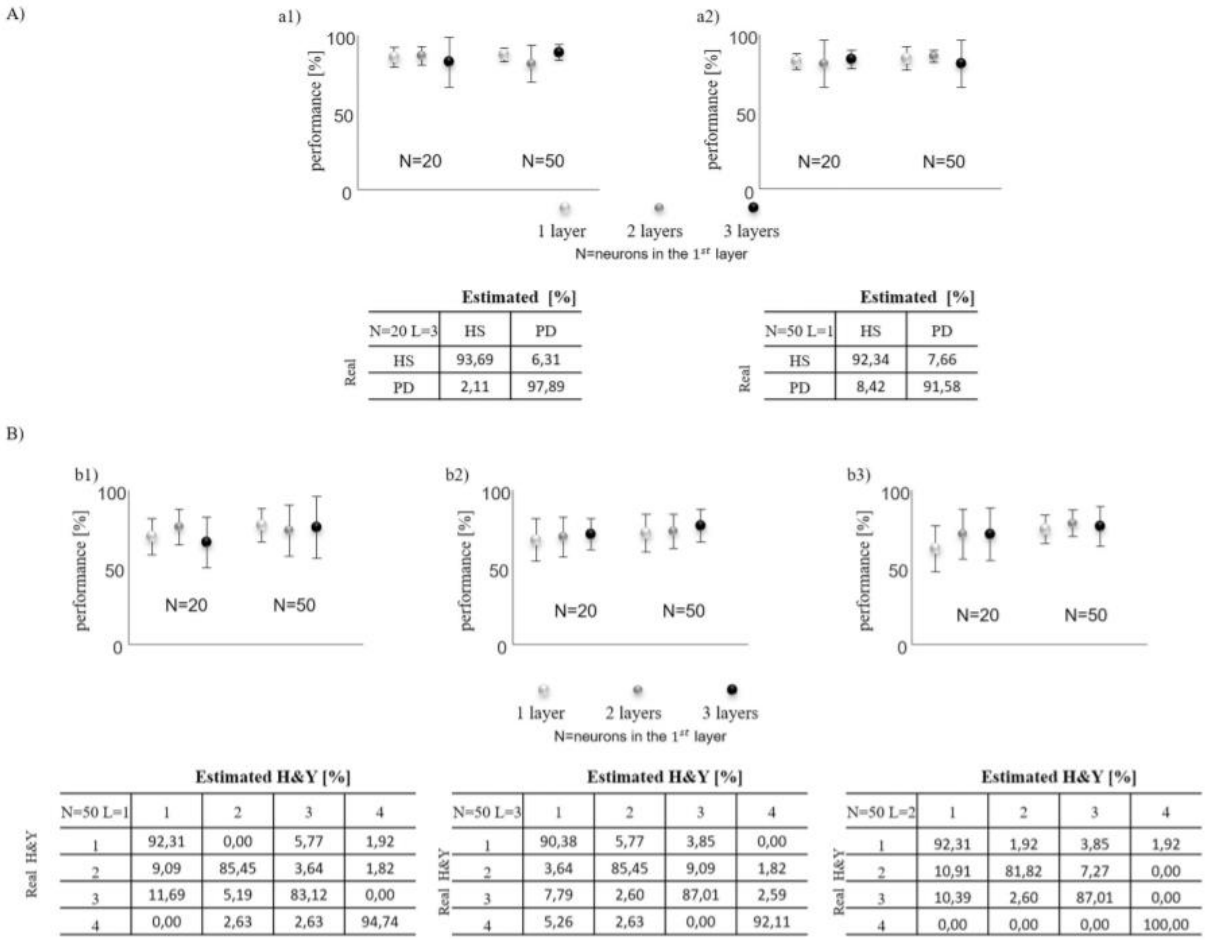

Figure 4.16 *Accuracy of artificial neural networks and the best mean confusion matrix. For diagnosis (A) and staging (B), in the first row the accuracy of artificial neural networks and in the second row the best mean confusion matrixes considering all PCA features as INPUT (a1 and b1) and subset of 2 features (knee RoM and trunk rotation RoM (a2)) and subsets of 4 features (walking speed, hip, knee and ankle RoMs (b2); walking speed, hip, knee and trunk rotation RoMs (b3)). Six different architectures of neural networks were represented by varying the numbers of hidden layers (1, 2, or 3) and the numbers of neurons in each hidden layer based on the numbers of nodes N in the first hidden layer.*

The results of the independent sample t–test and ROC curve analysis confirmed that the combination of knee and trunk rotation RoM values could significantly differentiate between PwPD and HS (t-statistic = −5.34, p<0.00) and to have good discriminative ability (AUC = 0.77). The numerical sum of knee and trunk rotation RoMs ≤ 66.23 was able to identify PwPD from HS with a 75% probability (Table 4.14).

The ANNs analysis revealed a mean performance range of 66.16–77.2% (Figure 4.11B), mean sensibility range of 66–77% (Table 4.13) and mean specificity range of 85–91% (Table 4.13) for all features detected by PCA for each number of neurons and HLs. The number of neurons had no effect on the performance (F1 = 2.82, p = 0.099), sensitivity (F1 = 0.41, p = 0.522), and specificity (F1 =

0.59, p = 0.448) in two-way ANOVA. Furthermore, the HL had no effect on the performances (F2 = 0.66, p = 0.522), sensitivity (F2 = 0.7, p = 0.499), and specificity (F2 = 0.29, p = 0.749) in two-way ANOVA.

By analyzing all the possible combinations, we found that two combinations of four features (walking speed and hip, knee, and ankle RoMs; walking speed and hip, knee, and trunk rotation RoMs) were the minimum set of gait parameters able to distinguish H-Y stage gait patterns from one another and whose performances (Figure 4.11B) did not differ significantly (p>0.05) from that of all PCA features. All combinations of two or three features showed a significant difference (p<0.05) from that of all PCA features. The numerical sums of speed, hip RoM, knee RoM, and ankle RoM (SET1) and speed, hip RoM, knee RoM, and trunk rotation RoM (SET2) were able to differentiate PwPD according to H-Y stage (F = 7.59, p<0.00 and F = 9.27, p<0.00, respectively).

Table 4.13 *Sensitivity and specificity.*

			HS vs PwPD classification.									PwPD staging classification														
	L	N	HS			PwPD			Mean			H&Y = 1			H&Y = 2			H&Y = 3			H&Y = 4			Mean		
sensibility [%]	1	20	93.2	±	2.03	78.32	±	11.2	85.76	±	5.66	87.88	±	5.52	61.27	±	15.99	69.09	±	8.41	61.05	±	17.4	69.83	±	7.36
	2	20	91.76	±	3.71	81.89	±	8.24	86.83	±	4.77	89.81	±	5.37	66.18	±	15.24	74.29	±	7.08	74.47	±	18.11	76.19	±	8.31
	3	20	91.89	±	4.53	73.58	±	27.59	82.74	±	12.54	87.69	±	9.34	52.36	±	21.66	70.65	±	12.61	53.95	±	21.1	66.16	±	13.1
	1	50	94.19	±	1.48	80.63	±	7.33	87.41	±	3.27	90.77	±	4.23	69.27	±	18.31	75.84	±	7.27	72.89	±	13.19	77.2	±	7.75
	2	50	92.97	±	1.69	70	±	22.21	81.49	±	10.85	86.92	±	11.13	66	±	20.21	71.04	±	12.78	71.58	±	22.32	73.89	±	11.23
	3	50	92.79	±	2.11	84.84	±	8.04	88.82	±	4.21	89.23	±	7.03	67.64	±	24.87	72.34	±	22.87	73.95	±	24.79	75.79	±	16.41
specificity [%]	1	20	78.32	±	11.2	93.2	±	2.03	85.76	±	5.66	72.32	±	7.03	92.12	±	5.05	90.66	±	10.85	96.86	±	5.14	87.99	±	3.58
	2	20	81.89	±	8.24	91.76	±	3.71	86.83	±	4.77	79.1	±	10.47	95.12	±	5.21	91.23	±	5.7	97.91	±	1.84	90.84	±	3.76
	3	20	73.58	±	27.59	91.89	±	4.53	82.74	±	12.54	67.5	±	17.57	91.71	±	5.63	87.11	±	11.05	97.5	±	3.04	85.95	±	7.11
	1	50	80.63	±	7.33	94.19	±	1.48	87.41	±	3.27	80.68	±	9.94	95.03	±	3.76	90.56	±	4.89	98.53	±	0.73	91.2	±	3.49
	2	50	70	±	22.21	92.97	±	1.69	81.49	±	10.85	75.07	±	17.92	95.32	±	2.73	92.24	±	7.43	98.39	±	1.43	90.26	±	4.24
	3	50	84.84	±	8.04	92.79	±	2.11	88.82	±	4.21	76.91	±	25.38	95.38	±	3.82	94.72	±	4.78	98.2	±	1.26	91.3	±	5.38

Sensitivity and Specificity of set with all PCA features for HS vs PwPD classification and for PwPD staging classification.

Post-hoc analysis revealed that SET1 was significantly different between H-Y stages 1 and 4 (p<0.00) and stages 3 and 4 (p = 0.02), while SET2 was able to differentiate between H-Y stages 1 and 2 (p = 0.03), 1 and 3 (p = 0.03), 1 and 4 (p<0.00), and 3 and 4 (p = 0.03). The AUCs, OCPs, sensitivity, specificity, LRs, and post-test probabilities of each set to discriminate PwPD across the H-Y stages are summarized in Table 4.14.

Table 4.14 *Ability to discriminate between PwPD and HS and between disability levels.*

	HS vs PwPD	HY 2 vs 1		HY 3 vs1		HY 4 vs 1		HY 4 vs 3	
	SET	SET1	SET2	SET1	SET2	SET1	SET2	SET1	SET2
AUC	0.77	n.a.	0.73	n.a.	0.76	0.88	0.88	0.77	0.78
OCP	≤ 66.23	n.a.	≤ 105.42	n.a.	≤ 103.91	≤111.71	≤98.09	≤99.28	≤81.35
Se (%)	72.37	n.a.	76.47	n.a.	81.48	91.67	75	66.67	58.35
Sp (%)	73.13	n.a.	60	n.a.	70	80	92	88.89	96.30
LR+	2.69	n.a.	1.91	n.a.	2.72	4.58	3.66	6	15.75
LR-	0.38	n.a.	0.39	n.a.	0.26	0.10	0.11	0.37	0.43
+PTP (%)	75	n.a.	62	n.a.	79	73	69	73	88
-PTP (%)	30	n.a.	25	n.a.	26	6	6	14	16

HS = Healthy Subjects; PwPD = people with Parkinson's Disease; HY = Hoehn & Yahr disability stage; SET = Knee RoM+Trunk rotation RoM; SET1 = combination of gait speed, hip, knee and ankle Roms values; SET2 = combination of gait speed, hip, knee and trunk rotation RoMs values; AUC = area under the curve; OCP = optimal cutoff point; Se = sensitivity; Sp = specificity; LR+ = positive likelihood ratio; LR- = negative likelihood ratio; +PTP = positive post-test probability: the probability to identify a true positive at OCP; -PTP = negative post-test probability: the probability to identify a false negative at OCP.

Briefly, PwPD at H-Y stage 1 were identified by cumulative SET1 values ≥ 111.71 and SET2 values ≥105.42, PwPD at H-Y stage 2 by cumulative SET2 values ≥ 103.91 and ≤ 105.42, PwPD at H-Y stage 3 by SET2 values ≥ 81.35 and ≤ 103.91, and PwPD at H-Y stage 4 by SET1 values ≤ 99.28 and SET2 values ≤ 81.35.

4.1.3 Hemiparesis

Patients with hemiparesis (HP), like those with Parkinson's disease and cerebellar ataxia, have abnormal gait patterns that include increased gait asymmetry, resulting in imbalance, inefficiency, risk of musculoskeletal injury in the nonparetic limb, loss of bone mass density in the paretic leg, difficulties maintaining a stable gait, and a high risk of falling [54]. Gait asymmetry has been quantified using spatiotemporal gait parameters such as step length, stance time, swing time, or an intralimb swing/stance time ratio. Furthermore, one of the main symptoms of hemiparetic gait is a change in trunk and pelvic biomechanics, which results in impaired trunk function, or as a secondary compensatory change caused by lower limb impairment during gait [55,56]. The aim of the study "*Ability of a set of trunk-acceleration derived gait indexes to characterize gait instability and asymmetry in stroke survivors*" (in progress) is to observe which of the trunk-acceleration indexes can accurately characterize the gait abnormalities of HP and reflect the gait asymmetry.

Subjects

Thirty-five stroke survivors (17 males, 18 females, aged 63.57 ± 15.31 years) were enrolled for this study at "ICOT" in Latina, Italy. 27 subjects suffered from ischemic stroke, 8 suffered from hemorrhagic stroke since 14.48 ± 22.71 months. 18 subjects were affected by right hemiparesis, 17 from left hemiparesis. Inclusion criteria were: (i) first ever subacute or chronic stroke; (ii) hemiparesis caused by a left or right subcortical or cortical lesion in the middle cerebral artery's territory; (iii) residual ability to walk independently for at least 30 meters. The control group consisted of 35 age-speed-matched healthy subjects (HS). All the participants were required to give their informed consent before they started the study, which complied with the Helsinki Declaration and was approved by the local ethics committee (CE Lazio2, protocol number: 0213481/2021).

Instrumentation and procedure

To collect data, an inertial sensor (BTS GWALK, BTS, Milan, Italy) was attached to an ergonomic belt at the level of L5 and Bluetooth-connected to a portable computer. At a sampling rate of 100 Hz, the sensor measures linear trunk accelerations as well as trunk angular velocities and displacements in three space directions (anterior-posterior, latero-lateral, and vertical).

Both patients and HS were asked to walk barefoot along a corridor at their self-selected speed (approximately 3 m wide and 30 m long). To avoid the effect of gait speed on other gait parameters, the HS repeated the tests a second time at a slower speed.

Data analysis

We calculated the following trunk-acceleration indexes: HR, iHR, CV, NJS, LDJ, RQA,LLE, RMS. To assess symmetry, we calculated the following indexes:

- Symmetry Index (SI) considering stance time, swing time and double support time. This index was calculated using the following equation [57]:

$$SI = \left[\frac{(V_{paretic} - V_{non\ paretic})}{0.5 * (V_{paretic} + V_{non\ paretic})}\right] * 100$$

The smaller the index value, the greater the gait symmetry.

- Symmetry Angle (SA) calculated using the angular ranges of pelvic movement in three directions of space as a parameter, distinguishing between the paretic and non-paretic side, according to the following equation [58]:

$$SA = \frac{[\left(45° - \arctan\left(\frac{V_{paretic}}{V_{non\ paretic}}\right)\right) * 100]}{90}$$

An SA value of 0% indicates perfect symmetry, while 100%indicates that the two values are equal and opposite in magnitude.

- Pelvis Symmetry Index (SI_{pelvis}) obtained from the correlation between the measures of the pelvic angles, using the following formula:

  $$SI = \frac{(r + 1) * 100}{2}$$

  Where r is the Pearson's correlation coefficients between the mean normalized pelvic angles signal of the left and right gait cycles, extracted from the whole pelvic angle signals. SI_{pelvis} values range from 0 to 100: the higher the symmetry index value, the more similar the pelvic angular displacements between the two sides will be.
- Step Regularity (SR) calculated used an unbiased autocorrelation procedure to measure the correlation of the acceleration signal for each step at different periods of time across each of the three accelerometer axes [59,60]. Step regularity was defined as the correlation between the original acceleration signal and the acceleration signal phase shifted to the average step time, and its values range from 0 to 1.

Statistical Analysis

We used MATLAB R2021b for statistical analysis. All data were expressed as mean ± standard deviation; $p < 0.05$ was considered statistically significant. We assessed the normality of distributions using the Shapiro-Wilk test. Mean and standard deviation within subjects were computed for all calculated indexes. We used the independent-samples t test to look for differences between the stability and symmetry indexes of HP vs. HS. Cohen's d index was used to assess the effect size of the stability and symmetry indexes in the three spatial directions. To assess the ability of the identified indexes to discriminate between HP and HS, area under the curves (AUCs) was calculated. The optimal cutoff points (OCPs) for each discriminative index were calculated as the points on the ROC curves that maximized the sum of sensitivity (Se) and specificity (Sp) values. Positive and negative likelihood ratios (LR+ and LR-) were also computed and transformed into post-test probabilities (PTP) by using Fagan's nomogram to analyze the probability of being correctly classified by a given index at the OCP. Partial correlation coefficients (r) after removing the effects of age and gait speed were calculated to identify correlations between the stability and symmetry indexes.

Results

Significant main effects ($p<0.05$) were identified on different gait stability indexes, as shown in Table 4.15. HR and RMSR, in particular, differ significantly between HS and HP in all three directions (Figure 4.17).

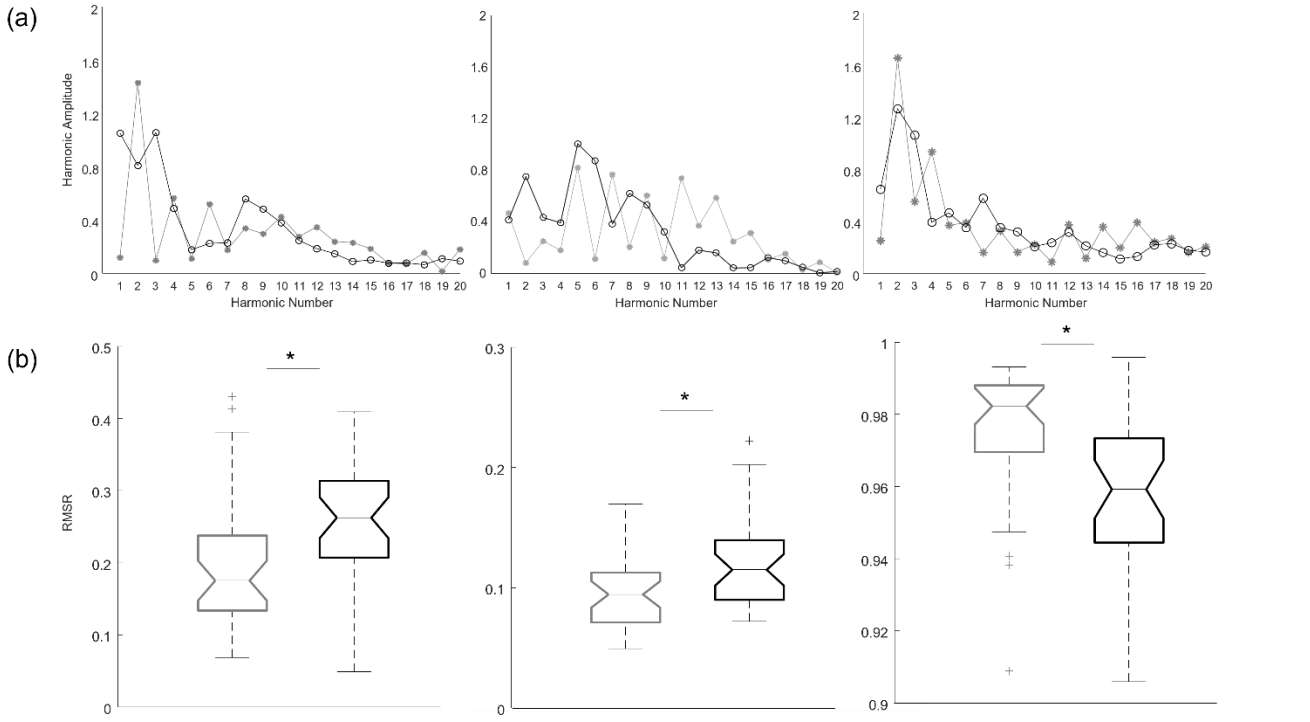

Figure 4.17 *(a) Graphical representation of the first 20 amplitude harmonics in the antero-posterior, medio-lateral, and vertical directions of a representative age-and-speed-matched healthy subject (grey) and a hemiplegic patient (black); (b) boxplot of the RMSR in the three directions.*

Table 4.15 *Comparison of the gait stability indexes between HP and $HS_{matched}$*

	HP		HS		t	p	d
	Mean	SD	Mean	SD			
HR_{AP}	1.44	0.34	1.95	0.41	5.63	**0.00**	1.35
HR_{ML}	1.44	0.31	1.84	0.38	4.82	**0.00**	1.15
HR_{V}	1.36	0.36	1.88	0.49	5.07	**0.00**	1.21
C_{V}	31.57	12.33	20.52	11.09	3.94	**0.00**	0.94
iHR_{AP}	61.64	9.63	71.24	13.53	3.42	**0.001**	0.82
iHR_{ML}	62.02	8.81	69.96	13.68	2.89	**0.005**	0.69
iHR_{V}	59.86	10.39	72.66	13.66	4.41	**0.00**	1.06
LDJ_{AP}	-7.73	1.14	-7.20	1.18	1.91	0.061	0.46
LDJ_{ML}	-10.21	0.74	-9.88	0.75	1.83	0.072	0.44
LDJ_{V}	-7.73	0.88	-7.19	1.05	2.32	**0.023**	0.55
LLE_{AP}	1.01	0.31	0.94	0.36	0.84	0.402	0.20
LLE_{ML}	0.64	0.26	0.59	0.30	0.74	0.462	0.18
LLE_{V}	0.82	0.43	0.60	0.30	2.42	**0.018**	0.58
RMS_{AP}	2.60	1.14	1.93	0.93	2.72	**0.008**	0.65
RMS_{ML}	1.20	0.38	0.93	0.28	3.39	**0.001**	0.81
RMS_{V}	9.40	0.44	9.57	0.27	470.50	0.095	0.45
$RMSR_{AP}$	0.26	0.11	0.20	0.09	2.69	**0.009**	0.64
$RMSR_{ML}$	0.12	0.04	0.09	0.03	3.37	**0.001**	0.81
$RMSR_{V}$	0.95	0.04	0.97	0.03	348.50	**0.002**	0.66
NJS_{AP}	1111.41	937.16	1910.89	1377.42	384.00	**0.007**	0.68
NJS_{ML}	1257.80	912.99	1864.89	1436.80	460.00	0.073	0.50
NJS_{V}	2728.50	1974.88	3943.45	2584.01	443.00	**0.04**	0.53
$\%rec_{AP}$	7.43	9.86	4.23	6.93	588.50	0.778	0.38
$\%rec_{ML}$	3.41	3.76	4.59	6.18	531.50	0.341	0.23
$\%rec_{V}$	13.12	11.73	7.83	13.29	432.50	**0.034**	0.42
$\%det_{AP}$	43.12	30.36	24.59	18.52	394.00	**0.01**	0.74
$\%det_{ML}$	45.84	31.87	33.74	24.47	489.00	0.147	0.43
$\%det_{V}$	58.26	31.53	40.53	26.17	408.00	**0.016**	0.61
SR_{AP}	0.602	0.195	0.719	0.173	366.500	**0.004**	0.638
SR_{ML}	0.191	0.124	0.233	0.152	1.247	0.217	0.298
SR_{V}	0.771	0.133	0.803	0.120	1.044	0.300	0.250

Mean ± standard deviation values, the results of the independent samples t-test and Cohen's d are reported. HS, Healthy Subjects; HP, Patients with Hemiparesis; HR, harmonic ratio; CV, coefficient of variation; iHR, improved Harmonic Ratio; LDJ, Log Dimensionless Jerk; LLE, largest Lyapunov exponent; RMS, Root Mean Square; RMSR, Root Mean Square Ratio; NJS, normalized Jerk score; %rec, percent recurrence; % det, percent determinism; SR, Step Regularity.

Statistically significant differences were also found for the symmetry parameters, specifically the SI calculated for the stance and swing parameters and the SA calculated for the pelvic obliquity, all in comparison to the respective parameters calculated in healthy subjects (Table 4.16).

Table 4.16 *Comparison of the symmetry indexes between HP and $HS_{matched}$*

	HP		HS		p	d
	Mean	SD	Mean	SD		
SI_{ST}	6.37	7.11	3.41	2.93	**0.03**	0.54
SI_{SW}	11.18	11.20	5.99	4.82	**0.02**	0.60
SI_{DS}	14.18	12.43	14.12	9.76	0.98	0.01
SA_{TILT}	3.09	3.35	2.54	2.60	0.50	0.18
$SA_{OBLIQUITY}$	3.30	2.97	1.56	1.44	**0.01**	0.74
$SA_{ROTATION}$	4.56	4.59	2.83	2.53	0.22	0.46
$SI_{pelvisTILT}$	65.543	28.280	53.149	39.067	0.240	0.363
$SI_{pelvisOBLIQUITY}$	49.346	56.083	93.851	13.465	**< .001**	1.091
$SI_{pelvisROTATION}$	55.469	61.403	94.242	12.677	**< .001**	0.875

Mean ± standard deviation values, the results of the independent samples t-test and Cohen's d are reported. HS, Healthy Subjects; HP, Patients with Hemiparesis; SI, Symmetry Index; SA, Symmetry Angle; SI_{pelvis}, pelvis Symmetry Index.

Finally, when the paretic and healthy sides of the HP were compared to the respective HS, significant differences in pelvic tilt of the paretic side compared to healthy subjects, as well as pelvic obliquity of both the healthy and paretic sides compared to healthy subjects, were observed. (Table 4.17).

Table 4.17 *Comparison of the spatiotemporal and pelvic parameters between HP and $HS_{matched}$*

	HS		HP							
			Paretic				non Paretic			
	Mean	**SD**	**Mean**	**SD**	**p**	**d**	**Mean**	**SD**	**p**	**d**
Stride Length	1.07	0.21	1.14	0.31	0.27	0.27	1.14	0.32	0.25	0.28
Stance phase duration (%)	62.23	3.80	61.19	5.25	0.34	0.22	62.69	4.99	0.58	0.13
Swing phase duration (%)	37.76	3.79	38.81	5.25	0.34	0.23	37.31	4.99	0.59	0.13
Double Support duration (%)	11.79	3.79	11.75	4.32	1.00	0.01	11.84	4.52	0.51	0.12
Pelvic tilt (°)	2.68	0.98	3.29	1.56	**0.04**	0.46	3.28	1.55	0.10	0.43
Pelvic obliquity (°)	4.84	2.41	3.43	2.17	**0.02**	0.61	3.47	2.12	**0.02**	0.61
Pelvic rotation (°)	6.66	2.99	5.93	3.36	0.21	0.23	5.97	3.30	0.40	0.15

Mean ± standard deviation values, the results of the independent samples t-test and Cohen's d are reported. HS, Healthy Subjects; HP, Patients with Hemiparesis.

A good ability (AUC > 0.70) to discriminate between HP and HS was identified for $HR_{AP,ML,V}$, $iHR_{AP,ML,V}$, CV, RMS_{ML} and $RMSR_{ML}$,V. HS and HP were discriminated by HR_{AP} values< 1.67 with 82% probability, HR_V values with 80% probability, HR_{ML} values<1.49, iHR_{AP} values<67.43 and iHR_V <68.04 with 81% probability (Table 4.18).

Table 4.18 *Discriminative ability and cutoff analysis*

Criterion	AUC	95% CI		OCP	Se	95% CI		Sp	95% CI		LR+	LR-	PTP+	PTP-
HR_{AP}	0.84	0.72	0.91	≤ 1.67	0.80	0.63	0.92	0.83	0.66	0.93	4.67	0.24	82%	19%
HR_{ML}	0.79	0.66	0.88	≤ 1.49	0.60	0.42	0.76	0.86	0.70	0.95	4.20	0.47	81%	32%
HR_{V}	0.79	0.66	0.88	≤ 1.48	0.69	0.51	0.83	0.83	0.66	0.93	4.00	0.38	80%	28%
iHR_{AP}	0.78	0.64	0.87	≤ 67.43	0.71	0.54	0.85	0.83	0.66	0.93	4.17	0.34	81%	25%
iHR_{ML}	0.76	0.62	0.86	≤ 70.09	0.80	0.63	0.92	0.71	0.54	0.85	2.80	0.28	74%	22%
iHR_{V}	0.82	0.68	0.90	≤ 68.04	0.74	0.57	0.88	0.83	0.66	0.93	4.33	0.31	81%	24%
CV	0.76	0.62	0.85	≥ 26.20	0.71	0.54	0.85	0.74	0.57	0.88	2.78	0.38	74%	28%
RMS_{ML}	0.72	0.58	0.82	≥ 1.13	0.57	0.39	0.74	0.83	0.66	0.93	3.33	0.52	77%	34%
$RMSR_{ML}$	0.72	0.58	0.82	≥ 0.12	0.51	0.34	0.69	0.83	0.66	0.93	3.00	0.59	75%	36%
$RMSR_{V}$	0.72	0.57	0.82	≤ 0.97	0.80	0.63	0.92	0.63	0.45	0.79	2.15	0.32	68%	24%
SR_{AP}	0.70	0.55	0.81	≤ 0.71	0.65	0.48	0.81	0.77	0.60	0.89	2.87	0.44	74%	31%

AUC, Area Under the ROC; OCP, optimal cutoff point; Se, sensitivity; Sp, specificity; LR-, negative likelihood ratio; PTP+, positive post-test probability; PTP-, negative post-test probability.HR, Harmonic Ratio; iHR, improved Harmonic Ratio; CV, Coefficient of Variation; RMS, Root Mean Square; RMSR, Root Mean Square Ratio; SR, Step Regularity.

After removing the effect of velocity, we obtained the following results by correlating the stability and symmetry indices (Table 4.19):

- a negative correlation between HR_V and SI_{ST}, $HR_{AP,ML,V}$ and SI_{SW} and a positive correlation between HR_V and $SI_{pelvis\ rotation}$;
- a negative correlation between $iHR_{AP,V}$ and SI_{SW} and a positive correlation between $iHR_{AP,ML}$ and SI_{pelvis} rotation;
- a negative correlation between RMS_{ML} and SI_{pelvis} obliquity and SI_{pelvis} rotation;
- a negative correlation between SR_{AP} and SI_{SW}.

Table 4.19 *Correlation analysis results between the stability indices and the symmetry indices*

		HR_{AP}	HR_{ML}	HR_{V}	CV	iHR_{AP}	iHR_{ML}	iHR_{V}	RMS_{AP}	RMS_{ML}	$RMSR_{AP}$	$RMSR_{ML}$	$RMSR_{V}$	SR_{AP}
SI_{ST}	r	-0.316	-0.191	**-0.394**	0.299	-0.274	-0.142	-0.336	0.088	-0.029	0.099	-0.009	-0.132	-0.318
	p	0.068	0.279	**0.021**	0.086	0.117	0.423	0.052	0.621	0.870	0.578	0.958	0.455	0.067
SI_{SW}	r	**-0.466**	**-0.345**	**-0.531**	0.010	**-0.432**	-0.302	**-0.464**	-0.037	0.021	-0.021	0.037	-0.027	**-0.341**
	p	**0.005**	**0.046**	**0.001**	0.954	**0.011**	0.082	**0.006**	0.835	0.907	0.907	0.834	0.881	**0.049**
SA OBLIQUITY	r	-0.137	-0.017	-0.066	0.017	-0.039	0.101	-0.084	0.082	0.236	0.080	0.240	-0.086	-0.103
	p	0.440	0.925	0.710	0.924	0.825	0.572	0.637	0.646	0.179	0.654	0.171	0.629	0.562
SI_{pelvis} OBLIQUITY	r	0.253	0.234	0.043	-0.031	0.267	0.207	0.065	-0.296	**-0.532**	-0.279	**-0.509**	0.295	-0.018
	p	0.149	0.184	0.810	0.862	0.127	0.241	0.717	0.089	**0.001**	0.110	**0.002**	0.091	0.917
SI_{pelvis} ROTATION	r	0.330	**0.355**	0.179	0.064	**0.397**	**0.359**	0.191	-0.229	**-0.455**	-0.201	**-0.430**	0.260	0.049
	p	0.057	**0.040**	0.311	0.718	**0.020**	**0.037**	0.279	0.194	**0.007**	0.254	**0.011**	0.138	0.782

The coefficient (r) and significance (p) of the correlations are reported. SI, Symmetry Index; SA, Symmetry Angle; SI_{pelvis}, pelvis Symmetry Index.

Bibliography

[1]. Morris ME, et al. 2001. The biomechanics and motor control of gait in Parkinson disease. Clinical Biomechanics, 10:459-470.

[2]. Martino G, Ivanenko YP, Serrao M, Ranavolo A, d'Avella A, Draicchio F, Conte C, Casali C, Lacquaniti F. 2014. Locomotor patterns in cerebellar ataxia. Journal of Neurophysiology, 112:2810-2821.

[3]. Tok F. Balaban B. Yas¸ar E. Alaca R. Tan AK. 2012. The effects of on a botulinum toxin A injection into rectus femoris muscle in hemiplegic stroke patients with stiff-knee gait: A placebo-controlled. nonrandomized trial. Am J Phys Med Rehabil, 91, 321-326.

[4]. Balaban B. Tok F. Yavuz F. Yas¸ar E. Alaca R. 2011. Early rehabilitation outcome in patients with middle cerebral artery stroke. Neurosci Lett, 498, 204-207.

[5]. Tok F. Ozçakar L. Safaz I. Alaca R. 2011. Effects of botulinum toxin-A on the muscle architecture of stroke patients: The first ultrasonographic study. J Rehabil Med, 43, 1016-1019.

[6]. Perry J. Garrett M. Gronley JK. Mulroy SJ. 1995. Classification of walking handicap in the stroke population. Stroke, 26, 982-989.

[7]. Krasovsky T. Levin MF. 2010. Review: Toward a better understanding of coordination in healthy and poststroke gait. Neurorehabil Neural Repair, 24, 213-224.

[8]. Varrecchia T, Serrao M, Rinaldi M, Ranavolo A, Conforto S, De Marchis C, Simonetti A, Poni I, Castellano S, Silvetti A, Tatarelli A, Fiori L, Conte C, Draicchio F. 2019. Common and specific gait patterns in people with varying anatomical levels of lower limb amputation and different prosthetic components. Human Movement Science 66 , 9–21.

[9]. Serrao M, Pierelli F, Ranavolo A, Draicchio F, Conte C, Don R, Di Fabio R, LeRose M, Padua L, Sandrini G, et al. 2012. Gait pattern in inherited cerebellar ataxias. Cerebellum Lond. Engl., 11, 194–211.

[10]. Serrao M, Ranavolo A, Casali C. 2018. Neurophysiology of gait. Handb. Clin. Neurol. 154, 299–303.

[11]. Chini G, Ranavolo A, Draicchio F, Casali C, Conte C, Martino G, Leonardi L, Padua L, Coppola G, Pierelli F, et al. 2017. Local Stability of the Trunk in Patients with Degenerative Cerebellar Ataxia DuringWalking. Cerebellum Lond. Engl., 16, 26–33.

[12]. Hoogkamer W, Bruijn S.M, Sunaert S, Swinnen S.P, Van Calenbergh F, Duysens, J. 2015. Toward new sensitive measures to evaluate gait stability in focal cerebellar lesion patients. Gait Posture, 41, 592–596.

[13]. Conte C, Pierelli F, Casali C, Ranavolo A, Draicchio F, Martino G, Harfoush M, Padua L, Coppola G, Sandrini G, et al. 2014. Upper body kinematics in patients with cerebellar ataxia. Cerebellum Lond. Engl., 13, 689–697.

[14]. Fonteyn EM, Schmitz-Hubsch T, Verstappen CC, Baliko L, Bloem R, Boesch S, et al. 2013. Prospective analysis of falls in dominant ataxias. Eur Neurol.;69:53–7.

[15]. Schniepp R,Wuehr M, Schlick C, Huth S, Pradhan C, Dieterich M, et al. 2014. Increased gait variability is associated with the history of falls in patients with cerebellar ataxia. J Neurol.,261:213–23.

[16]. Bodranghien F, Bastian A, Casali C, Hallett M, Louis ED, Manto M, et al. 2015. Consensus paper: revisiting the symptoms and signs of cerebellar syndrome. Cerebellum, 15 (3):369–91.

[17]. Ilg W, Timmann D. 2013. Gait ataxia—specific cerebellar influences and their rehabilitation. Mov Disord, 28:1566–75.

[18]. Marquer A, Barbieri G, Perennou D. 2014. The assessment and treatment of postural disorders in cerebellar ataxia: a systematic review. Ann Phys Rehabil Med., 57:67–78.

[19]. Gordt K, Gerhardy T, Najafi B, Schwenk M. 2017. Effects of wearable sensor-based balance and gait training on balance, gait, and functional performance in healthy and patient populations: a systematic review and meta-analysis of randomized controlled trials. Gerontology, 64:74–89.

[20]. Serrao M, Casali C, Ranavolo A, Mari S, Conte C, Chini G, et al. 2017. Use of dynamic movement orthoses to improve gait stability and trunk control in ataxic patients. Eur J Phys Rehabil Med., 53:735–43.

[21]. Morton SM, Bastian AJ. 2004. Cerebellar control of balance and locomotion. Neurosci , 10:247–59.

[22]. Konczak J, Timmann D. 2007. The effect of damage to the cerebellum on sensorimotor and cognitive function in children and adolescents. Neurosci Biobehav Rev, 31:1101–13.

[23]. Bodranghien F, Bastian A, Casali C, Hallett M, Louis ED, Manto M, et al. 2016. Consensus paper: revisiting the symptoms and signs of cerebellar syndrome. The Cerebellum, 15:369–91. https://doi.org/10. 1007/s12311-015-0687-3

[24]. Vasco G, Gazzellini S, Petrarca M, Lispi ML, Pisano A, Zazza M, et al. 2016. Functional and gait assessment in children and adolescents affected by Friedreich's ataxia: A One-Year Longitudinal Study. Palau F, editor. PLoS One, 11:e0162463. https:// doi.org/10.1371/journal.pone.0162463

[25]. Caliandro P, Iacovelli C, Conte C, Simbolotti C, Rossini PM, Padua L, et al. 2017. Trunk-lower limb coordination pattern during gait in patients with ataxia.Gait Posture, 57:252–7.

[26]. Schmitz-Hubsch T, Montcel ST du, Baliko L, Berciano J, Boesch S, Depondt C, et al. Scale for the assessment and rating of ataxia. 2006. Neurology, 66:1717–20.

[27]. Holmes G. The cerebellum of man. Brain 1939;62:1-30.

[28]. Tatarelli A, Serrao M, Varrecchia T, Fiori L, Draicchio F, Silvetti A, Conforto S, De Marchis C, Ranavolo A. 2020. Global Muscle Coactivation of the Sound Limb in Gait of People with Transfemoral and Transtibial Amputation. Sensors , 29, 20(9):2543. doi: 10.3390/s20092543.

[29]. Saini M, Kerrigan DC, Thirunarayan MA, Duff-Raffaele M. 1998. The vertical displacement of the center of mass during walking: a comparison of four measurement methods. J Biomech Eng., 120(1):133-9. doi: 10.1115/1.2834293

[30]. Hof AL, Gazendam M, Sinke WE. 2005. The condition for dynamic stability. J Biomech., 38:1–8.

[31]. Hoogkamer W, Bruijn S.M, Sunaert S, Swinnen S.P, Van Calenbergh F, Duysens J. 2015. Toward new sensitive measures to evaluate gait stability in focal cerebellar lesion patients. Gait Posture, 41, 592–596.

[32]. Caliandro P, Iacovelli C, Conte C, Simbolotti C, Rossini P.M, Padua L, Casali C, Pierelli F, Reale G, Serrao M. 2017. Trunk-lower limb coordination pattern during gait in patients with ataxia. Gait Posture, 57: 252–257

[33]. Filippeschi A, Schmitz N, Miezal M, Bleser G, Rualdi E, Stricker D. 2017. Survey of Motion Tracking Methods Based on Inertial Sensors: A Focus on Upper Limb Human Motion. Sensors, 17, 1257.

[34]. Picerno P. 2017. 25 years of lower limb joint kinematics by using inertial and magnetic sensors: A review of methodological approaches. Gait Posture, 51, 239–246.

[35]. Iosa M, Picerno P, Paolucci S, Morone G. 2016. Wearable inertial sensors for human movement analysis. Expert Rev. Med. Devices, 13, 641–659.

[36]. Bloem BR, Boesch S, et al. 2010. Falls in spinocerebellar ataxias: results of the EuroSCA fall study. Cerebellum, 9:232–9.

[37]. Kallner A. 2018. Bayes' theorem, the roc diagram and reference values: definition and use in clinical diagnosis. Biochem Medica [Internet]. Biochemia Medica, 15;28(1):010101.

[38]. Morrone M, Miccinilli S, Bravi M, et al. 2016. Perceptive rehabilitation and trunk posture alignment in patients with Parkinson disease: a single blind randomized controlled trial. Eur J Phys Rehabil Med., 52(6): 799–809.

[39]. Viitanen M, Mortimer JA, Webster DD. 1994. Association between presenting motor symptoms and the risk of cognitive impairment in Parkinson's disease. J Neurol Neurosurg Psychiatry, 57(10): 1203–1207.

[40]. Czech M, Demanuele C, Erb M.K, Ramos V, Zhang H, Ho B, Patel S. 2020. The impact of reducing the number of wearable devices on measuring gait in parkinson disease: Noninterventional exploratory study. JMIR Rehabil. Assist. Technol., 21;7(2):e17986

[41]. Paul S.S, Allen N.E, Sherrington C, Heller G, Fung V.S.C, Close J.C.T, Lord S.R, Canning C.G. 2014. Risk factors for frequent falls in people with Parkinson's disease. J. Parkinsons Dis., 4, 699–703.

[42]. Castiglia S.F, Tatarelli A, Trabassi D, De Icco R, Grillo V, Ranavolo A, Varrecchia T, Magnifica F, Di Lenola D, Coppola G, Ferrari D, Denaro A, Tassorelli C, Serrao M. 2021. Ability of a set of trunk inertial indexes of gait to identify gait instability and recurrent fallers in Parkinson's disease. Sensors, 15;21(10):3449.

[43]. Husted J.A, Cook R.J, Farewell V.T, Gladman D.D. 2000. Methods for assessing responsiveness: a critical review and recommendations, J. Clin. Epidemiol., 53,459–468.

[44]. Zurada J, Karwowski W, Marras W. 1997. A neural network-based system for classification of industrial jobs with respect to risk of low back disorders due to workplace design. Appl Ergon., 28(1): 49–58.

[45]. Chen CL, Kaber DB, Dempsey PG. 2004. Using feedforward neural networks and forward selection of input variables for an ergonomics data classification problem. Hum Factors Ergon Manuf., 14(1): 31– 49.

[46]. Zhang S, Poon SK, Vuong K, Sneddon A, Loy CT. 2019. A Deep Learning-Based Approach for Gait Analysis in Huntington Disease. Stud Health Technol Inform., 64: 477–481

[47]. Rovini E, Maremmani C, Cavallo F. 2017. How wearable sensors can support parkinson's disease diagnosis and treatment: A systematic review. Front Neurosci., 11: 555.

[48]. Caramia C, Torricelli D, Schmid M, et al. 2018. IMU-Based Classification of Parkinson's Disease From Gait: A Sensitivity Analysis on Sensor Location and Feature Selection. IEEE J Biomed Health Inform., 22(6): 1765–1774.

[49]. Pickle NT, Shearin SM, Fey NP. 2018. A machine learning approach to targeted balance rehabilitation in people with Parkinson's disease using a sparse sensor set. Conf Proc IEEE Eng Med Biol Soc., 1202–1205.

[50]. Hughes AJ, Daniel SE, Kilford L, Lees AJ. 1992. Accuracy of clinical diagnosis of idiopathic Parkinson's disease: a clinico-pathological study of 100 cases. J Neurol Neurosurg Psychiatry, 55: 181–4.

[51]. Rumelhart DE et al.1986. Learning internal representations by error propagation. In: Parallel Distributed Processing, vol. 1, pp. 318-362.

[52]. Deeks JJ, Altman DG. 2004. Diagnostic tests 4: likelihood ratios. BMJ ,329(7458): 168–9. https:// doi.org/10.1136/bmj.329.7458.168

[53]. Wald NJ, Bestwick JP. 2014. The area under the ROC curve: is it a valid measure of screening performance? J Med Screen, 21(4): 220.

[54]. Langhorne P, Stott D. J, Robertson L, MacDonald J, Jones L, McAlpine, C. 2000. Medical complications after stroke. Stroke, 31, 1223–1229

[55]. Van Criekinge T, Saeys W, Hallemans A, Velghe S, Viskens PJ, Vereeck L, De Hertogh W, Truijen S. Trunk biomechanics during hemiplegic gait after stroke: A systematic review. Gait Posture. 2017 May;54:133-143.

[56]. Bower K, Thilarajah S, Pua YH, Williams G, Tan D, Mentiplay B, Denehy L, Clark R. 2019. Dynamic balance and instrumented gait variables are independent predictors of falls following stroke. J Neuroeng Rehabil., 7;16(1):3.

[57]. Patterson KK, Gage WH, Brooks D, Black SE, McIlroy WE. 2010. Evaluation of gait symmetry after stroke: a comparison of current methods and recommendations for standardization. Gait Posture, 31(2):241-6.

[58]. Zifchock RA, Davis I, Higginson J, Royer T. 2008. The symmetry angle: a novel, robust method of quantifying asymmetry. Gait Posture, 27(4):622-7.

[59]. Moe-Nilssen R, and Helbostad J. L. 2004. Estimation of gait cycle characteristics by truck accelerometry. J. Biomech., 37, 121–126.

[60]. Kobsar D, Olson C, Paranjape R, Hadjistavropoulos T, Barden J. M. 2014a. Evaluation of age-related differences in the stride-to-stride fluctuations, regularity and symmetry of gait using a waist-mounted tri-axial accelerometer. Gait Posture, 39, 553–557.

CHAPTER 5

5. GAIT ANALYSIS OF PEOPLE WITH LOWER LIMB AMPUTATION

Lower limb amputation causes considerable neuronal remodeling within the central nervous system (CNS), owing mostly to the loss of sensory function produced by the amputation [1,2]. From a motor control standpoint, people with amputation must adapt their walking patterns to their new physical conditions, and this adaptation may result in changes in the way the central nervous system (CNS) controls the movement. The two factors influencing the gait in people with amputation are the level of the amputation [3,4] and the type of prostheses [5,12]. People with amputations above the knee appear to be more asymmetric than those with amputations below the knee, with increased compensatory strategies that may be detrimental to individuals over time [13]. In terms of prosthesis design, materials, and technology, advancements have been made in recent years to make them more effective in terms of ambulation efficiency, asymmetries reduction, and compensatory movements reduction. Actually, subjects with lower limb amputation wear different type of prostheses, such as the old concept mechanical prostheses or the most recent and technologically advanced prostheses (Microprocessor Controlled Knees (MPKs)), i.e. CLeg and Genium [7, 14, 15]. Taking these aspects into account, quantifying and characterizing the gait of persons with a prosthesis is an essential element to improve the development of new and ergonomic prosthetic devices, and to optimize the rehabilitation programs [16-19].

In the perspective article "*Characterizing the Gait of People With Different Types of Amputation and Prosthetic Components Through Multimodal Measurements: A Methodological Perspective*" (2022) we provide a methodological perspective related to multimodal prosthetic gait assessment reporting and discussing the results obtained in a series of studies in which we investigated the kinematic, kinetic and electromyographic aspects of the gait of subjects with unilateral lower limb amputation.

In this study we considered the results of 5 studies with a total of 57 recordings of subjects with unilateral TFA, 20 recordings of subjects with unilateral TTA and 40 recordings of age–sex–speed matched healthy subjects , all performed at the Rome site of the INAIL Prosthesis Centre at the CTO Andrea Alesini hospital in Rome.

Subjects with TFA wore three different types of prosthesis: mechanical prosthesis (TFA_M) and two types of prosthesis microprocessor-controlled knees (MPK), namely C-Leg (TFA_C) and Genium (TFA_G) (Ottobock, Duderstadt, Germany).

Walking tests were conducted on a 9-m long walkway equipped with two force platforms at a self-selected comfortable speed (Kistler 9286AA, Winterthur, Switzerland). To match the TFA and TTA groups, control subjects were also asked to walk at a slower speed. An optoelectronic motion analysis system with six infrared cameras (SMART-DX 6000 System, BTS, Milan, Italy) was used, with passive spherical markers placed according to a modified Davis' protocol [20]. The amputated limb markers were placed over symmetrical points with respect to the position of the homologous marker on the non-amputated limb in subjects with TTA and TFA. A wireless system (FreeEMG 1000 System, BTS, Milan, Italy) was used to record electromyographic (EMG) signals. The activity of 12 muscles on the sound side was recorded (right side for the controls) in accordance with Atlas of Muscle Innervation Zones [21] and the European Recommendations for Surface Electromyography [22].

5.1. Kinematic, Kinetic, and Energy Consumption

In the study "*Common and specific gait patterns in people with varying anatomical levels of lower limb amputation and different prosthetic components*" (2019) fifty-five subjects with lower limb amputation were analyzed, including 15 subjects with transtibial amputation and 40 subjects with transfemoral amputation. Forty healthy subjects were recruited as a control group and matched for age-sex-velocity to subjects with TFA, and of these 12 were matched for age-sex-velocity to subjects with TTA. We calculated time-distance parameters, kinematic and kinetic data and energy consumption measurement.

5.1.1 Kinematic data

5.1.1.1 Spatio-temporal parameters

Significantly increased step width, step length, and double support duration in both sides were found in both TTA and TFA groups compared to the C (Cm_{TTA} and Cm_{TFA}). Stance duration was significantly increased in the NA side in both TTA and TFA groups, and significantly decreased in the A side in the TFA group. Conversely, the swing duration was significantly decreased in the NA

side in both TTA and TFA groups, and significantly increased in the A side in TFA group (Table 5.1). Significantly shorter stance duration and longer swing duration were found in the A side than in the NA side (Table 5.1, Fig. 5.1) in TTA and TFA groups.

Table 5.1 *The means, standard deviations, and statistical results (p value) of walking speed, cadence, step width, step length, stance duration, swing duration, and double support duration.*

		People with amputation vs controls						Type of prostheses				TTAm vs TFAm		
Time-distance parameters		C_{mTTA}	TTA	p group	C_{mTFA}	TFA	p group	TFA_M	TFA_C	TFA_G	p group	TTA_m	TFA_m	p group
Walking speed (m/s)		0.97±0.20	1.08±0.16	0.1163	0.93±0.25	0.92±0.20	0.813	0.82±0.20	0.91±0.23	1.01±0.12	0.064	1.05±0.15	0.94±0.16	0.084
Cadence (cycle/s)	A	0.84±0.07	0.83±0.07	0.52	0.81±0.12	0.78±0.08	0.289	0.75±0.07	0.79±0.09	0.80±0.06	0.309	0.82±0.10	0.77±0.07	0.077
	NA		0.82±0.07	0.481		0.78±0.08	0.397	0.74±0.07	0.79±0.09	0.80±0.06	0.16	0.81±0.07	0.77±0.07	0.11
	p side		0.083			0.439		0.269	0.158	0.619		0.114	0.973	
Step width (% limb length)		0.20±0.05	0.28±0.06	**<0.001**	0.19±0.06	0.30±0.09	**<0.001**	0.33±0.10	0.32±0.08	0.27±0.09	0.214	0.27±0.05	0.29±0.09	0.538
Step length (% limb length)	A	0.61±0.12	0.74±0.09	**0.002**	0.60±0.10	0.66±0.09	**0.014**	0.63±0.11	0.65±0.12	0.66±0.08	0.729	0.74±0.10	0.64±0.11	0.058
	NA		0.75±0.07	**0.001**		0.67±0.09	**0.003**	0.64±0.12	0.65±0.09	0.72±0.05	**0.048**	0.74±0.07	0.70±0.08	0.182
	p side		0.903			0.241		0.681	0.877	**0.046**		0.946	0.38	
Stance duration (% cycle)	A	61.78±1.78	61.89±1.79	0.871	62.38±2.88	59.63±2.57	**<0.001**	60.14±2.31	60.09±3.02	58.74±2.02	0.285	61.68±1.80	58.71±0.88	**<0.001**
	NA		64.17±3.44	**0.009**		67.99±3.31	**<0.001**	67.21±3.02	69.27±3.92	66.94±2.14	0.107	64.68±3.42	67.99±3.15	**0.017**
	p side		**0.014**			**<0.001**		**0.004**	**<0.001**	**<0.001**		**0.01**	**<0.01**	
Swing duration (% cycle)	A	38.85±3.29	38.09±1.80	0.648	38.30±2.99	39.88±2.98	**<0.001**	39.9±2.93	39.01±2.33	40.91±2.05	0.205	38.28±1.82	40.58±2.20	**0.002**
	NA		35.82±3.43	**0.009**		31.91±3.30	**<0.001**	31.6±2.53	31.11±4.24	33.08±2.04	0.25	35.3±3.4	31.64±3.18	**0.011**
	p side		**0.015**			**<0.001**		**0.004**	**<0.001**	**<0.001**		**<0.01**	**<0.01**	
Double support duration (% cycle)	A	23.17±3.15	26.07±4.46	**0.049**	23.54±5.76	27.72±5.01	**0.001**	28.54±3.73	28.97±6.36	25.66±3.12	0.161	26.38±4.74	27.08±3.54	0.677
	NA		26.08±4.50	**0.037**		27.44±6.58	**<0.001**	24.28±9.03	30.26±6.47	26.04±2.98	0.05	24.4±4.77	27.41±4.09	0.568
	p side		0.670			0.367[b]		0.125	0.081	0.298		0.672	0.698	

Cm_{TTA}: healthy subjects age-sex-speed matched with TTA; TTA: subjects with transtibial amputation; Cm_{TFA}: healthy subjects age-sex-speed matched with TFA; TFA: subjects with transfemoral amputation; TFA_M: subjects with transfemoral amputation with mechanical prosthesis; TFA_C: subjects with transfemoral amputation with CLeg prosthesis; TFA_G: subjects with transfemoral amputation with Genium prosthesis; TFA_m: a subgroup of 13 age-sex-speed matched subjects with a subgroup of TTA; TTA_m: a subgroup of 13 age-sex-speed matched subjects with a subgroup of TFA.

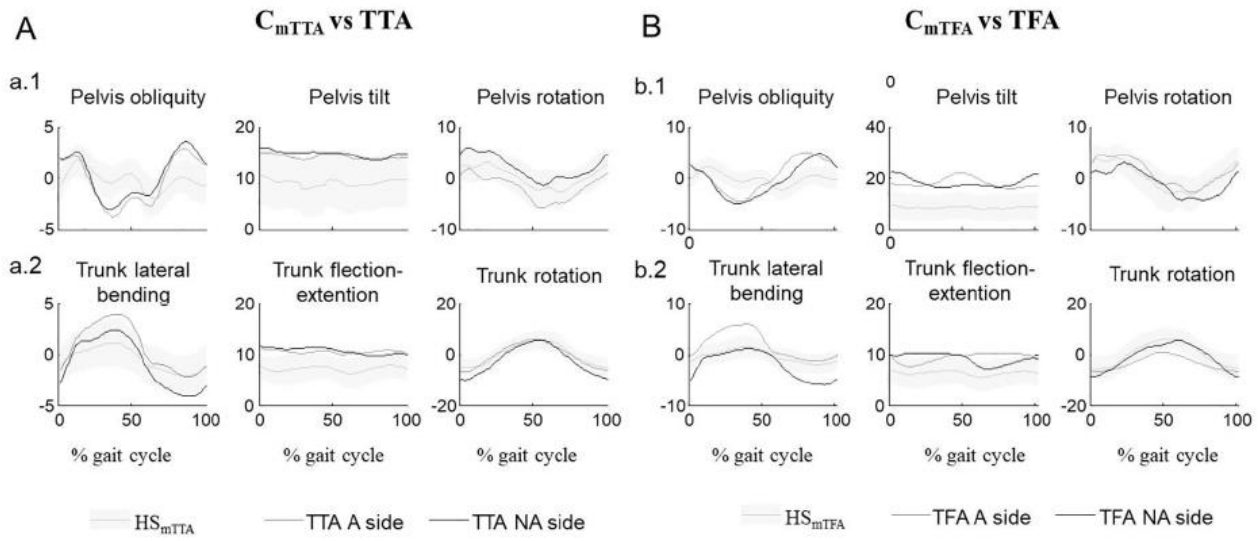

Figure 5.1 *Pelvic obliquity, pelvic tilt, pelvic rotation, trunk lateral bending, trunk flection-extension, and trunk rotation in both sides were found in both TTA and TFA groups compared to controls. Cm_{TTA}: healthy subjects age-sex-speed matched with TTA; TTA: subjects with transtibial amputation; Cm_{TFA}: healthy subjects age-sex-speed matched with TFA; TFA: subjects with transfemoral amputation.*

A significant effect of the type of prosthesis on the step length of the NA side was detected. Post hoc analysis revealed higher values for the Genium prosthesis compared to mechanical prosthesis (Table 5.1). A significantly shorter step length in A side than in the NA one (Table 5.1) was found in TFA_G subgroup. Furthermore, significantly shorter stance duration and longer swing duration in the A side than in the NA one (Table 5.1) were found in all three TFA_M, TFA_C and TFA_G subgroups

.

A significant effect of the type of amputation (TTA_m vs. TFA_m) on the stance and swing duration was found in both sides, with the stance significantly increased and the swing significantly decreased in the NA side in TFA_m group compared to TTA_m group, (Table 5.1). Conversely, the stance significantly decreased and the swing significantly increased in the A side in TFA_m group compared to TTA_m group (Table 5.1). Significantly shorter stance duration and longer swing duration in the A side than in the NA one (Table 5.1) were found both in TTA_m and TFA_m.

5.1.1.2 Joint angles

Significantly increased hip and knee RoMs in NA side were found in TFA compared to Cm_{TFA} (Figure 5.2). Furthermore, significantly decreased ankle RoMs in A side were detected in both TTA and TFA compared to the speed matched C (Cm_{TTA} and Cm_{TFA}) (Figure 5.2). Significantly increased pelvic obliquity, trunk lateral bending, and trunk rotation RoMs of both sides were found in both TTA and TFA groups compared to C (Figure 5.1 and 5.2). Moreover, pelvic tilt, pelvic rotation, and trunk flection-extension RoMs of both sides were significantly increased in TFA group compared to Cm_{TFA}

group (Figure 5.1 and 5.2). Figure 5.1 also shows that people with amputation walked with the pelvis and trunk ante-flexed (flexed in a forward direction) compared to C. A significantly shorter hip and knee RoMs were found in the A side than in the NA side (Figure 5.2) in TFA group. Furthermore, a significantly shorter ankle RoMs were found in the A side than in the NA side (Figure 5.2)in both TTA and TFA groups.

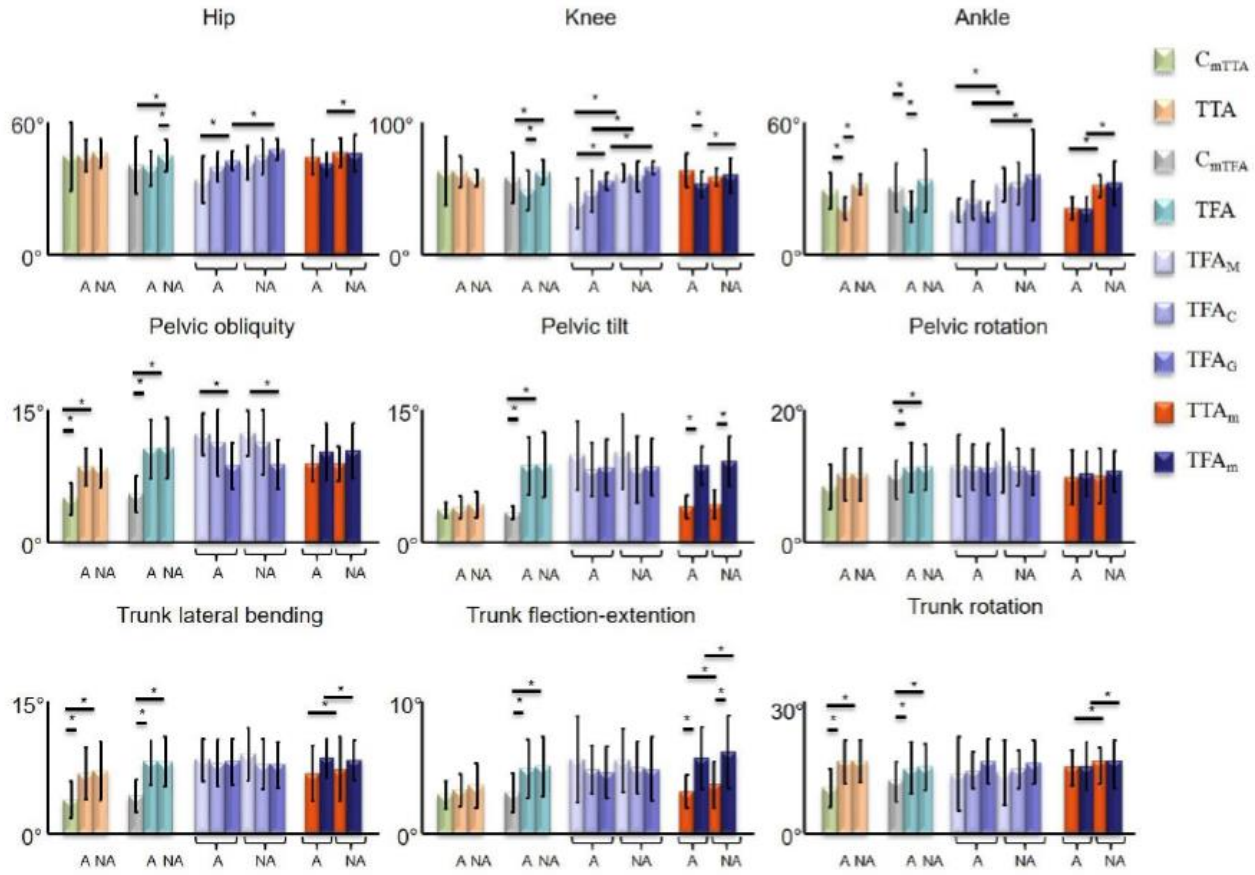

Figure 5.2 *The means, standard deviations, and statistical results of range of motion for the hip, knee, ankle, pelvic, and trunk for each group. Cm_{TTA}: healthy subjects age-sex-speed matched with TTA; TTA: subjects with transtibial amputation; Cm_{TFA}: healthy subjects age-sex-speed matched with TFA; TFA: subjects with transfemoral amputation; TFA_M: subjects with transfemoral amputation with mechanical prosthesis; TFA_C: subjects with transfemoral amputation with CLeg prosthesis; TFA_G: subjects with transfemoral amputation with Genium prosthesis; TFA_m: a subgroup of 13 age-sex-speed matched subjects with a subgroup of TTA; TTA_m: a subgroup of 13 age-sex-speed matched subjects with a subgroup of TFA.*

Figure 5.2 depicts increased hip and knee RoMs in TFA on the NA side compared to Cm_{TFA}, and significantly decreased ankle RoMs in TTA and TFA on the A side compared to the control group. When compared to healthy subjects, both TTA and TFA groups had significantly higher pelvic obliquity, trunk lateral bending, and trunk rotation RoMs on both sides (Figure 5.2). Furthermore, the TFA group had significantly higher pelvic tilt, pelvic rotation, and trunk flection-extension RoMs on both sides than the Cm_{TFA} group. In the TFA group, the A side had significantly shorter hip and knee

RoMs than the NA side. Furthermore, in both TTA, the A side had significantly shorter ankle RoMs than the NA side.

A significant effect of the type of prosthesis on the hip and knee RoMs in the A side and on the pelvic obliquity RoM was found in both sides. Post hoc analysis revealed higher values of the hip and knee RoMs in the A side of TFA_G subgroup compared to TFA_M subgroup (Figure 5.2) and lower values of the pelvic obliquity RoMs for the Genium prosthesis (TFA_G) compared to mechanical prosthesis (TFA_M) in both sides (Figure 5.2). Significantly decreased knee and ankle RoMs in the A side than in NA side were found in TFA_M, TFA_C, and TFA_G subgroups (Figure 5.2). Furthermore, a significantly decreased hip RoM in A side than in NA side (Figure 5.2) was detected in TFA_G subgroup.

A significant effect of the type of amputation (TTA_m vs. TFA_m) on the knee, pelvic tilt, and trunk flexion-extension RoMs was found, with the knee RoM significantly decreased in the A side in TFA_m subgroup compared to TTA_m subgroup (Figure 5.2) and the pelvic tilt and trunk flexion-extension RoMs significantly increased in both sides in TFA_m subgroup compared to TTA_m subgroup (Figure 5.2). A significantly shorter hip and knee RoMs were found in the A side than in the NA side (Figure 5.2) in TFA_m subgroup. Furthermore, a significantly shorter ankle RoM was found in the A side than in the NA side (Figure 5.2) in both TTA_m and TFA_m subgroups. Significantly shorter trunk lateral bending, trunk flexion-extension, and trunk rotation RoMs were found in the A side than in the NA side (Figure 5.2) in both TTA_m and TFA_m subgroups.

5.1.2 Kinetic data

The curves of the vertical force for Cm_{TTA} and TTA (Figure 5.3A) and for Cm_{TFA} and TFA (Figure 5.3B) are shown in Cartesian coordinates as mean curves (Figure 5.3 a.1 and b.1), and in polar

coordinates as mean curve (a.2 and b.2), as well as single and mean CoA values (a.3 and b.3), all expressed as percentage of gait cycle.

The means, standard deviations, and statistical results of VF for each group are reported in Table 5.2.

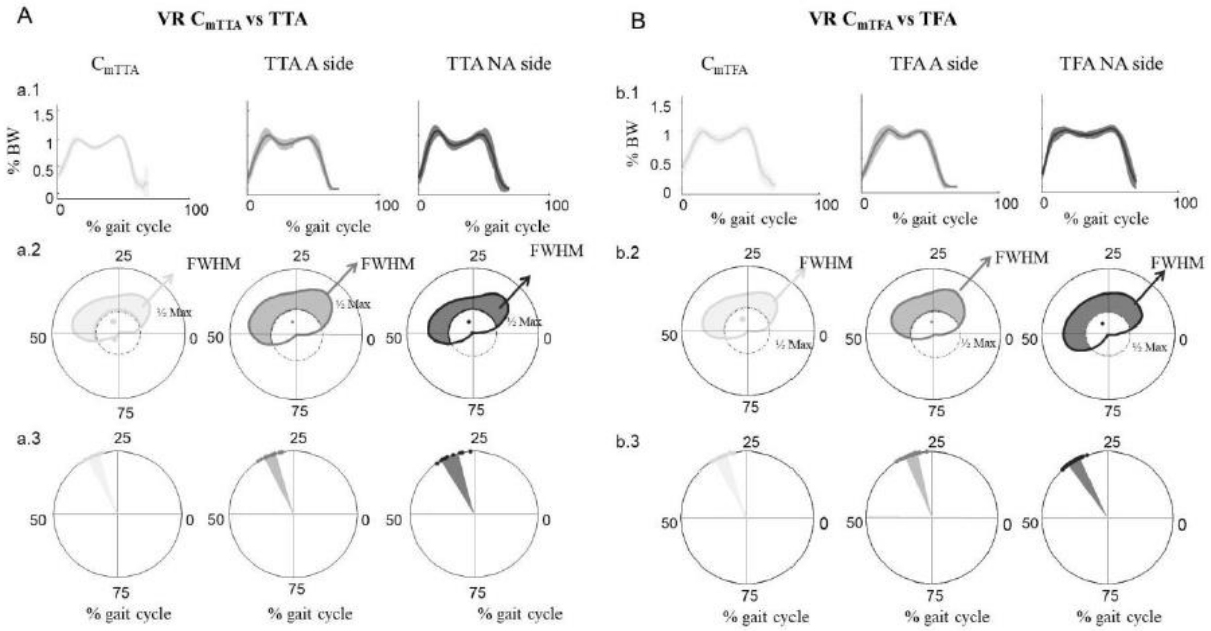

Figure 5.3 *Curves of the vertical force for Cm_{TTA} and TTA and for Cm_{TFA} and TFA shown in Cartesian coordinates as mean curves (a.1 and b.1), and in polar coordinates as mean curve (a.2 and b.2), as well as single and mean CoA values (a.3 and b.3), all expressed as percentage of gait cycle. Cm_{TTA}: healthy subjects age-sex-speed matched with TTA; TTA: subjects with transtibial amputation; Cm_{TFA}: healthy subjects age-sex-speed matched with TFA; TFA: subjects with transfemoral amputation*

A significantly increased $Peak1_{VF}$ value in NA side and a significantly decreased $Peak2_{VF}$ value in A side were found in TTA group compared to Cm_{TTA} group (Table 5.2). Significantly increased $Peak1_{VF}$, CoA_{VF}, and $FWHM_{VF}$ values in NA side were found in TFA compared to Cm_{TFA} (Table 5.2). Furthermore, significantly increased $Peak1_{VF}$ value and significantly decreased $FWHM_{VF}$ and CoA_{VF} values in A side were found in TFA compared to Cm_{TFA} (Table 5.2). $Peak1_{VF}$ was significantly lower in the A side than in the NA side (Table 5.2) in TTA group. A significantly lower $Peak2_{VF}$ value was found in the A side than in the NA side (Table 5.2) in both TTA and TFA groups. Furthermore, significantly higher $Peak1_{VF}$ and lower $FWHM_{VF}$ and CoA_{VF} values were found in the A side than in the NA side (Table 5.2) in TFA.

Table 5.2 *The means, standard deviations, and statistical results (p value) of parameters evaluated on vertical force (VF) curves (Peak1$_{VF}$ and Peak2$_{VF}$: 2 peaks, CoA$_{VF}$: center of activity and FWHM$_{VF}$: full width at half maximum).*

		People with amputation vs controls						Type of prostheses				TTA$_m$ vs TFA$_m$		
Kinetic parameters		Cm_{TTA}	TTA	p group	Cm_{TFA}	TFA	p group	TFA_M	TFA_C	TFA_G	p group	TTA_m	TFA_m	p group
Peak1$_{VF}$	A)	1.014±0.061	1.049±0.083	0.125	0.973±0.114	1.04±0.064	**<0.001**	1.065±0.068	1.052±0.051	1.03±0.075	0.423	1.021±0.039	1.043±0.071	0.336
	NA)		1.109±0.10	**0.005**		1.016±0.062	**0.1**	1.002±0.056	1.008±0.043	1.03±0.083	0.421	1.094±0.103	1.001±0.07	**0.014**
	p side		**0.029**			**0.011**		0.098	**0.013**	0.883		**0.02**	0.1	
Peak2$_{VF}$	A)	1.054±0.051	0.985±0.032	**<0.001**	1.00±0.124	0.989±0.048	0.355	0.997±0.054	0.986±0.043	0.987±0.054	0.838	0.982±0.032	0.976±0.046	0.538
	NA)		1.063±0.079	0.733		0.992±0.071	0.379	0.999±0.075	1.042±0.066	1.011±0.074	0.288	1.0584±0.083	1.007±0.063	0.084
	p side		**<0.001**			**0.008**		0.82	**0.001**	**0.288**		**0.002**	0.168	
CoA$_{VF}$ (% gait cicle)	A)	31.25±1.599	30.87±1.68	0.654	31.43±1.77	30.09±1.67	**<0.001**	29.98±1.62	30.38±1.99	29.84±1.31	0.666	30.81±1.78	29.60±1.56	0.091
	NA)		31.40±2.45	0.475		33.57±1.74	**<0.001**	33.73±1.86	34.08±1.72	32.85±1.56	0.142	31.86±2.28	33.57±1.62	0.095
	p side		0.281			**<0.001**		**<0.001**	**<0.001**	**<0.001**		0.07	**<0.001**	
FWHM$_{VF}$	A)	50±1.604	47.667±3.457	0.066	47.179±1.798	44.051±3.809	**<0.001**	43.222±3.961	43.941±4.322	44.712±3.148	0.659	47.153±3.412	43.231±3.678	**0.01**
	NA)		50.47±2.446	0.652		56.72±2.611	**<0.001**	57.11±2.315	56.18±3.005	57.12±2.318	0.542	50.85±2.267	57.46±2.696	**<0.001**
	p side		0.076			**<0.001**		**<0.001**	**<0.001**	**<0.001**		**0.03**	**<0.001**	

Cm_{TTA}: healthy subjects age-sex-speed matched with TTA; TTA: subjects with transtibial amputation; Cm_{TFA}: healthy subjects age-sex-speed matched with TFA; TFA: subjects with transfemoral amputation; TFA_M: subjects with transfemoral amputation with mechanical prosthesis; TFA_C: subjects with transfemoral amputation with CLeg prosthesis; TFA_G: subjects with transfemoral amputation with Genium prosthesis; TFA_m: a subgroup of 13 age-sex-speed matched subjects with a subgroup of TTA; TTA_m: a subgroup of 13 age-sex-speed matched subjects with a subgroup of TFA.

No significant effects of the type of prosthesis on the VF values were detected for both sides (Table 5.2). A significantly increased Peak1$_{VF}$ value was found in A side than in the NA side (Table 5.2) in TFA_C and significantly decreased ($p < 0.05$) Peak2$_{VF}$ values were found in A side than in the NA side (Table 5.2) in TFA_C and in TFA_G subgroups. Furthermore, significantly decreased FWHM$_{VF}$ and CoA$_{VF}$ values were found in A side than in the NA side (Table 5.2) in all three TFA_M, TFA_C, and TFA_G subgroups.

A significant effect of the type of amputation (TTA_m vs. TFA_m) on the VF values was detected. Peak1$_{VF}$ was significantly decreased in the NA side in TFA_m group compared to TTA_m group (Table 5.2). FWHM$_{VF}$ was significantly increased in the NA side and significantly decreased in the A side in TFA_m group compared to TTA_m group (Table 5.2). Significantly lower values were found in the A side than in the NA side for Peak1$_{VF}$ and Peak2$_{VF}$ in TTA_m, for FWHM$_{VF}$ in both TTA_m and TFA_m group, and for CoA$_{VF}$ in TFA_m (Table 5.2).

5.1.3 Energy consumption

A significantly lower value of R-step in TFA subgroup compared to Cm_{TFA} subgroup was found (Figure 5.4). No significant differences of TEC values were detected.

No significant effects of the type of prosthesis were found on both R-step and TEC (Figure 5.4).

A significant effect of the type of amputation on R-step was found, with R-step value of TTA_m subgroup being significantly higher than that of TFA_m. Instead, no significant effect of the type of amputation on TEC was detected (Figure 5.4).

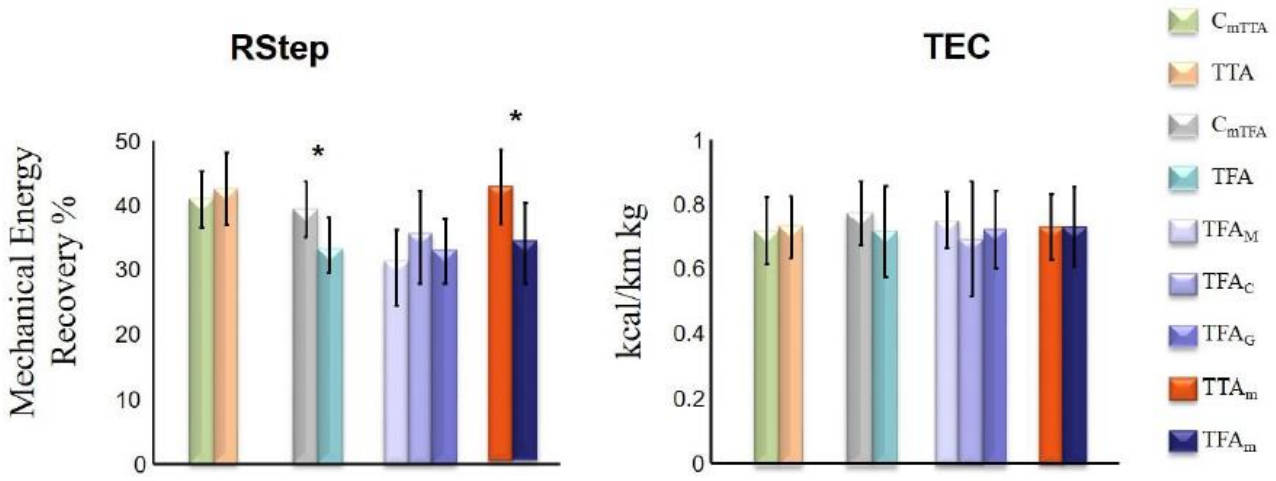

Figure 5.4 *Means, standard deviations, and statistical results of fraction of mechanical energy recovered during each walking step (R-step) and total energy consumption (TEC) values for each group. Cm_{TTA}: healthy subjects age-sex-speed matched with TTA; TTA: subjects with transtibial amputation; Cm_{TFA}: healthy subjects age-sex-speed matched with TFA; TFA: subjects with transfemoral amputation; TFAM: subjects with transfemoral amputation with mechanical prosthesis; TFAC: subjects with transfemoral amputation with CLeg prosthesis; TFA_G: subjects with transfemoral amputation with Genium prosthesis; TFAm: a subgroup of 13 age-sex-speed matched subjects with a subgroup of TTA; TTAm: a subgroup of 13 age-sex-speed matched subjects with a subgroup of TFA.*

Thus, abnormal patterns found in the gait of subjects with lower limb amputations, and in particular in TFA, are associated with a decreased ability to recover mechanical energy (R-step) [23] and an increased metabolic cost of walking [24,25], both of which contribute to decreased autonomy [26] and a reluctance to use the prosthesis [27]. Prosthetic advances have resulted in devices that improve walking performance by reducing compensatory patterns while optimizing energetic cost [16]. Understanding which biomechanical gait abnormalities are primarily and specifically associated with energy recovery is important for developing prosthetic devices aimed at restoring the most effective gait function.

The aims of the study *"Pelvic obliquity as a compensatory mechanism leading to lower energy recovery: Characterization among the types of prostheses in subjects with transfemoral amputation"*(2020) were to identify the spatiotemporal and kinematic gait variables most strongly associated with energy recovery in TFA subjects and to assess the ability of such parameters to discriminate between TFA and healthy subjects based on prosthesis type.

We used the data from the previous study, specifically those related to TFA. Each parameter for the prosthetic and sound side was calculated for TFA subjects. Parameters for the control group were evaluated without regard to side. The walking speed (m/s), cadence (step/s), step width (m), step length (m), and durations of the stance, swing, and double support phases were calculated for each subject. The difference between the maximum and minimum joint range of motion values during the gait cycle was used to calculate the anatomical and prosthetic joint angles for the hip, knee, ankle, trunk, and pelvis (frontal, sagittal, and transverse planes). Energy recovery was measured trough the R-step parameter.

Table 5.3 *Correlations between R-step, spatio-temporal and kinematic parameters.*

R-step				
	Pearson's correlation		Partial correlations (speed-corrected)	
speed (m/s)	r	−0.34		
	p	0.03		
Stance duration A	r	0.33	r	0.21
	p	0.04	p	0.09
Double support	r	0.35	r	0.15
duration A	p	0.03	p	0.18
Knee range of motion	r	−0.34	r	−0.15
	p	0.03	p	0.17
Pelvic obliquity A	r	0.42	r	0.28
	p	**0.01**	**p**	**0.04**
Pelvic obliquity NA	r	0.41	r	0.26
	p	0.01	p	0.06
Multiple linear regression analysis				
	B	t	p	95 %CI
Constant	0.284	8.94	0.00	0.22–0.35
Pelvic Obliquity A	0.01	2.90	0.00	0.00–0.01
Adjusted $R^2 = 0.159 \pm 0.60$; $F = 8.36$; $p = 0.00$				

R-step: The fraction of mechanical energy recovered during each walking step; r: correlation coefficient; p: 95 % significance level; A: prosthetic limb; NA: sound limb; B: unstandardized coefficients; CI: confidence interval; Adjusted R^2: goodness of fitting parameter; F: Fisher's test in ANOVA.

Pelvic obliquity on both sides, stance and double support duration of the prosthetic limb, and knee range of motion of the prosthetic side showed significant positive correlations with R-step. In contrast, gait speed showed a negative correlation (Table 5.3). After correcting for gait speed, partial

correlation analysis showed a fair but significant positive correlation only between pelvic obliquity of the prosthetic side and Rstep. Among gait variables, only pelvic obliquity of the prosthetic side was significantly associated with the R-step value (Table 5.3).

Pelvic obliquity of the prosthetic side showed an excellent ability to discriminate TFA from Cm_{HS} subjects (AUC=0.90; Table 5.4, Figure 5.5/a). Pelvic obliquity values ≥ 6.13° identified subjects with TFA with a 74 % probability. Pelvic obliquity showed an excellent discriminative ability to identify TFA_m and TFA_c subjects from Cm_{HS} subjects (AUC=0.97 and 0.92, respectively; Table 5.4, Figure 5.5/b). Values ≥ 11.10° and ≥ 6.37° identified TFA_m and TFA_c subjects from Cm_{HS} subjects, respectively, with 89 % and 59 % probability. Pelvic obliquity showed a good discriminative ability to identify TFA_g from Cm_{HS} subjects (AUC=0.84; Table 5.4, Figure 5.5/b). Values ≥ 5.56° identify TFA_g subjects with a 45 % probability

Table 5.4 *Discriminative ability of pelvic obliquity and cut-off analysis.*

	AUC (95 % CI)	OCP	Se	Sp	LR+	LR-	+PTP	-PTP
CmTFA vs TFA	0.90 (0.82 – 0.95)	≥ 6.13°	0.95	0.67	2.92	0.07	74 %	7 %
CmTFA vs TFAm	0.97 (0.82 – 0.97)	≥ 11.10°	0.89	0.97	35.55	0.11	89 %	2 %
CmTFA vs TFAc	0.92 (0.82 – 0.97)	≥ 6.37°	0.94	0.72	3.42	0.08	59 %	3 %
CmTFA vs TFAg	0.84 (0.69 – 0.92)	≥ 5.56°	0.93	0.60	2.32	0.12	45 %	4 %

AUC: area under the receiver operating characteristics curve with 95 % Confidence Intervals (CI); OCP: optimal cutoff point; Se: sensitivity; Sp: specificity; LR+: positive likelihood ratio; LR-: negative likelihood ratio; +PTP: positive post-test probability; -PTP: negative post-test probability; Cm_{TFA}: healthy subjects age-sex-speed matched with TFA; TFA: subjects with transfemoral amputation; TFA_m: subjects wearing a mechanical prosthesis; TFA_c: subjects wearing C-Leg prosthesis; TFA_g: subjects wearing Genium prosthesis.

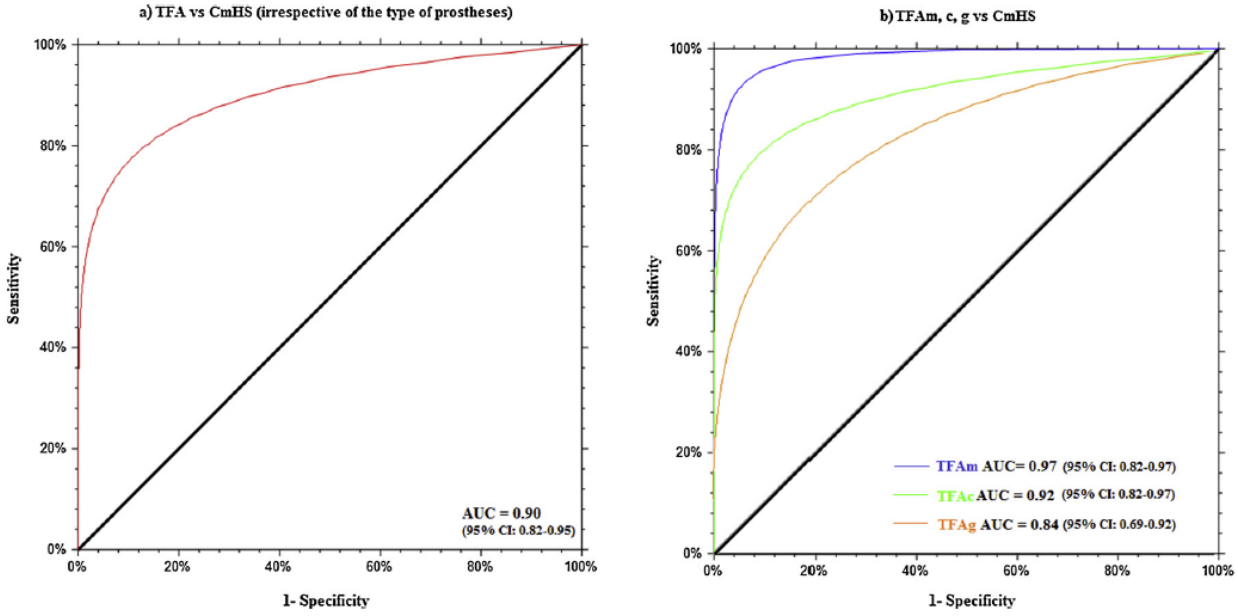

Figure 5.5 *Receiver operating characteristics curve. Ability of pelvic obliquity to discriminate between CmHS and subjects with TFA. This figure illustrates the area under the receiver operating characteristics curve (AUC) of pelvic obliquity in identifying subjects with TFA from CmHS, irrespective of the type of prosthesis (a) and according to the type of prostheses (b). The diagonal black line represents the non–significance threshold of AUC=0.50, the colored lines represent the true positive rate and the false positive rate at each threshold. AUC values and their 95 % confidence intervals (CI) are reported.*

5.2. Electrophysiological Features of Prosthetic Gait

One of the primary goals of gait analysis studies in people with amputation should be to improve the development of new and ergonomic prostheses, as well as the people's ability to adapt to the most recent and technologically advanced prosthetic devices [7,16,28]. The ideal prosthetic device should enable people with amputation to maintain an efficient and ecological gait function while also minimizing gait asymmetries and reducing the need for compensatory activation of the muscles of the sound limb. However, no studies on the effect of various prosthetic devices on muscle activation in the sound limb have been conducted thus far. Such studies are required to determine the amounts of compensation in the neuromuscular strategies used for various prostheses.

The goal of the study *"Global Muscle Coactivation of the Sound Limb in Gait of People with Transfemoral and Transtibial Amputation"* (2020) was to investigate the effect of three different types of prosthetic devices (mechanical, electronic, and bionic) on the activation of the sound limb muscles. The time-varying multimuscle coactivation function (TMCf) method [29,30] was used, which is a compact indicator that allows one to understand the central nervous system's (CNS) global strategy in modulating the simultaneous activation/deactivation of many lower limb muscles during

gait, regardless of the magnitude of the single muscle activation, to the agonist-antagonist interaction at the single joint level, and to the modular architecture.

Forty eight subjects with lower-limb unilateral TFA and TTA, consequent to workplace traumatic accidents, were enrolled from the Rome branch of the Prosthetics Center of Italian Workers' Compensation Authority (INAIL). Twenty two healthy subjects were enrolled as the control group (C) and were age-sex-speed matched with people with amputation.

Walking tests were performed using a six infrared cameras optoelectronic motion analysis system at sample frequency of 340 Hz (SMART-DX 6000 System, BTS, Milan, Italy). Twenty-seven passive spherical markers were placed on the following prominent bony landmarks, according to a modified Davis' protocol [20], as shown in Figure 5.6.

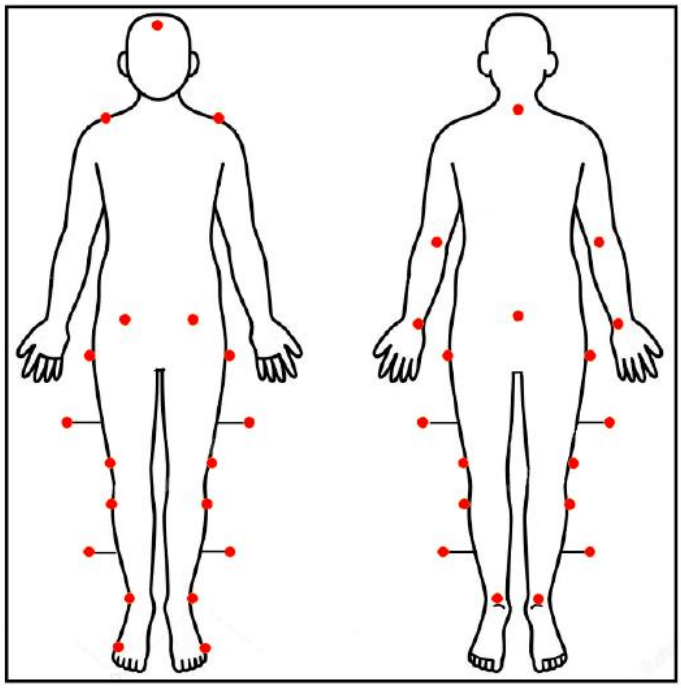

Figure 5.6 *Modified Davis' protocol for marker placement.*

Gait analysis started with the standing position on a platform. Subsequently, controls and subjects with amputation were asked to walk at their preferred speed with their shoes. Furthermore, controls were asked to walk also at a slower speed. At least ten trials, at each velocity, were recorded for both subject groups.

We recorded sEMG signals using a bipolar 16-channel wireless system (FreeEMG 1000 System, BTS) with a sample frequency of 1000 Hz from the sound limb of the people with amputation and on the dominant side of the controls on the gluteus medius, rectus femoris, vastus lateralis, vastus

medialis, tensor fascia latae, semitendinosus, biceps femoris, tibialis anterior, gastrocnemius medialis, gastrocnemius lateralis, soleus, and peroneus longus in accordance with Atlas of Muscle Innervation Zones [21] and the European Recommendations for Surface Electromyography [22].

We calculated the time-varying multimuscle coactivation function (TMCf) and the Coactivation Index to evaluate the global muscle coactivation, and two indexes, FWHM and CoA, to characterize in terms of time amplitude the TMCf curves and to understand where most coactivation is concentrated within the gait cycle. We also calculated the Coefficient of Multiple Correlation to evaluate the waveform similarity of the curves.
The following time-distance parameters were calculated for each subject with amputation: walking speed (m/s), cadence (steps/s), step length (m), and step width (m) normalized to the limb length; stance, swing, and double support phase duration expressed as percentages of the gait cycle duration. Symmetry index was calculated for each time-distance parameter. Mechanical energy expenditure and recovery was also assessed by calculating the TEC and R-step parameters.

Both TFA and TTA groups showed significantly higher CI values when compared with the corresponding controls (Table 5.5).

Table 5.5 *The means, standard deviations, and statistical results (p-values) of parameters evaluated on TMCf curves*

	People with Amputation versus Controls						Type of Prosthesis			
	TFA	C_{TFA}	p_{group}	TTA	C_{TTA}	p_{group}	TFA_M	TFA_C	TFA_G	p_{group}
CI	3.06 ± 0.58	2.43 ± 0.57	<0.01	3.11 ± 1.07	2.25 ± 0.31	<0.01	3.36 ± 0.55	2.78 ± 0.58	3.24 ± 0.48	0.02
CMC_{IS}	0.84 ± 0.06	0.85 ± 0.05	>0.05	0.88 ± 0.04	0.88 ± 0.04	>0.05	0.86 ± 0.06	0.84 ± 0.05	0.84 ± 0.06	>0.05
DP	1.36 ± 0.31	1.07 ± 0.3	<0.01	1.28 ± 0.41	0.9 ± 0.2	0.01	1.43 ± 0.28	1.21 ± 0.26	1.41 ± 0.21	0.04

CI: coactivation index, CMC_{IS}: coefficient of multiple correlation intra-subjects, DP: deviation phase. People with transfemoral amputation (TFA), control group matched with TFA (C_{TFA}), people with transtibial amputation (TTA), control group matched with TTA (C_{TTA}), people with transfemoral amputation with mechanical (TFA_M), CLeg (TFA_C), and Genium prostheses (TFA_G).

Both TFA and TTA groups showed significantly higher FWHM values when compared with the corresponding controls (TFA vs. C_{TFA}: $p = 0.03$ and TTA vs. C_{TTA}: $p = 0.04$) (Figure 5.7). Both TFA and TTA groups showed significantly higher DP values than those of the corresponding controls (Table 5.5). No significant differences in the CMC_{IS} were found between the TFA and TTA groups when compared with the corresponding controls (Table 5.5). The level of amputation had no statistically significant effect on CoA evaluated on TMCf curves (Figure 5.7).

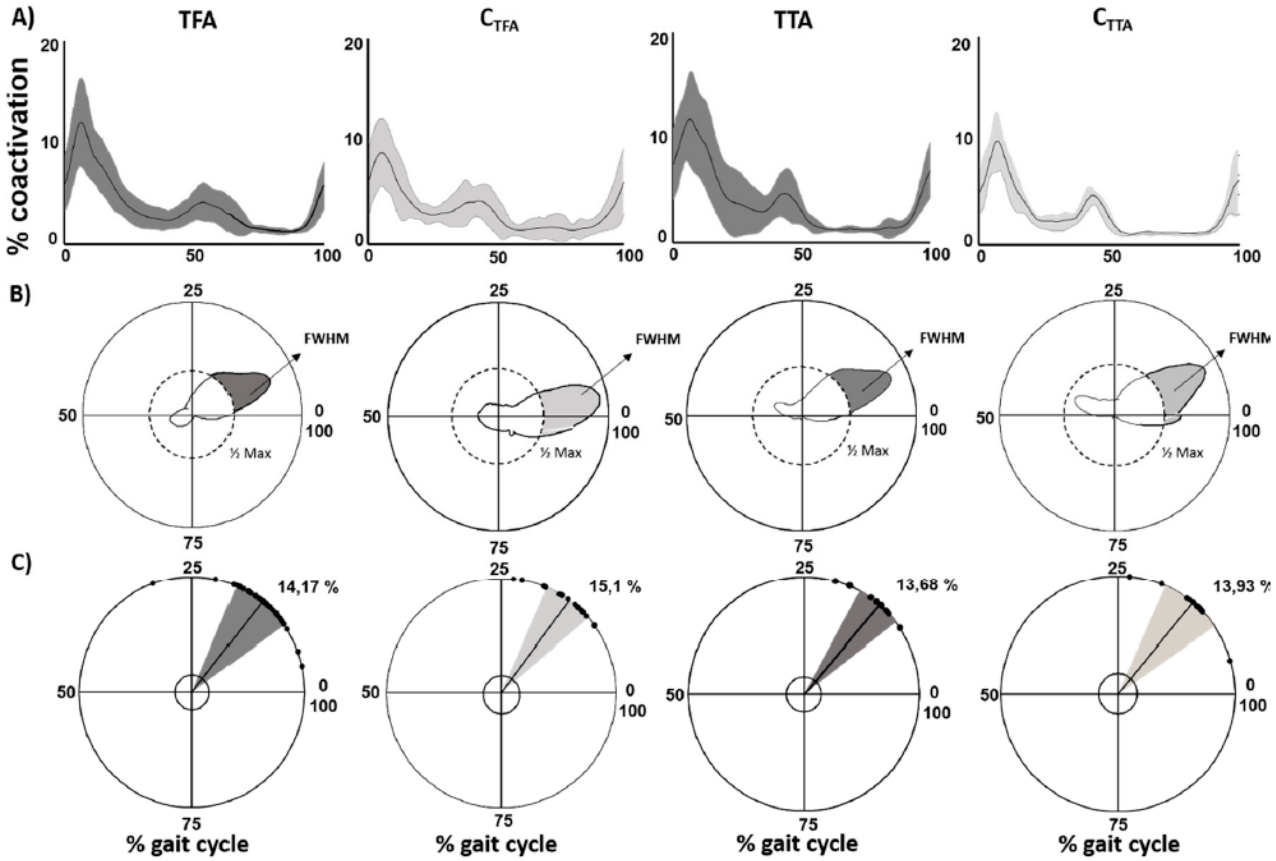

Figure 5.7 *(A) Time-varying multimuscle coactivation function (TMCf) curves shown as mean curves with standard deviations for people with transfemoral amputation (TFA), the control group matched with TFA (C_{TFA}), for people with transtibial amputation (TTA), and the control group matched with TTA (C_{TTA}). (B) Full width at half maximum (FWHM) of the TMCf for each group shown in polar coordinates. (C) Center of activity (CoA) of the TMCf for each group: each dot represents the mean CoA value of a subject, whereas the solid line and the width of the circular sector represent the mean and standard deviation values of the CoA of all subjects, respectively. All parameters are shown as percentages of the gait cycle.*

A significant main effect of the type of prosthesis was found on the CI values. TFA_C showed lower values when compared with both TFA_M and TFA_G at post-hoc analysis (Table 5.5). A significant main effect of the type of prosthesis was found on the FWHM values (Figure 5.8). TFA_C showed lower values when compared with both TFA_M and TFA_G at post-hoc analysis ($p = 0.036$). A significant main effect of the type of prosthesis was found on DP values. TFA_C showed lower values when compared with TFA_M and TFA_G (Table 5.5). No significant effect of the type of prosthesis was found on CMC_{IS} values (Table 5.5). The type of prosthesis had no statistically significant effect on CoA evaluated on TMCf curves (Figure 5.8).

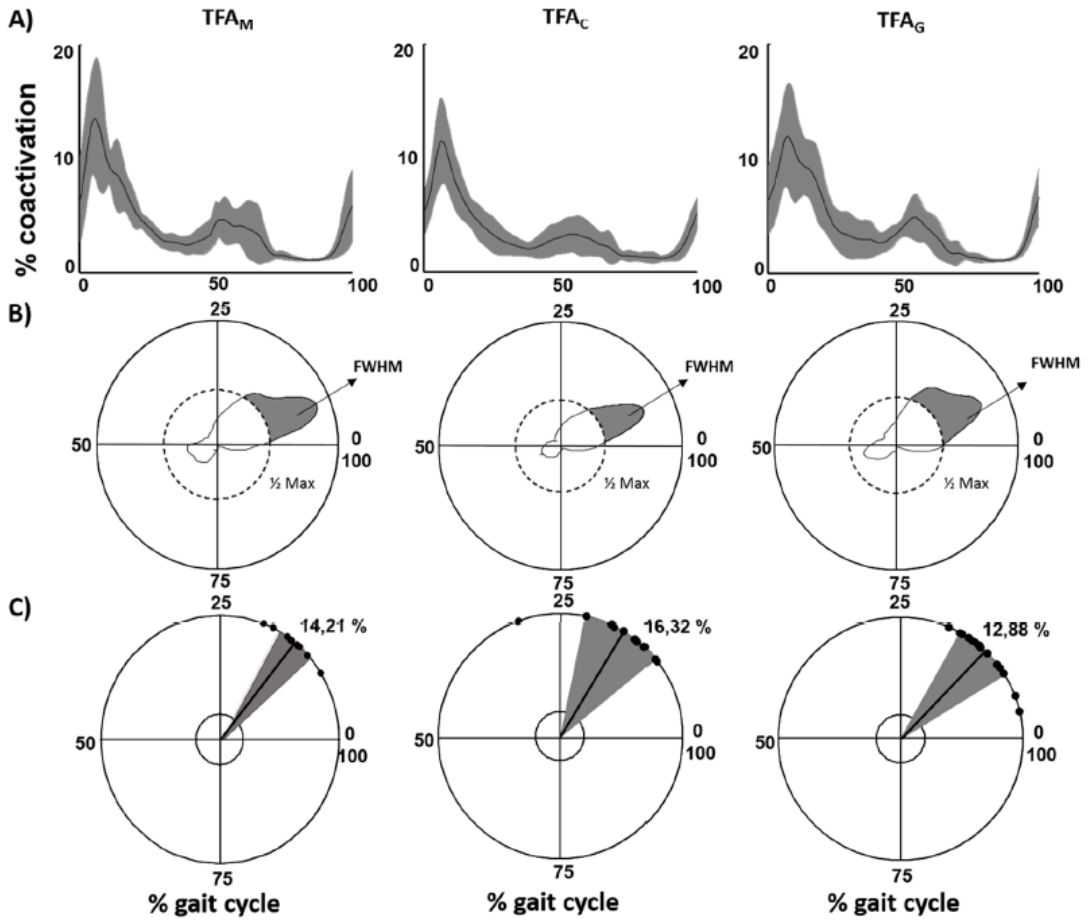

Figure 5.8 *(A) TMCf curves shown as mean curves with standard deviations for people with transfemoral amputation with mechanical (TFA_M), CLeg (TFA_C), and Genium prostheses (TFA_G). (B) Full width at half maximum (FWHM) of the TMCf for each group shown in polar coordinates. (C) Center of activity (CoA) of the TMCf for each group: each dot represents the mean CoA value of a subject, whereas the solid line and the width of the circular sector represent the mean and standard deviation values of the CoA of all subjects, respectively. All parameters are shown as percentages*

A moderate positive correlation was found between CI and gait speed values in people with TFA ($p = 0.03$, $r = 0.36$). Correcting for gait speed, partial correlation analysis showed a moderate positive correlation between CI and stance duration values ($p = 0.04$, $r = 0.38$). Furthermore, people with TFA also showed a moderate positive correlation between CI and TEC values ($p = 0.04$, $r = 0.52$) and a negative correlation between the DP and symmetry index evaluated on double support duration ($p = 0.04$, $r = -0.33$)

All of the considerations from the related studies emphasize the importance of using a multimodal approach when analyzing gait in people who have had a lower limb amputation; in fact, despite the massive scientific effort of the last two decades, this condition is still partially unknown to date, and

the compensations that are required for achieving stable gait with a prosthesis are highly complex and cannot be characterized as a whole without a complete record.

Bibliography

[1]. Geurts A.C, Mulder T.W, Nienhuis B, Rijken R.A. 1991. Dual-task assessment of reorganization of postural control in persons with lower limb amputation. Arch. Phys. Med. Rehabil., 72, 1059–1064.

[2]. Chen R, Corwell B, Yaseen Z, Hallett M, Cohen L.G. 1998. Mechanisms of cortical reorganization in lower-limb amputees. J. Neurosci., 18, 3443–3450.

[3]. Baum BS, Schnall BL, Tis JE, Lipton JS. 2008. Correlation of residual limb length and gait parameters in amputees. Injury, 39:728–33.

[4]. Bell JC, Wolf EJ, Schnall BL, Tis JE, Tis LL, Potter MBK. 2013. Transfemoral amputations: the effect of residual limb length and orientation on gait analysis outcome measures. JBJS, 95:408–14. doi: 10.2106/JBJS.K.01446

[5]. Kannenberg A, Zacharias B, Pröbsting E. 2014. Benefits of microprocessor controlled prosthetic knees to limited community ambulators: systematic review. J Rehabil Res Dev., 51:1469.

[6]. Segal AD, Orendurff MS, Klute GK, McDowell ML. 2006. Kinematic and kinetic comparisons of transfemoral amputee gait using C-LegR and Mauch SNSR prosthetic knees. J Rehabil Res Dev., 43:857.

[7]. Highsmith MJ, Kahle JT, Miro RM, Cress ME, Lura DJ, Quillen WS, et al. 2016. Functional performance differences between the Genium and C-Leg prosthetic knees and intact knees. J Rehabil Res Dev., 53:753.

[8]. Kahle JT, Highsmith MJ, Hubbard SL. 2008. Comparison of non-microprocessor knee mechanism versus C-Leg on prosthesis evaluation questionnaire, stumbles, falls, walking tests, stair descent, and knee preference. J Rehabil Res Dev., 45:1–14.

[9]. Thiele J, Westebbe B, Bellmann M, Kraft M. 2014. Designs and performance of microprocessor-controlled knee joints. Biomed Tech., 59:65– 77.

[10]. Kaufman KR, Bernhardt KA, Symms K. 2018. Functional assessment and satisfaction of transfemoral amputees with low mobility (FASTK2): a clinical trial of microprocessor-controlled vs. non-microprocessor-controlled knees. Clin Biomech., 58:116–22.

[11]. Uchytil J, Jandacka D, Zahradnik D, Farana R, Janura M. 2014. Temporal– spatial parameters of gait in transfemoral amputees: comparison of bionic and mechanically passive knee joints. Prosthet Orthot Int., 38:199– 203.

[12]. Mileusnic MP, Rettinger L, Highsmith MJ, Hahn A. 2021. Benefits of the Genium microprocessor controlled prosthetic knee on ambulation, mobility, activities of daily living and quality of life: a systematic literature review. Disabil Rehabil Assist Technol., 16:453–64.

[13]. Sivapuratharasu B, Bull AM, McGregor AH. 2019. Understanding low back pain in traumatic lower limb amputees: a systematic review. Arch Rehabil Res Clin Transl., 1:100007.

[14]. Cutti A. G, Lettieri E, Del Maestro M, Radaelli G, Luchetti M, Verni G, Masella C. 2017. Stratified cost-utility analysis of C-Leg versus mechanical knees: Findings from an Italian sample of transfemoral amputees. Prosthetics and Orthotics International, 41(3), 227–236.

[15]. Kannenberg A, Zacharias B, Mileusnic M, Seyr M. 2013. Activities of daily living. JPO Journal of Prosthetics and Orthotics, 25(3), 110–117.

[16]. Schafer ZA, Perry JL, Vanicek N. 2018. A personalised exercise programme for individuals with lower limb amputation reduces falls and improves gait biomechanics: a block randomised controlled trial. Gait Posture, 63:282–9.

[17]. Crenshaw JR, Kaufman KR, Grabiner MD. 2013. Compensatory-step training of healthy, mobile people with unilateral, transfemoral or knee disarticulation amputations: a potential intervention for trip-related falls. Gait Posture, 38:500–6.

[18]. Major MJ, Fey NP. 2017. Considering passive mechanical properties and patient user motor performance in lower limb prosthesis design optimization to enhance rehabilitation outcomes. Phys Ther Rev., 22:202– 16.

[19]. Mohanty RK, Mohanty RC, Sabut SK. 2020. A systematic review on design technology and application of polycentric prosthetic knee in amputee rehabilitation. Phys Eng Sci Med., 43:781–98.

[20]. Tatarelli A, Serrao M, Varrecchia T, Fiori L, Draicchio F, Silvetti A, Conforto S, De Marchis C, Ranavolo A. 2020. Global Muscle Coactivation of the Sound Limb in Gait of People with Transfemoral and Transtibial Amputation. Sensors, 20(9):2543.

[21]. Barbero M, Merletti R, Rainoldi A. 2012. Atlas of Muscle Innervation Zones; Springer: Milan, Italy.

[22]. Hermens H.J, Freriks B, Disselhorst-Klug C, Rau G. 2000. Development of recommendations for SEMG sensors and sensor placement procedures. J. Electromyogr. Kinesiol., 10, 361–374.

[23]. Varrecchia, et al. 2019. Common and specific gait patterns in people with varying anatomical levels of lower limb amputation and different prosthetic components, Hum. Mov. Sci., 66,9–21.

[24]. S Li, W Cao, H Yu, Q Meng, W Chen. 2019. Physiological parameters analysis of transfemoral amputees with different prosthetic knees, Acta Bioeng. Biomech., 21,135–142.

[25]. Highsmith M.J, et al. 2010. Safety, energy efficiency, and cost efficacy of the C-Leg for transfemoral amputees: a review of the literature, Prosthet. Orthot. Int., 34, 362–377.

[26]. Czerniecki J.M, Morgenroth D.C. 2017. Metabolic energy expenditure of ambulation in lower extremity amputees: what have we learned and what are the next steps? Disabil. Rehabil., 39, 143–151.

[27]. Gholizadeh H, Abu Osman N.A, Eshraghi A, Ali S. 2014. Transfemoral prosthesis suspension systems: a systematic review of the literature, Am. J. Phys. Med. Rehabil. 93, 809–823.

[28]. Hsu M.-J, Nielsen D.H, Lin S.-J, Shurr D. 2006. The effects of prosthetic foot design on physiologic measurements, self-selected walking velocity, and physical activity in people with transtibial amputation. Arch. Phys. Med. Rehabil., 87, 123–129.

[29]. Ranavolo A, Mari S, Conte C, Serrao M, Silvetti A, Iavicoli S, Draicchio F. 2015. A new muscle co-activation index for biomechanical load evaluation in work activities. Ergonomics, 58, 966–979.

[30]. Varrecchia T, Rinaldi M, Serrao M, Draicchio F, Conte C, Conforto S, Schmid M, Ranavolo A. 2018. Global lower limb muscle coactivation during walking at different speeds: Relationship between spatio-temporal, kinematic, kinetic, and energetic parameters. J. Electromyogr. Kinesiol., 43, 148–157.

CHAPTER 6

6. JOB INTEGRATION/REINTEGRATION OF PEOPLE WITH NEUROMUSCULAR DISORDERS

Individuals of working age with neuromuscular illnesses frequently struggle with employability, work challenges, and premature job stoppage [1–3]. In any case, employment integration and reintegration have been shown to improve pathological people's overall quality of life [1, 4, 5]. Indeed, increasing their working life should be an important element of neuromuscular disorder care in terms of psychological, social, and health wellness [6]. An increase in self-esteem and social wellness, as well as a reduction in workplace prejudice against disabled people, can be achieved by designing an adequate job accommodation [7– 9], assistance and improving, among other things, the social environment, support from colleagues and supervisors, job expectations, and ergonomic interventions [10]. Furthermore, understanding of specific work-related difficulties, as well as focused rehabilitative, ergonomic, and training interventions, can enable individuals to return to work. Rehabilitation can play a constructive role by removing barriers to obtaining, retaining, or returning to work [11– 18]. This concept is supported by these people's contextual ability to maintain an effective motor strategy by adopting different compensatory behaviors during the disease, despite disease progression and motor decline [19–22]. Neuropathies, multiple sclerosis, stroke, spastic paraplegia, cerebellar ataxia, dystonia, traumatic spine and brain lesions, and encephalitis are degenerative and acquired neurological diseases that can impact motor function throughout working age and severely limit workers' autonomy and efficiency [6, 23–27]. Therefore, workers with neurological illnesses may have motor impairment in numerous motor domains, including hand function, balance, and locomotion, placing a significant burden on society in terms of lower job productivity and expense. Clinicians manage their patients' premature work interruptions [28, 29] by developing appropriate standard and new pharmacological, surgical, and rehabilitation treatments, such as robotic rehabilitation, virtual reality, and neuromodulation [30–34]. Indeed, these treatments have the primary goal of restoring patients' motor performance, autonomy, and everyday life, allowing them to return to work and optimize their work capabilities. Furthermore, novel ergonomic solutions, such as work task rehabilitation and workplace interventions, are being added to job accommodation plans [35–37]. Indeed, the fourth industrial revolution has lately opened up new occupational scenarios in which crucial human–robot collaboration (HRC) technologies, such as collaborative robots and exoskeletons, aid workers in their workplaces [3]. When a worker affected

by a neurological pathology with motor disorders is reintegrated at work, an exhaustive assessment of his/her residual motor function is of primary importance to design and/or optimally adapt his/her workplace. Therefore, biomechanical and physiological indexes are useful for monitoring motor and muscle performance and verifying the effectiveness of interventions for job integration/reintegration [3]. Furthermore, the efficiency Furthermore, the efficiency of these ergonomic interventions should be verified and monitored throughout time [3]. Kinematic, kinetic, and surface electromyography (sEMG) measurements are now widely used in research laboratories by movement scientists and could be used more and more in clinical practice by health operators, to define quantitatively the form and degree of motor dysfunction, assess the complicated interaction between the fundamental deficit and the adaptive and compensating mechanisms, categorize patients based on their specific neurological condition, and finally monitor pre–post-treatment [3].

The aim of the study " *Indexes for motor performance assessment in Job Integration/Reintegration of People with Neuromuscular Disorders-A Systematic Review*" (2022) is to identify which of these indexes are the most suited for assessing the effectiveness and efficiency of return-to-work programs. This research employs a systematic literature review process to suggest present and future important indexes to achieve this purpose.

6.1 Materials and Methods

This study was performed using the systematic review method proposed by the Preferred Reporting Items for Systematic Reviews and Meta-Analysis (PRISMA) [38].

Literature search strategy

This systematic review considered English articles published from 2011 to March 30, 2021, and the literature search was performed in a systematic manner using the following selected databases: Scopus, Web of Science, and PubMed. According to the database, the annual article production related to this research is starting to grow significantly from 2011, which is the starting year of the analyzed period. There were four issues of interest in this systematic review [39]: job reintegration, indexes, neurological, and quality. For each issue identified according to the method proposed in the study mentioned in [39], the following keywords were identified as related to that topic and used for online database searching:

- Job Reintegration: "Job Integration," "Job Reintegration," "work Integration," "work Reintegration," "workplace," "Return to work Rehabilitation," "work ability";

- Indexes: “kinematic index,” “kinetic index,” “force index,” “sEMG index,” “surface electromyography index,” “motor index”;
- Neurological: “Neurological motor disease,” “Neurological motor disorders,” “Neuromuscular motor disease,” “Neuromuscular motor disorders”;
- Quality: “performance,” “monitoring,” “ergonomics,” “quantitative,” “instrumental”.

Screening criteria

A total of two, three, and four groups of keywords (one for each issue) were combined in the literature search (1,657 combinations). We then entered each combination of one, two, three, or four keywords into each of the selected online databases (PubMed, Scopus, andWeb of Science) to search for articles. The articles obtained were imported into Mendeley, and duplicates were removed. Our search was limited to peer-reviewed journal publications, reviews, chapters of books, and conference proceedings. The collected publications were then screened in three steps: (i) the titles were assessed for relevance; (ii) the abstracts were considered; and (iii) the complete text were downloaded when the information was deemed relevant.

Inclusion and exclusion criteria of articles in the review

Studies were considered eligible if they were written in English, and they investigated subjects using biomechanical and physiological quantitative indexes. The common goal of these eligible studies was to perform a quantitative evaluation of programs/strategies to make patients sufficiently able to return to work. Excluded were narrative and systematic reviews or meta-analyses and purely clinical studies not aimed at evaluating job placement/reintegration. Furthermore, the studies with the following characteristics were also excluded:

- studies that do not consider indexes (biomechanical and physiological indexes) of motor performance for job integration/reintegration;
- studies on simulated data and not on people;
- studies with all or almost all participants of non-working age (>67 years, since the maximum range of retirement age in Italy is 67 years for most professions);
- studies on children/teenagers (<18 years, since in Italy, it is forbidden to work if you are younger than 18 years);
- studies on only work risks assessment.

In addition to searching databases with the aforementioned keywords, once the authors had identified articles for inclusion in the systematic review, they also examined the bibliography of the selected

articles to check whether there were any additional articles that could be included in this systematic review.

Data extraction

From the articles selected as eligible, the authors extracted the data that provided detailed information for each study, using the Population Intervention Comparison Outcome (PICO) framework as a guide when analyzing the eligible articles [40]. More in detail, the authors followed the following steps to extract the data from the selected articles:

- The authors looked for an existing extraction form or tool to help guide them and used existing systematic reviews on our topic to identify what information to collect if they are not sure what to do [41, 42].
- Train the review team on the extraction categories and what type of data would be expected.
- The authors performed a pilot extraction to ensure data extractors were recording similar data and revised the extraction form if needed.
- The authors discussed any discrepancies in extraction throughout the process.
- The review team documented any changes to the process or the form, kept track of the decisions the team made, and the reasoning behind them.

At the end of this procedure, the extracted information included the following:

- characteristics of the participants involved in the study: number of subjects (N), gender (F and M), age (years), height (H) in meters, weight (W) in kg, and/or body mass index (BMI) in kg/m2;
- measurement details: motor task, parameters/indexes names and acronyms if applicable, instrumentation used, and investigated body part;
- aims of the study;
- findings of the study.

Assessment of bias

A bias represents a characteristic of a study that can introduce a systematic error in the magnitude or direction findings. The potential risk of bias was assessed independently by the authors according to the Cochrane Handbook for Systematic Reviews of Interventions [43] and by using the tool ROBINS-I [44, 45], which was developed for the risk of bias assessment of nonrandomized studies of interventions. The authors assessed the following risks of bias [44, 45]:

- confounding [D1]: occurs when one or more prognostic factors can also predict the baseline intervention;
- selection of participants into study [D2]: even though the effects of the interventions are the same, there will be a connection between interventions and outcomes when exclusion of some eligible participants, initial follow-up times for some participants, or certain outcome events are connected to both the intervention and the outcome;
- classification of interventions [D3]: by misclassification of intervention status;
- deviation from the intended study [D4]: when there are consistent discrepancies between experimental intervention and comparison groups, which represent a deviation from the intended intervention;
- missing data [D5]: when later follow-up or information is missing for individuals initially included and followed;
- measurement of outcomes [D6]: introduced by errors in measurement of outcome data;
- selection of the reported result [D7]: selective reporting of results in a way that depends on the findings.

6.2 Results

The study selection process started from the results of the literature database search that yielded 231,793 records, as shown in Figure 6.1. In particular, 71,317 were found on Scopus, 93,406 on Web of Science, and 67,070 PubMed. After removing the duplicates, the articles were 142,968. These articles were screened by deleting articles on the basis of not connected words (e.g., animal, astronomy, and human resources) and journals([e.g., International Journal of Molecular Science), obtaining 4,119 articles. These articles were screened based on their title, obtaining 1,187 articles. From this group, abstracts were read, and 1,133 were excluded by the screening criteria. Consequently, 54 full text articles were assessed for eligibility. Finally, after having removed 39 articles by the eligibility criteria, a total of 15 articles were included in this systematic review.

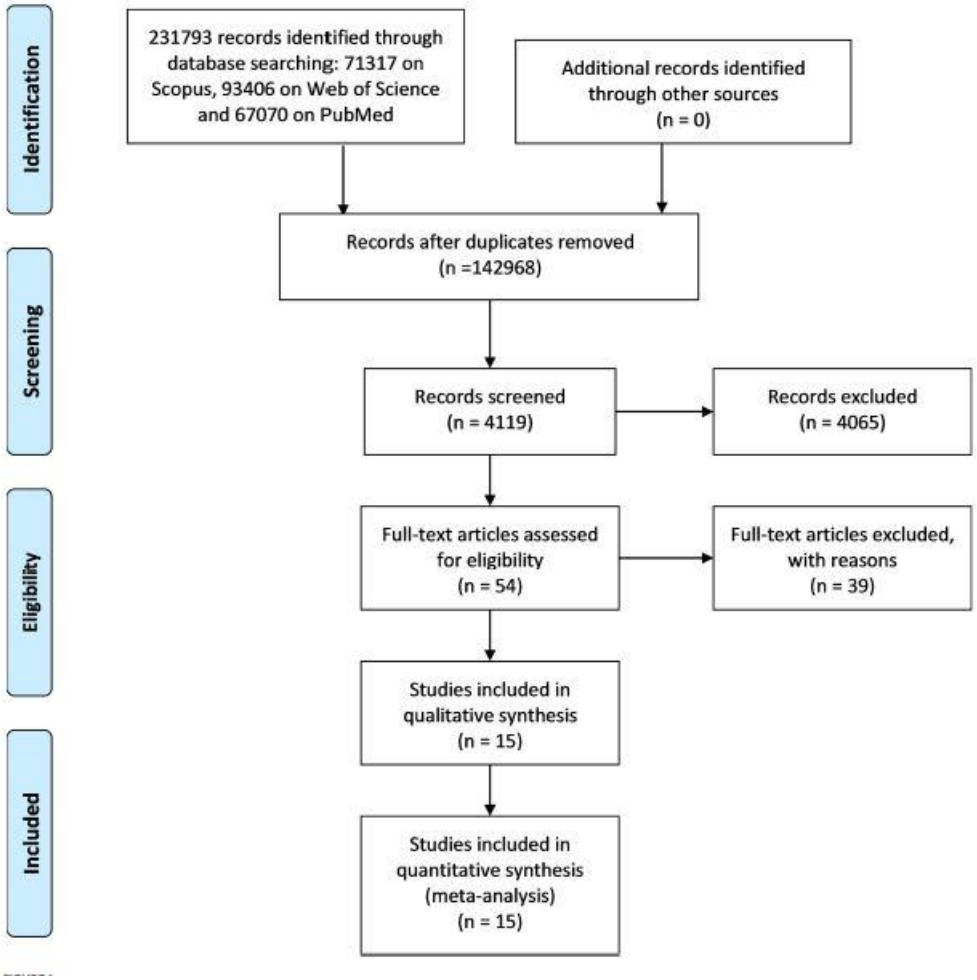

Figure 6.1 *PRISMA flowchart related to the steps of a systematic review provided by the journal Frontiers in Neurology.*

Table 6.1 shows an overview of the main characteristics of the 15 considered studies [46–60] following the PICO model [40] and highlighting the biomechanical and physiological indexes used. All the articles that met the eligibility criteria are very recent: five were published in 2020, one in 2019, six between 2013 and 2016, and three, the oldest, in 2012. A total of 1,300 subjects were recruited in the included studies, with 618 males (M) and 612 females (F), and only in one study [60], the gender was not specified. The subjects' mean age varied from <21.36 [57] to 74 [55] years. A total of eight studies dealt with subjects with low back pain (LBP) [46, 49, 52, 53, 56, 58–60], two studies considered subjects who have survived stroke (SS) [50, 55], one study considered subjects with multiple sclerosis (MS) [48], three subjects with spinal cord injury (SCI) [51, 52, 57], and finally, two addressed healthy subjects (HS) [47, 54]. All studies were carried out in the laboratory [46–60], and three of them also in real-life environments [47, 52, 55]. The following tasks were analyzed (see Table 6.1):

- lifting task, one study [60];
- rehabilitation exercises, three studies [46, 53, 56];
- daily activities, two studies [47, 55];
- walking task, two studies [47, 48];
- balance, three studies [54, 57, 59];
- reaching and grasping activities, three studies [50, 51, 57];
- typical working activities, one study [52];
- lumbar flexion–extension, one study [49];
- physical performance task, one study [54];
- trunk stability test, one study [58];
- gross arm and fine hand movements, one study [47];
- sitting test, one study [57];
- dexterity task, one study [59].

In total, 41 different kinematic [46–55, 57, 60], 12 kinetic [51, 53, 54, 57], 5 sEMG [46, 56, 59, 60], 3 postural [55, 57], and 4 other indexes [47, 49, 50] were investigated (see Tables 6.1, 6.2).

Table 6.1. *Descriptive analysis of the studies considered in the review according to the PICO method.*

References	Participants involved in the study	Measurement details				Aims	Findings
		Motor task	Parameters/indexes name (acronym)	Instrumentation	Body part		
Monticone et al. (46)	$N = 20$: • 10 LBP (7 F, 3 M; Age = 58.9 ± 16.4 y; BMI = 27.4 ± 4.9 kg/m^2); • 10 HS (4 F, 6 M; Age = 56.6 ± 14.4 y; BMI = 25.2 ± 3.1 kg/m^2).	Spinal stabilizing exercises in addition to usual-care rehabilitation (passive mobilisatio, stretching, and postural control); • Individual cognitive–behavioral training.	**Gait parameters**: velocity, cadence, step length, step time, and single support time of both sides.	GAITRite-Walkway System (CIR System Inc., Clifton, NJ).	-	To evaluate the effect of a multidisciplinary rehabilitation program on disability, kinesiophobia, catastrophizing, pain, quality of life and gait disturbances in patients with chronic LBP.	The findings indicate that the treatment was beneficial in terms of gait cadence, as well as the positive impact of cognitive–behavioral therapy on non-spinal motor tasks, which improved health and favored a return to work and usual activities.
Lee et al. (47)	$N = 35$ HS: • 18 (5 F, 13 M; Age = 21.7 ± 2.3 y) participated in the in-laboratory experiments; • 18 (4 F, 14 M; Age = 23.4 ± 4.2 y) in the free-living experiments; one subject participated in both.	•**Laboratory experiments:** Walking; Buttoning a shirt Bilateral; Tying shoelaces; Typing on a keyboard; Folding a towel; Cutting putty dough with a fork and a knife; Opening a screw-top jar; Taking the cap off of a bottle and drinking; Flipping pages of a magazine. • **Free-living experiments:** Normal daily routines.	The ratio of limb use; • Limb-use intensity (i.e., acceleration magnitude).	Miniaturized sensor (Arcus, ArcSecond Inc., USA) consisted of a three-axis accelerometer, a local memory for data storage, a 170 mAh battery, and an ultra-low-power 32-bit microprocessor in a waterproof enclosure.	Hands.	To investigate the use of finger-worn accelerometers to monitor gross arm and fine hand movement; to examine the validity of the proposed approach by collecting and analyzing data from neurologically intact individuals in a laboratory and a free-living environment as a preliminary step toward developing a system suitable to monitor stroke survivors in the home and community setting; to describe a comprehensive approach integrating both a clinical- and functional status-based pathology and an adapted rehabilitation prescription.	The results establish the validity of the proposed measure of real-world upper-limb function derived using data collected by means of finger-worn accelerometers.

Richmond et al. (48)	$N = 56$: • 29 HS (21 F, 8 M; Age = 47 ± 15 y; $H = 1.69 \pm 0.08$ m; $W = 72.4 \pm 14.2$ kg; BMI = 25.3 ± 4.0 kg/m^2); • 27 MS (20 F, 7 M; Age = 48 ± 12 y; $H = 1.66 \pm 0.08$ m; $W = 68.6 \pm 9.2$ kg; BMI = 24.9 ± 3.8 kg/m^2).	Walking task.	Phase coordination index (PCI).	Six tri-axial Opal^{TM} body-worn inertial monitoring units (IMUs).	Sternum, lower back (L4/L5 region), wrists and feet.	To identify the temporal actions underlying bilateral coordination in people with MS and how bilateral coordination is affected by gait speed augmentation in these individuals.	People with MS exhibited poorer left-right coordinated stepping patterns during gait compared to neurotypical peers across walking conditions. This assessment highlights Phase Coordination Index as a potential target for future rehabilitative interventions for subjects with MS and individualized rehabilitation strategies aimed at improving the health span and overall quality of life for subjects with MS.
Cimarras-Otal et al., (49)	$N = 18$: • 10 LBP (2 F, 8 M; Age = 42.25 ± 7.28 y; $H = 1.69 \pm 0.05$ m; $W = 72.75 \pm 15.79$ kg; BMI = 25.12 ± 4.69 kg/m^2); • 8 HS (4 F, 4 M; Age = 42.20 ± 5.59 y; $H = 1.68 \pm 0.09$ m; $W = 68.27 \pm 12.80$ kg; BMI = 23.80 ± 2.34 kg/m^2).	Flexion-lumbar extension.	• Angle and flexion; • Bending speed; • Root mean square (RMS) of EMG signal; • Angle, bending speed, and flexion-extension ratio (FER).	SMART-DX (BTS Bioengineering, Italy): BTS FREEEMG 300 electromyographic probes; Six BTS Bioengineering—SDX-C2 3D; Two video cameras BTS VISTA.	Trunk.	To investigate whether an exercise program adapted to the characteristics of the workplace is a useful supplement to general exercise recommendations in assembly line workers with chronic LBP.	Results demonstrated that the implementation of a physical exercise program adapted to the characteristics of the workplace, for workers with chronic LBP, could be an effective treatment to reduce the interference of pain and to improve the functionality of the lumbar spine.
Schaefer et al. (50)	$N = 28$: • 16 subjects with SS (7 F, 9 M; Age = 58 ± 11 y); • 12 HS (6 F, 6 M; Age = 53 ± 16 y).	Reach-to-grasp.	• **Reaching performance**: reach path ratio, peak reach velocity, reach time, contact velocity; • **Grasping performance**: peak aperture, peak grip force.	Electromagnetic tracking system with nine sensors (The Motion Monitor, Innovative Sports Training, Chicago, IL).	Midsternum; upper arm; forearm; hand; fingernail of each digit.	To determine whether performance of a functional reach-to-grasp movement in people with poststroke hemiparesis is influenced by grip type and/or task goal; to directly test how stroke might alter patterns of performance when moving with multiple grip types and task goals.	Results suggest that even though the ability to move one's arm and hand is often impaired after stroke, reaching and grasping performance can still be modified based on how and why an object will be grasped. Information about how different movement contexts influence performance poststroke may assist therapists in planning how and what to practice during task specific upper extremity training.
Correia et al. (51)	13 SCI at level C4–C7 (Age = 54.54 ± 16.23 y).	Grasping.	• Activities of daily living using the Jebsen Taylor Hand; • Active range of motion of the fingers; • Grasp strength for power; • Pinch grasps.	SOFT ROBOTIC GLOVE, Goniometer, pressure sensor mat.	Hand.	To evaluate the performance of the optimized soft robotic glove in restoring activities of daily living for individuals with tetraplegia resulting from SCI.	Results demonstrated the effectiveness of a fabric based soft robotic glove to improve independent performance of activities of daily living in individuals with hand paralysis resulting from SCI.
Kim and Martin (52)	$N = 29$: • 10 HS (7 M, 3 F; Age = 28.0 ± 11.3 y; $W = 81.3 \pm 20.3$ kg); • 10 SCI (10 M; Age = 39.0 ± 13.7 y; $W = 75.2 \pm 17.4$ kg). • 9 LBP (5M, 4F; Age = 47.8 ± 11.6 y; $W = 84.0 \pm 29.2$ kg).	Manually moving a hand-held box from an initial position to one of four target shelves.	Precedence Index (PI).	-	Upper body segments.	To characterize the temporal coordination between the torso and hands in SCI and LBP individuals.	Results demonstrated that hands and torso movements show adapted patterns of coordination in the population with injury. Altogether, it is suggested that patterns of temporal coordination, can be effectively used to assess the gravity of injury, progress of rehabilitation and work capacity measurements.

Bruce-Low et al. (53)	$N = 72$ LBP (42 M, 30 F; Age = 45.5 ± 14.1 y).	• Maximal lumbar isometric strength; • modified-modified Schober's flexion test; • completion of the Oswestry disability index (ODI); • the visual analog scale (VAS).	Maximal Strength; • Range of Motion (ROM); • Scober's flexion.	Lumbar extension machine (MedX, Ocala, FL).	Lumbar part of the spine.	To examine whether the second weekly dynamic training session is actually beneficial in increasing isometric strength, range of motion (ROM) and decreasing perceived pain in subjects with chronic LBP.	Results suggest that in the rehabilitation of workers suffering from chronic lower back pain, resistance training of the lumbar muscles improves isometric strength and ROM.
Lebde et al. (54)	$N = 720$ HS (364M, 356F; Age = 52.3 ± 20.9 y; $W = 71.4 \pm 14.0$ kg; $H = 1.69 \pm 0.1$ m; BMI = 24.8 ± 3.8 kg/m^2).	Isometric muscle strength of 13 muscle groups; • flexibility of six joints; • 11 functional measures classified as gross motor, fine motor or balance tasks.	• **Isometric muscle strength (N):** Shoulder internal/external rotation, Elbow flexion/extension, Grip; Hip abduction, Hip internal/external rotation, Knee flexion/extension, Ankle dorsi/plantarflexion, Toe flexion; • **Joint flexibility:** Neck flexion/extension, Shoulder internal/external rotation, Elbow flexion/extension, Hip flexion, Hip internal/external rotation, Knee flexion/extension, Ankle dorsi/plantarflexion, walk distance, gait velocity.	Fixed dynamometry (CSMi; HUMAC NORM, Stoughton, Massachusetts, USA); Hand-held dynamometry (Citec dynamometer CT 3001; CIT Technics, Groningen, the Netherlands); A universal goniometer (Baseline, Fabrication Enterprises, White Plains, New York, USA) or digital inclinometer (ankle dorsiflexion lunge test).	Full body.	To generate an age-stratified dataset of normative reference values for work ability in a healthy adult Australian population using the Work Ability Score (WAS) and investigate the association of physical performance factors.	Results identified physical factors associated with work ability that can potentially be targeted to maintain longevity in work. Physical tests may assist in the development of objective job-specific screening tools to assess work ability, supplementing subjective evaluation.
Taylor-Piliae et al. (55)	$N = 20$: • 10 HS (2M, 8F; Age = 74.0 ± 7.0 y); • 10 SS (3M, 7F; Age = 70.0 ± 8.0 y).	Daily activities.	• Trunk tilt (°); • Type of the participant's postural transitions (e.g., sit-to-stand); • Duration of the participant's postural transitions; • Duration of the participant's locomotion; • Characterization of the participant's locomotion (gait speed and number of steps); • Type of the participant's postures (walking, sitting, standing, lying).	Kinematic motion sensor (PAMSys, Biosensics LLC, MA, USA)	Trunk.	To determine the feasibility of using a kinematic motion sensor to objectively monitor fall risk and gait in naturalistic environments in community-dwelling stroke survivors.	Results highlight the utility of using objective kinematic motion sensors to monitor fall risk and gait in community-welling stroke survivors—so that strategies can be implemented early on, to reduce the risk of falling in this vulnerable population. As sensor algorithms become increasingly more predictive with less obtrusive applications, for home and community settings.
Brooks et al. (56)	$N = 64$ LBP: • 32 in Group1 (12 M, 20 F; Age = 36.2 ± 8.2 y; $H = 171 \pm 8.0$ cm; $W = 80.0 \pm 13.8$ kg); • 32 in Group2 (12 M, 20 F; Age = (Missing Data) ± 6.3 y; $H = 171 \pm 9.0$ cm; $W = 85.5 \pm 17.8$ kg).	• Specific Exercise Group (SEG); • general Exercise Group (GEG).	The onset time.	Electromyography ML138 Bio Amp (common mode rejection ratio >85 dB at 50 Hz, input impedance 200 M Ω) with 16-bit analog-to-digital conversion, sampled at 2000 Hz (ADI instruments, Analog Digital Instruments, Sydney, Australia).	Trunk.	To measure self-rated disability, pain, and the onsets of various trunk muscles in response to a rapid shoulder movement as a measure of anticipatory postural adjustments (APAs), before and after 8 weeks of specific trunk or general exercise in patients with LBP. To verify that that selfrated disability and pain scores would decrease after specific trunk exercise and APAs, whether delayed or not at baseline, would change only after specific trunk exercise	Results show similar between-group changes in trunk muscle onsets were observed. The motor control adaptation seems to reflect a strategy of improved coordination between the trunk muscles with the unilateral shoulder movement. Trunk muscle onsets during rapid limb movement do not seem to be a valid mechanism of action for specific trunk exercise rehabilitation programs

Shin and Sosnoff (57)	$N = 36$: • 18 HS (10 M, 8 F; Age = 22.14 ± 3.07 y; Sitting H = 84.95 ± 4.65 cm; W = 63.03 ± 8.15 kg); • 7 High SCI (5 M, 2 F; Age = 23.27 ± 3.67 y; Sitting H = 78.56 ± 9.57 cm; W = 62.87 ± 13.35 kg); • 11 Low SCI (5 M, 6 F; Age = 21.36 ± 2.29 cm; Sitting H = 86.13 ± 10.95 cm; W = 62.88 ± 9.79 kg).	• Functional reach test; • leaned forward, backward, side to side, and diagonally by pivoting at the hip joints to trace a circle while leaning as far as possible without losing balance for 1 min; • sitting still for 30	• Center of pressure (CoP); • Root mean square (RMS); • Median velocity; • Virtual time to contact (VTC); • Instability index.	Force platform; AMTI, Inc., 176 Waltham St, Watertown, MA 02472-4800.	Upper body.	To investigate seated postural control in persons with SCI compared with age-matched controls.	Results suggest that VTC analysis is appropriate to investigate seated postural control. It is proposed that including VTC of seated postural control as an outcome measure will provide novel information concerning the effectiveness of various rehabilitation approaches and/or technologies aimed at improving seated postural control in persons with SCI.
Moreside et al. (58)	$N = 81$ • 30 LBP (14 M, 16 F; Age = 40.7 ± 12 y; H = 169.9 ± 9 cm; W =77 7.6 ± 20 kg; BMI = 26.6 ± 6 kg/m^2); • 51 HS (24 M, 27 F; Age = 31.5 ± 8 y; H = 171.1 ± 9 cm; W = 71.5 ± 15 kg; BMI = 24.3 ± 4 kg/m^2).	Trunk stability test.	EMG principal component score.	Surface electrodes (Meditrace silver/silver chloride electrodes); 3 AMT-8 EMG systems; An electromagnetic Flock of Birds Motion Capture system.	Trunk.	To compare temporal activation patterns from 24 abdominal and lumbar muscles between healthy subjects and those who reported recovery from recent low back injury.	Results demonstrated that despite perceived readiness to return to work and low pain scores, muscle activation patterns remained altered in this low back injury group, including reduced synergistic coactivation and increased overall amplitudes as well as greater relative amplitude differences during specific phases of the movement. Electromyographic measures provide objective information to help guide therapy and may assist with determining the level of healing and return-to-work readiness after a low back injury.
Rowley et al. (59)	$N = 38$: • 19 LBP (7 M, 12 F; Age = 23.5 ± 2.8 y; H = 170.4 ± 8.4 cm; W = 68.7 ± 10.3 kg; BMI = 23.6 ± 2.47 kg/m^2); • 19 HS (2 M, 12 F; Age = 23.9 ± 3.3 y; H = 169.1 ± 10.4 cm; W = 67.1 ± 10.8 kg; BMI = 23.3 ± 1.8 kg/m^2).	The Balance-Dexterity Task protocol.	Mean muscle activation.	Surface EMG (Noraxon Wireless EMG; Scottsdale, AZ; 3,000 Hz); Advanced Medical Technology Inc. force plates (Watertown, MA; 3,000 Hz).	Trunk and hip.	To examine the association between hip and trunk muscle activity during dynamically perturbed single-limb balance using the Balance-Dexterity Task in persons with and without LBP.	Results demonstrated that there were no between-group differences in activation amplitude for any muscle groups tested. Back-healthy control participants increased hip and trunk muscle activation amplitudes in response to the added instability of the spring in a coordinated way, while those in remission from LBP did not. Instead, hip muscle activation and task performance were associated in those with LBP. These findings suggest persons with LBP preferentially, and potentially excessively, utilize hip musculature during challenging dynamic balance tasks. This represents an extrapolation of previous findings where persons with symptomatic LBP had greater hip muscle activity than controls, and this may help explain the dissociated trunk motion observed in those in remission from LBP during the Balance-Dexterity Task.

6.2.1 Kinematic parameters

In 13 studies, five on LBP [46, 49, 52, 53, 60], two on SS [50, 55], one on MS [48], three on SCI [51, 52, 57], and two on HS [47, 54], 31 kinematic indexes were reported as useful for motor performance

assessment (Table 2). More in detail, with regard to the gait: velocity [46, 48, 54], number of steps [55], gait duration [55], cadence [46], step length [46], step time [46], single support time [46], stride length [48], and phase coordination index [48]. With regard to other motor tasks, different from gait: limb-use intensity [47], flexion angle [49], bending/flexion speed [49], peak reach velocity [50], reach time [50], contact velocity [50], peak aperture [50], peak grip force [50], fingers range of motion [51], movement duration [52], hand peak velocity [52], torso peak velocity [52], time at torso peak velocity [52], shoulder-to-hand distance at hand peak velocity [52], precedence index [52], lumbar ROM [53], Schober's flexion [53], neck flexion/extension [54], shoulder external rotation [54], hip flexion, internal/external rotation [54], knee flexion/extension [54], virtual time to contact (VTC) [57], and maximum angular displacement [60]. The following kinematic parameters were found to be less significant for characterizing the motor performance of analyzed subjects. Regarding the gait: velocity [55], single support time [48], stance [48], swing [48], double support time [48], and walk distance [54]. In other tasks: bending/flexion speed [49], torso travel distance [52], hand travel distance [52], time at hand peak velocity [52], shoulder internal rotation [54], ankle plantar/dorsi flexion [54], and functional boundary [57].

6.2.2 Kinetic parameters

In three studies, one on LBP [53], one on SCI [51], one on HS [54], and five kinetic indexes have been identified as useful for the assessment of motor functions in tasks not including gait: palmar maximum grasp strength [51], pinch maximum grasp strength [51], maximal voluntary isometric torque [53], muscle strength knee flexor/extensor [54], and muscle strength toe flexor [54]. Other kinetic indexes [Table 2] were found to be less significant for characterizing the motor performance of analyzed subjects: muscle strength shoulder internal/external rotators [54], muscle strength elbow flexors/extensor [54], muscle strength hip abductors [54], muscle strength hip internal/external rotators [54], muscle strength ankle plantar flexors/dorsiflexors [54], center of pressure (CoP) velocity [57], and CoP root mean square (RMS) [57].

6.2.3 sEMG parameters

In three studies [56, 58, 60], four sEMG indexes were identified to be useful results for guiding therapy and determining the level of return to work of subjects with LBP: muscle onset [56], latency time [56], principal component score [58, 60]; and EMG ensemble average waveforms [60]. The other sEMG parameter (Table 6.2), mean muscle activation [59], was found to be less significant for characterizing the motor performance of LBP subjects.

6.2.4 Postural parameters

In two studies, three indexes referring to posture were identified, which provide novel information concerning the effectiveness of various rehabilitation approaches for individuals with SS [55] and SCI [57], with the aim of adequate job reintegration: postural transition duration [55], aborted postural transition attempts [55], and instability index [57].

6.2.5 Other parameters

In two studies, one on HS [47] and one on SS [50], three other indexes were identified to be useful for assessing motor performance: mean of magnitude ratio of activity intensity [47], upper-limb performance [47], and reach path ratio [50], while the flexion/extension ratio evaluated in Cimarras-Otal et al. [49] was found to be less significant for characterizing the motor performance of LBP subjects (Table 6.2).

Table 6.2 *Description of all the outcome parameters from the eligible studies.*

Outcome type	Outcome measure	Unit	Description and/or calculation	Neuromuscolar disorder	References
Kinematic	Velocity	(m/s)	Speed adopted by the subject to walk.	LBP/MS/HS/SS	(46, 48, 54, 55)
	Number of steps and cadence#	(a.u.)	Number of steps performed during the test or in 1 min.	SS/LBP	(46, 55)
	Gait duration	(% of total activity)	Percentage of total activity dedicated to walking.	SS	
	Step time#	(s)	The time between the point of initial contact of one foot and the point of initial contact of the opposite foot.	LBP	
	Single and double support duration	(s), (%GCT: Gait cycle time)	The time or gait cycle percentage during which just one foot or both feet are in touch with the ground.	LBP/MS	(46, 48)
	Stance duration	(%GCT: Gait cycle time)	The gait cycle percentage during which the foot is in contact with the ground.	MS	(46, 48)
	Swing duration	(%GCT: Gait cycle time)	The gait cycle percentage during which the foot is not in contact with the ground.	MS	
	Stride and step length	(m)	The distance between successive points of initial contact of the same foot or between the points of initial contact of one foot and the opposite foot.	MS/LBP	
	Phase coordination index	(%)	Bilateral limb coordination calculated by modeling the gait cycle as 360 degrees with a step equating a phase (ϕ) within the cycle: $PCI = \varphi_{CV} + P_{\varphi_{ABS}}$ [%] where ϕ_ABS and ϕ_CV represent the accuracy and consistency of phase generation, respectively	MS	
	Limb-use intensity	(m/s^2)	Limb acceleration magnitude calculated as follows: $\lvert a_l \rvert = \sqrt{a_{l,x}^2 + a_{l,y}^2 + a_{l,z}^2} - g$; $\lvert a_r \rvert = \sqrt{a_{r,x}^2 + a_{r,y}^2 + a_{r,z}^2} - g$ where a_r [t] and a_l [t] are the accelerations of the right and left limbs respectively.	HS	(47)
	Flexion angle	(°)	Measurement of maximum lumbar flexion recorded through a motion capture system	LBP	(49)
	Bending/flexion speed	(°/s)	Speed at which forward bending is performed measured with a motion analysis system.	LBP	
	Peak reach velocity	(mm/s)	Maximum three-dimensional resultant velocity of the hand during the reach.	SS	(50)
	Reach time	(ms)	Duration from reach start to reach end.	SS	
	Contact velocity	(mm/s)	Three-dimensional resultant velocity of the hand at reach end.	SS	
	Peak aperture	(mm)	Maximum three-dimensional distance between the thumbnail and the index fingernail during the reaching phase.	SS	
	Peak grip force	(grams)	Maximum grip force of the object during the hold task or the lift task.	SS	
	Fingers range of motion	(°)	Active range of motion (ROM) of the fingers measured with a goniometer for the metacarpophalangeal (MCP) and proximal interphalangeal (PIP) joints of the index finger, and for the MCP joint of the thumb.	SCI	(51)

	Torso travel distance	(cm)	The distance traveled by the torso from the initial position ($t = 0$) to reaching the target ($t = T$), calculated as follow: $D(T) = \int_0^T \left\| \dot{\mathbf{p}}(t) \right\| dt$ Where $\left\| \dot{\mathbf{p}}(t) \right\|$ is the magnitude of the C7/T1 landmark's instantaneous velocity vector.	SCI	(52)
	Hand travel distance	(cm)	The distance traveled by the Hand from the initial position ($t = 0$) to reaching the target ($t = T$), calculated as follow: $D(T) = \int_0^T \left\| \dot{\mathbf{p}}(t) \right\| dt$ Where $\left\| \dot{\mathbf{p}}(t) \right\|$ is the magnitude of the instantaneous velocity vector of the right hand grip.	SCI	
	Movement duration	(s)	The difference between the start and end movement times.	SCI	
	Hand peak velocity	(cm/s)	Maximum speed achieved by the hand.	SCI	
	Torso peak velocity	(cm/s)	Maximum speed achieved by the Torso.	SCI	
	Time at hand peak velocity	(a.u.)	Time instant (normalized to movement time) at which the maximum velocity is achieved by the hand.	SCI	
	Time at torso peak velocity	(a.u.)	Time instant (normalized to movement time) at which the maximum velocity is achieved by the Torso.	SCI	
	Shoulder-to-hand distance at hand peak velocity	(cm)	The distance between the shoulder (acromion process) and the hand (middle point of the dorsal surface) at the maximum hand speed.	SCI/LBP	
	Precedence index (PI)		Index expressing the coordination of movement between torso and hand. PI = 0 when the hand and torso move in synchrony. PI > 0 indicating that hand movement precedes torso movement. In contrast, when the torso precedes the hand, PI is <0. calculated as follow: $PI = \frac{1}{T_{MT}} \int_0^{T_{MT}} [N_{hand}(t) - N_{Torso}(t)]\, dt$ where $N_{hand}(t)$ and $N_{Torso}(t)$ indicate the normalized travel distance of the hand and torso at time t, respectively, and T_{MT} denotes the total movement time.	SCI/LBP	
	Lumbar ROM	(°)	Lumbar movement range calculated with the goniometer within the MedX lumbar extension machine.	LBP	(53)
	Schober's flexion	(cm)	ROM of the lumbar spine. In order to undertake the modified-modified Schober's test pen marks were made at each of the posterior superior iliac spines (PSIS). Another mark was made at the midline of the lumbar spines horizontal to the PSIS and a final mark was then made 15 cm above this mark. Whilst holding a tape measure close to the participant's skin, he or she bent over as though to touch the toes whilst a reading was obtained to ascertain any change in the original 15 cm measure.	LBP	
	Flexion/extension of neck, hip and knee	(°)	Joint flexibility of the neck, hip and knee in terms of range of motion, measured using a universal goniometer or digital inclinometer	HS	(53)
	Shoulder and hip internal/external rotation	(°)	Joint flexibility of the shoulder and hip in terms of range of motion, measured using a universal goniometer or digital inclinometer	HS	
	Ankle plantar/dorsiflexion	(°)	Joint flexibility of the Ankle in terms of range of motion, measured using a universal goniometer or digital inclinometer.	HS	
	Walk distance	(m)	Distance walked during the 6-min walking test.	HS	
	Functional boundary	(mm^2)	Stability area drawn during movements, performed in a sitting position, forward, backward, diagonally and side to side without losing balance, calculated using a direct least square fitting method.	SCI	(57)
	Virtual time to contact (VTC)	(s)	Parameter that specifies the spatiotemporal proximity of the CoP to the postural stability boundary taking into account acceleration, velocity, and position of the COP trajectory.	SCI	
	Maximum angular displacement	(°)	Maximum angular displacement of hands in the three planes of space measured with an electromagnetic Flock of BirdsTM (FOB) Motion Capture system.	LBP	(60)
Kinetic	Palmar maximum grasp strength	(N)	Maximum force expressed in the palmar grasp.	SCI	(51)
	Pinch maximum grasp strength	(N)	Maximum force expressed in the pinch grasp.	SCI	
	Maximal voluntary isometric torque	(N*m)	The extension torque expressed by the trunk, in isometric condition. Calculated at intervals of 12° from 0° to 72° of lumbar flexion with a 10 s rest between each joint angle.	LBP	(53)
	Muscle strength shoulder internal/external rotators	(N)	Physical performance of the shoulder muscles measured using hand-held dynamometry.	HS	(54)
	Muscle strength elbow flexors/extensor	(N)	Physical performance of the elbow muscles measured using hand-held dynamometry.	HS	
	Muscle strength hip abductors	(N)	Physical performance of the hip muscles measured using hand-held dynamometry.	HS	
	Muscle strength hip internal/external rotatators	(N)	Physical performance of the hip muscles measured using hand-held dynamometry.	HS	
	Muscle strength Knee flexor/extensor	(N*m)	Physical performance of the knee muscles measured using fixed dynamometry.	HS	
	Muscle strength Ankle plantar-flexors/dorsiflexors	(N)	Physical performance of the Ankle muscles measured using hand-held dynamometry.	HS	
	Muscle strength Toe flexor	(N)	Physical performance of the Toe muscles measured using the Paper Grip Test and a composite score out of six was summed based on the number of successful trials of Paper Grip Test-1 (hallux strength) and Paper Grip Test-2 (lesser toes strength).	HS	

	Center of pressure (CoP) velocity	(mm/s)	Center of pressure speed.	SCI	(57)
	CoP Root mean square (RMS)	(mm)	The mean square error of the CoP's trajectory described during task execution between the subject and the seat equipped with a force platform.	SCI	
Electromyography	Muscles onset	(ms)	The onset of the abdominal and lumbar muscles during rapid right arm shoulder flexion was measured using surface electromyography.	LBP	(56)
	Latency time	(ms)	The time between the onset of each trunk muscle and the anterior deltoid.	LBP	
	Principal component score	(a.u.)	Abdominals and back extensors muscles score, calculated with the principal component analysis model, that provide a weighting factor for the contribution of the Principal Component to the measured EMG waveform.	LBP	(58, 60)
	Mean muscle activation	(%)	Average activation of hip and trunk muscles during the Balance-Dexterity Task protocol measured with surface and fine-wire electromyography. Muscle activations were reported as a percent of activation during the stable block condition and thus represent additional muscle activation utilized in response to instability of the spring	LBP	(59)
	EMG ensemble average waveforms	(%MVIC)	Average waveforms for the right sided abdominal and back extensor muscles recorded with surface electrodes.	LBP	(60)
Postural	Postural transition duration	[s]	Postural transition duration are identified by measuring the pattern recognition of the trunk tilt with kinematic motion sensor PAMSys.	SS	(55)
	Aborted postural transition attempts	(Number/day)	Unsuccessful attempts rising from a chair quantified by kinematic motion sensor PAMSys.	SS	
	Instability index	(a.u.)	The ratio of the area defined by the COP's trajectory described during the task to the functional boundary; high index values indicate poor postural stability.	SCI	(57)
Other	Mean of magnitude ratio of activity intensity	(a.u.)	Mean of magnitude ratio of the acceleration of one limb in comparison to the other during daily activities and calculated as the mean of this quantity: $r[t] = ln(\lvert a_r[t] \rvert) - ln(\lvert a_l[t] \rvert)$ where $a_r[t]$ and $a_l[t]$ are the accelerations of the right and left limbs, respectively.	HS	(47)
	Upper-limb performance	(a.u.)	A measure of how much one limb is used in comparison to the other during activities of daily living calculated as follow: $M = \frac{\lvert t \in \{r[t] > \delta, \lvert a_r[t] \rvert > \beta\} \rvert}{T} - \frac{\lvert t \in \{r[t] < -\delta, \lvert a_l[t] \rvert > \beta\} \rvert}{T}$ where $r[t]$, $a_r[t]$ and $a_l[t]$ are the magnitude ratio of activity intensity and accelerations of the right and left limbs, respectively. T is the total monitoring duration in seconds, β represents a parameter identifying upper limb activities (epochs) and δ is a threshold.	HS	
	Flexion-extension ratio (F/R ratio)	(a.u)	Ratio between the maximum EMG value during flexion and the minimum resting EMG.	LBP	(49)
	Reach path ratio	(a.u.)	Total distance traveled by the wrist sensor divided by the length of a straight-line path from the reach's starting point to ending point.	SS	(50)

6.2.6 Risk of bias

The results of the risk of bias assessment are reported in the risk of bias summary (Figure 6.2)—where the authors' judgments are shown for all the seven considered domains and for each study included in this review, according to Higgins and Green [43], McGuinness [44], and Sterne et al. [45]—and in the risk of bias graph (Figure 6.3), where the authors' judgments are reported for each risk of bias as percentages across the different studies included in this review. None of the studies considered was associated with the risk of bias due to confounding [D1], in classifications of interventions [D3], due to deviations from intended interventions [D4], due to missing data [D5], and in selection of the reported result [D7]. Instead, there was a moderate risk of bias due to participant selection [D2] in a single study [47], owing to a poor description of the subjects involved. Furthermore, due to a lack of results for some of the subjects studied, three studies [49, 53, 56] had a moderate risk of bias in outcome measurement [D6].

Figure 6.2 *Risk of bias summary: authors' judgments for 15 included studies and for each considered domain*

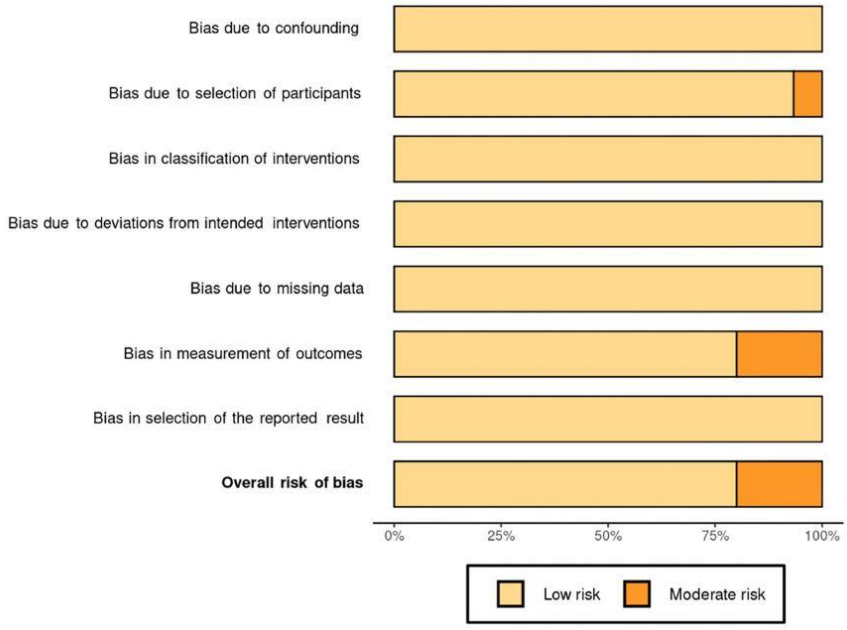

Figure 6.3 *Risk of bias graph: authors' judgments for each risk of bias reported as percentages of the different studies included in the review.*

Bibliography

[1]. Miller A, Dishon S. 2006. Health-related quality of life in multiple sclerosis: the impact of disability, gender and employment status. Qual Life Res., 15:259– 71.

[2]. Klockgether T. 2010. Sporadic ataxia with adult onset: classification and diagnostic criteria. Lancet Neurol., 9:94–104.

[3]. Ranavolo A, Serrao M, Draicchio F. 2020. Critical issues and imminent challenges in the use of sEMG in return-to-work rehabilitation of patients affected by neurological disorders in the epoch of Human–Robot collaborative technologies. Front Neurol., 11:572069.

[4]. Persechino B, Fontana L, Buresti G, Fortuna G, Valenti A, Iavicoli S. 2019. Improving the job-retention strategies in multiple sclerosis workers: the role of occupational physicians. Ind Health., 57:52–69.

[5]. Benedict RH, Wahlig E, Bakshi R, Fishman I,Munschauer F, Zivadinov R, et al. 2005. Predicting quality of life in multiple sclerosis: accounting for physical disability, fatigue, cognition, mood disorder, personality, and behavior change. J Neurol Sci., 231:29–34.

[6]. Ranavolo A, Serrao M, Varrecchia T, Casali C, Filla A, Roca A, et al. 2019. The working life of people with degenerative cerebellar ataxia. Cerebellum, 18:910–21.

[7]. Henderson M, Harvey SB, Overland S, Mykletun A, Hotopf M. 2011. Work and common psychiatric disorders. J R Soc Med., 104:198–207.

[8]. Matt SB, Butterfield P. 2006. Changing the disability climate: promoting tolerance in the workplace. AAOHN J., 54:129–35.

[9]. Gates LB. 2000. Workplace accommodation as a social process. J Occup Rehabil., 10:1.

[10]. Merz MA, Bricout JC, Koch LC. 2001. Disability and job stress: implications for vocational rehabilitation planning.Work., 17:85–95.

[11]. Frank AO, Sawney P. 2003. Vocational rehabilitation. J R Soc Med., 96:522– 4.

[12]. Reneman MF. 2015. State of vocational rehabilitation and disability evaluation in chronic musculoskeletal pain conditions. In: Escorpizo R, Brage S, Homa D, Stucki G, editors. Handbook of Vocational Rehabilitation and Disability Evaluation. Handbooks in Health,Work, and Disability. Cham: Springer, p. 187–98.

[13]. Staubli S, Schwegler U, Schmitt K, Trezzini B. 2015. ICF-based process management in vocational rehabilitation for people with spinal cord injury. In: Escorpizo R, Brage S, Homa D, Stucki G, editors. Handbook of Vocational Rehabilitation and Disability Evaluation. Handbooks in Health, Work, and Disability. Cham: Springer, p. 371–96.

[14]. Bond GR, Campbell K, Becker DR. 2013. A test of the occupational matching hypothesis for rehabilitation clients with severe mental illness. J Occup Rehabil., 23:261–9.

[15]. Escorpizo R, Reneman MF, Ekholm J, Fritz J, Krupa T, Marnetoft SU, et al. 2011. Conceptual definition of vocational rehabilitation based on the ICF: building a shared global model. J Occup Rehabil., 21:126–33.

[16]. Schultz IZ, Stowell AW, Feuerstein M, Gatchel RJ. 2007. Models of return to work for musculoskeletal disorders. J Occup Rehabil., 17:327– 52.

[17]. Isernhagen SJ. 2006. Job matching and return to work: occupational rehabilitation as the link.Work., 26:237–42.

[18]. Frank A. 2016. Vocational rehabilitation: supporting ill or disabled individuals in (to) work: a UK perspective. Healthcare, 4:46.

[19]. Serrao M, Chini G, Casali C, Conte C, Rinaldi M, Ranavolo A, et al. 2017. Progression of gait ataxia in patients with degenerative cerebellar disorders: a 4-year follow-up study. Cerebellum, 16:629–37.

[20]. Jacobi H, du Montcel ST, Bauer P, Giunti P, Cook A, Labrum R, et al. 2015. Long-term disease progression in spinocerebellar ataxia types 1, 2, 3, and 6: a longitudinal cohort study. Lancet Neurol., 14:1101– 8.

[21]. Dubbioso R, Pellegrino G, Antenora A, De Michele G, Filla A, Santoro L, et al. 2015. The effect of cerebellar degeneration on human sensori-motor plasticity. Brain Stimul., 8:1144–50.

[22]. Serrao M, Chini G, Bergantino M, Sarnari D, Casali C, Conte C, et al. 2017. Dataset on gait patterns in degenerative neurological diseases. Data Brief., 16:806es.c

[23]. Vinci P, Serrao M, Millul A, Deidda A, De Santis F, Capici S, et al. 2005. Quality of life in patients with Charcot-Marie-Tooth disease. Neurology, 922– 24.

[24]. Doogan C, Playford ED. 2014. Supporting work for people with multiple sclerosis. Mult Scler., 20:646–50.

[25]. Raggi A, Covelli V, Schiavolin S, Scaratti C, Leonardi M, Willems M. 2016. Work-related problems in multiple sclerosis: a literature review on its associates and determinants. Disabil Rehabil., 38:936–44.

[26]. Hendricks DJ, Sampson E. 2017. Accommodating individuals with traumatic brain injury: an analysis of employer-initiated cases handled by the Job Accommodation Network.Work., 58:29–34.

[27]. van der Kemp J, Kruithof WJ, Nijboer TCW, van Bennekom CAM, van Heugten C, Visser-Meily JMA. 2019. Return to work after mild-to-moderate stroke: work satisfaction and predictive factors. Neuropsychol Rehabil., 29:638– 53.

[28]. Toldrá RC, Santos MC. 2013. People with disabilities in the labor market: facilitators and barriers. Work., 45:553 63.

[29]. Honan CA, Brown RF, Hine DW, Vowels L, Wollin JA, Simmons RD, et al. 2012. The multiple sclerosis work difficulties questionnaire. Mult Scler., 18:871–80.

[30]. Karamians R, Proffitt R, Kline D, Gauthier LV. 2020. Effectiveness of virtual reality- and gaming-based interventions for upper extremity rehabilitation poststroke: a meta-analysis. Arch Phys Med Rehabil., 101:885–96.

[31]. Triegaardt J, Han TS, Sada C, Sharma S, Sharma P. 2020. The role of virtual reality on outcomes in rehabilitation of Parkinson's disease: metaanalysis and systematic review in 1031 participants. Neurol Sci., 41:529– 36.

[32]. Naro A, Leo A, Russo M, Casella C, Buda A, Crespantini A, et al. 2017. Breakthroughs in the spasticity management: are non-pharmacological treatments the future? J Clin Neurosci., 39:16–27.

[33]. Iosa M, Morone G, Cherubini A, Paolucci S. 2016. The three laws of neurorobotics: a review on what neurorehabilitation robots should do for patients and clinicians. J Med Biol Eng., 36:1–11.

[34]. Mangone M, Agostini F, de Sire A, Cacchio A, Chiaramonte A, Butterini G, et al. 2022. Effect of virtual reality rehabilitation on functional outcomes for return-towork patients with Parkinson's disease: an umbrella review of systematic reviews. Neuro Rehabilitation, 1–11.

[35]. Ashley KD, Lee LT, Heaton K. 2019. Return to work among stroke survivors. Workplace Health Saf., 67:87–94.

[36]. Skamagki G, King A, Duncan M, Wåhlin C. 2018. A systematic review on workplace interventions tomanage chronic musculoskeletal conditions. Physiother Res Int., 23:e1738.

[37]. Hoosain M, de Klerk S, Burger M. 2019. Workplace-based rehabilitation of upper limb conditions: a systematic review. J Occup Rehabil., 29:175– 93.

[38]. Moher D, Shamseer L, Clarke M, Ghersi D, Liberati A, Petticrew M, et al. 2015. Preferred reporting items for systematic review and meta-analysis protocols (PRISMA-P) 2015 statement. Syst Rev., 4:1.

[39]. Grant MJ, Booth A. 2009. A typology of reviews: an analysis of 14 review types and associated methodologies. Health Info Libr J., 26:91– 108.

[40]. Leonardo R. 2018. PICO model for clinical questions. Evid Based Med Pract., 3:2.

[41]. Del Ferraro S, Falcone T, Ranavolo A, Molinaro V. 2020. The effects of upper-body exoskeletons on human metabolic cost and thermal response during work tasks-a systematic review. Int J Environ Res Public Health., 17:7374.

[42]. Falcone T, Cordella F, Molinaro V, Zollo L, Del Ferraro S. 2021. Real time human core temperature estimation methods and their application in the occupational field: a systematic review. Measurement, 183:109776.

[43]. Higgins J, Green S. 2019. Cochrane handbook for systematic reviews of interventions. Cochrane Handb Syst Rev Interv.

[44]. McGuinness LA. 2020. Robvis: An R Package and Web Application for Visualising Risk-of-bias Assessments. https://github.com/mcguinlu/robvis).

[45]. Sterne JA, Hernán MA, Reeves BC, Savovi´c J, Berkman ND, Viswanathan M, e al. 2016. ROBINS-I: a tool for assessing risk of bias in non-randomised studies of interventions. BMJ, 12:bmj.14919.

[46]. Monticone M, Ambrosini E, Rocca B, Magni S, Brivio F, Ferrante S, et al. 2014. Multidisciplinary rehabilitation programme improves disability, kinesiophobia and walking ability in subjects with chronic low back pain: results of a randomised controlled pilot study. Eur Spine J., 23:2105–13.

[47]. Lee SI, Liu X, Rajan S, Ramasarma N, Choe EK, Bonato P, et al. 2019. Novel upperlimb function measure derived from finger-worn sensor data collected in a freeliving setting. PLoS One, 14:e0212484.

[48]. Richmond SB, Swanson CW, Peterson DS, Fling BW. 2020. A temporal analysis of bilateral gait coordination in people with multiple sclerosis.Mult Scler Relat Disord., 45:102445.

[49]. Cimarras-Otal C, Marcen-Cinca N, Rabal-Pelay J, Lacrcel-Tejero B, Alczar- Crevilln A, Villalba-Ruete J, et al. 2020. Adapted exercises versus general exercise recommendations on chronic low back pain in industrial workers: a randomized control pilot study.Work., 67:733–40.

[50]. Schaefer S, DeJong S, Cherry K, Lang C. 2012. Grip type and task goal modify reach-to-grasp performance in post-stroke hemiparesis. Motor Control., 16:2.

[51]. Correia C, Nuckols K, Wagner D, Zhou YM, Clarke M, Orzel D, et al. 2020. Improving grasp function after spinal cord injury with a soft robotic glove. IEEE Trans Neural Syst Rehabil Eng., 28:1407–15.

[52]. Kim K, Martin B. 2013. Manual movement coordination adapted to spinal cord injury and low back pain. Int J Ind Ergon., 43:1–8.

[53]. Bruce-Low S, Smith D, Burnet S, Fisher J, Bissell G, Webster L. 2012. One lumbar extension training session per week is sufficient for strength gains and reductions in pain in patients with chronic low back pain ergonomics. Ergonomics, 55:500–07.

[54]. Lebde N, Burns J, Mackey M, Baldwin J, McKay M. 2020. Normative reference values and physical factors associated with work ability: a cross-sectional observational study. Occup Environ Med., 77:231–7.

[55]. Taylor-Piliae RE, Mohler MJ, Najafi B, Coull BM. 2016. Objective fall risk detection in stroke survivors using wearable sensor technology: a feasibility study. Top Stroke Rehabil., 23:393–9.

[56]. Brooks C, Kennedy S, Marshall P. 2012. Specific trunk and general exercise elicit similar changes in anticipatory postural adjustments in patients with chronic low back pain: a randomized controlled trial. Spine, 37:E1543– 50.

[57]. Shin S, Sosnoff JJ. 2013. Spinal cord injury and time to instability in seated posture. Arch Phys Med Rehabil., 94:1615–20.

[58]. Moreside JM, Quirk DA, Hubley-Kozey CL. 2014. Temporal patterns of the trunk muscles remain altered in a low back-injured population despite subjective reports of recovery. Arch Phys Med Rehabil., 95:686– 98.

[59]. Rowley KM, Engel T, Kulig K. 2020. Trunk and hip muscle activity during the Balance-Dexterity task in persons with and without recurrent low back pain. J Electromyogr Kinesiol., 50:102378.

[60]. Hubley-Kozey C, Moreside JM, Quirk DA. 2014. Trunk neuromuscular pattern alterations during a controlled functional task in a low back injured group deemed ready to resume regular activities. Work, 47:87– 100.

CHAPTER 7

7. DISCUSSION AND CONCLUSION

Below I describe the kinematic, kinetic, and electromyographic indices implemented, and the behavior assumed and highlighted in literature studies.

7.1 Kinematic indices

The kinematic analysis mainly involves the study of the instantaneous angular positions in the sagittal, frontal and transverse planes and the ranges of motions (RoMs) understood as joint excursions. Additional useful information is represented by spatio-temporal parameters and energy variables such as energy recovery and consumption. The former is an index of the capacity to store and reuse kinetic energy during walking while the letter is an index of energy expenditure per unit distance walked.
Many studies in the literature have shown these parameters to be altered and thus distinctive of the motor disorders that characterize neurological disease [1]. This is why we decided to include these kinematic indices in our research.

Spatio-temporal parameters

- Patients with cerebellar ataxia (PwCA), compared to healthy subjects (HS), show significantly lower values of stride length and higher values of stride width, as well as a high variability of stride length, stride width and step length [2]. These findings support previous research [3,4] and are distinct features of ataxic gait developed to compensate for poor balance and dynamic stability [4-7]. Patients who wear the passive soft trunk exoskeleton, on the other hand, have less variability in step length [8], which is likely due to the device's restraining properties, which allow them to take more regular steps while walking.

- In patients with Parkinson's disease (PwPD), we found a lower stride length and higher cadence [9,10] and a lower stride length [9]. These findings support those found in the literature [11,12], and these temporal alterations in gait are thought to be neural system strategies to reduce the risk of falls, allowing greater postural control.

- People with transfemoral (TFA) and transtibial (TTA) amputation, in general, regardless of the level of amputation and type of prosthesis, showed a common gait pattern characterized by a symmetric increase of step length, step width and double support duration. Almost all these gait deficits reflect compensatory mechanisms adopted by people with amputation presumably to increase their stability in the frontal plane (increased step width), to maintain the most stable configuration (increased double support duration), while increasing the time of the stance and in the unaffected limb.

  People with TFA showed a specific gait pattern that differed from that of HS and people with TTA; in particular they reduced the duration of the stance and increased the duration of the swing in the prosthetic limb.

  Altogether these findings deeply reflect the essence of the asymmetric gait [14] that characterizes people with lower limb amputation.

Joint Range of Motion

- Several studies have examined the biomechanical characteristics of PwCA, discovering significant variability in all values of global and segmental gait parameters, such as marked trunk oscillations [4-7]. As a result, we examined trunk ROMs to assess the effectiveness of the passive soft exoskeleton [8]. We observed a significant improvement in trunk movements in all three planes of space, which is most likely due to the soft passive exoskeleton's restraining factor, which ensures a better and more physiological trunk oscillation.

- One of the hallmark symptoms of Parkinson's disease (PD) is decreased amplitude of joint movement [15,16]. This affects not only the distal joints but also the trunk [17-19], affecting the patients' performance in daily activities and function [20,21]. Trunk mobility is an important component of physical therapy treatment in Parkinson's disease patients, so an accurate measurement of trunk range of motion [ROM] is frequently regarded as an essential component in a rehabilitation context [22]. Confirming these considerations, we obtained improved pelvic rotation and obliquity after rehabilitation [10], which is consistent with studies in the literature indicating that trunk-focused excercises have beneficial effects on both trunk and pelvic mobility [23]. We also found that PwPD had decreased hip, knee, and ankle ROM, as well as decreased trunk and pelvic rotation [9]. We demonstrated how a small set of these parameters, specifically knee and trunk rotation ROM, can distinguish patients from

healthy subjects using machine learning algorithms. Thus knee and trunk rotation RoM abnormalities characterize the gait pattern of PwPD, as found in previous studies [23-28].

- People with TFA and TTA showed a symmetric increase of pelvic obliquity, trunk lateral bending, and trunk rotation range of motions with increased pelvis and trunk ante-flexed posture [13]. These features reflect the compensatory mechanisms used by patients to help lift the affected limb. The reduced range of motion of the ankle joint in the prosthetic limb, which is the common prosthetic joint in both TTA and TFA subjects, on the other hand, is directly related to the use of the prosthesis. However, it is not possible to exclude that the lack of sensory feedback [29] might have played a role in determining a hypermetric foot placement in the prosthetic limb, which, in turn, would have influenced the foot placement of the unaffected limb, as adaptive mechanism of the new support base schema [30,31].

  People with TFA wearing Genium prosthesis (TFA_G) showed an increased hip and knee range of motions in the prosthetic side compared to subjects with mechanical prosthesis, who, conversely, showed a symmetric increased pelvic obliquity. These findings indicate that the type of prosthesis influences the gait pattern of people with amputation both in terms of gait performance and adaptation [32]. In this view, the increased hip and knee ranges of motion, together with other parameters, might reflect a better gait performance for the Genium vs mechanical prostheses. Conversely, the increased pelvic obliquity seems to reflect a greater compensatory effort in subjects with mechanical prostheses, likely aimed to lift the limbs during the gait progression.

  We also demonstrated that pelvic obliquity was positively correlated with the energy recovery during walking and had an optimal discriminative ability between people with TFA and HS. These findings strongly indicate that it may be one of the most appropriate parameter to be considered for monitoring a subject's adaptation to a prosthesis.

Energy variables

- In terms of energy behavior, we discovered that PwCA had significantly lower R-Step values than HS [2], indicating that the compensation strategies used prevent the patient from recovering energy while walking. Our study evaluating the passive trunk exoskeleton, on the other hand, demonstrated how the device, by improving other kinematic parameters, allows for greater recovery and lower energy expenditure [8].

- Subjects with lower limb amputation, and in particular people with TFA, showed significantly lower R-step values than healthy matched subjects [13]. This could be related to the fact that the specific gait patterns that characterize these subjects prevent them from recovering energy.

Harmonic Ratio

The Harmonic Ratio (HR) is a measure used to quantify smoothness of walking [33-35]. In gait research, the HR is most commonly extracted from trunk accelerations in the anteroposterior (AP), vertical (VT) and mediolateral (ML) directions. HRs have discriminated between the gait of young and older adults [36,37], older adults who have and have not fallen [33], and the gait of healthy older adults and individuals with neurologic disorders [38-40].

- In our study we found that HR of PwCA significantly differed from that of HS in all three spatial planes [41] . This means that ataxic patients, compared to healthy subjects, exhibit a substantial reduction of trunk movement smoothness. This result suggest that HR can substantially describe trunk accelerative behavior abnormalities among patients with degenerative ataxia, as shown by other studies in the literature [42]. However, we found no correlation between HR and the number of falls and the severity of the disease. This is probably due to the small sample size. Indeed, by increasing the sample size, we confirmed that HR is the most appropriate accurate trunk acceleration-derived marker for detecting the loss of the ability to organize a fluid and rhythmically effective gait in PwCA due to cerebellar degeneration, which leads to inter- and inter-segmental incoordination [43].

  We also found that HR values were correlated with the history of falls, SARA gait and posture subscores, and temporal gait instability variables, confirming the results of other studies reporting the HRs of trunk acceleration during gait as predictors of falls among older people [44] or persons with Parkinson's disease [45], multiple sclerosis [46], and stroke survivors [47].

- In PwPD we found that the HRs calculated for the three spatial planes were able to discriminate between PwPD at moderate stages of disease progression and HS [45]. HR_{AP}, in particular, was also able to discriminate between PwPD at the moderate disability stage and PwPD at lower disability stages. Furthermore, HR_{AP} exhibited good ability to characterize

the gait of recurrent fallers. These results are in line with those from previous studies reporting that PwPD exhibit disruptions in the rhythmicity of pelvic acceleration [38,39].
In a subsequent study [10] we found that the HR_{AP} and the HR_{ML}, can significantly improve up to normative values after rehabilitation, with medium-to-high internal and optimal external responsiveness. Our results are consistent with previous studies reporting the HR_{AP} and the HR_{ML} to significantly improve after rehabilitation [48]. In particular Lowry et al. [39] showed that internal cognitive and verbal amplitude-based cueing aiming to increase stride length is effective in improving HRs.

- Even in patients with hemiparesis [HP] [49], we discovered that HR values in all three directions can distinguish patients from HS with high accuracy. We found that HP showed decreased HR values and it may occur as a result of various compensation strategies due to the force deficit that does not allow patients to exploit the pendular mechanism of walking for generating harmonic movements [47].

Coefficient of Variation of step length

The coefficient of variation of step length is a measure of gait spatial variability that has been studied in several studies in the literature [50,52].

- In PwCA we found that the CV of step length was higher than the controls and significantly correlated with the clinical scales scores and with the number of falls per year [41,43]. In fact, it has been shown in the literature that during the progression of the disease subjects with degenerative ataxia tend to lose the ability to both enlarge their step width and fasten their walking speed and they shorten their step length in order to reduce their single support time [53], with a significant increase in step length CV that can lead to an increased risk of falls.

- We found significantly altered values of the coefficient of variation of step length only in patients with a severe stage of Parkinson's disease [45], which is consistent with previous studies that did not observe step length CV alterations in subjects at milder disease stages [53]. However, the low probability of correctly discriminating PwPD (58%) at the cutoff value and a lack of correlations with clinical variables and spatiotemporal gait parameters do not allow us to consider this index as a marker of gait stability that is independent of speed.

Simultaneously, we discovered no improvement in the parameter following rehabilitation treatment [10].

- CV step length was found to be a good parameter to discriminate HP from HS [49], confirming the variety in gait ability and compensatory strategy among the stroke patients.

Largest Lyapunov Exponent

The LLE quantifies gait stability as the average logarithmic rate of divergence of the system's trajectory to its nearest neighboring trajectory. When trajectories converge, the observed system is considered to have local dynamic stability, whereas divergence indicates local dynamic instability.

- We found that higher values of LLE, as calculated in the three spatial directions, characterize the gait of PwCA, regardless of gait speed [43]. Our results are in line with previous studies [54,55] reporting higher LLEs values in subjects with cerebellar involvement, compared with non-speed-matched healthy subjects, as an expression of gait instability due to the inability to recover from small perturbations. However, LLE is highly influenced by lower gait speed [56-58], leading to higher LLE values. Because we did not find speed-independent correlations between the LLEs and the disease severity or the history of falls, we can further confirm that the LLE is dependent on the gait speed compensation experienced by PwCA and cannot be considered as a marker of fall risk, regardless of gait speed.

- We identified no differences for LLE in PwPD when compared with HS [45]. In contrast, other studies have reported significant group differences between PwPD and HS [59] and between walking at self-selected speeds and dual-task walking in terms of LLE. These contrasting results can be attributed to varying matching procedures and testing conditions. Given that the goals of the these studies were different, combining their interpretations with our results may suggest that the gait of PwPD is characterized by dynamic instability, but that LLE is speed dependent.

Root mean square

The RMS and RMSR quantify the magnitude of the acceleration signals [60,61] as an expression of the degree of body sway during gait [59].

- In our study [43], we found that these indices can capture the inability of the trunk of the PwCA to damp the gait-related oscillations and the transmission of accelerations in all directions [62,63], regardless of gait speed. However, because of the lack of speed-independent correlation with the history of falls, our results confirm that RMS and RMSR are speed-dependent parameters [61] and cannot be considered indexes of fall risk, regardless of gait speed.

- Furthermore, we identified RMS and RMSR as good indices to discriminate HP from HS [49]. These results show that HP are characterized by altered movement patterns of the trunk. This is most likely due to compensatory strategies that, on the one hand, allow for an increase in gait ability but, on the other hand, reduce gait stability [47].

Recurrence Quantification Analysis

RQA is a nonlinear technique that can provide useful information about system dynamics patterns and structures. It characterizes a variety of features of a given time series, including the quantification of deterministic structures and non-stationarity, using recurrence plots.

- It represents how often a subject's trunk accelerations revisit similar locations in the three spatial planes during their gait. Previous studies [64-66] have shown that RQA_{det} is the most convenient RQA index for objectively separating PwPD from HS. Accordingly, we identified lower RQA_{det} values in the AP direction in PwPD compared to $HS_{matched}$, regardless of the disability stage [45]. Therefore, we can argue that PwPD exhibit disruptions in the quasi-periodic recurrence of their gaits in the early stages of PD, which reflects the early temporal gait alterations experienced by PwPD [67]. This consideration is further reinforced by the correlation we identified between RQA_{detAP} and temporal gait parameters, such as cadence and stride duration. Since the earliest stages of PD, PwPD exhibit shorter step lengths and stride times with an increased cadence [28, 68] as a part of the abnormal gait pattern that progressively deteriorates into festination [69]. The reduced predictability of AP trunk accelerations may reflect systemic instability caused by altered temporal gait patterns. Therefore, RQA_{detAP} can be considered as a temporal marker of gait stability that can identify PwPD independently of gait speed. Therefore, the positive correlation between RQA_{detAP} and UPDRS-III may reflect its ability to capture gait impairment besides other symptoms such as reduced hand dexterity, facial mimicry, or altered posture.

However, in a subsequent study [10] we obtained that RQA_{detAP} did not show significant modifications after the rehabilitation period, so our results do not allow it to be considered as an outcome measure in rehabilitation trials and clinical contexts.

Normalized Jerk Score and Log Dimensionless Jerk

The NJS is an index that provides information on the smoothness of trunk accelerations.

- In PwCA we found that NJS and LDJ-A failed to accurately describe the loss of smoothness of the trunk acceleration patterns during walking [43]. One possible explanation is that they better reflect upper limb motor impairment with fast changes in directions and jerks during rhythmic task-oriented movements [70].

- Previous studies have reported [71,72] significantly lower NJS values in the ML and V directions in PwPD compared to age-matched HS. These differences have been interpreted as a reflection of PD-related bradykinesia, which parallels lower gait speed and reduced arm swing movements. Furthermore, the NJS in the ML and V directions has been reported to be responsive to dopaminergic medication in subjects with improved gait speed. In our study [45], we identified no differences in NJS between PwPD and age-and speed-matched HS, indicating that NJS is a marker of a general loss in complexity of the motor control system that depends on gait speed.

Kinematic parameters appear to be the most commonly used for biomechanical characterization, and many of these are chosen for motor performance assessment, as demonstrated by our systematic review. The wide use of kinematics is likely to be associated with easier use even directly in the work environment, thanks to wearable technologies that are becoming increasingly popular in recent years and that are also easy to use even with user-friendly interfaces.

7.2 Kinetic indices

The ground reaction force data in vector form is surely the most important signal studied in the kinetic analysis of movement. This force represents a global information because it represents the environment's reaction to the actions of the entire human system. The components of this force

provide important information to clinicians about load acceptance and forward propulsion generation capabilities [1].

- In PwCA, when compared with HS, we found a significant decrease in the center of activity of the ground reaction force, but no correlation with muscle activity [2]. This may imply that PwCA have the same spatiotemporal relationship between muscle activation and foot-ground interaction torque as HS, suggesting that the cerebellum is not involved in such motor control mechanism.

  In the second study [8], we obtained for PwCA a ground reaction force profile while walking without the exoskeleton with a peak even at 10% of the stance phase, as Martino et colleagues demonstrated [3]. This indicates an imbalance in control and foot touch preparation. This peak, as well as the FWHM of the reaction force, disappears in presence of the device. This is most likely due to the device's characteristics, which allow the subject to have more control of limb loading.

- People with TFA showed a significant increase in the first peak of the ground reaction force in the affected limb, which seems to indicate their inability to control the prosthesis during the heel strike, likely caused by a reduced deceleration of the prosthetic limb from the late swing to initial contact [13]. In contrast, the FWHM of the reaction force decreases, showing that the amputated limb is unable to produce and maintain an appropriate force during the stance phase. As a compensation, the FWHM of the reaction force of the healthy limb increases, as it produces a more intense and longer-lasting force. Overall, these findings reflect the greater effort made by people with TFA to compensate for reduced motor performance by increasing movement and force production in the unaffected limb.

Kinetic parameters, which are mainly limited to the laboratory environment, are still used very little in the evaluation of workers' motor performance in job integration/reintegration programs. Sensorized shoes that can replace force platforms have become increasingly popular in recent years [74], and it is therefore essential to include this type of evaluation in order to develop an ergonomic rehabilitation pathway.

7.3 Surface electromyography indices

Surface electromyography [sEMG] is a tool that can detect muscle contractions in agonist and antagonist muscles and monitor their evolution over time [75,76]. As a result, we decided to investigate muscle coactivation, the mechanism that controls the simultaneous activity of agonist and antagonist muscles crossing the same joint [77].

To quantify muscle co-activation, several computational approaches have been used: ratio, overlapping, or cross-sectional areas of simultaneous activation of opposite muscles [75]. These mathematical tools are based on an agonist-antagonist approach to EMG signals recorded from two antagonist muscles or from two antagonist muscles in the same joint. In our study we used the method proposed by Ranavolo et al. [78] based on the time-varying multi-muscle co- activation function (TMCf). In some ways, this approach could be studied together with muscle synergies, a mechanism that demonstrates how the central nervous system manages the complex musculoskeletal system's high number of degrees of freedom to best organize movement [79].

Many studies in the literature have demonstrated that the spinal motor system is actively involved in the production of movements ranging from simple to complex. These findings have confirmed the existence of modules whose combination results in movement. This modular structure of spinal cord circuits is based on functional units known as muscle synergies, which generate motor output by imposing together a specific pattern of muscle activations. This is an interesting method, but in our studies, we chose to use the synthetic approach provided by the TMCf, which is a time-varying function capable of expressing global stiffness and does not need to distinguish between agonist and antagonist muscle, allowing us to study the coactivation of more than two muscles at the same time.

The decision to investigate this parameter in our studies stems from the fact that other studies in literature have shown that patients with various central nervous system lesions, such as Parkinson's disease [80] and hereditary spastic paraparesis, have high levels of muscular coactivation and how this is related to the primary deficits of the disease. In particular, we investigated muscle coactivation using TMCf in patients with cerebellar ataxia and lower limb amputation.

- In the case of PwCA, we obtained high values of muscle coactivation in terms of both the synthetic indexes of TMCf, such as the coactivation index and the FWHM [2]. Another significant finding is that the TMCf center of activity shifts toward the earlier subphase of the gait cycle in comparison to HS. These findings appear to imply that PwCA increase coactivation as a compensatory mechanism primarily during the loading response subphase,

which represents the most difficult biomechanical condition, when body weight is shifted from one limb to another. Furthermore, the increase in muscle coactivation could be a global compensatory mechanism to cope with the enlarged lateral body sway resulting from the lack of interjoint coordination and hypotonia, which are caused by cerebellar degeneration.

- The same synthetic indices of coactivation and FWHM appear to have high values even in subjects with lower limb amputation [81], indicating their need to increase the level of the simultaneous activation of many muscles and for a longer time when compared with HS. This is an expected result and well reflects the compensatory increase in stiffness demonstrated in previous studies [82]. The coactivation function's characteristic shape curve, combined with the lack of significant differences in CoA values when compared to the control, suggests that the global coactivation temporal profile in people with amputation is similar to that of healthy subjects. The observation that the spatiotemporal modular architecture of muscle synergies in the sound limb is preserved in people with TFA reinforces this notion [83]. In addition, we found elevated DP values, which express the variance of the global coactivation curves and thus indicate an increased inter-subject variation in the global coactivation function. Together with the lack of a significant difference in intrasubject variability, it suggests that people with amputation exert a variable compensatory increase in global coactivation of the sound limb muscles from subject to subject, but remains stable within each subject.

  Furthermore, we found that people with TFA wearing C-Leg prosthesis (TFA_C) performed better than people with TFA wearing Genium prosthesis (TFA_G). This finding may come as a surprise given that previous research [84] found that TFA_G demonstrated greater flexibility, balance, and upper body strength than TFA_C during both walking and stair climbing. Previous findings suggest that coactivation of the sound limb muscles is less necessary in TFA_G than in TFA_C. In our case, the increased muscle activation found in the TFA_G could have a multifactorial interpretation: the Genium device, by allowing for the programming of multiple activities, could cause performance losses on specific tasks. Two other factors stem from the device's technical features: the increased weight of the prosthesis and the introduction of a pre-bending of the knee in the double stance phase, which is frequently not well managed by the patient

Based on these findings, it is possible to conclude that the global coactivation measure may be a useful tool for characterizing motor control and improving physicians' ability to optimize rehabilitation treatment and design new types of orthoses and prostheses.

The results of our systematic review of motor performance indices used in return to work programs revealed that those derived from surface electromyography are still underutilized. This is most likely due to technical, methodological, and cultural limitations. Fortunately, there are tutorials and other materials available to overcome these challenges, so the sEMG approach should be included in return to work rehabilitation plans.

In conclusion, I believe that the indices identified in this thesis work can be an effective tool for proposing appropriate clinical and ergonomic rehabilitation interventions. They are also a reliable tool to: (i) assess the rehabilitation efficacy by comparing their values before and after treatment; (ii) provide useful clinical information regarding gait instability or alterations in subjects with motor disorders, which are not directly observable through routine clinical assessments; (iii) design of new and ergonomic prostheses and orthoses; (iv) control collaborative robots that can support people to carry out their activities.

Finally, because new technologies are becoming more transparent and accepted by individuals, we now have the opportunity of evaluating motor patterns not only in the laboratory but directly in the patient's/worker's daily life environment.

Bibliography

[1]. Giorgio Sandrini. 2012. Compendio di Neuroriabilitazione. Dai quadri clinici alla presa in carico della disabilità - Adulto ed età evolutive.

[2]. Fiori L, Ranavolo A, Varrecchia T, Tatarelli A, Conte C, Draicchio F, Castiglia SF, Coppola G, Casali C, Pierelli F, Serrao M. 2020. Impairment of Global Lower Limb Muscle Coactivation During Walking in Cerebellar Ataxias. Cerebellum, 19(4):583-596.

[3]. Martino G, Ivanenko YP, Serrao M, Ranavolo A, d'Avella A, Draicchio F, Conte C, Casali C, Lacquaniti F. 2014. Locomotor patterns in cerebellar ataxia. J Neurophysiol.,1, 112(11):2810-21.

[4]. Serrao M, Pierelli F, Ranavolo A, Draicchio F, Conte C, Don R, Di Fabio R, LeRose M, Padua L, Sandrini G, Casali C. 2012. Gait pattern in inherited cerebellar ataxias. Cerebellum, 11: 194–211.

[5]. Palliyath S, Hallett M, Thomas SL, Lebiedowska MK. 1998. Gait in patients with cerebellar ataxia. Mov Disord., 13: 958–964.

[6]. Ilg W, Golla H, Thier P, Giese MA. 2007. Specific influences of cerebellar dysfunctions on gait. Brain J Neurol., 130: 786–798..

[7]. Wuehr M, Schniepp R, Ilmberger J, Brandt T, Jahn K. 2013. Speed-dependent temporospatial gait variability and long-range correlations in cerebellar ataxia. Gait Posture37: 214–218.

[8]. The effectiveness of a soft passive trunk exoskeleton on the motor coordination in patients with cerebellar ataxia (in progress)

[9]. Varrecchia T, Castiglia SF, Ranavolo A, Conte C, Tatarelli A, Coppola G, Di Lorenzo C, Draicchio F, Pierelli F, Serrao M. 2021. An artificial neural network approach to detect presence and severity of Parkinson's disease via gait parameters. PLoS One, 19, 16(2):e0244396.

[10]. Castiglia SF, Trabassi D, De Icco R, Tatarelli A, Avenali M, Corrado M, Grillo V, Coppola G, Denaro A, Tassorelli C, Serrao M. 2022. Harmonic ratio is the most responsive trunk-acceleration derived gait index to rehabilitation in people with Parkinson's disease at moderate disease stages. Gait Posture, 97:152-158.

[11]. Pistacchi M, Gioulis M, Sanson F, De Giovannini E, Filippi G, Rossetto F, Zambito Marsala S. 2017. Gait analysis and clinical correlations in early Parkinson's disease. Funct Neurol., 32(1):28-34.

[12]. Zanardi APJ, da Silva ES, Costa RR, Passos-Monteiro E, Dos Santos IO, Kruel LFM, Peyré-Tartaruga LA. 2021. Gait parameters of Parkinson's disease compared with healthy controls: a systematic review and meta-analysis. Sci Rep., 11(1):752.

[13]. Varrecchia T, Serrao M, Rinaldi M, Ranavolo A, Conforto S, De Marchis C, Simonetti A, Poni I, Castellano S, Silvetti A, Tatarelli A, Fiori L, Conte C, Draicchio F. 2019. Common and specific gait patterns in people with varying anatomical levels of lower limb amputation and different prosthetic components. Hum Mov Sci., 66:9-21.

[14]. Iosa M, Paradisi F, Brunelli S, Delussu A. S, Pellegrini R, Zenardi D, ... Traballesi M. 2014. Assessment of gait stability, harmony, and symmetry in subjects with lower-limb amputation evaluated by trunk accelerations. Journal of Rehabilitation Research and Development, 51(4):623–634.

[15]. Schilder J.C.M, Overmars S.S, Marinus J, van Hilten J.J, Koehler P.J. 2017. The Terminology of Akinesia, Bradykinesia and Hypokinesia: Past, Present and Future. Parkinsonism Relat. Disord., 37:27–35

[16]. Ling H, Massey, L.A, Lees A.J, Brown P, Day B.L. 2012. Hypokinesia Without Decrement Distinguishes Progressive Supranuclear Palsy From Parkinson's Disease. Brain, 135, 1141:1153.

[17]. Van Emmerik R.E, Wagenaar R.C, Winogrodzka A, Wolters E.C. 1999. Identification of Axial Rigidity during Locomotion in Parkinson Disease.Arch. Phys. Med. Rehabil., 80:186–191.

[18]. Mak M.K, Wong E.C, Hui-Chan C.W. 2007. Quantitative Measurement of Trunk Rigidity in Parkinsonian Patients.J. Neurol.,254: 202–209.

[19]. Wright W, Gurfinkel V, Nutt J, Horak F, Cordo P. 2007. Axial Hypertonicity in Parkinson's Disease: Direct Measurements of Trunk and Hip Torque. Exp. Neurol., 208:38–46.

[20]. Bridgewater K.J, Sharpe M.H. 1998. Trunk Muscle Performance in Early Parkinson's Disease. Phys. Ther.,78: 566–576.

[21]. Koh S.B, Park Y.M, Kim M.J, Kim W.S. 2019. Influences of Elbow, Shoulder, Trunk Motion and Temporospatial Parameters on Arm Swing Asymmetry of Parkinson's Disease during Walking. Hum. Mov. Sci.,68, 102527.

[22]. Krishnamurthi N, Murphey C, Driver-Dunckley E. 2019. A Comprehensive Movement and Motion Training Program Improves Mobility in Parkinson's Disease. Aging Clin. Exp. Res.,32: 633–643.

[23]. Serrao M, Pierelli F, Sinibaldi E, Chini G, Castiglia S.F, Priori M, Gimma D, Sellitto G, Ranavolo A, Conte C, Bartolo M, Monari G. 2019. Progressive modular rebalancing system and visual cueing for gait rehabilitation in parkinson's disease: a pilot, randomized, controlled trial with crossover, Front. Neurol., 10.

[24]. Vieregge P, Stolze H, Klein C, Heberlein I. 1997. Gait quantitation in Parkinson's disease? locomotor disability and correlation to clinical rating scales. J Neural Transm., 104: 237–48.

[25]. Morris ME, Huxham FE, McGinley J, Iansek R. 2001. Gait disorders and gait rehabilitation in Parkinson's disease. Adv Neurol., 87: 347–61.

[26]. Morris M, Iansek R, McGinley J, Matyas T, Huxham F. 2005. Three-dimensional gait biomechanics in Parkinson's disease: evidence for a centrally mediated amplitude regulation disorder. Mov Disord., 20: 40–50.

[27]. Sofuwa O, Nieuwboer A, Desloovere K, Willems AM, Chavret F, Jonkers I. 2005. Quantitative Gait Analysis in Parkinson's Disease: Comparison With Healthy Control Group. Arch Phys Med Rehabil., 86(5): 1007–1013.

[28]. Serrao M, Chini G, Caramanico G, et al. 2019. Prediction of Responsiveness of Gait Variables to Rehabilitation Training in Parkinson's Disease. Front Neurol., 10: 826.

[29]. Fan R. E, Culjat M. O, King C.-H, Franco M. L, Sedrak M, Bisley J. W, ... Grundfest W. S. 2008. A prototype haptic feedback system for lower-limb prostheses and sensory neuropathy. Retrieved from Studies in Health Technology and Informatics, 132:115–119.

[30]. Head H, Holmes G. 1911. Sensory disturbances from cerebral lesions. Brain, 34(2–3): 102–254.

[31]. Ivanenko Y. P, Dominici N, Daprati E, Nico D, Cappellini G, Lacquaniti F. 2011. Locomotor body scheme. Human Movement Science, 30(2): 341–351.

[32]. Highsmith M. J, Kahle J. T, Miro R. M, Cress M. E, Lura D. J, Quillen W. S, ... Mengelkoch L. J. 2016. Functional performance differences between the Genium and C-Leg prosthetic knees and intact knees. Journal of Rehabilitation Research and Development, 53(6): 753–766.

[33]. Menz HB, Lord SR, Fitzpatrick RC. 2003. Acceleration patterns of the head and pelvis when walking on level and irregular surfaces. Gait & posture, 18:35–46.

[34]. Smidt GL, Arora JS, Johnston RC. 1971. Accelerographic analysis of several types of walking. American journal of physical medicine, 50:285–300.

[35]. Yack HJ, Berger RC. 1993. Dynamic stability in the elderly: identifying a possible measure. Journal of gerontology, 48:M225–230.

[36]. Brach JS, McGurl D, Wert D, et al. 2011. Validation of a measure of smoothness of walking. The journals of gerontology. Biological sciences and medical sciences, 66:136–141.

[37]. Kavanagh JJ, Barrett RS, Morrison S. 2005. Age-related differences in head and trunk coordination during walking. Human movement science, 24:574–587.

[38]. Latt MD, Menz HB, Fung VS, Lord SR. 2009. Acceleration patterns of the head and pelvis during gait in older people with Parkinson's disease: a comparison of fallers and nonfallers. The journals of gerontology. Biological sciences and medical sciences, 64:700–706.

[39]. Lowry KA, Smiley-Oyen AL, Carrel AJ, Kerr JP. 2009. Walking stability using harmonic ratios in Parkinson's disease. Movement disorders official journal of the Movement Disorder Society, 24:261–267.

[40]. Menz HB, Lord SR, St George R, Fitzpatrick RC. 2004. Walking stability and sensorimotor function in older people with diabetic peripheral neuropathy. Archives of physical medicine and rehabilitation, 85:245–252.

[41]. Caliandro P, Conte C, Iacovelli C, Tatarelli A, Castiglia SF, Reale G, Serrao M. 2019. Exploring Risk of Falls and Dynamic Unbalance in Cerebellar Ataxia by Inertial Sensor Assessment. Sensors, 19(24):5571.

[42]. Kelley K, Preacher K.J. 2012. On effect size. Psychol. Methods, 17: 137–152.

[43]. Castiglia SF, Trabassi D, Tatarelli A, Ranavolo A, Varrecchia T, Fiori L, Di Lenola D, Cioffi E, Raju M, Coppola G, Caliandro P, Casali C, Serrao M. 2022. Identification of Gait Unbalance and Fallers Among Subjects with Cerebellar Ataxia by a Set of Trunk Acceleration-Derived Indices of Gait. Cerebellum.

[44]. Doi T, Hirata S, Ono R, Tsutsumimoto K, Misu S, Ando H. 2013. The harmonic ratio of trunk acceleration predicts falling among older people: results of a 1-year prospective study. J Neuroeng Rehabil., 10:7.

[45]. Castiglia SF, Tatarelli A, Trabassi D, De Icco R, Grillo V, Ranavolo A, et al. 2021. Ability of a set of trunk inertial indexes of gait to identify gait instability and recurrent fallers in Parkinson's disease. Sensors, 21.

[46]. Psarakis M, Greene DA, Cole MH, Lord SR, Hoang P, Brodie M. 2018. Wearable technology reveals gait compensations, unstable walking patterns and fatigue in people with multiple sclerosis. Physiol Meas., 39:075004.

[47]. Iosa M, Bini F, Marinozzi F, Fusco A, Morone G, Koch G, et al. 2016. Stability and harmony of gait in patients with subacute stroke. J Med Biol Eng., 36:635.

[48]. Hubble R.P, Naughton G, Silburn P.A, Cole M.H. 2018. Trunk exercises improve gait symmetry in Parkinson disease: a blind phase II randomized controlled trial, Am. J. Phys. Med. Rehabil., 97:151–159

[49]. Ability of a set of trunk-acceleration derived gait indexes to characterize gait instability and asymmetry in stroke survivors (in progress).

[50]. Siragy T, Nantel J. 2018. Quantifying Dynamic Balance in Young, Elderly and Parkinson's Individuals: A Systematic Review. Front. Aging Neurosci., 10, 387.

[51]. Noh B, Youm, C, Lee, M, Cheon S.M. 2020. Gait characteristics in individuals with Parkinson's disease during 1-minute treadmill walking. PeerJ, 2020.

[52]. Bovonsunthonchai S, Vachalathiti R, Pisarnpong A, Khobhun F, Hiengkaew V. 2014. Spatiotemporal Gait Parameters for Patients with Parkinson's Disease Compared with Normal Individuals. Physiother. Res. Int., 19: 158–165.

[53]. Serrao M, Chini G, Casali C, Conte C, Rinaldi M, Ranavolo A, Marcotulli C, Leonardi L, Fragiotta G, Bini F, et al. 2017. Progression of Gait Ataxia in Patients with Degenerative Cerebellar Disorders: A 4-Year Follow-Up Study. Cerebellum Lond. Engl., 16: 629–637.

[54]. Chini G, Ranavolo A, Draicchio F, Casali C, Conte C, Martino G, et al. 2016. Local stability of the trunk in patients with degenerative cerebellar ataxia during walking. Cerebellum, 16:26–33.

[55]. Hoogkamer W, Bruijn SM, Sunaert S, Swinnen SP, Van Calenbergh F, Duysens J. 2015. Toward new sensitive measures to evaluate gait stability in focal cerebellar lesion patients. Gait Posture, 41:592–6.

[56]. Mehdizadeh S. 2018. The largest Lyapunov exponent of gait in young and elderly individuals: a systematic review. Gait Posture, 60:241–50.

[57]. Bruijn SM, van Dieen JH, Meijer OG, Beek PJ. 2009. Is slow walking more stable? J Biomech Elsevier, 42:1506–12.

[58]. Caronni A, Gervasoni E, Ferrarin M, Anastasi D, Brichetto G, Confalonieri P, et al. 2020. Local dynamic stability of gait in people with early multiple sclerosis and no-to-mild neurological impairment. IEEE Trans Neural Syst Rehabil Eng., 28:1389–96.

[59]. Peterson D.S, Mancini M, Fino P.C, Horak F, Smulders K. 2020. Speeding Up Gait in Parkinson's Disease. J. Parkinsons Dis., 10: 245–253.

[60]. Wada O, Asai T, Hiyama Y, Nitta S, Mizuno K. 2017. Root mean square of lower trunk acceleration during walking in patients with unilateral total hip replacement. Gait Posture Elsevier, 58:19–22.

[61]. Moe-Nilssen R, Helbostad JL. 2004. Estimation of gait cycle characteristics by trunk accelerometry. J Biomech Elsevier, 37:121–6.

[62]. Prince F, Winter D, Stergiou P, Walt S. 1994. Anticipatory control of upper body balance during human locomotion. Gait Posture Elsevier, 2:19–25.

[63]. Morrison S, Russell DM, Kelleran K, Walker ML. 2015. Bracing of the trunk and neck has a differential effect on head control during gait. J Neurophysiol., 114:1773–83.

[64]. Afsar O, Tirnakli U, Marwan N. 2018. Recurrence Quantification Analysis at work: Quasi-periodicity based interpretation of gait force profiles for patients with Parkinson disease. Sci. Rep., 8.

[65]. Afsar, Ö. 2018. Recurrence Quantification Analysis on Gait Reaction Forces of Elderly Adults for Determination of Pathological States. Celal Bayar Univ. Fen Bilim. Derg., 14: 309–314.

[66]. Pham, T.D. 2018. Pattern analysis of computer keystroke time series in healthy control and early-stage Parkinson's disease subjects using fuzzy recurrence and scalable recurrence network features. J. Neurosci. Methods, 307: 194–202.

[67]. Djuri´c-Jovi˘ci´c M, Beli´c M, Stankovi´c I, Radovanovi´c S, Kosti´c V.S. 2017. Selection of gait parameters for differential diagnostics of patients with de novo Parkinson's disease. Neurol. Res., 39: 853–861.

[68]. Kwon K.Y, Lee H.M, Kang S.H, Pyo S.J, Kim H.J, Koh S.B. 2017. Recuperation of slow walking in de novo Parkinson's disease is more closely associated with increased cadence, rather than with expanded stride length. Gait Posture, 58:1–6.

[69]. Mirelman A, Bonato P, Camicioli R, Ellis T.D, Giladi N, Hamilton J.L, Hass C.J, Hausdorff, J.M, Pelosin E, Almeida Q.J. 2019. Gait impairments in Parkinson's disease. Lancet Neurol., 18, 697–708.

[70]. Germanotta M, Vasco G, Petrarca M, Rossi S, Carniel S, Bertini E, et al. 2015. Robotic and clinical evaluation of upper limb motor performance in patients with Friedreich's Ataxia: an observational study. J NeuroEngineering Rehabil., 12:1–13.

[71]. Palmerini L, Mellone S, Avanzolini G, Valzania F, Chiari L. 2013. Quantification of motor impairment in Parkinson's disease using an instrumented timed up and go test. IEEE Trans. Neural Syst. Rehabil. Eng., 21: 664–673.

[72]. Warabi T, Furuyama H, Kato M. 2020. Gait bradykinesia: Difficulty in switching posture/gait measured by the anatomical y-axis vector of the sole in Parkinson's disease. Exp. Brain Res., 238:139–151.

[73]. Ranavolo A, Draicchio F, Varrecchia T, Silvetti A, Iavicoli S, Alberto R, et al. 2018. Erratum: wearable monitoring devices for biomechanical risk assessment at work: current status and future challenges-a systematic review. Int J Environ Res Public Health., 15:2569.

[74]. Fonseca ST, Silva PLP ST, Ocarino JM, Ursine PGS. 2001. Analysis of an EMG method for quantification of muscular co-contraction. Rev Bras Ciên e Mov., 9(3):23-30.

[75]. Fonseca ST, Silva PLP, Ocarino JM, Guimaràes RB, Oliveira MTC, Lage CA. 2004. Analyses of dynamic co-contraction level in individuals with anterior cruciate ligament injury. J Electromyogr Kinesiol, 14:239-47.

[76]. Busse ME, Wiles CM, et al. 2005. Muscle co-activation in neurological conditions. Phys Ther Rev., 7(4):247–53.

[77]. Ranavolo A, Mari S, Conte C, Serrao M, Silvetti A, Iavicoli S, Draicchio F. 2015. A new muscle co-activation index for biomechanical load evaluation in work activities. Ergonomics, 58(6):966-79.

[78]. Bernstein NA. 1967. The Coordination and Regulation of Movements. Pergamon Press.

[79]. Dietz V, Zijlstra W, Prokop T, Berger W. 1995. Leg muscle activation during gait in Parkinson's disease: adaptation and interlimb coordination. Electroencephalography and Clinical Neurophysiology 97:408–415.

[80]. Tatarelli A, Serrao M, Varrecchia T, Fiori L, Draicchio F, Silvetti A, Conforto S, De Marchis C, Ranavolo A. 2020. Global Muscle Coactivation of the Sound Limb in Gait of People with Transfemoral and Transtibial Amputation. Sensors, 20(9):2543.

[81]. Gailey, R. 2008. Review of secondary physical conditions associated with lower-limb amputation and long-term prosthesis use. J. Rehabil. Res. Dev., 45: 15–30.

[82]. De Marchis C, Ranaldi S, Serrao M, Ranavolo A, Draicchio F, Lacquaniti F, Conforto S. 2019. Modular motor control of the sound limb in gait of people with trans-femoral amputation. J. Neuroeng. Rehabil., 16, 132.

[83]. Lura D.J, Wernke, M.M, Carey S.L, Kahle J.T, Miro R.M, Highsmith M.J. 2015. Differences in knee flexion between the Genium and C-Leg microprocessor knees while walking on level ground and ramps. Clin. Biomech., 30, 175–181